Corrosion of steel in concrete

Tuutti, Kyösti

1982

Corrosion of steel in concrete

Kyösti Tuutti

CBI forskning research

fo 4·82

CORROSION OF STEEL IN CONCRETE

ERRATA

The most severe errors are given. Minor errors still occur, however, but should not affect the understanding of the contents.

The temperature in the laboratory tests, if there is no other comments, was $(20 \pm 2)^{\circ}C$.

Page/line	has been written	should be written
87-88	blended cement	slag cement
159 and 160 FIGS 91-92		Kucera pers. comm.
163/9 FIG 94	W/C approximately 0.9	0.8
176-178	W/C = 0.9	W/C = o.8
186/8	FIG 107	FIG 108
199/2	plotted	numbered
207/14	at right angles ... ... the bar but,	for bars at right angles to concrete surface but,
219/6	... so that	(Gullman and Kucera pers. comm.) so that ...
232-235	blended cement	slag cement
265/7	-	Portland cement paste, W/C = 0.60
266/3	-	Portland cement mortar, W/C = 0.40
266/6	-	Portland cement mortar, W/C = 0.60
275 in FIG	RH 80%	RH 50%
281 in FIG	no text at vertical axis	Free Cl^- (g/l)
320/4	-	Gullman, J, The Swedish Corrosion Institute
320/4	Kučera, V, The Swedish ...	Kučera, V, The Swedish Corrosion Institute
342-347	cell cement	cell current

CORROSION OF STEEL IN CONCRETE

av

Kyösti Tuutti
civ ing

Akademisk avhandling som med tillstånd av Kungliga Tekniska Högskolan i Stockholm framlägges till offentlig granskning för avläggande av teknisk doktorsexamen torsdagen den 21 oktober 1982 kl 09.00 i Kollegiesalen, Administrationsbyggnaden, KTH, Valhallavägen 79, Stockholm. Disputationen kommer att hållas på engelska.

Stockholm 1982

Tuutti, K: Corrosion of steel in concrete.
1982, Stockholm. Swedish Cement and Concrete Research Institute, ISSN 0346-6906.
Royal Institute of Technology, Stockholm.
Department of Building Materials.

A B S T R A C T

The research work that is presented in this thesis aims at mapping out the various mechanisms which control the process of steel corrosion in concrete.
The process of corrosion is illustrated with a schematic model where the service life is divided into a period of initiation and a period of propagation.
The time up to the initiation of the corrosion process is determined by the flow of penetrating substances into the concrete cover and by the threshold concentration for corrosion to start. Theoretical models have been produced to approximate the time of initiation.
The rate of corrosion in the propagation period can be described by the relative humidity in the concrete and the mean temperature of the structure. Different relations between these factors and the rate of corrosion have been put up for different initiation mechanisms.
The final state, cracked concrete covers, reduced cross-section area of the steel etc. is discussed in the model.
Other important factors, which have not been dealt with in the model, are also discussed.
A method for predicting service life of concrete structures is presented. The report also includes applications in various forms of the method.
The report is concluded with a documentation of laboratory investigations carried out by the author. (Author)

Descriptors: Corrosion, carbonation, chloride penetration, threshold values, free and bound chloride, acceptable depth of corrosion, corrosion products, environment types, cracks, cement type, service life calculations, test methods.

Document publisher

Swedish Cement and Concrete
Research Institute
S-100 44 STOCKHOLM

☐ Reports
☒ Research

No Year
Fo 4 1982

Project name

Author

Kyösti Tuutti

Initiator or sponsoring organization

Swedish Foundation for Concrete Research
Swedish Board for Technical Development

Document title

CORROSION OF STEEL IN CONCRETE

Keyword

Reinforcement corrosion
Carbonation
Chloride penetration
Rate of corrosion
Service life

Language

English

ISSN and key title

0346-6906 CBI forskning/research

Number of pages

469

GOTAB 71743 Stockholm 1982

CONTENTS

NOTATIONS

		PAGE
A	= area	151
A_{CO_2}	= depth of corrosion, initiation by CO_2	114
A_{Cl^-}	= depth of corrosion, initiation by Cl^-	114
a	= constant	26
$\bar{b}$	= retardation factor	26
C	= cement content	61
c, c_{index}	= concentration of different substances	26
$cover_D$	= concrete cover measured from the dry surface	187
$cover_W$	= concrete cover measured from the wet surface	187
D, D_{index}	= diffusion coefficient of different substances	30
D_{eff}	= effective diffusion coefficient	26
erf	= error function	34
erfc	= 1 - erf	34
I	= cell current	85
J, J_{index}	= flux of different substances	30
K	= transfer coefficient	147
(K)	= weight share of K in cement	61
k	= constant	26
k_d	= relation between free chloride in a pore solution (g/l) and bound chloride per cement weight (kg)	64
L	= life time	21
l	= diffusion length	72
l_o	= air content in fresh concrete	61
m	= constant	30
(Na)	= weight share of Na in cement	61
P	= Slite Portland cement	49
p	= porosity	61
R	= constant, specifies the quantity of bound chlorides in relation to the quantity of free chlorides	268
R_c	= electrical resistance	158
RH	= relative humidity	31
r	= rate of corrosion	21
S	= slag cement	49
T	= temperature	51
t	= time, exposure time	26

V_v	= external emf	158
W/C	= water cement ratio	29
X, x	= penetration depth	26
X_∞	= penetration depth after infinite time	26
z	= length, distance	30
α	= degree of hydration	29
β	= angle	40
δ	= distance	147
ρ	= density	97
ϕ	= bar diameter	99

ACKNOWLEDGEMENT

The present publication is the result of the mutual efforts of several persons to whom I wish to express my deepest thanks.

Those who contributed were:

Sven Gabriel Bergström	has been my supervisor and has contributed his knowledge, inspiration and personality in a most decisive way.
Eva Bergman, Lars Rombén	have in a most sacrifising and skilful way been engaged in the work. I would like to point out that several test methods have been developed by them.
Göran Fagerlund (Cementa AB), Vladimir Kucera (Swedish Corrosion Institute),	have given a great deal of good advice.
Olof Gewalli	has designed and made most of the test equipments.
Lars Olof Victorin, Greger Ysberg	have been engaged in some of the experimental works.
Bertil Johnsson, Gustav Westergren, Kjell Waern	have mixed the concrete and handled the test specimens.
Iréne Fahlberg, Ulla Jardinger (Cementa AB)	have done the word processing brilliantly.
Ann-Thérése Söderquist	has made all the 200 drawings.
Margit Hattenbach	has organised the printing procedure.
Ragna Adolfsson, Magdalena Carlsson-Gram, Maria Jerkland-Åberg, Tuula Ojala	who found all the literature

Patrick Smith (AB Exportspråk) has translated the report from my hand-written manuscript.

As this work has been a part of a joint-project between the Swedish Cement and Concrete Research Institute, Korrosionscentralen ATV in Denmark and The Technical Research Centre of Finland, I wish to thank Hans Arup, Frits Grönvold and Tenho Sneck.

Also many thanks to Kurt Eriksson, chairman of the advisory group for the Swedish project and all members of the advisory group.

Further, I would like to express my thanks to the Swedish Foundation for Concrete Research and the Swedish Board for Technical Development who sponsored the investigation.

Finally, if I have forgotten someone, please, forgive me.

Kyösti Tuutti

SUMMARY

This report presents the work aiming at mapping out the various mechanisms which control the process of steel corrosion in concrete.

Chapter 2 deals with a schematic corrosion model. Steel embedded in concrete is protected both chemically and physically by the concrete. Corrosion theories, laboratory experiments and field investigations have shown that the steel does not corrode immediately after embedment. In principle, the corrosion process is initiated by the causes:

- Neutralization of the environment surrounding the metal, e.g. carbonation.
- Activation of strongly corrosive anions, e.g. chlorides.

The time up to the initiation of the corrosion process is determined by the flow of penetration substances in the concrete cover and by the threshold concentration for the process. Theoretical models have been produced to approximate the time of initiation.

The rate of corrosion after initiation can suitably be described by means of the following parameters:

- the relative humidity in the pore system which effects both the electrolyte and the supply of O_2
- the mean temperature of the structure.

Different relations between these factors and the rate of corrosion have been put up for different initiation mechanisms and chemical composition of the pore solution.

The mean corrosion rate in Sweden can also be set to about

- 50 µm/year in carbonated concrete
- 100 µm/year for chloride initiated corrosion (low concentrations)
- up to 1 mm/year for chloride initiated corrosion (high concentrations or combination of CO_2 and Cl^-),

using the practical cases as a basis.

The final state, cracked concrete covers, reduced cross-section area of the steel etc. is also discussed in the model.

The service life of a concrete structure with regard to reinforcement corrosion is thus divided into an initiation stage and a propagation stage.

Other important factors, which have not been dealt with in the model, are discussed in Chapter 3. Environment types were divided by the main parameters: concentrations of initiating substances, moisture and temperature conditions. Cracked concrete can often be regarded as though they were uncracked, because repassivation occurs and the rate of corrosion must be low in the crack zone. The corrosion model was used to compare slag cement and Portland cement. The organisation of this subproject intended to provide answers to the following questions:

- do the substances in the slag cement initiate corrosion?
- how rapidly is the corrosion process initiated by the usual initiators CO_2 and Cl^-?
- is the propagation time affected by the cement type?
- what effects, if any, does the slag cement have on the final state?

Chapter 4 contains a summary of useful interrelationships and how these should be linked together to provide an approximate assessment of the service life of the structure. The report also includes applications of the methods in various forms.

The report is concluded with the documentation of laboratory investigations carried out by the author:

- Measurement of oxygen diffusion coefficient for concrete.
- Corrosion investigations with corrosion cells.
- Measuring the rate of corrosion by means of the weight loss method.
- Analysis of pore solution squeezed out of cement paste and mortar.
- Chloride threshold values.
- Porosity and pore size distribution in corrosion products.
- Relative humidity in cracks.
- Potential measurements.

1 INTRODUCTION

1.1 Background

There is a considerable need of reliable methods for predicting the risk of corrosion for steel embedded in concrete under given conditions, for example for a given environment and concrete quality. This problem is directly linked to the choice of cover thickness and quality of the concrete in the structure. There are examples of structures which have been severely damaged in corrosive environments.

Considerable research work has also been devoted in many countries to mapping out the interdependencies between the rate of corrosion and different variables in the concrete composition, workmanship and environment - for example the cement type, cement content, water-cement ratio, carbonation, moisture, temperature, cracking, cover thickness etc. Attempts have also been made to summarize the influence of a small number of important parameters, such as crack width and environment.

By the beginning of the 1970s it had been established that the surrounding environment, the quality of the concrete, the thickness of the cover and the crack width were primary variables. No one had, however, attempted to make a synthesis of the influence of these factors.

The Programme Council for Swedish Concrete Research has made the following statement: "The problem is to determine the risk of corrosion and its danger for a certain environment and under certain given conditions with regard to the porosity and crack width. As is always the case in connection with durability, it is difficult to convert the results from laboratory tests to practical conditions."

Against this background, a research project was started in 1975 at the Swedish Cement and Concrete Research Institute with the title: "Corrosion of steel in concrete - a synthesis".

1.2 Project objectives

The objectives of the project were to:

- map out the various mechanisms which control the decomposition of reinforcement in concrete by determining the interrelationships between the primary factors environment, concrete quality, concrete cover, crack width and corrosion rate.

- using known research material, supplemented where necessary with special or controlled experiments carried out within the framework for the project, quantify the significance of the primary variables for the corrosion process.

- attempt, if possible, to specify a method for documenting whether or not the reinforcement in a concrete structure is sufficiently protected against corrosion.

1.3 Organization in principle of the project

The project was started in July 1975 and was scheduled to last for three years but was extended for a further 1.5 years.

The original tasks set up for the project were:

- Review of the literature and collection of experimental data.
- Definition and description of various environment types.
- Synthesis of the factors environment, concrete quality and concrete cover.
- Control experiments with regard to this synthesis and, if applicable, a modification of the synthesis.
- A compilation of the significance of the crack width.
- Control experiments with regard to the preceding item and, if applicable, modification.
- Adjustment with regard to lightweight concrete.
- If possible, to specify a method for documenting corrosion protection in a finished structure.

In January 1976 an agreement was reached with Valtion Teknillinen Tutkimuskeskus in Finland on collaboration on this subject. As a result, the original 8-item schedule was changed so that the main responsibility for the various tasks was subdivided amongst the two institutions and so that the project was extended with the following two items:

- The significance of the steel type, including prestressing steel.
- The influence of slag cement.

The project was extended once more in May 1977 when an agreement on collaboration was reached with the Korrosionscentralen in Denmark. Once again, the main responsibility for all of the tasks embraced by the project was subdivided and the project was extended with the following items:

- Mechanism studies.
- Special studies in chloride environments.
- The effect of zinc-plating.
- Presentation of a method for estimating the service life of concrete structures.

Each of the three institutions have published their scientific reports within the framework for the project. The author of the present report has published reports dealing with the following tasks during the course of the project: review of literature, synthesis of the factors environment, concrete quality and concrete cover, compilation of the significance of the crack width and the effect of the cement type, see e.g. Tuutti /1977/.

Theories which have been produced at various stages during the project have been tested in practical cases in which the three institutions have been involved.

1.4 Organization of this report

The usual layout of a report with documentary research, processing of other researchers' results, construction of in-depth theories etc has not been followed here due to the fact that several reports have already been published. This report is rather a summary of the results presented in the previous publications combined with unpublished work and a docu-

mentation of all experiments which have been carried out within the framework for the project at the Swedish Cement and Concrete Research Institute.

It should also be noted that all the models that have been designed for various stages of the corrosion process by no means provide a precise description of reality. The intention has rather been to offer an overall picture of the service life of a concrete structure so as to provide a possibility of approximating the effects of various parameter values and of calculating a rough minimum service life for the structure.

The report begins with a schematic corrosion model which is then followed by a more detailed description of the various stages in the corrosion process, important parameters and measured values for the parameters. The model applies to an uncracked homogeneous Swedish Portland cement concrete with standard reinforcement.

Other important factors, which have not been dealt with in the model - such as the effect of the cement type, cracks etc - are discussed in Chapter 3.

Chapter 4 contains a summary of useful interrelationships and of how these should be linked together to provide an approximate assessment of the life of the structure.

The report is concluded with the documentation of laboratory investigations carried out by the author, see Chapter 5.

2 CORROSION MODEL

2.1 General

The pore solution which surrounds embedded steel is highly alkaline from the beginning with a pH value between 13 and 14. An environment of this type causes the steel to be passivated. This means that corrosion products, which are difficult to dissolve, are formed on the surface of the metal with a permeability so high that the rate of corrosion becomes practically zero.

Nevertheless, corrosion occurs on steel in concrete. In cases in which this happens, the environment closest to the steel has been changed to such an extent that the passive state has been counteracted. This can take place locally or over a large part of the reinforcement area. A certain length of time is normally required before the corrosion process is initiated.

The question of when initiation takes place immediately leads to the next question: What initiates the process? Practical experience has shown that activating substances such as chlorides, which penetrate to the steel, can counteract the passivity locally when the electrolyte is highly alkaline, and that the concrete cover is changed chemically when CO_2 penetrates into the material, whereupon the pore solution is neutralised. The latter is called carbonation of the concrete. Neutralisation can also occur in other ways besides through carbonation. Carbonation is, however, the completely dominating neutralisation mechanism for concrete in air.

When corrosion has been initiated, the rate of attack is determined both by the rate of the anode and cathode reactions and by the manner in which the physical contact between the reaction areas functions. The rate of corrosion after initiation can vary between high and low. The shorter the initiation time, the more interesting the questions concerning the corrosion rate become.

Corrosion of reinforcement leads to a reduced steel area which much absorb the stresses to which the material is subjected. Furthermore, corrosion products are usually accumulated around the anodic areas and since the corrosion products have a greater volume than the steel,

stresses occur in the concrete cover. After a certain amount of attack the cover cracks parallel to the reinforcement and finally exposes the reinforcement. The consequences are sometimes limited, however, to a leaching of the corrosion products without cracks occurring in the cover.

2.2 Parameters in the corrosion model

The model is illustrated in FIG 1.

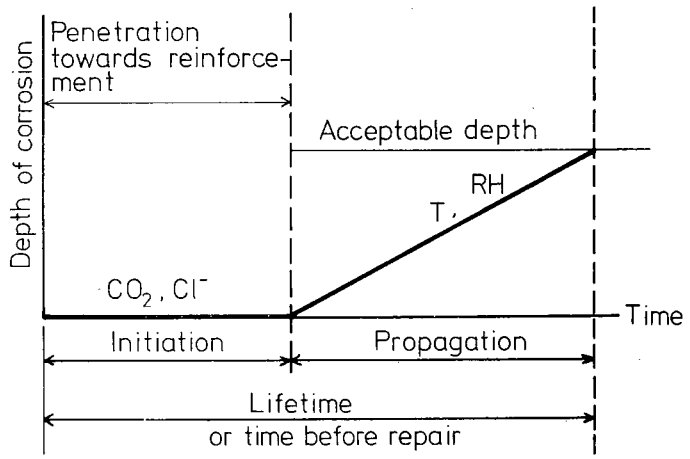

FIG 1. Schematic sketch of steel corrosion sequence in concrete.

From the point of view of reinforcement corrosion the service life of a concrete structure is subdivided into an initiation stage and a propogation stage. This subdivision is suitable since the primary parameters differ in the two subprocesses.

The length of the initiation period is determined by how rapidly the concrete cover is changed as a result of the fact that neutralising or activating substances penetrate to the steel, and by the concentrations of those substances which are required for the start of the corrosion process. A boundary case which is usually utilised in this context is to regard the penetration sequence as a diffusion process. In practice, the transport is not always quite so clear-cut but is rather a combination of convection and diffusion. One example of this is the fact that partly dried-out concrete absorbs a chloride solution through capillary action.

Mass transport as a result of diffusion gives the following parameters when studying the initiation period.

- Concentration difference, the ambient concentration minus the initial concentration which occurs in the material of the substance which diffuses.
- Transport distance, the thickness of the concrete cover.
- The permeability of the concrete against the substance which is penetrating it.
- The capacity of the concrete for binding the substance which is penetrating it.
- The threshold value, if applicable, which is required for initiating the corrosion process.

The corrosion process has started in the propagation stage and factors which determine the rate of corrosion decide the length of this stage.

Steel embedded in concrete can be said to have more clearly defined conditions than steel freely exposed in air. The concrete cover equalizes the effects of different variations in the surroundings and protects the steel against solid impurities.

The following are the factors which markedly influence the rate of corrosion:

- The moisture content of the concrete expressed by means of relative humidities in the pore system.
- The temperatures around the corrosion areas.
- The chemical composition of the pore solution around the embedded steel.
- The porosity of the concrete.
- The thickness of the concrete cover.
- Other factors which are difficult to define such as environmental variations along the metal etc.

For the same concrete and specimen in a certain stage, the two first factors in the list above are those which control the rate of corrosion. In the

case of chloride initiation, we can also presume that the chemical composition around the steel becomes more and more corrosive the longer the specimen is exposed to the environment.

The average loss of material or the depth of pitting which causes damage to the concrete cover is determined by which corrosion products are formed, in other words by their increase in volume in relation to the original metal, by the porosity of the concrete closest to the metal surface since this concrete serves as a storage space for the first corrosion products, and by the quantity of ferric ions which are diffused away from the area closest to the anode.

It should be noted that the model in FIG 1 is a rough schmetisation of reality. The rate of corrosion during the initiation stage, for example, is not zero but is very low. Nor is the rate of corrosion constant during the propagation stage, assuming constant conditions, but can increase locally as a result of migrating ions or decrease as a result of the formation of a diffusion barrier formed by the corrosion products.

Furthermore, the model applies to a homogeneous and uncracked concrete with reinforcement of standard type.

2.3 The significance of the model

All the subprocesses involved must be assessed when studying the effects which various parameters can have on the reinforcement corrosion and the service life of a concrete structure in a given environment. Completely erroneous conclusions can be drawn if an assessment or a selection is made on the basis of results obtained from only one parameter, for example the rate of corrosion after initiation, the rate of carbonation etc, see FIGS 2 and 3.

Corrosion studies of steel embedded in concrete should, consequently, be made in concrete. All experiments in which a completely different environment, for example, a saturated $Ca(OH)_2$ solution, is converted to conditions in concrete entail a further variable whose effect can be misinterpreted. Conflicting research results which have previously been reported on this subject may be due to the causes indicated here.

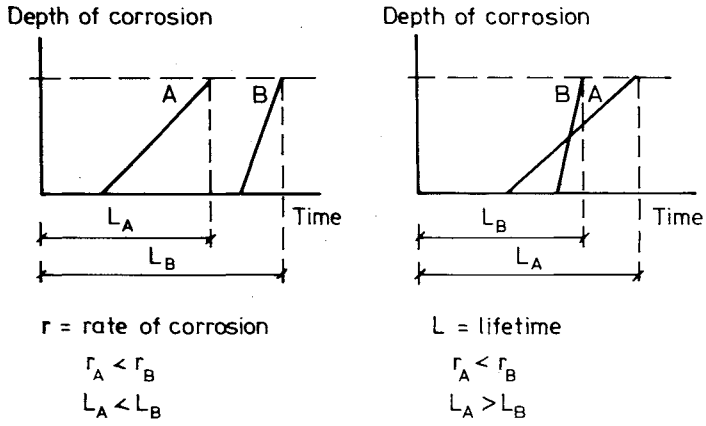

FIG 2. If only the rate of corrosion after initiation is taken into consideration, the life of a concrete structure cannot be assessed. The initiation time can be completely decisive for the life of the structure.

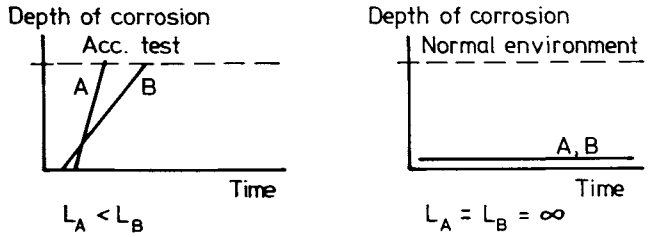

FIG 3. The corrosion process is often accelerated in laboratory experiments. This can lead to misleading results since the corrosion rate is frequently limited in practical cases for one reason or another.

The basic approach adopted in the investigations carried out in the present project has been to avoid accelerations and to carry out measurements in concrete with methods which are reliable.

2.4 Verification of corrosion model

The principles for the corrosion model were drawn up during an early stage of the project. When previous research results were processed on the basis of the significance of the primary factors - concrete quality, concrete cover and environment - the interrelationships illustrated in FIGS 4 and 5 were obtained. In the figures the concrete quality has been

converted to water permeability according to the results obtained by Ruettger, Vidal and Wing /1935/. A impermeable concrete had less corrosion attack than had a more permeable concrete. It could, however, also be established that damage occured in extremely low permeable concrete but that this took place in a later stage. Other published experiments followed the same pattern. See also Tuutti /1977/.

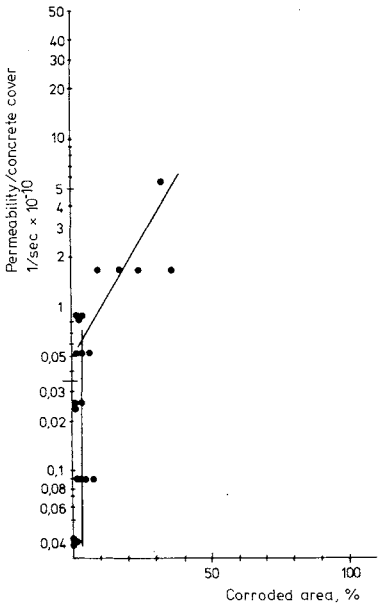

FIG 4. Corroded area as a function of the specific permeability. Exposure time: 6 months. The specimens were sprayed daily with 3% NaCl solution. The calculations were carried out with values from Houston, Atimtay and Ferguson /1972/.

A subdivision of the life of the structure into two periods thus constituted the first stage in the development. Practical investigations also confirmed this principle. It could be seen from practical cases studied that the initiation mechanisms were completely dominated by the carbonation of the concrete and by an excessively high chloride content around the embedded steel.

Tuutti /1979a/ presents an investigation in which balconies were studied in 50 different buildings. The balconies which were investigated represented the most seriously damaged balconies in Sweden. 80% of them were in such a state that they showed visible damage. Most of the damage occurred in

the edge zones of the balconies. The cause of the damage was an insufficient concrete quality for the concrete cover in question, leading to the carbonation front penetrating to and past the reinforcement in most cases. Sometimes frost damage had reduced the cover. Those balconies which had an extra surface finish, such as klinker tiles, terazzo etc, had been satisfactorily protected against carbonation although many of them had concrete which had been damaged by frost during an early stage. The age of the investigated balconies was around 20-30 years.

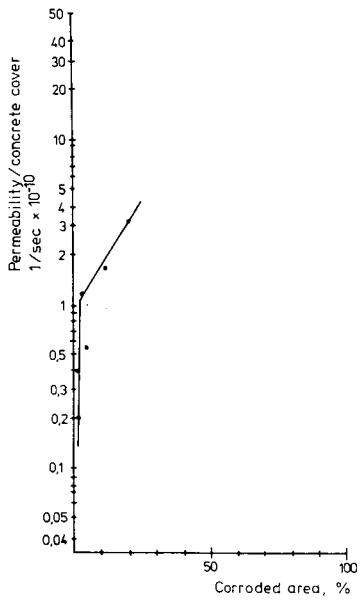

FIG 5. Corrosion area as a function of the specific permeability for lightweight concrete. Exposure time: 12 months. In other respects as for FIG 4.

In an investigation, as yet unpublished, of a traffic facility called Slussen in Stockholm in which the author acted as advisor, concrete cores were drilled out of the structure at about 100 points. The state of the reinforcement was also mapped out adjacent to the sampling points. The investigation confirmed that both chlorides and carbonation had acted as corrosion initiating factors.

All of the studies of damaged cases carried out at the Swedish Cement and Concrete Research Institute showed the same pattern for initiation and

propagation as the two abovementioned investigations. Nor has the author found, in his own laboratory experiments or in the literature, any indication of factors conflicting with the principle on which the model is based. On the contrary, Brown /1979/ has constructed a similar model without any knowledge of the Swedish report, Tuutti /1977/.

The practical case histories are further discussed in the presentation of the subprocesses and the other parameters involved are also verified in conjunction with this, see Chapters 2.6.4, 2.7.4 and 3.2.4.

2.5 Initiation

2.5.1 General

Most of all corrosion damage is caused by the neutralisation of the concrete through carbonation or by the fact that the pore solution surrounding the reinforcement has too high a concentration of chlorides. Rarer initiation mechanisms, in which other corrosive substances penetrate to the steel, for example bromides, cyanates etc, or which are due to the fact that the environment along the reinforcement differs, for example air gaps and voids along the reinforcement, are not dealt with directly in the model. A number of special factors are, however, discussed later in the report.

2.5.2 Carbonation

Model

Concrete contains a number of substances which give basic solutions such as CaO, Na_2O and K_2O.

The pore solution thus has a very high concentration of hydroxide or, as it can also be expressed, a high pH value.

$Ca(OH)_2$ has a limited solubility which is markedly dependent on the OH^- concentration in the solution. Na and K are, on the other hand, considerably more soluble and are almost completely dissolved in the concrete pore solution. As a result of alkalis, very small quantities of $Ca(OH)_2$ are dissolved in the concrete pore solution, see Longuet et al /1976/. CaO is,

however, the dominating substance in cement. As a result, extremely large quantities of $Ca(OH)_2$ are crystallised in the pores. The impermeability of the concrete, this reserve of hydroxide and the low CO_2 concentrations which occur in air are the primary reasons why the carbonation process proceeds slowly in the concrete. The carbonation entails

$$Ca(OH)_2 + CO_2 \rightarrow CaCO_3 + H_2O$$

The reaction gives rise to a neutralisation of the pore solution to pH values under 9. The process is not, however, as simple as might appear from the above. The neutralisation takes place in stages and several intermediate reactions occur. One of the final products is, however, always $CaCO_3$. The part played by the alkalis in the carbonation process is probably quite small. When CO_2 diffuses into the concrete, NaOH and KOH carbonate, thus increasing the solubility for $Ca(OH)_2$. We therefore get a diffusion process in concrete of CO_2 and a diffusion process of NaOH, KOH and $Ca(OH)_2$ to the carbonation front, see FIG 6.

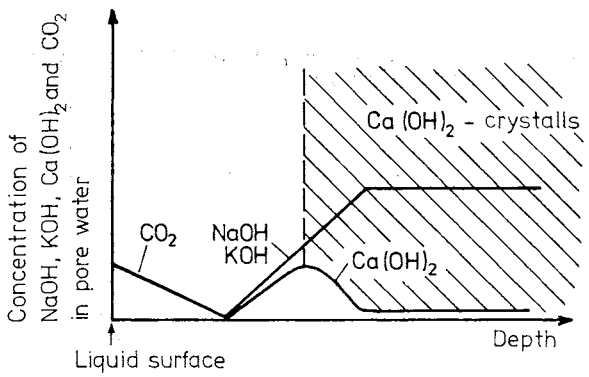

FIG 6. Schematic sketch of concentration profile for concrete carbonation.

The literature contains two basically different concepts of which mathematical function the carbonation process follows. The oldest theory is based on the square root principle

$$X = k\sqrt{t} \quad \text{---------} \quad (1)$$

where X = penetration depth

t = exposure time

k = a constant which is dependent on the effective diffusivity for CO_2 through concrete, the concentration difference and the quantity of bound CO_2.

Emperical values indicate, however, that the exponent for the time is less than 0.5. A new theory put forward by Schiessl /1976/ therefore has a retardation factor $\bar{b}$. The interdependency thus inserted leads to an infinity value X_∞ for the position of the carbonation front, see FIG 7.

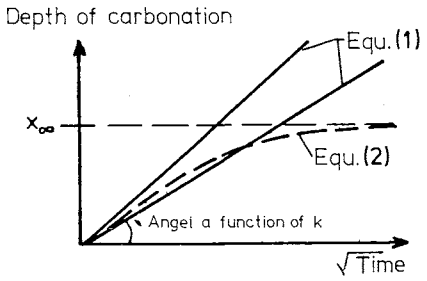

FIG 7. Two different mathematical principles for describing the penetration of the carbonation front in concrete.

$$t = -\frac{a}{\bar{b}}\left(X + X_\infty \cdot \ln\left(1 - \frac{X}{X_\infty}\right)\right) \quad \text{---} \quad (2)$$

where $X_\infty = \dfrac{D_{eff}\,\Delta c}{\bar{b}}$

D_{eff} = effective diffusion coefficient

Δc = concentration difference

a = constant

$\bar{b}$ = retardation factor

Equation 2 cannot be completely correct unless the concrete becomes more impermeable the more it is carbonated until, at a carbonation depth of a few tenths of a millimetre, it becomes absolutely impermeable against CO_2. After an infinite length of time the concrete will have been carbonated.

Furthermore, at the depth at which the carbonation front comes to a halt, we should have an extremely large quantity of reaction products, for example $CaCO_3$ which is extremely difficult to dissolve. While admittedly rendering the material impermeable, this would also give rise to an internal stress since the pore system would be completely filled with solid compounds.

It seems more likely that the truth is to be found somewhere in between these two equations. The deviations which have been noted from equation (1) can, for example, be the effect of an decrease in the permeability of the concrete the further into the material one penetrates. The surface layer does not have at all the same properties as concrete further in due to different curing conditions, moisture content etc which affect the permeability of the material. Consequently, one cannot make any direct comparisons between different concretes even if the mix proportions are the same. The moisture transport out of and into the concrete is also markedly affected by the ambient environment.

The carbonation depth, which is normally measured with the aid of a meter after a phenolphtalein solution has been sprayed on the concrete is a fairly rough method with an accuracy of a few millimetres and in turn requires extremely lengthy exposure times if a better interrelationship is to be obtained for this process.

The phenolphtalein measurement is also limited to providing an indication of the position of the pH value limit 9 and does not show the changes which may occur in partly carbonated concrete, see FIG 8.

Concrete has pores measuring from a few Ångström to several millimetres, see FIGS 9-11. The linking channels in concrete are called capillary pores and various substances are mainly transported through these pores and cracks. The diffusion of CO_2 and other gases such as O_2, which are transported through a porous material, takes place partly through a gas phase and partly through a liquid phase. For a certain concentration of CO_2 or O_2 in the gas phase there is another, considerably smaller, concentration of the same gas in the liquid phase.

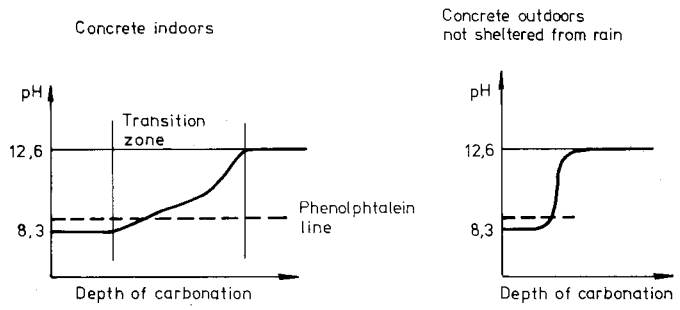

FIG 8 Basic sketch of the pH profile in the concrete cover when the concrete has been carbonated to a certain depth. (Schiessl /1976/).

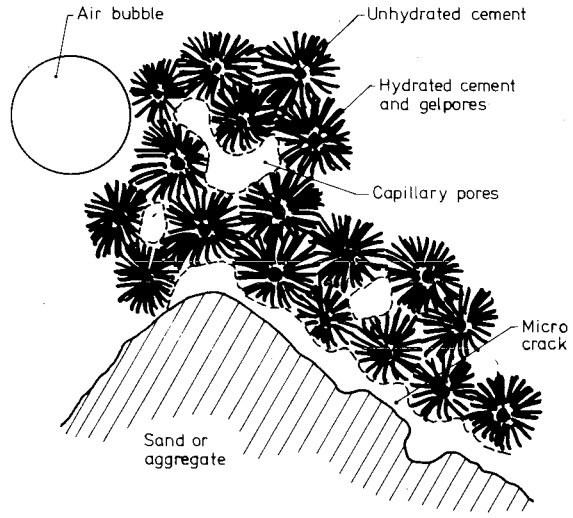

FIG 9. Schematic sketch of the microstructure in concrete, Fagerlund /1980/.

Both phases must, however, be penetrated. This results in a state where the resistence is completely dependent on the liquid phase. When calculating the gradient for the concentration in the liquid and gas phases, which is the driving force in a diffusion process, the following are obtained for CO_2 and O_2.

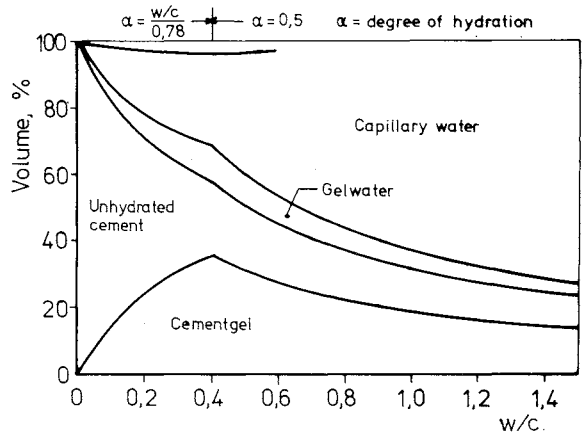

FIG 10. Volumetric distribution of the constituents of the cement paste at half the maximum possible degree of hydration (= 0,5 for W/C $\geq$ 0.40). Bergström /1967/.

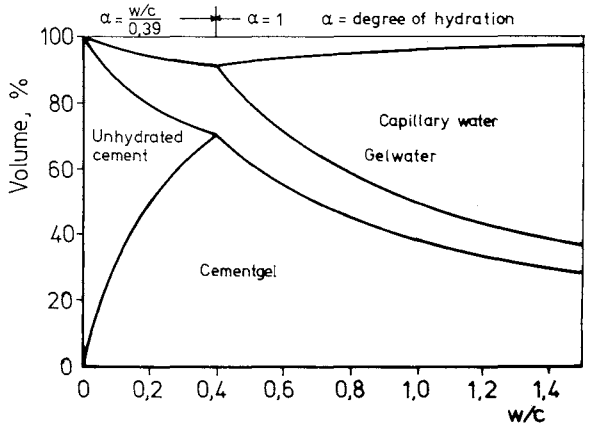

FIG 11. Volumetric distribution of the constituents of the cement paste at the maximum possible degree of hydration (= 1 for W/C $\geq$ 0.40). Bergström /1967/.

The flow in the gas phase is equal to the flow in the liquid phase. It has been assumed in conjunction with this that there is no major transition resistance between the two phases.

$$J_{CO_2} = -D_{CO_2\ gas} \cdot c_{tot_{gas}} \cdot \frac{dc_{y_{CO_2}}}{dz} = -D_{CO_2\ H_2O} \cdot c_{tot\ H_2O} \cdot \frac{dc_{x_{CO_2}}}{dz}$$

where $c_{y_{CO_2}} = m \cdot c_{x_{CO_2}}$

J = flux of CO_2 or O_2

D = diffusion coefficient

c = concentrations (index x,y = relative concentrations)

$$\frac{dc_{x_{CO_2}}/dz}{dc_{y_{CO_2}}/dz} \approx 1 \cdot 10^4$$

$$\frac{dc_{x_{O_2}}/dz}{dc_{y_{O_2}}/dz} \approx 3 \cdot 10^5$$

Designations according to FIG 12.

The difference between O_2 and CO_2 is caused by the fact that CO_2 is more soluble in water than is O_2.

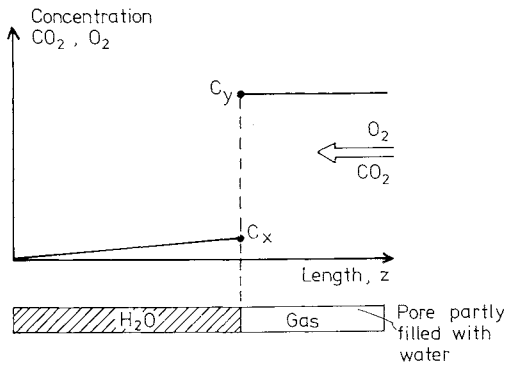

FIG 12. Schematic concentration profile in a pore which is partly filled with water.

The moisture content in the concrete is thus of considerable significance for how rapidly a gas can penetrate the material, see Chapter 5.1, where the experimental results confirm this claim.

If the degree to which a pore is filled is studied as a function of the relative humidity of the ambient air when a state of equilibrium prevails, it can be seen in FIG 13 that the capillary pores are not filled until the relative humidity reaches 100% and that small changes in the relative humidity at high values entail considerable changes in the moisture content of the concrete, see FIG 14.

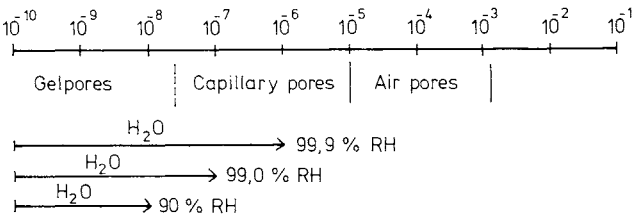

FIG 13. Degree with which different pore types are filled with water for varying RH values.

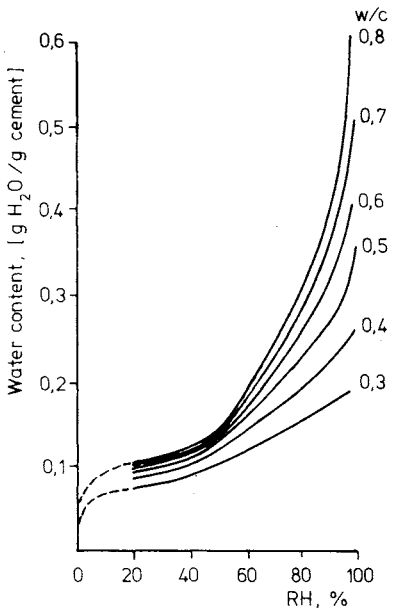

FIG 14. Desorptions isotherms for different concrete qualities. Degree of hydration 0.8. Nilsson /1977/.

If we return to the carbonation of the concrete and a study of the design of a suitable model for the process, we can schematically sketch the pore system of the concrete according to FIG 15. The concrete has a heterogeneous pore system with large and small pores intermingled and connected with each other. When the concrete carbonates, the CO_2 flow rapidly penetrates through the large air-filled pores but is effectively retarded by the small water-filled pores. Carbonation takes place throughout the entire pore system, as long as water is available. In dry concrete (relative humidity below 80%) only incomplete carbonation takes place, see Chapter 5.3,5.

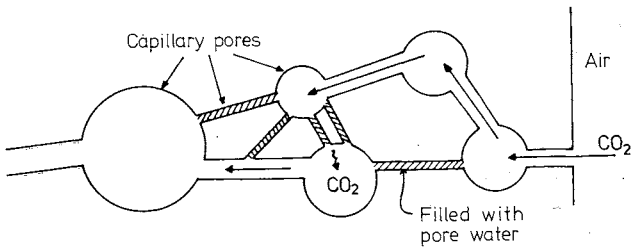

FIG 15. Schematic sketch of CO_2 diffusion in concrete. The large capillary pores which are not filled with water function as transport channels. The channel system which is filled with air is interrupted by smaller channels which are filled with pore solution. These smaller channels retard the penetration of the carbonation front.

On the other hand, it can be seen that the carbonation must be a local occurrence since the entire pore system is not filled with water as a result of the fact that alkalis further into the concrete are not capable of diffusing to the point of reaction. The reason for this is, quite simply, that there are no transport paths for this diffusion due to the occurrence of air-filled pores. A thin layer of pore solution is, admittedly, adsorbed to the pore surfaces but the resistance in these is far too great to permit an active participation in the carbonation process. This opposed diffusion does, however, occur locally at points where a plentiful supply of water is available.

OH^-, on the other hand, is always diffused outwards in completely water-saturated concrete but in such cases it is not normally the carbonation process which is the deciding factor for the initiation of corrosion.

An outward diffusion of OH^- also probably takes place in concrete which has been exposed to rain, in which the moisture state is for the most part high and in which the capillary pores are sometimes filled. The more impermeable the concrete, the closer to the concrete surface this diffusion occurs.

Concrete which is protected against rain has a moisture state in which the relative humidity in the pores mainly lies under 90%, in other words the capillary pores are filled with air and the carbonation process should follow a square root relation for each layer in the material in which the permeability is constant. In an extremely low permeable concrete, $W/C < 0.40$, the capillary pore system will, on the other hand, constitute no more than a small part of the total porosity. For concretes of this type OH^- will diffuse outwards even in this semi-moist state. The dimensions of a structure can also influence the moisture state in the concrete pore system. A thin structure follows the temperature changes in the outdoor air and is not, consequently, subjected to condensation to the same extent as is a solid structure. Furthermore, complete drying out takes place at a considerably slower rate in a thick structure than it does in a thin structure.

Against the background of the above line of reasoning, it seems that concrete which is not exposed to rain usually follows a square root relationship. It thus becomes a question of a diffusion process with the complication that the diffusing CO_2 is eliminated from the process. It is, on the other hand, impossible to specify precisely a limit where the carbonation-retarding outward diffusion of OH^- becomes decisive. This is illustrated in the next section. The square root relationship is, however, an upper limit value for the penetration of the carbonation front, in other words the shortest conceivable initiation time is obtained when assessing the service life of the structure. As a result, this theory can be utilized in most cases.

If we assume that the pH value profile is discontinuous, i.e. that a thin layer in the material is completely carbonated on one surface and not carbonated on the other, the process can be described mathematically as a moving boundary with the equations given below and taken from Crank /1975/, see FIG 16.

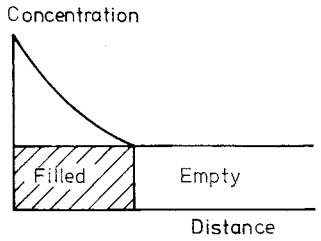

FIG 16 Concentration profile in conjunction with diffusion of particles in a material which is capable, physically or chemically, of eliminating the particles from the diffusion process.

$$\frac{c_x - c_1}{g(k/2\sqrt{D_1})} + \frac{c_x - c_2}{f(k/2\sqrt{D_2})} = 0$$

where c_x = concentration at discontinuity

D_1 and D_2 = diffusion constants on either side of the boundary

c_1 = concentration in surroundings

c_2 = concentration in material

The functions g and f can be written as follows:

$$g\left(\frac{k}{2\sqrt{D_1}}\right) = \sqrt{\pi}\,\frac{k}{2\sqrt{D_1}}\,e^{\frac{k^2}{4D_1}}\,\mathrm{erf}\,\frac{k}{2\sqrt{D_1}}$$

$$f\left(\frac{k}{2\sqrt{D_2}}\right) = \sqrt{\pi}\,\frac{k}{2\sqrt{D_2}}\,e^{\frac{k^2}{4D_2}}\,\mathrm{erfc}\,\frac{k}{2\sqrt{D_2}}$$

The constant k can be calculated with the aid of these equations.

The special case which applies to CO_2 diffusion in concrete can have the following simpler solution

$$\frac{c_x - c_1}{g(k/2\sqrt{D})} + c_x - c_2 = 0 \quad \text{---} \quad (3)$$

Furthermore, the following applies:

$$X = k \sqrt{t}$$

where X = carbonation depth
t = time

The carbonation rate is thus dependent on

- the surrounding concentration of CO_2
- the possible absorption of CO_2 in the concrete
- the permeability of the material

The problem can be solved when these three parameters are known. A number of calculated examples are presented in FIG 17 to indicate the significance of the various parameters. In this model, the carbonation depth, X, as function of the time, t, becomes a straight line in a log-log chart and undergoes a parallel displacement for a change in any of the variable values.

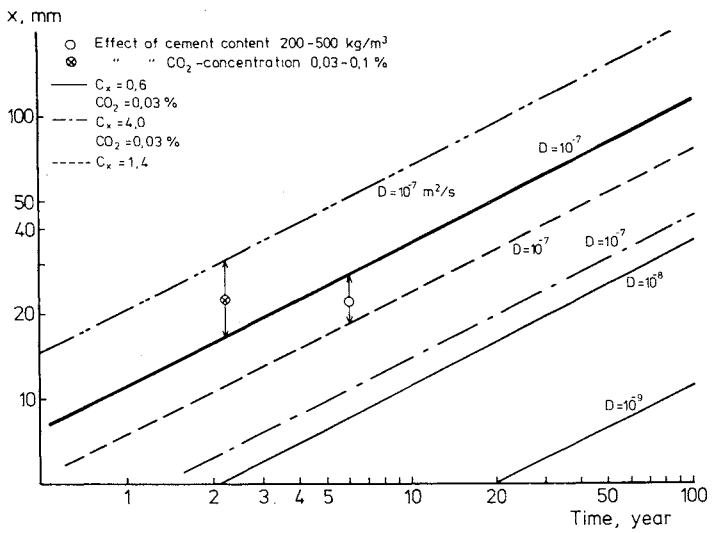

FIG 17. Calculated depth of carbonation for variations in bound CO_2 quantities (c_x), cement content (the permeability is assumed to be unchanged; this is not the case when the cement content is changed), CO_2 concentration in surrounding atmosphere and the permeability of the material (D).

Test of carbonation model

The carbonation process is an initiation mechanism in the corrosion process and has been thoroughly studied with numerous detailed reports in the literature. Consequently, the author has not carried out any laboratory experiments of his own but has confined himself to processing his own results from a number of investigations of damage cases and the results provided in various publications, primarily the three German publications which have been reported by Moll /1965/, Kleinschmidt /1965/, Forschungsinstitut der Zementindustrie in Düsseldorf /1965/, Meyer et al /1967/, Schröder et al /1967/. To begin with, the carbonation depth was plotted as a function of the age and W/C, FIG 18. The water cement ratio is the primary factor for the strength and permeability of the concrete, in other words, it is an indirect measure of the rate of carbonation for the concrete.

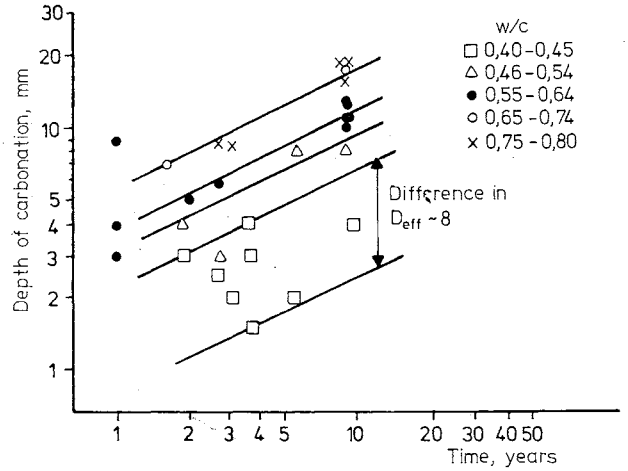

FIG 18. Measured mean carbonation depth at various times for Portland cement concrete. After casting the specimens were cured in water for seven days and then stored in the laboratory (50% relative humidity). The values have been obtained from results by Meyer, Wierig and Husmann /1967/.

The specimens in FIG 18 had all gone through the usual laboratory conditioning with 7 days in water followed by storage in 50% relative humidity. A fairly good agreement was obtained for the higher W/C ratios with the

theoretical model (see the upper curves). Very low W/C ratios give a wide distribution, however. The explanation for this can consist of the difference in permeability in the concrete surfaces due to environmental differences. But differences in the constituent materials, poor measuring accuracy or, quite simply, a smaller proportion of capillary pores and an outward diffusion of OH^- give this effect. The carbonation depth measured in all structures and published in the abovementioned German investigations and the author's own results have been plotted in FIGS 19-22 as a function of the time. The structures which have been exposed to rain and the structures which have been sheltered from rain respectively have been differentiated. The cement types, on the other hand, varied in quality although all were of Portland cement type. The structures varied from thin beams to thick slabs and walls. Bearing in mind the considerable significance of the moisture content for the gas diffusion, the results should show a very large distribution despite the fact that structures with different W/C ratios have been differentiated. The result also showed a cluster of dots across almost all of the figures. It can, however, be noted that structures not exposed to rain have a considerably higher carbonation depth than do structures exposed to rain. Furthermore, the depth of carbonation increases with increases in the W/C ratio. This can be seen if an upper boundary line is drawn for the points (see FIG 23).

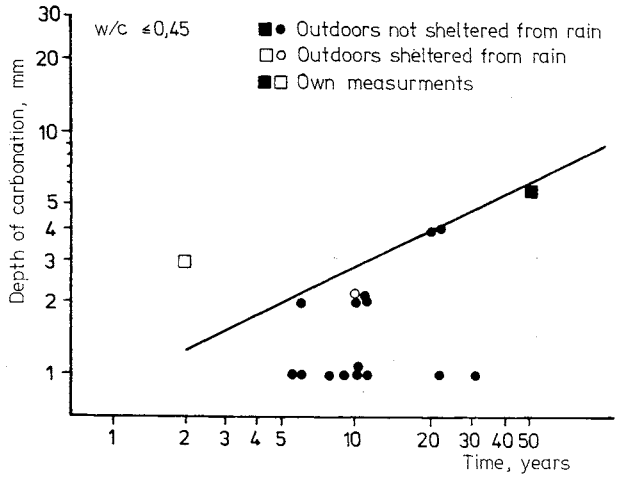

FIG 19. Measured mean carbonation depth. An upper boundary line on the measured carbonation depth has been drawn for the two environment types. This line has a gradient of 1:2 according to the model.

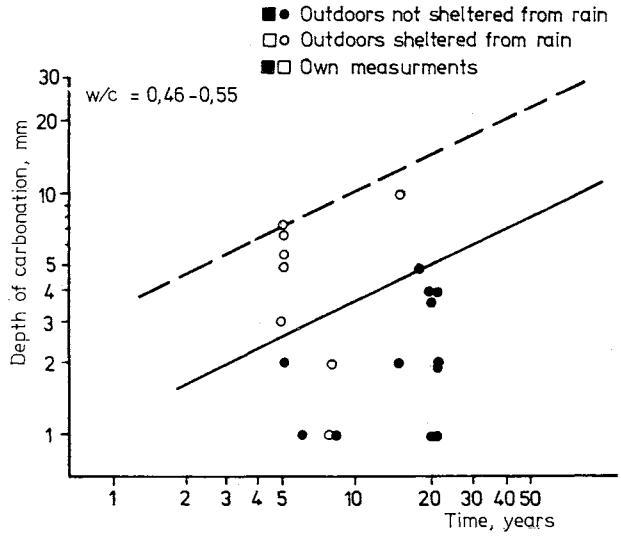

FIG 20. Measured mean carbonation depth. An upper boundary line on the measured carbonation depth has been drawn for the two environment types. This line has a gradient of 1:2 according to the model.

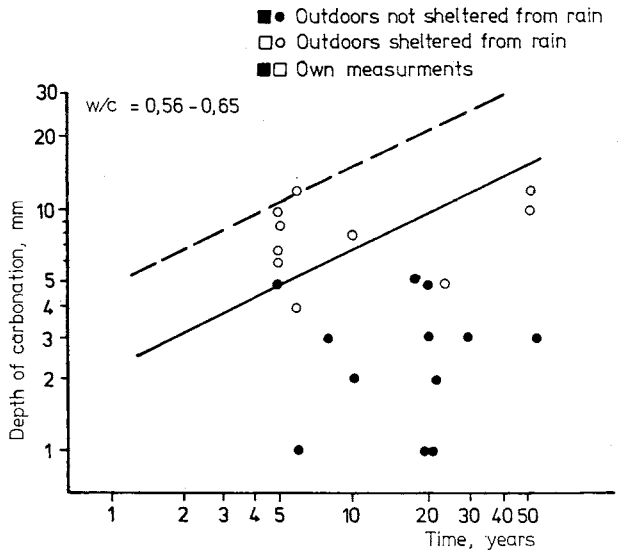

FIG 21. Measured mean carbonation depth. An upper boundary line on the measured carbonation depth has been drawn for the two environment types. This line has a gradient of 1:2 according to the model.

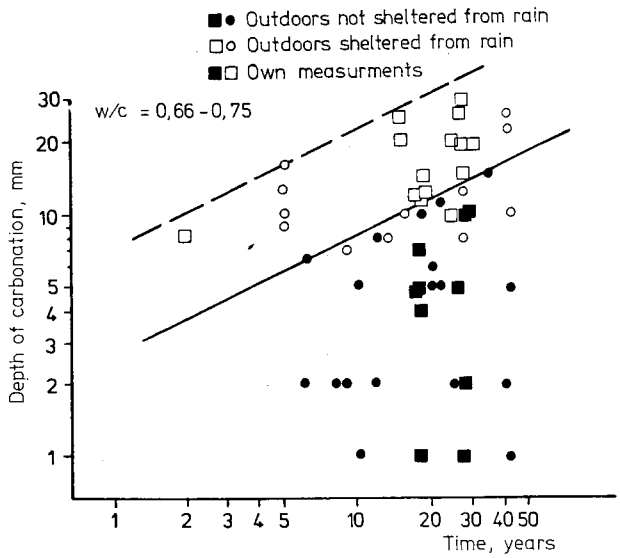

FIG 22. Measured mean carbonation depth. An upper boundary line on the measured carbonation depth has been drawn for the two environment types. This line has a gradient of 1:2 according to the model.

In only one report, Meyer Wierig and Husmann /1967/, were the same specimens investigated after several different exposure times. When the measured carbonation depth was plotted for these experiments, a very close agreement was obtained with the square root model for the carbonation process if the first stabilization stage is ignored, see FIG 24.

Concrete is a brittle material which has visible and invisible cracks. CO_2 and other gases are transported rapidly in these channels. As a result, the carbonation front is by no means uniform but has penetrated deeper into the material here and there. Because of this, the maximum depth for the pH value limit 9 has been measured in addition to the mean carbonation depth.

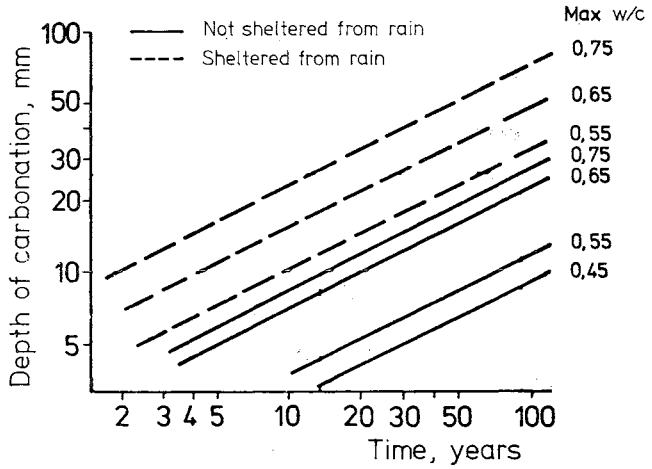

FIG 23. Upper boundary lines for measured mean carbonation depth in Portland cement concrete with varying W/C ratios. The curves have been taken directly from FIGS 19-22.

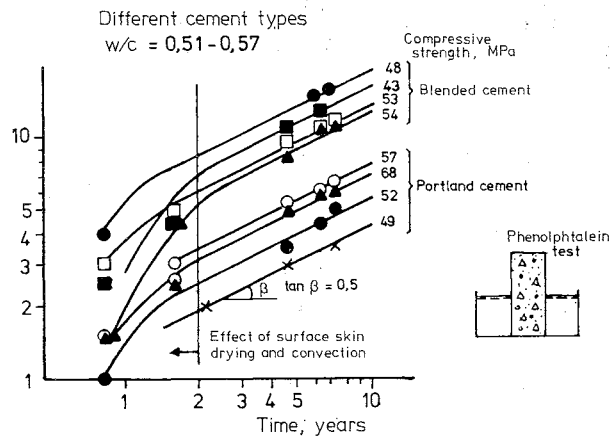

FIG 24. Measured mean carbonation depth as a function of the time for each different concrete specimen. The cement type was varied while the cement content remained constant at about 350 kg/m^3. Unbroken curves with a gradient of 1:2 according to the carbonation model have been drawn between the points. The results have been taken from Meyer, Wierig and Husmann /1967/.

A number of points for the absolute maximum and for the mean carbonation depth for each object measured have been plotted in FIG 25. Regardless of the age of the concrete, a greater difference is obtained between the

maximum values and the mean values the higher the W/C ratio of the concrete. This agrees with the simple model which says that the less permeable the matrix the fewer the capillary pores and large transport channels which are connected to each other, thus giving a more uniform depth of penetration. This is unlike cracked concrete where the carbonation depth in the crack becomes greater with reductions in the W/C ratio, see Schiessl /1976/.

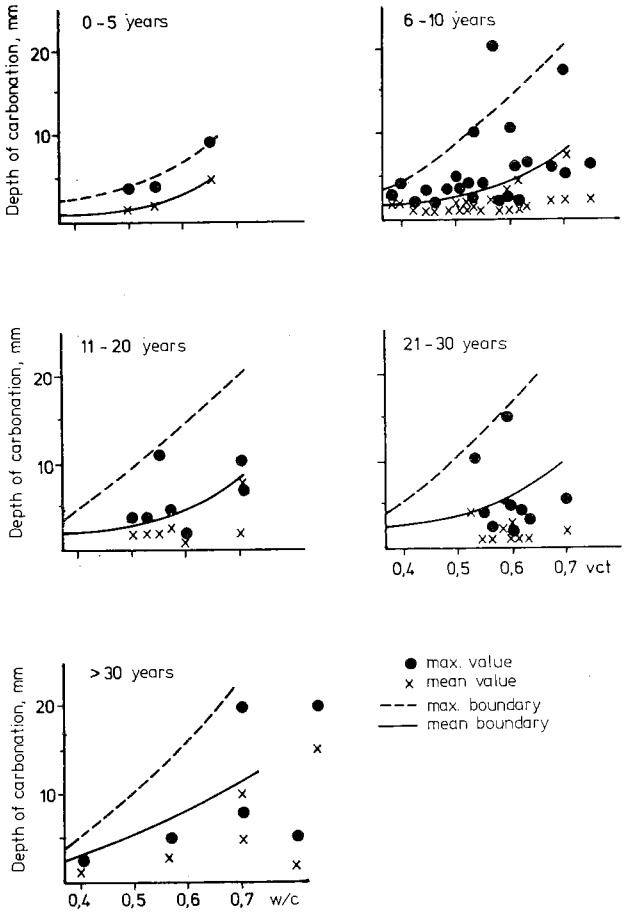

FIG 25. Measured mean and maximum carbonation depth. The values have been taken from DAfS publication 170.

In order to devote particular study to the effect of the treatment to which precast concrete elements are subjected during industrial manufacture, the Swedish Cement and Concrete Research Institute has obtained the measured results from about 30 objects. The measurements were carried out by AB Strängbetong and A-betong AB. The results have been compiled in Tables 1 and 2. All concrete was manufactured with Swedish Portland cement.

A distinction can be made between the measurements carried out by Strängbetong and those carried out by A-Betong insofar as Strängbetong carried out all its measurements on thin structures while A-Betong carried out measurements on fairly thick structures.

The effect of this is particularly marked since the thinner structures have a more variable moisture state and are thus provided with a greater possibility of carbonating.

The values in Table 1 and 2 have been plotted in FIG 26 so as to provide a comparison between these measurements and the previous measurements. A satisfactory level of agreement can be noted.

In this way, the square root model can be used for assessing the rate of the carbonation process in different concretes and environments. Given better material coefficients in a later stage, one need not worry about the assessments previously made since the rate of the process was over estimated, see FIG 27.

The model has also been used for a theoretical calculation of the penetration of the carbonation front in concrete. The following material coefficients must be known in connection with this.

- the ambient concentration of CO_2
- the possible absorption of CO_2 in the concrete
- the permeability of the material vis-à-vis CO_2

Table 1. Measurements carried out by AB Strängbetong.

Structure	Concrete data MPa *	W/C	Environment exposed to rain	not exposed to rain	Number of measurement	Age years	Carbonation depth mm
Column	40 MPa	0.50	X		5	6	1.5
"	"	"		X	5	6	2
Precast element	"	0.52	X		5	5.5	1.2
"	"	"		X	5	5.5	3
TT-element	60 MPa	0.42	X		5	4.5	1.5
"	"	0.45					
"	"	"		X	10	4.5	3
"	"	"		X	5	4.5	1.5
CDf element	60 MPa	0.39	X		6	8.5	1.2
"	"	"		X	6	8.5	1.5
"	60 MPa	0.36		X	10	11.5	1.0
"	"	"		X		11.5	0.5
"	"	0.39		X		8.5	1.5
"	"	"		X	14	"	2.5
"	"	"		X		"	0.5
"	"	"	X		5	"	1.0
"	"	"	X		5	"	0.5
TT-element	60 MPa	0.39	X		9	10.5	1.5
Beam	60 MPa	0.36		X	6	13	0.8
"	60 MPa	0.37	X		3	10.5	0.5
"	"	"		X	6	"	1.5
"	"	"		X	6	"	1.0
Slab	60 MPa	0.36		X	3	10.5	1.0

* Lower five percent fractile for compressive strength results for cube testing at an age of 28 days.

Table 2. Measurements carried out by A-Betong AB

Structure	Concrete data W/C	Environment exposed to rain	Environment not exposed to rain	Number of measurement points	Age years	Carbonation depth mm
Column	0.40-0.45	X		2	11	<1
"	"		X	2	13	<1
External wall	"	X		2	13	<1
"	"	X		2	15	<1
Column	"	X		2	"	<1
"	"			2	"	<1
"	"		X	2	11	8
"	"		X	2	13	<1
External wall	"			2	8	<1
Column	"	X		2	18	<1
"	"	X		2	11	<1
"	"	X		2	16	<1
"	"	X		2	19	<1
"	"	X		2	22	<1

CO_2 concentration in air surrounding concrete

The concentration of carbon dioxide generally varies between 0.03 -0.1%. The higher value is an approximation for densely built-up areas while the lower value is a mean value for rural areas. In the case of particularly exposed structures, for example adjacent to major traffic facilities or to industrial facilities etc, concentrations should be measured.

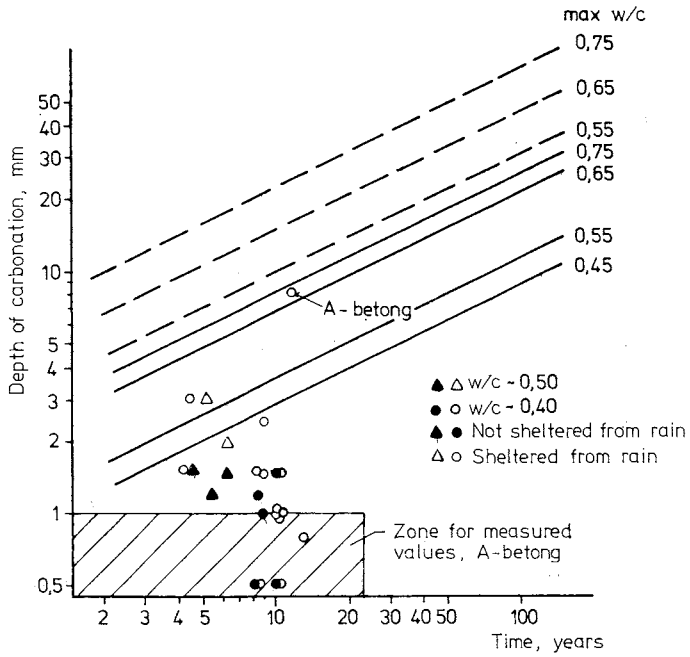

FIG 26. Values provided in Tables 1 and 2 for carbonation depth plotted in FIG 23.

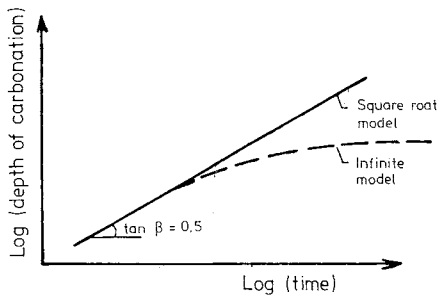

FIG 27. Using the square root model provides a value for the initiation time which is on the safe side. Since the infinite model gives a lower initiation time. The initiation times can even become infinitely long using the infinite model.

As an example of special conditions it can be noted that the CO_2 concentration in silos which contain grain can amount to 1%. This was observed in an investigation of a damage case in which the extremely deep carbonation was a direct result of a high CO_2 content in the surrounding air.

Bound CO_2 in carbonated concrete

At the request of the author, Peterson /1979/ developed a method for determining bound CO_2 in concrete.

In principle, this method is as follows:

- A concrete specimen is drilled or sawn out of the object which is to be tested.
- The depth of carbonation is determined with the aid of a phenolphtalein indicator.
- The specimen is dried in CO_2-free air at an increased temperature to avoid later carbonation.
- Thin layers were extracted from the specimen with the aid of a carbide-tipped tool.
- The chips were analyzed for calcium oxide and carbon dioxide.

See also the report published by Peterson /1979/.

In a preliminary investigation of two specimens which had been cured for 28 days in water and then conditioned in laboratory air to an age of about 500 days, the CO_2 bound in the concrete was measured. The specimens were of two qualities, one with a W/C ratio of 0.70 and the other with a W/C ratio of 0.41. The binder used was Slite Standard Portland cement.

The analysis results have been compiled in Table 3 where the ratio between the indicated quantity of carbon dioxide and calcium oxide has been calculated.

The calcium oxide content thus decreases with increases in depth for both concrete types. This applies to the first millimetres, which means that the cement paste content is greater at the surface.

Table 3. Measured quantity of CO_2 and CaO in chip milled from two concrete specimens.

Specimen	Layer mm from surface	CO_2 %	CaO %	Mol CO_2/Mol CaO
Concrete 25L	0- 1	10.6	15.8	0.855
W/C = 0.70	1- 2	7.6	12.0	0.807
Cement content	2- 3	6.9	11.2	0.785
= 250 kg/m^3	3- 4	6.0	9.1	0.840
Fluid	4- 5	5.1	8.1	0.802
consistence	5- 6	5.1	8.1	0.802
	6- 8	3.3	8.3	0.507
	8-10	1.2	8.3	0.184
	10-12	1.1	8.6	0.163
	12-14	0.9	9.2	0.125
	14-16	0.9	8.7	0.132
	Approx. 40	1.0	7.5	0.170
Concrete 50 T	0.0-0.5	12.9	22.6	0.727
W/C = 0.41	0.5-1.0	11.4	21.1	0.688
Cement content	1.0-1.5	9.7	18.8	0.657
= 500 kg/m^3	1.5-2.0	8.1	17.3	0.597
Semi-fluid	2.0-2.5	6.6	15.9	0.529
consistence	2.5-3.0	5.1	14.9	0.436
	3.0-3.5	3.9	13.7	0.363
	3.5-4.0	3.8	12.8	0.378
	Approx. 20	1.0	12.8	0.100

The phenophtalein limit for 25 L concrete was measured at 6-10 mm and for 50 T concrete at 2-5 mm.

The carbonation does not become complete (CO_2/CaO $\geq$1.0) even at the surface despite 500 days curing in air. For the 25 L concrete specimen, the CO_2/CaO ratios specified in Table 3 have been plotted in FIG 28. It can be seen there that the carbonation boundary is relatively sharp for this concrete despite the fact that it was cured in air. The boundary would probably have been even more marked if the carbonation front had

been more uniform. The theory that the reactions are almost completed before the process proceeds on its way into the concrete is not, consequently, upset. If the transition zone had been longer, where the phenolphtalein boundary only marked the end point of the carbonation front, it would have been necessary to replace and revise both the phenolphtalein test and the carbonation model.

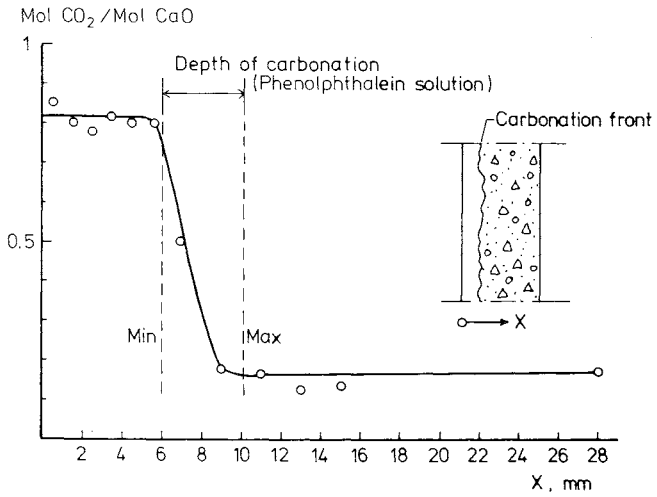

FIG 28. Measured CO_2/CaO in carbonated concrete designated 25 L concrete.

These experiments cannot, however, be used to show that the pH boundary is discontinuous. And this is not likely to be the case. Instead, the experiments have shown that the pH values jump from a low to a high level over a distance of a few millimetres.

The abovementioned experiments were repeated on specimens which had been cured in water for 7 days and then for 6 months in 50% relative humidity. The specimens were then placed in a climate chamber with 80% relative humidity and a raised CO_2 content, approximately 1% CO_2. The specimens were carbonated in the climate chamber for 3 months.

The concretes were cast at the same time as the corrosion cells in Series 4. The values of the concrete parameters are presented in Appendix 4. In

addition to studying Portland cement, the capacity of slag cement (65% slag plus 35% Portland) to bind CO_2 was also studied. The results are presented in FIG 29.

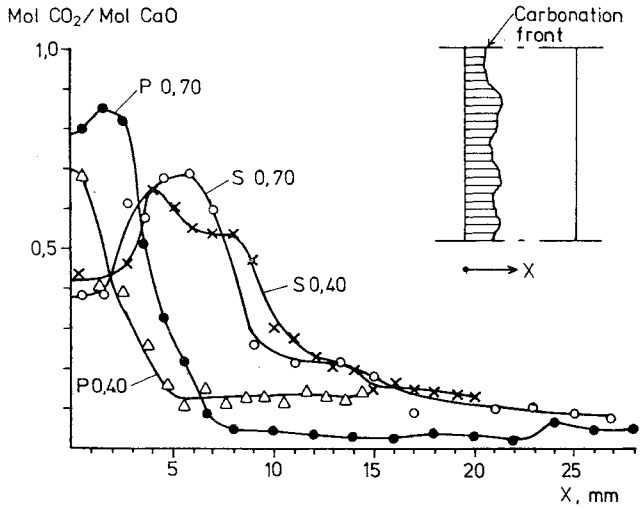

FIG 29. Bound quantity of CO_2 in carbonated concrete.
S = Slag cement
P = Portland cement
The figure indicates the W/C.

Phenolphtalein limits
P 0.70 = 3- 7 mm
P 0.40 = 1- 4 mm
S 0.70 = 7-15 mm
S 0.40 = 4-11 mm

The experiment with Portland cement shows a satifactory agreement with the first investigation. The slag cement specimen, on the other hand, proved to have a poorer storage capacity in the surface layer compared with the Portland cement specimens. Even further into the material, the slag cement does not achieve the same level of CO_2 binding as does the Portland cement.

One explanation for the surface effect may be the slower hydration of the slag cement and the fact that the surface layer has not had time to receive the same level of moisture curing as the concrete further in.

The CO_2/CaO ratio also indicates that the degree of binding is determined by the degree of hydration of the cement, in other words only hydrated cement participates in the absorption of CO_2. One can also logically assume that water reaches unhydrated cement much more easily than do the considerably less soluble CO_2 molecules.

When carbonation takes place the quantity of bound CO_2 can thus be set equal to the quantity of hydrated lime which occurs in each layer of concrete. Standard Portland cement contains about 65% CaO and the degree of hydration is roughly as indicated in Table 4 from one year to a considerable age.

Table 4. Approximate degree of hydration in Portland cement Byfors /1980/.

W/C	Degree of hydration %
0.4	60
0.6	70
0.8	80

The permeability of concrete vis-à-vis CO_2

A number of measurements of the effective diffusion coefficient, D_{eff}, for O_2 in concrete are presented in Chapter 5.1. The theory which says that the moisture content of the concrete is the determining parameter for D_{eff} was verified in the experiment. Consequently, the permeability parameter is also the most uncertain parameter when assessing the carbonation of concrete. Small changes in the moisture content give rise to major effects on the diffusion coefficient. Measurements with O_2 were carried out in the experiments. Major differences do, admittedly, exist between gases O_2 and CO_2 but since the moisture content of the concrete is the determinant parameter for CO_2 diffusion - as has previously been shown in this report for CO_2 and O_2 - a satisfactory relative measure should be obtained.

The effective diffusion coefficient for O_2 as a function of W/C and the moisture conditions are presented in FIGS 30 and 31.

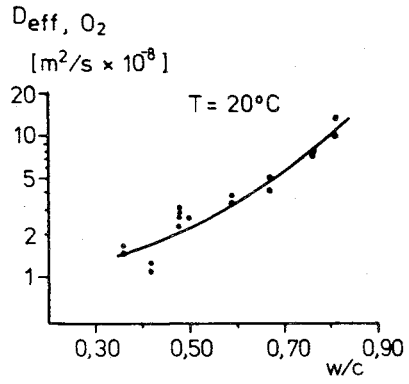

FIG 30 Measured effective diffusion coefficient for O_2 as a function of W/C. Cement type was Slite Portland cement. The measurement was carried out at 20°C and 50% RH. Specimen age approximately 1 year.

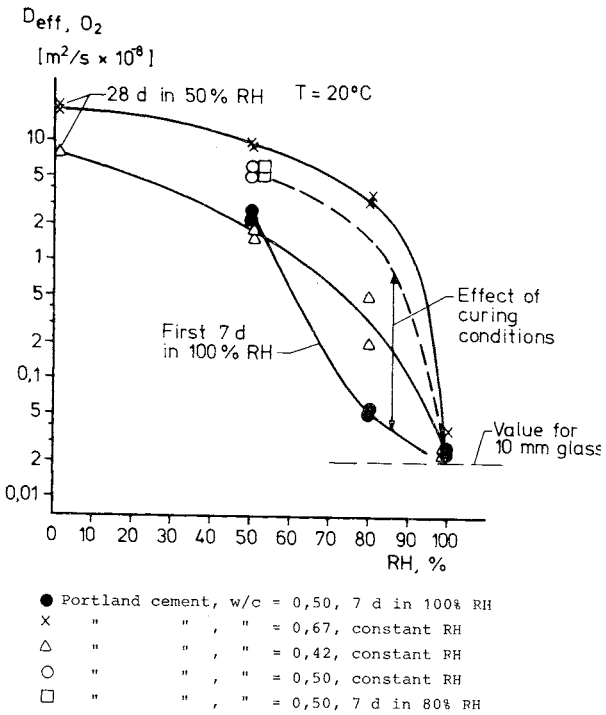

FIG 31 Measured effective diffusion coefficient for O_2 with varying conditioning and moisture state. Cement type was Slite Portland cement. The measurement was carried out at 20°C. Specimen age 6-12 months.

Changing the W/C ratio from 0.40 to 0.80 thus gives increased permeability by a factor of slightly less than 10, while changing the moisture content from 50% to 100% relative humidity in the specimen reduces the permeability by at least twice the power of 10. In a given environment, however, only the W/C ratio and the concrete cover can affect the time taken for the penetration of the carbonation front to the reinforcement.

Practical applications of the model

A theoretical evalution of, for example, the significance of the concrete cover for different concrete qualities is fully possible.

It should be noted that the values which are calculated here are not by any means absolute numbers but rather a comparison on a relative basis. The effective diffusion coefficients are not identical for O_2 and CO_2. The ratios should, on the other hand, be the same for fictitious values and real values.

The fictitious carbonation sequences are calculated for three concrete qualities:

1) W/C = 0.70. The water content is usually constant in concrete at a level of about 180-200 l/m^3.

   The water content is assumed to be 180 l/m^3 in all mixes. This gives the following input data in the calculations:

D_{eff} according to FIG 30	$= 6 \cdot 10^{-8}$ m^2/s
Cement content	$= 257$ kg/m^3
CaO (65%)	$= 2.98$ kmol CaO/m^3
Bound CO_2 (75%) according to Table 4	$= 2.24$ kmol CO_2/m^3

2) W/C = 0.50

Water content	$= 180$ l/m^3
D_{eff}	$= 2 \cdot 10^{-8}$ m^2/s
Cement content	$= 360$ kg/m^3
CaO (65%)	$= 4.18$ kmol CaO/m^3
Bound CO_2 (65%)	$= 2.72$ kmol CO_2/m^3

3) W/C = 0.36 - 0.40

Water content	= 180 l/m^3
D_{eff}	= $1.5 \cdot 10^{-8}$ m^2/s
Cement content	= 500 kg/m^3
CaO (65%)	= 5.80 kmol CaO/m^3
Bound CO_2 (60%)	= 3.48 kmol CO_2/m^3

The effective diffusivity is selected for the measured values at 50% RH from FIG 30. These values can also be related to approximately 80% RH, since the curve for W/C = 0.67 and 0.42 lie at about the same distance from each other at 50% RH and 80% RH respectively, see FIG 31.

The calculated carbonation sequences are presented in FIG 32.

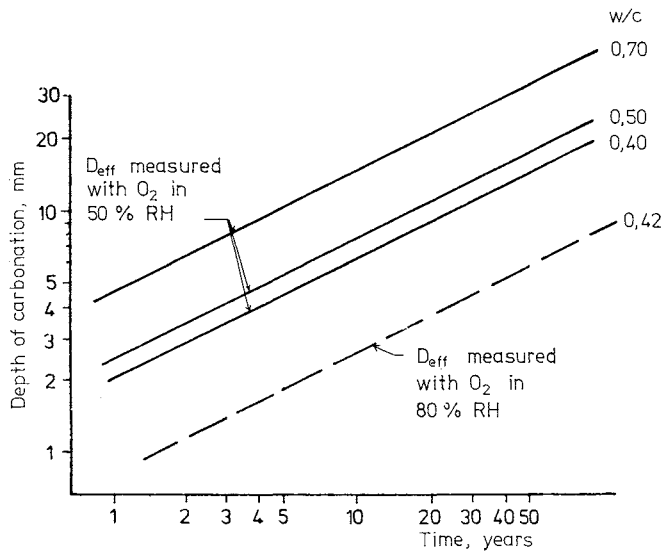

FIG 32. Calculated fictitious carbonation sequences for concrete with W/C = 0.70, 0.50 and 0.40 respectively at 50% RH and for W/C = 0.42 for 80% RH.

The result thus shows that if the concrete cover or initiation time is kept constant, the following relations are obtained between the three different concrete types:

	W/C=0.70	W/C=0.50	W/C=0.40
Constant cover			
ratio between initiation times	1.0	3.4	5.0
Constant initiation			
time cover required	1.00	0.53	0.40

A concrete structure with a cover of 25 mm and a W/C ratio of 0.70 thus has an equally long initiation time as a concrete structure with 25 x 0.40 = 10 mm cover and W/C = 0.40.

It should be noted that these values are on the safe side since we can assume that the denser concrete receives a greater addition of $Ca(OH)_2$ from the area in front of the carbonation front due to a pore system which is more saturated with water for the same relative humidity in the surroundings.

1:0.53:0.40 were the relations obtained in the theoretical processing for the required concrete cover when the W/C was 0.70:0.50:0.40. 1:0.68:0.45 were the relations obtained for the boundaries plotted in FIG 23 for concrete not exposed to rain and 1:0.82:0.44:0.34 were the corresponding ratios obtained for concrete exposed to rain when the W/C was the maximum of 0.75:0.65:0.55:0.45. For the measured carbonation depths, the difference then becomes somewhat larger between the different water-cement ratios.

On the other hand, these results have been obtained from a number of measurements and with an upper boundary which might, perhaps, have received a different position if more measurement results had been available for plotting.

It seems quite clear, however, that the practical values agree well with the theoretical reasoning which has been put forward. This can also be seen in FIG 33 where the theoretical line for W/C =0.42, 80% RH has been plotted amongst the practical results. The approximate size also appears to be correct for the theoretical value, since the curve falls outside the upper boundary amongst the plotted values. The distance between the water-cement ratio curve for the two groups (sheltered concrete and unsheltered

concrete) is approximately the same. This agrees with the results in FIG 31 where D_{eff} for O_2 was measured for concrete in different climates, in other words the distance between the curves is roughly constant if water curing is poor.

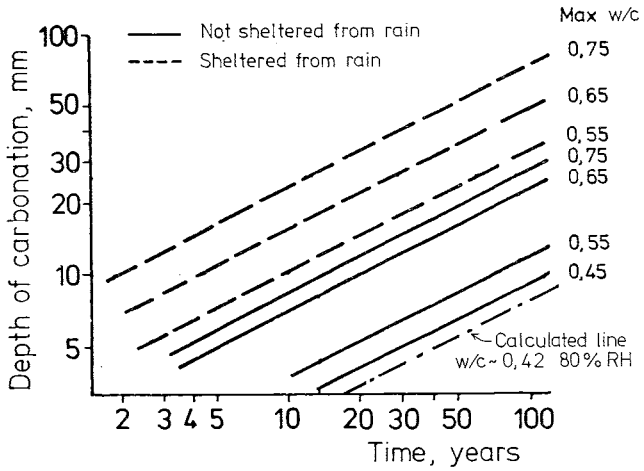

FIG 33. Upper bounding lines for measured mean carbonation depth in Portland cement concrete with varying W/C ratios and the theoretical line for W/C = 0.42, 80% RH.

In most cases it is, however, unpractical to attempt to calculate the precise carbonation sequence due to the large number of parameters which are difficult to determine and unreliable. Instead, guiding values can be obtained from FIG 23 where the surrounding environment has been broken down into outdoor structures sheltered against rain and outdoor structures not sheltered against rain.

As far as the difference in distance between the curves for W/C 0.65 and 0.55 for unsheltered concrete is concerned, we can note that the carbonation sequence is changed drastically around W/C = 0.60, see FIG 34. This is probably due to the fact that the continuous capillary pores are not capable of retaining contact with each other when their quantity and volume are reduced, in other words, in principle the same effect as that which gives concrete such permeable properties that the requirements for water thightness are fulfilled.

A more accurate assessment is, of course, fully possible but this would require a check of the CO_2 concentration and of the current moisture state in the atmosphere. The diffusivity would then be determined for the concrete in the same climate.

The absolutely most reliable calculation of the carbonation sequence can be carried out on structures which have been in use for at least 2 years. This is because the current carbonation depth is a summary parameter for all factors which effect the carbonation rate. The carbonation sequence can also be extrapolated since the mathematical relation follows the actual sequence sufficiently closely. In any case, the value obtained lies on the safe side. The estimated initiation time is shorter than the actual initiation time.

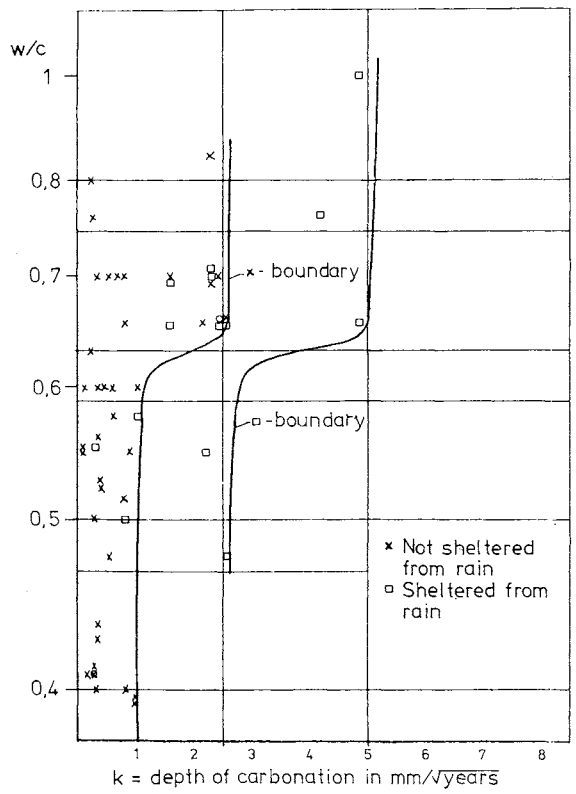

FIG 34

The relationship for the relative carbonation rate of Portland cement, the permeability of the concrete and the conditioning of the concrete. The calculations have been carried out with values from Forschungsinstitut der Zementindustrie des Vereins Deutschen Zementwerke e.v., Düsseldorf /1965/.

2.5.3 Chloride initiation

Model

When the corrosion process is initiated by an excessively high chloride concentration, the problem becomes more complicated. We are no longer dealing with a clearly separated front which penetrates the material, as is the case for carbonation initiation, but rather with a situation where the chloride concentration increases gradually if the surroundings contain chlorides with a greater concentration than that in the pore solution.

Chlorides can also be supplied to the concrete by adding $CaCl_2$ with the aim of accelerating the binding process.

It should, however, be noted that adding materials containing chlorides when manufacturing concrete always increases the risk of corrosion.

The corrosion process first begins when a certain chloride concentration has been reached around the steel. This concentration is called the threshold value hereinafter.

On the other hand, the threshold value is not a precise limit. Instead, the metal liberation increases with increases in the concentration. The passive state has changed over to a low-level active state with a uniform general corrosion. The general corrosion becomes particularly noticeable at very high OH^- concentrations since high chloride concentrations are not capable of giving rise to pitting. General corrosion leads to a dark oxide formation on the surface of the steel, see Chapter 5.5.3. This type of corrosion is, however, very slow and can in fact be compared with a passive state. The threshold value when the chloride concentration is so large that local corrosion occurs in the solution can, according to Hausmann /1977/, be approximated as follows:

$$\frac{c_{Cl^-}}{c_{OH^-}} = 0.61 \qquad \text{(concentration in equiv/l)}$$

Experiments carried out by the author and described in Chapter 5.5 have agreed well with the results obtained by Hausmann. It should, however, be noted that the experiments described in Chapter 5.5 were carried out

in a simulated pore solution and not only in a strongly basic solution. The threshold value is therefore dependent on the OH^- concentration. We can also assume that other negative ions have the same effect. Different ions always compete to obtain contact with the surface of the steel. The affinity of the ions or the substances with the surface of the steel and their corrosion-promoting or metal- liberating effect determine the concentration at which corrosion occurs at a given potential in the metals. If the potential (moisture state) is changed, the threshold value is also changed. The situation is thus highly complex. Consequently, I shall deal mainly here with what happens when the chloride concentration increases but the pore solution remains unchanged in other respects.

Experiments which have been carried out all over the world show a very wide distribution for the chloride concentrations which can be accepted in concrete. Construction activities in the Middle East and other hot climates, in particular, have entailed a tightening up of the requirements applied to the constituents in concrete. In Sweden and many other countries, mode rate chloride admixtures have been accepted in concrete during manufacture. Just above a level of 2% $CaCl_2$ per cement quantity has been found to constitute a critical limit for the initiation of the corrosion process. Consequently, the limit has been a maximum of 1.5% admixture of $CaCl_2$ per cement quantity. This will be discussed later and compared with the model which has been set up.

One complication in previous corrosion studies has been a lack of knowledge of which concentrations of different substances have surrounded the embedded steel. Chloride occurs in concrete in three different forms - chemically bound, physically adsorbed to the pore wall and as free chlorides, see FIG 35.

Equilibrium always prevails between the different phases, in other words if the concentration in the free phase is increased larger quantities are also fixed physically and chemically. Embedded steel is surrounded and influenced only by the free chloride ions in the pore solution. This means that the concentration of chlorides increases in the immediate surroundings of the reinforcement if the concrete dries, see FIG 36. On the other hand, the concentration of OH^-, which counteracts the initiation of corrosion, also increases when this happens. Furthermore, we can assume that when

an increase in concentration of this type occurs, chlorides are bound to a greater extent than is the case for the OH ions.

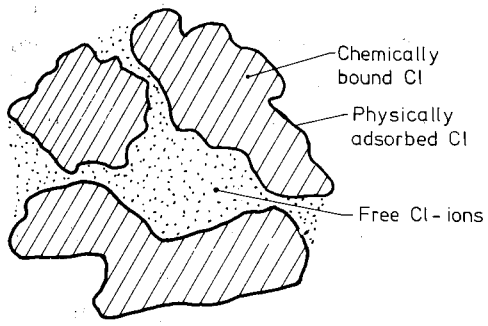

FIG 35. Chlorides occur in three different forms in concrete.

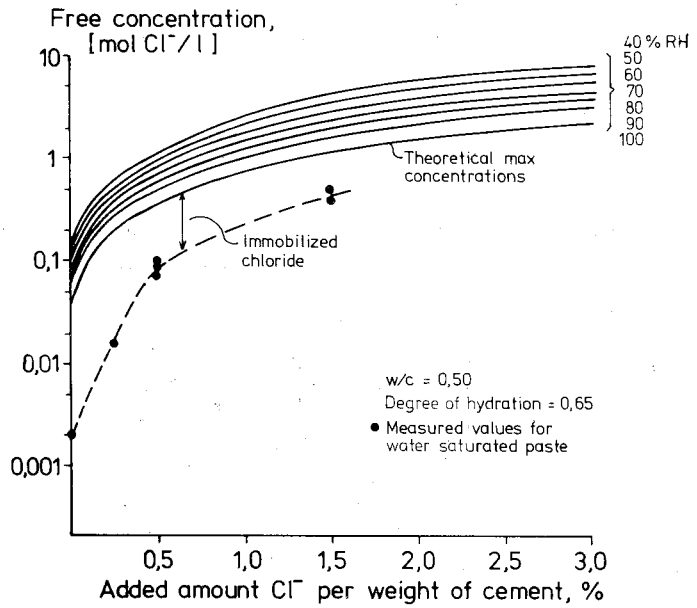

FIG 36. Chloride concentrations in paste as a function of the quantity added during manufacture.

Drying-out always entails an increased risk of corrosion, however, but this depends on the collaboration of other factors with the chlorides, for example local neutralization, higher O_2 consumption at the oxygen electrode which entails peaks and oscillations in the anode and cathode processes

which, in turn, can accumulate high chloride concentrations locally. A impermeable concrete prevents the chlorides from being transported rapidly between neighbouring areas.

Finally, one must also know how different substances are transported in concrete and the rates at which this takes place. The first approximation is always a transport controlled by diffusion. This gives a value which indicates the maximum values for the initiation periods. The problem is not, however, always confined to studying chloride penetration. Concrete which is completely submerged in water also undergoes a neutralisation as a result of the outward diffusion of OH^-. Alternative calculation methods must be used for these cases. Nor do pure diffusion sequences occur in practice but rather convective transports often take place in the concrete cover.

This applies, for example, to dried-out concrete which absorbs water through capillary action or for structures which are exposed to one-sided liquid pressure.

By way of summary, it can thus be said that the model must

- using the hydroxide concentration in the pore solution as a basis, calculate the threshold value for the free chloride content at which the corrosion process is initiated.

- calculate how rapidly the threshold value is reached for different transport mechanisms and varying surrounding chloride concentrations. The interdependency between free chloride and total chloride in the concrete must be mapped out in connection with this.

Hydroxide concentration in pore solution

In Portland cement concrete the pore solution has a high OH^- concentration. The concentration is determined for the most part by the cement's content of Na and K and by the concrete's liquid content. Concrete made with Slite Portland cement with W/C = 0.4 - 0.6 has a free OH^- concentration of 1.0-0.3 equiv/l according to Chapters 5.4.4 and 5.5.4. Note that the highest concentration applies to the lowest W/C. The relevant OH^-

concentration can be calculated or measured. The above values have been both theoretically calculated and measured for a pore solution which was pressed out of pastes and mortar.

If the K and Na contents of the cement are known, and if the concrete constituents are known, the concentration in the pore solution can be calculated as follows:

Assume that all Na and K are dissolved.

$$C_{OH^-} = \frac{\frac{C \cdot (Na)}{23} + \frac{C \cdot (K)}{39}}{p} \cdot 100$$

c_{OH^-} = OH^- concentration in equiv/l
C = cement content kg/m^3
(Na), (K) = weight share Na and K respectively in cement
p = porosity of the concrete in % by volume

where p can be calculated according to Bergström /1967/.

$$p = \frac{C}{10} (W/C - 0.19\ \alpha) + l_o$$

W/C = water-cement ratio
α = degree of hydration, see Table 4
l_o = air content of fresh concrete

Leaching out or pressing out pore solution and then carrying out titration with regard to OH^- is another method for determining the OH^- concentration.

Threshold values for chloride

The preceding section showed that the pore solution which occurs in concrete has a high concentration of hydroxide ions. The experiments which were carried out with the aim of determining the threshold values which initiate the corrosion process were all executed in simulated pore solutions, see Hausmann /1967/, Gouda /1970/ and Chapter 5.5. The environment in concrete must be less corrosive than a purely liquid environment.

The following relation can be used (see FIG 37) until better values have been produced from experiments in concrete and the interdependency between the free hydroxide and chloride concentrations and other factors have been mapped out.

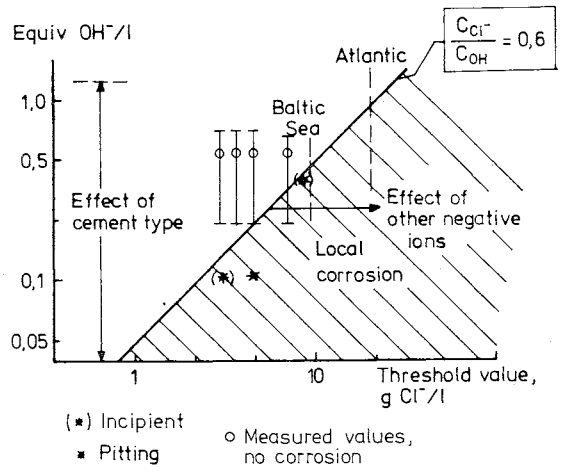

FIG 37. Relation between hydroxyl concentration and threshold value for chloride concentration. Four values from practical measurements have been plotted in the figure. The corrosion process was not initiated in these cases. The values are, however, fairly uncertain since the free chloride concentration has been calculated from the measured total cloride content. The value of the constant k_d (relation between free chloride and bound chloride according to Chapter 5.4) has been assumed to be 0.7. The possible variation range for the theoretically calculated OH concentration has been indicated.

It has also been shown that other negative ions can affect the threshold values in both a negative and positive direction. If other corrosion-initiating substances occur in the concrete, FIG 37 cannot be used directly, see Thorsén /1979/, where bromides and sulphides in larger quantities than normal cause the initiation of corrosion.

Relation between free and bound chloride

Extensive experiments have been carried out in which the chloride concentration has been studied as a function of the total chloride content, see Chapter 5.4. The measurements were made on a pore solution which had

been pressed out of concrete for free chloride and on solid specimens where the chloride quantity was determined in relation to the cement content.

A high chloride concentration was obtained in mortar and paste specimens through direct admixture during casting, capillary absorption and the diffusion process respectively.

A higher degree of binding could be noted for a slow penetration of chlorides than was the case for rapid transports. The relation between free chloride in a pore solution (g/l) and bound chloride per cement weight (gCl^-/kgC), the factor k_d, amounted to about 0.7 for mortar specimens with a W/C ratio between 0.40 and 0.60, see FIGS 38 and 39.

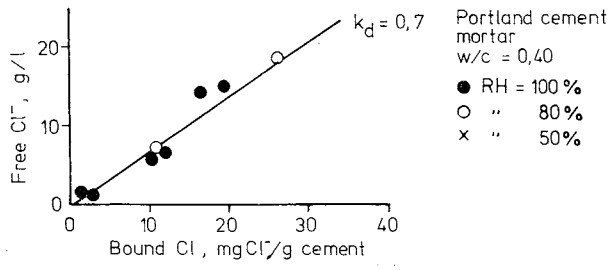

FIG 38. Measured free chloride concentration as a function of bound chloride per weight unit cement.

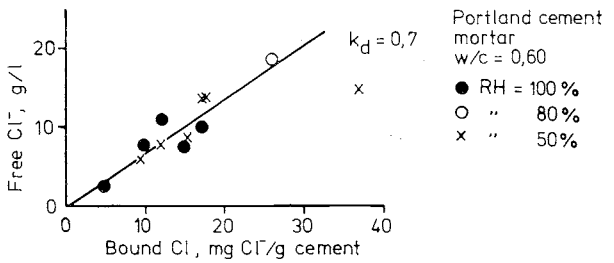

FIG 39. Measured free chloride concentration as a function of bound chloride per weight unit cement.

The degree of binding measured in cement paste was not as high as in mortar specimens, see FIGS 40 and 41.

For the case involving a lengthy exposure time in which chlorides diffuse into the concrete, the same values were obtained for k_d as for the case in which $CaCl_2$ was mixed directly into the concrete, see FIGS 40-42. The type of salt involved, on the other hand, was of major significance for the amount which was fixed in the structure and the pore walls, see FIG 42.

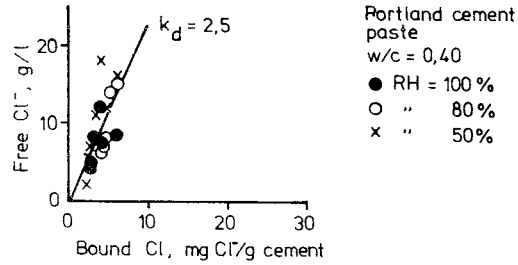

FIG 40. Measured free chloride concentration as a function of bound chloride per weight unit cement.

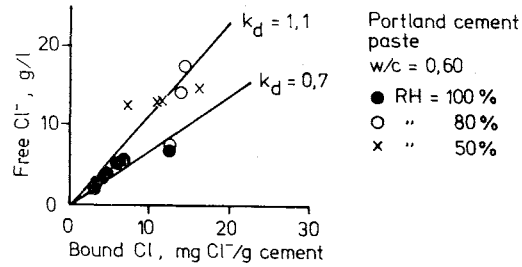

FIG 41. Measured free chloride concentration as a function of bound chloride per weight unit cement.

The free chloride concentrations in concretes can thus be approximated with the aid of the factor k_d.

$$k_d = \frac{c_{free} \cdot 10^{-4}}{\frac{c_{bound}}{c_{tot}} \cdot c_{\%}}$$

where c_{tot} = c_{bound} + c_{free}
c_{bound} = bound chloride (mg/l)
c_{free} = free chloride in pore solution (mg/l)
$c_{\%}$ = chloride content in % of cement weight

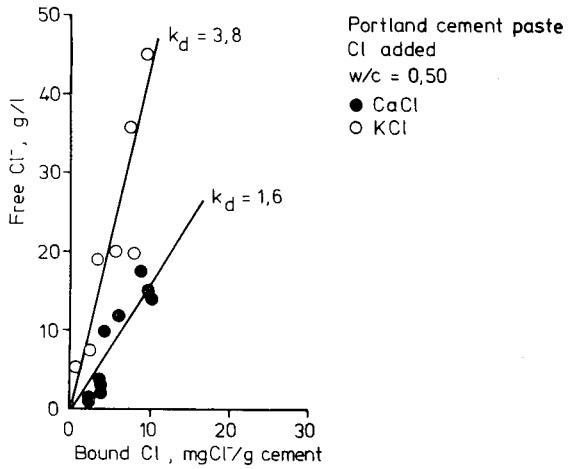

FIG 42. Measured free chloride concentration as a function of bound chloride per weight unit cement.

Porosity determination and dilution can be dealt with in the same way as has previously been presented for OH^- concentrations.

For cases involving slow transports and in which chloride is mixed with the concrete, the value for k_d can be set to 0.7 for Slite Portland cement. In the case of convective transports the concentrations should be analysed.

An important consequence of the results which have been obtained is that the cement content is by no means of subordinate significance for the initiation process, when a concrete structure is exposed to external chloride effects. A higher cement content without any doubt provides the concrete with a better capacity for binding the chlorides. The cement content has no significance, however, in cases where the chlorides are added to the concrete during manufacture and reach the same procentage Cl^-/cement content.

Effective diffusion coefficients for OH^- and Cl^-

The penetration of chloride ions in concrete can occur with varying rates. Dry concretes which are exposed to liquids absorb the liquid through capillary action. This transport takes place at considerable speed. The chlorides do not, however, have the same rate of penetration as does water. Instead, a certain time lag, which results from physical and chemical binding, entails a lower rate of penetration, see Table 5.

Table 5. Relation between chloride penetration and water penetration for mortar specimens of varying quality, see Chapter 5.4.6.

	Cl^- : H_2O penetration
Portland cement W/C = 0.4	1:3
Slag* cement W/C = 0.6	1:3
Slag* cement W/C = 0.4	1:6

* (30% Portland + 70% slag)

In concrete which is completely saturated in water, the transport occurs only as a result of differences in concentrations. This is the slowest of all transport mechanisms. Between the two extreme cases capillary suction and diffusion, other modes of transport occur which are a combination of pure transport mechanisms such as diffusion, non-stationary conditions as a result of drying out, chemical constriction and capillary flow.

Furthermore, it is not just the chloride transports which are significant for the initiation of corrosion - the hydroxide transports must also be taken into consideration. With the aid of the experimental results presented in Chapter 5.4 we can allocate the values specified in Table 6 to the effective diffusion coefficient.

Note that transport systems other than diffusion must be dealt with in a different manner and that we can always assume that the quantity of penetrated chloride is a function of the quantity of water which has flowed through or penetrated the concrete.

Table 6. Estimated effective diffusion coefficient from measured free chloride and hydroxide concentrations in water, see Chapter 5.4. Slite Portland cement was used in the experiment.

W/C	D_{eff} ($m^2/s \cdot 10^{-12}$)	
	Cl^-	OH^-
0.40	0.8-5	6-10
0.60	4-12	10-30

Practical applications of the model

The range for the threshold values for chloride concentrations specified in the literature varies from 30 ppm for experiments in weak basic solutions up to 2-3% $CaCl_2$ admixture when manufacturing concrete see, for example, Bergström and Holst /1960/, Roberts /1970/. How do these results agree with FIG 37?

The following principles can be adopted to limit the experimental variables previously used in corrosion investigations involving the direct admixture of chloride.

- The W/C can be assumed to vary between 0.5 and 0.7.

- The cement content can be assumed to vary between 250-350 kg/m^3. An accelerator has not normally been required for higher cement contents.

- The cement can have contained a large or a small quantity of the substances Na_2O and K_2O which determine the OH^- concentration in the pore solution. Assume two cement types for extreme cases.
  Low-alkaline cement $Na_2O = 0.1\%$ $K_2O = 0.5\%$
  High-alkaline cement $Na_2O = 0.2\%$ $K_2O = 1.5\%$

- In the Swedish concrete regulations, 1.5% $CaCl_2$/cement weight has been regarded as harmless, at least in concrete which does not later come in contact with chlorides.

- Corrosion initiation can be considered to occur directly when the steel comes in contact with the fresh concrete. Both the chlorides and the alkali can then be assumed, as an approximation, to be completely dissolved in the mixing water. The quantity of water in concrete is normally 180 l/m^3.

- Corrosion initiation can also be considered to occur after a certain period of time when the pore system has developed and when the porosity determines the maximum degree of dilution. In this case, the factor k_d can be allocated a value 0.7.

Against this background, the results presented in Table 7 were obtained.

Table 7 Calculated threshold values when the relation in FIG 37 was used and for a number of different assumptions.

Cement content (kg/m^3)	260	360
Water content (l/m^3)	180	180
W/C	0.7	0.5
Chloride content in mixing water at 1.5% $CaCl_2$/C (g/l)	14	19
Calculated threshold value for direct initiation (g/l)		
low-alkaline cement	4	6
high-alkaline cement	12	17
Calculated threshold value when k_d = 0.7 (% $CaCl_2$/cement content)		
Low-alkaline cement	1.6	2.1
High-alkaline cement	4.3	5.7

The results concerning possible threshold values thus show an extremely good agreement with the practical experiences which have been reported. It does not seem likely that the chlorides added in moderate quantities during concrete manufacture directly cause a corrosion attack. A certain time is normally required before the attack starts, see Gouda /1970/ and

Chapter 5.5. If, on the other hand, initiation takes place immediately the risk is greatest at the beginning since small chloride quantites have been bound. The threshold values will lie around a level of 1.6-5.7% $CaCl_2$/ /cement content if we assume that the degree of binding k_d = 0.7. The cement type is extremely important in this model.

The relation in FIG 37 thus constitutes a good approximation of the threshold values for the initiation of the corrosion process in the concrete.

In recent years the permissible chloride content in concrete has, however, been reduced in most countries. One reason for this is the large number of concrete structures in recent years which have been damaged as a result of corroding reinforcement. This applies in particular to those cases in which considerable quantities of chloride were added to the concrete during manufacture.

The storage capacity of the concrete has, in these cases, already been utilized to a considerable extent directly after casting. Furthermore, the environment in the concrete cover changes with increases in age. The carbonation process occurs even if chloride has been added to the constituents during the mixing. Carbonating concrete does not have at all the same capacity for binding chlorides as does non-carbonated concrete, see FIG 43. This means that the equilibrium which occurs between the free chloride and bound chloride is displaced so that the free chloride increases in the pore solution. In a concrete which was homogeneous from the beginning, a difference in concentration is gradually built up for the chlorides with the greatest concentration at the surface. The difference in concentration leads to a diffusion process. In popular terms one might say that the carbonation process ploughs the chlorides into the concrete. A chloride level at the reinforcement which was acceptable from the beginning can thus become too high before the carbonation front reaches the reinforcement. In these cases initiation takes place very rapidly as a single crack or void which is carbonated leads to an attack. The corrosion process cannot be stopped once this has occured since the corrosion flows have transported chlorides to the anodes. The concentration of chlorides thus increases within the zones which corrode.

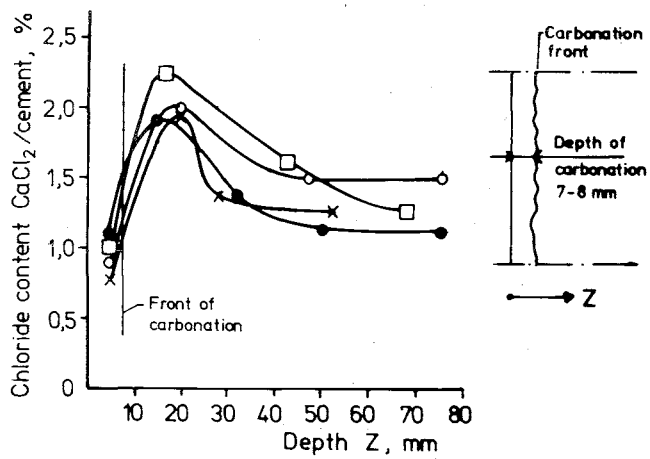

FIG 43. Measured chloride concentration in partly carbonated concrete. The original chloride admixture was 1-1.5% $CaCl_2$/cement quantity.

Since all the parameters in the model are now known for chloride initiation, the length of the initiation periods can be calculated in the same way as was used for the carbonation case. A number of boundaries are presented in FIG 44 to provide readers with an idea of the periods of time involved.

Note that an iterative procedure must be applied if OH^- is also to have a possibility of diffusing out of the concrete. FIG 45 can be used as a need for calculating concentration profiles at different times. The effective diffusivity is obtained from Table 6. Fick's diffusion equation is used in other respects:

$$\frac{\partial c}{\partial t} = D_{eff} \frac{\partial^2 c}{\partial x^2}$$

It can be seen from FIG 44 that the chloride concentration which gives rise to corrosion is reached very rapidly even in good concrete. An initiation in chloride environments normally occurs within a period of 10 years. This has also been confirmed by the measurements which the author carried out with corrosion cells, see Chapter 5.2.3. For a concrete with W/C = 0.32 and a compressive strength around 75 MPa, corrosion attacks began within a period of four years with normal concrete covers. The

practical "experiments" carried out in the USA also confirmed this. Bridges with low W/C values and a concrete cover of 100 mm have been damaged within a period of 20-30 years and extremely expensive repairs are now required. It can thus be seen that reality and theory do not give conflicting results.

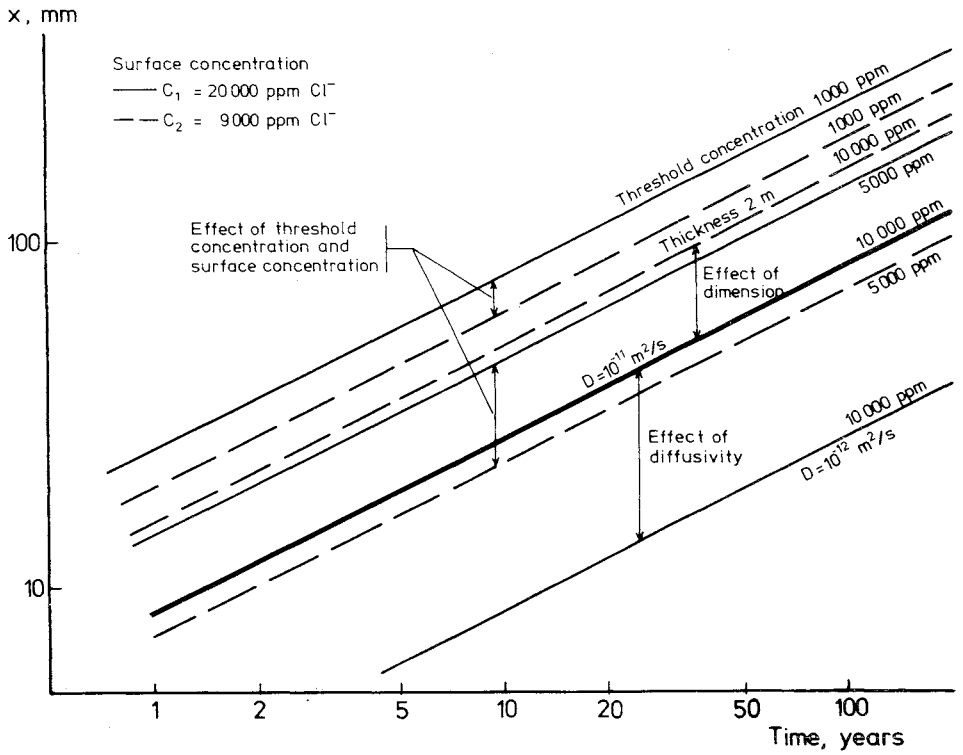

FIG 44. Calculated initiation times for chloride penetration. The effect of the concrete cover, x, the threshold concentration, C, and the permeability of the material, D_{eff} are presented in the figure. Compare D_{eff} in Table 6.

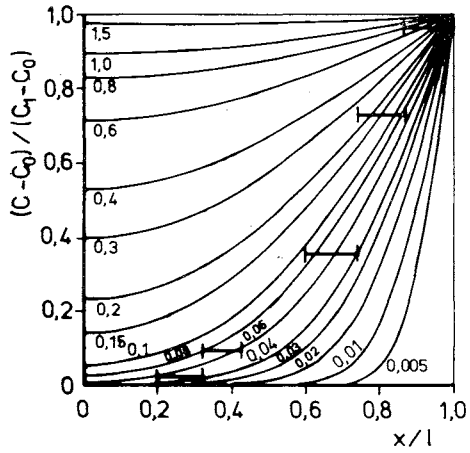

FIG 45. Concentration profile for varying times in one dimension
c = concentration at various depths and varying times
c_o = original concentration
c_1 = surface concentration
l = diffusion length
t = time
The numbers on the curve indicate $D_{eff}\ t/l^2$

2.6 Propagation

2.6.1 Model

Steel in concrete has both physical and electro-chemical protection. The physical effect limits the mobility of various substances around the metal and prevents the penetration of various substances through the concrete. Consequently, the corrosion condition becomes simpler than is the case for atmospheric corrosion of steel where all the substances which occur in the air, such as solid particles, solutions and gases, are in contact with the metal surface. The atmospheric general corrosion on freely exposed steel has a rate of 50-100 µm/year. We can therefore assume that the corrosion of steel in concrete should be on roughly the same level, in other words, 20-200 µm/year.

The electrochemical effect is favourable for steel due to the high hydroxide concentration which occurs in the pore solution in the concrete - as distinct from other metals such as aluminium which corrode at a very high

rate in solutions with high pH values. On the other hand, steel in large local defects in the concrete, such as large water-filled cracks or steel protruding from concrete, has very high rate of local corrosion as a result of galvanic effect.

Certain substances must be transported to the corrosion area if this type of electro-chemical process is to proceed. Furthermore, an electron exchange and certain local movements of substances between the electrodes and around the electrodes respectively also occur. The following factors affect the mean corrosion rate of steel after initiation.

- the chemical composition of the liquid which surrounds the steel, this can be decisive for the rate of liberation.
- the conductivity of the electrolyte, which determines the contact between the anodic and cathodic areas.
- the O_2 supply, which is required if the cathode reaction is to proceed.
- the temperature, which affects the solubility of various substances such as O_2 and the mobility of the substances which participate in the corrosion process.

Numerous other factors have been mentioned in the literature as controlling corrosion but these are often factors which either directly or indirectly control the above primary factors or vice versa. It can, however, be suitable to make use of the indirect variables due to existing measurement technology or due to their clearly established interdependencies with the primary parameters etc.

A number of factors which often occur in the literature are listed below together with a description of their effect on the corrosion process.

- The moisture content in the finely porous material which surrounds the steel expressed with the relative humidity in the pore system. The relative humidity is a measure of the quantity of electrolyte in the pore system. The quantity of liquid is, in turn, a measure of the permeability of the material against gases according to the line of reasoning previously presented in Chapter 2.5.2.

- The chemical composition of the material which surrounds the steel expressed with the cement type controls the corrosion process with regard to promoting local or general corrosion. The chemical composition of the material also determines the composition of the pore solution to a considerable extent. The hygroscopicity of the material is also dependent on which salts are dissolved in the pore solution. The hygroscopicity affects the quantity of liquid etc.

- The porosity of the concrete is mainly a physical factor which affects the mobility of water and substances around the steel. A less permeable matrix gives, for example, a lower effective diffusion coefficient for O_2. The conductivity is not, on the other hand, markedly influenced by the W/C ratio, the porosity, see FIG 46.

- Like the porosity, the concrete cover for reinforcement is a physical factor. A thicker concrete cover reduces the penetration of O_2 to the cathode.

- Potential differences which have been measured along the reinforcement constitute an expression for the variations of the other factors along the metal. The supply of O_2 can be higher locally, thus giving rise to a change in potential. Concentration differences in chloride, hydroxide etc. affect the potentials.

- The chloride content is a factor in the chemical composition. The chloride content in concrete does admittedly affect the conductivity of the electrolyte but this is no more than marginal. The chlorides have their primary significance in the initiation sequence. During the propagation stage, they control the corrosion process, however, so that the attacks are concentrated to smaller areas. The mean corrosion is still dependent on the supply of O_2 but the pitting effect of the chloride gives a high corrosion rate locally. The rate of corrosion therefore increases with an increase in the chloride content.

- Temperature variations can give rise to other effects besides directly influencing the rate of corrosion. If rapid temperature switches take place in the ambient air, water can condense on the surface of the concrete and thus change the moisture content of the material.

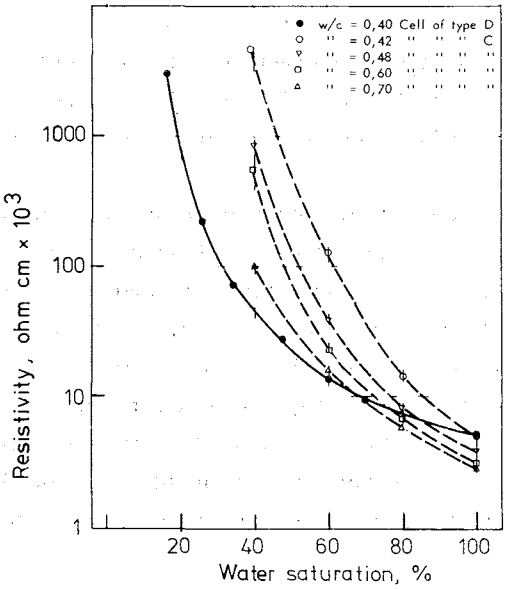

FIG 46. Effect of water saturation on the resitivity. Gjörv et al /1977/.

It can be seen from the above list that certain factors are constant during the corrosion sequence while others vary with time. The environment around the steel is a factor of primary importance. Structures which have been exposed to chlorides receive a constantly increasing chloride concentration closest to the steel until a state of equilibrium is reached. Local corrosion occurs at a certain concentration according to the line of reasoning previously presented. From this time onwards, the concentration increases particularly within the anodic areas, partly as a result of penetrating chlorides and partly as a result of a redistribution of chlorides through the corrosion flows which occur. An increase in chloride concentration thus entails an increase in the rate of corrosion.

The corrosion areas do not have the same shape throughout the entire corrosion period. For a constant moisture content in the concrete and a chloride-initiated corrosion, the chloride concentration gradually increases at the anodes until the concentration of chlorides is so high that a diffusion transport in the other direction bridges over the effect of the corro-

sion potential. When this occurs, the anodic area is extended through a local extension or through the occurrence of new anodes.

If the corrosion process is assumed to proceed while the relative humidity is decreasing, the mean distance between the anodic and cathodic areas first decreases and new anodes are formed. The attacks then become similar to the general corrosion which carbonated concrete gives rise to.

Nor is the corrosion rate constant during the propogation stage even if the environment around the steel is not changed. This is because the corrosion products are extremely impermeable and form diffusion barriers which lead to a reduction in the rate of corrosion with time, see FIGS 47 and 48. The corrosion products first formed are also exposed to a stress when new corrosion products are formed. One type of rust, magnatite, is a material which is not as tough as steel. Consequently, the rust deposit on the steel will crack and the diffusion barrier will be unable to grow infinitely. We can therefore assume that the corrosion rate is practically constant after a few years.

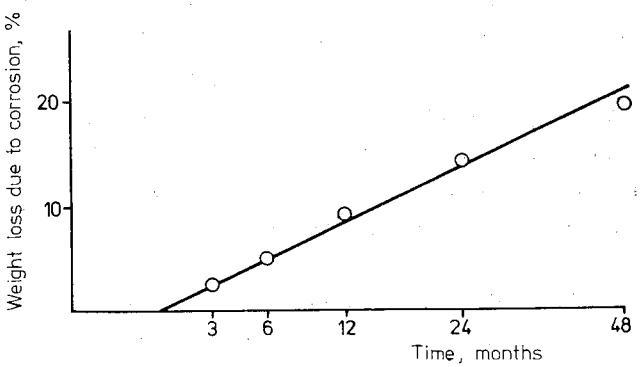

FIG 47. Maximum corroded quantity as a function of the time. Initiation has occurred as a result of mixing chlorides when manufacturing the specimens. Shalon and Raphael /1959/.

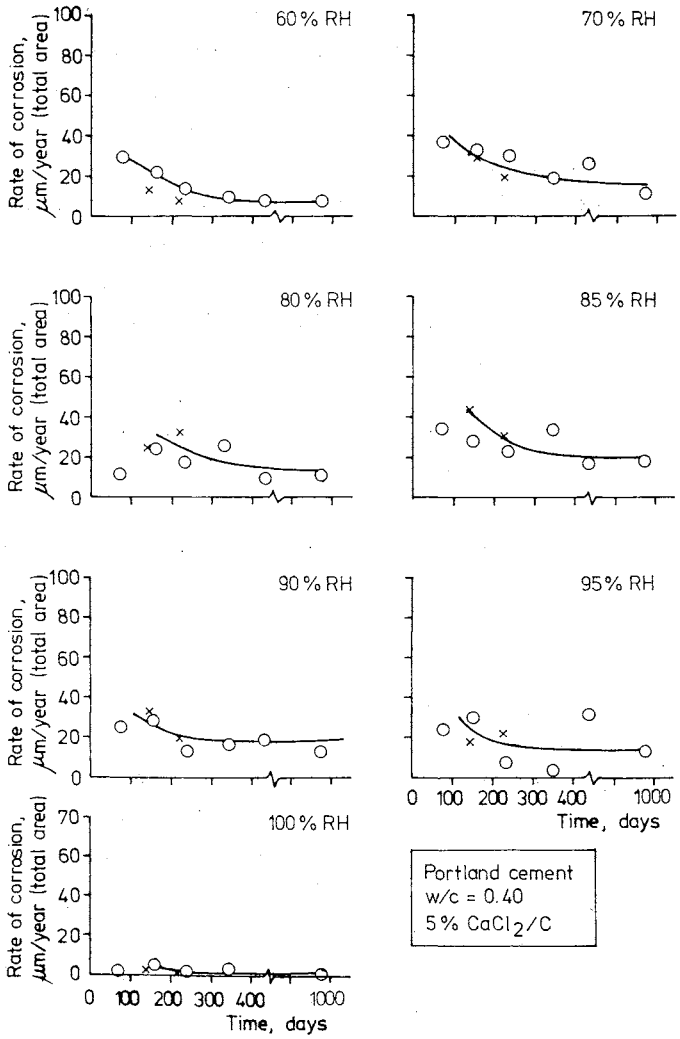

FIG 48. Measured rate of corrosion as a function of the time for different relative humidities according to Chapter 5.3.

The corrosion rate in the propagation stage can suitably be described by means of the following parameters:

- the relative humidity in the pore system which effects both the electrolyte and the supply of O_2
- the mean temperature for the structure.

The initiation mechanism and the effect of the chemical composition is taken into consideration by means of various relations between these factors and the rate of corrosion.

A review of the literature shows that very few studies have been devoted to the propagation stage. Efforts have mainly been concentrated on the initiation processes and on investigating the status of the structure in damage cases. Because of this, the author studied the propagation stage partly with the aid of a type of cell and partly with conventional weight loss measurement, see Chapter 5.2 and 5.3.

2.6.2 The conductivity of the concrete and the O_2 diffusion coefficient as a function of the relative humidity

The resistivity of the concrete is effected no more than very moderately by the thickness of the sample, the W/C value and the chloride content according to Gjörv et al /1977/.

The resistivity of the concrete is changed by a factor of 2 when the W/C ratio is changed from 0.70 to 0.40 and when the chloride content is changed from 0 to 4% $CaCl_2$ per cement quantity, see FIGS 49 and 50. The reason for the limited influence of these factors is the excellent conductivity of the alkali hydroxides. A small contribution of chlorides has no major effect.

If, on the other hand, the material is dried the conductivity is changed by several times the power of 10 for a change from 100% to 50% relatively humidity. This effect can be seen in FIG 51 which is a processing of FIG 46.

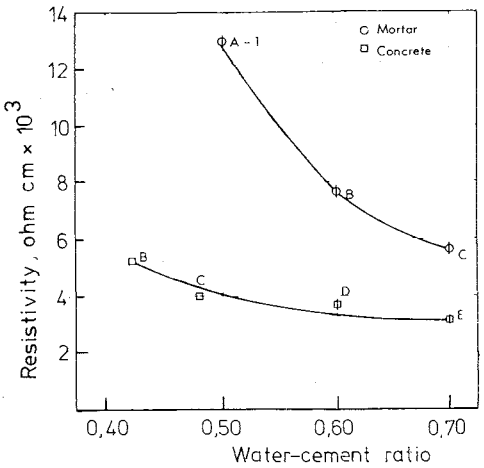

FIG 49. Effect of water-cement ratio on the resistivity. Gjörv et al/1977/.

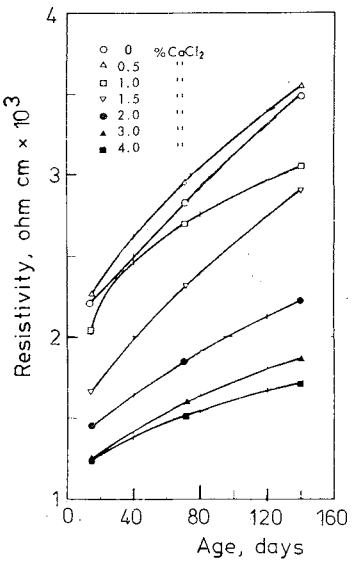

FIG 50. Effect of hydration on the resistivity. Gjörv et al /1977/.

The impermeability of the concrete against O_2 increases with increases in the relative humidity according to FIG 31 which has previously been presented. The cathode process, which consumes oxygen, can be a limiting factor in certain cases. If we assume that the O_2 which reaches the rein-

forcement is consumed and that the diffusion sequence takes place in one dimension, then $D_{eff,\ O2} = 10^{-8}$ m^2/s and given a concrete thickness of 20 mm, corresponds to a rate of corrosion of 750 µm Fe/year. The corrosion product has been assumed to be Fe_3O_4, which has been seen to occur in many damage cases.

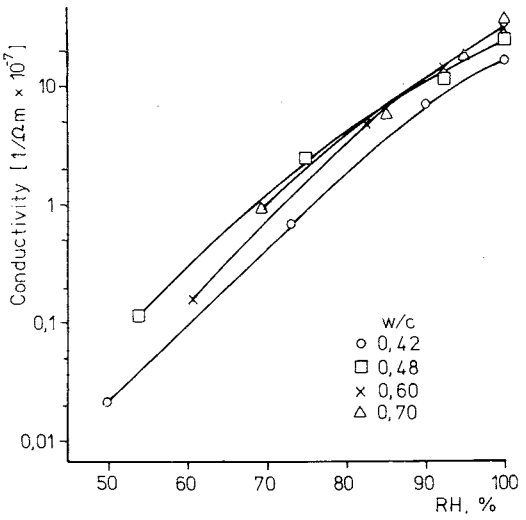

FIG 51. Numbers from FIG 46 converted with the conductivity expressed as a function of the relative humidity. FIG 14 was used when converting the moisture content to relative humidity. The moisture in the specimen was assumed to be homogeneously distributed.

The conductivity of the concrete and the effective diffusion coefficient for O_2 in concrete have been compiled in FIG 52. When the relative humidity increases, these two factors have opposite effects on the rate of corrosion. The gas impermeability has a limiting affect while the conductivity stimulates the corrosion process. The cathodic control will not, consequently, become noticeable until the diffusion coefficient falls below a value of $0.3 \cdot 10^{-8}$ m^2/s and the corrosion rate is a maximum of about 200 µm/year. In the case of high W/C values, a limitation then takes place at relative humidities in excess of about 95% while the value becomes about 90% for low W/C ratios.

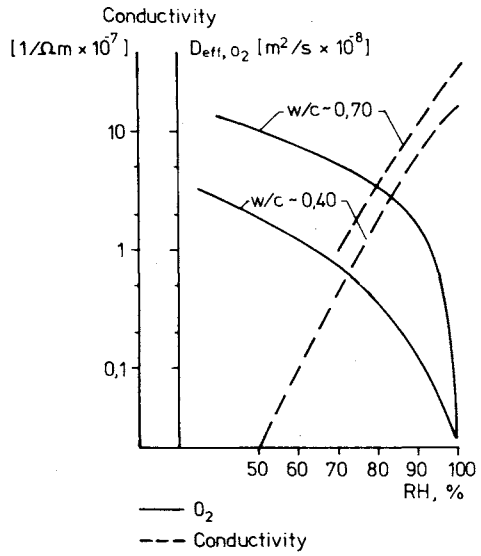

FIG 52. Compilation of effective diffusion coefficient and conductivity and their relation to the relative humidity.

It should be noted that the corrosion rate which occurs for the moisture contents mentioned above is by no means directly proportional to the conductivity of the electrolyte. Improved conductivity does, on the other hand, improve the possibility for the electrodes to function.

2.6.3 Rate of corrosion - laboratory experiment

Corrosion cells

A type of corrosion cell has been developed at the Swedish Corrosion Institute in Stockholm, see Kucera and Collin /1977/. This type of cell has been used in the author's investigations in which it was cast in concrete, see Chapter 5.2.

The method is based on casting steel electrodes in concrete closely adjacent to each other. Half of these steel electrodes are given a very slightly higher potential than the other half. The current which passes between the electrodes is then recorded and an increase in current indi-

cates either that the resistivity has decreased and/or that the rate of corrosion has increased.

The results obtained with these cells indicated the initiation time by means of a marked increase in current. They also provided an idea of the relative corrosion rate for variations in the environmental and concrete parameters, see FIGS 53 and 54.

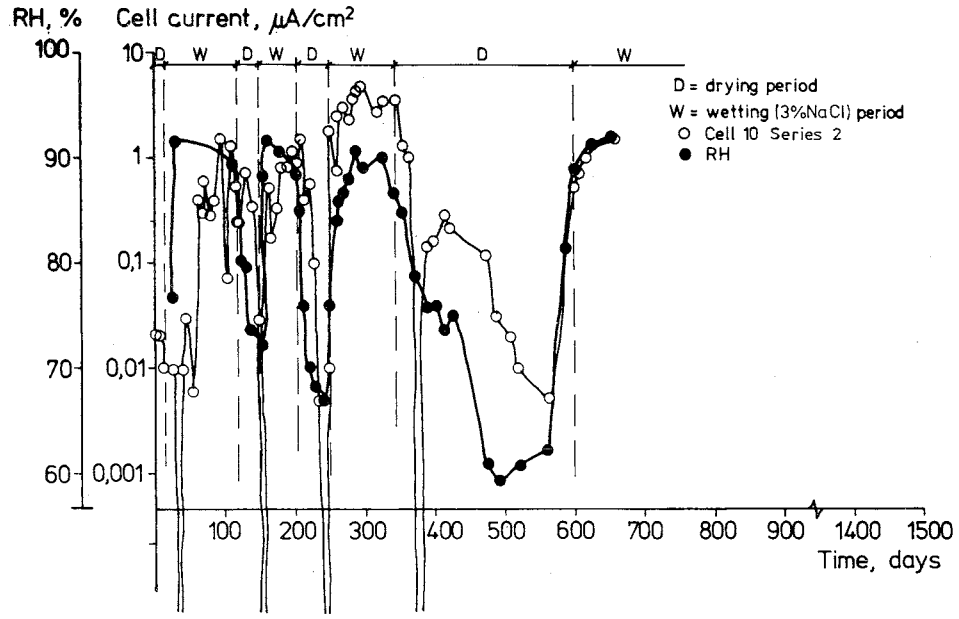

FIG 53. Cell current and relative humidity as a function of exposure time.

FIG 53 presents a cell current as a function of the time when the specimen was alternately moistened in 3% NaCl solution and dried in air. It is not possible to make a direct conversion of the cell currents to loss of steel through corrosion. It is not certain that all corrosion current was recorded. Studies of freely exposed cells in air gave currents which were approximately 10-15% of the actual rate of corrosion. The concrete environment should, however, provide a better effect, particularly for high moisture levels. According to Columb's law, 1 $\mu A/cm^2$ corresponds to 12 μm Fe/year if the corrosion occurs uniformly over the anode.

If we assume that a cell current is equal to the rate of corrosion, the specimen in FIG 53 would have a maximum corrosion rate of 60 µm/year which would decrease by several times the power of 10 during drying out. The cell current follows the relative humidity quite closely. Generally speaking, we can say that when the cells exceeded 1 $\mu A/cm^2$ we can feel convinced that the corrosion process had been initiated and that the rate of corrosion was considerable.

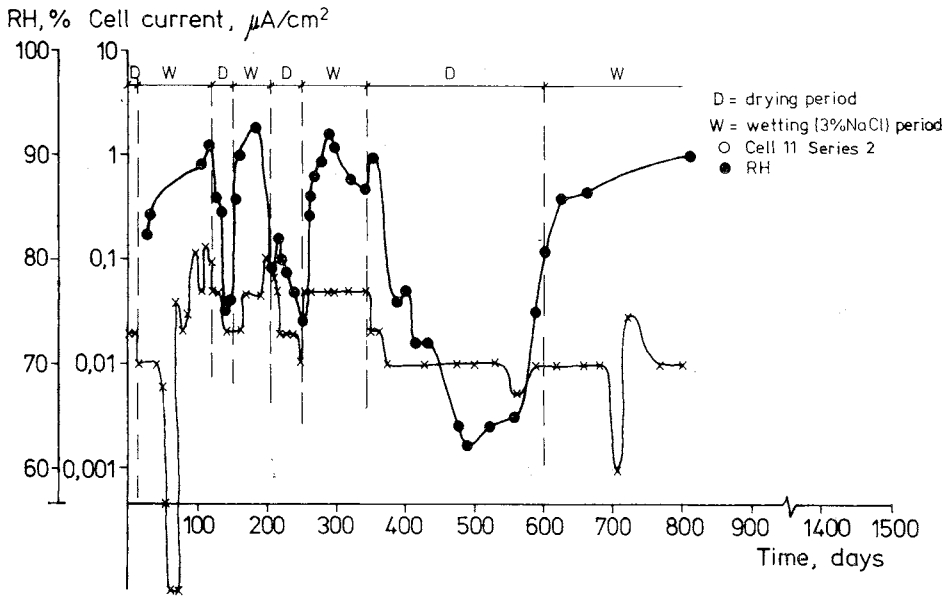

FIG 54. Cell current and relative humidity as a function of exposure time.

FIG 54 presents another specimen in which the concrete cover was increased from 5 mm, which was the concrete cover used in the specimen in FIG 53, to about 15 mm. Apart from that, the specimen was treated in the same way as the specimen in FIG 53. The cell currents are low and do not follow the curve for the relative humidity at all. No noteworthy corrosion is considered to be in progress.

When the measured values in FIG 53 are plotted as a function of the relative humidity, we get a cluster of points according to FIG 55. The contours have the appearance which one might expect according to the discussion presented in the proceeding section. The concrete quality was

very high, W/C = 0.32. The cathodic control begins to work effectively at 90% relative humidity, while the corrosion current increased under this level due to better conductivity in connection with moistening.

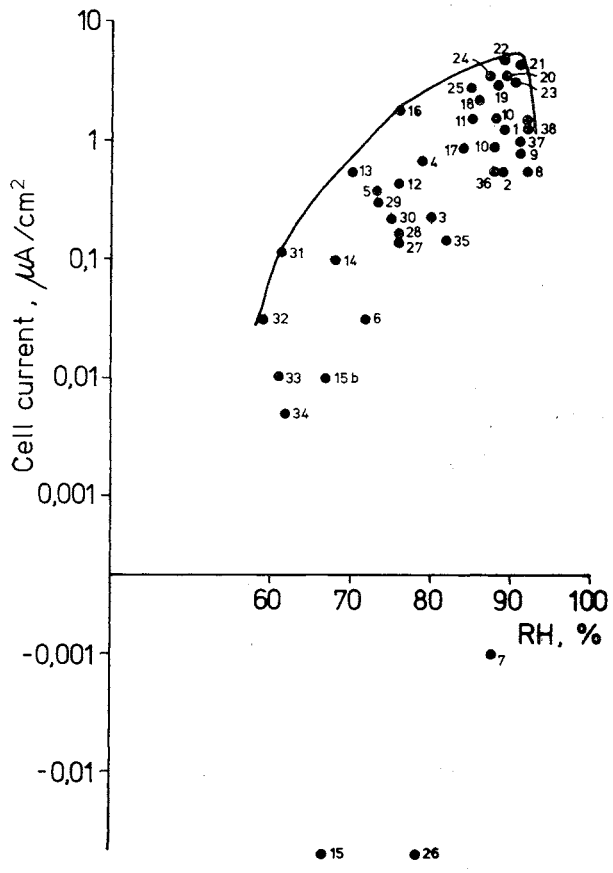

FIG 55. Measured cell current as a function of the relative humidity in a cell which is corroding. The values have been plotted in the sequence in which they occurred.

Corrosion currents have been recorded in the same ways for a carbonated concrete, see FIG 56. The pattern is the same, an optimum level around 95% relative humidity which decreases on either side of this limit. The rate of corrosion is low in all cases at 100% RH - the cell current indicates about 0.1 µm/ year - since the resistivity is at its maximum, but the absolute value for the cell current is on a level with that for extremely dry

specimens. The carbonated specimen in the example above was also used at varying temperatures. The results are presented in FIG 57.

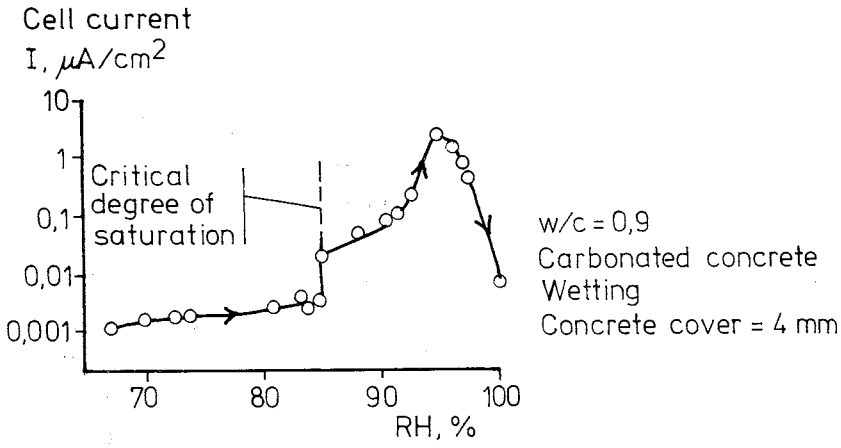

FIG 56. Measured cell current as a function of the relative humidity. The specimen is gradually moistened. Concrete quality KC6-78, see Appendix 4.

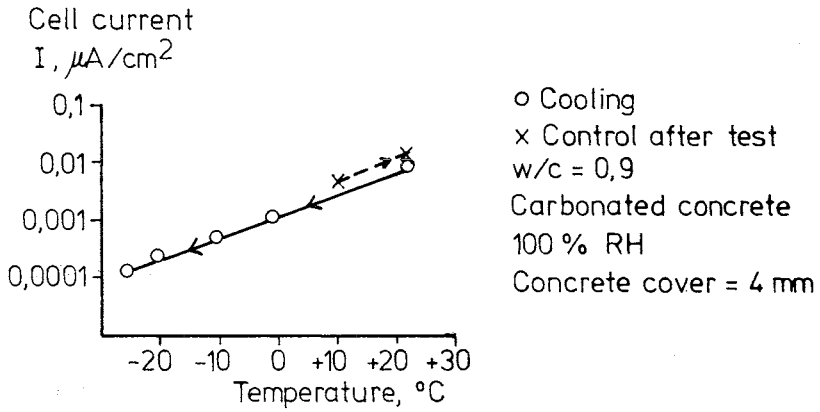

FIG 57. Measured cell current as a function of the temperature. Concrete quality KC6-78, see Appendix 4.

Since the specimen was saturated with moisture, the measured currents can be regarded as thoroughly representative for the corrosion sequence in

embedded steel. The corrosion rate thus follows approximately the same relations as other corrosion processes, which entails doubling the corrosion rate for a temperature increase of $10^{o}C$.

Weight loss measurements

Extensive weight loss measurements were carried out to provide a better basis for the values for the corrosion rate after initiation, see Chapter 5.3. These measurements were also intended to provide information on the value of the corrosion cell in the studies which had been carried out.

Plain bars were cast in a container with a concrete cover of 3-4 mm. Test tubes were used as moulds and the concrete cover was equally thick in all directions. Unfortunately, for reasons explained elsewhere, this probably did not provide values which can be regarded as representative for reinforcement in concrete (see Chapter 5.3.5). The corrosion process was initiated by carbonating the concrete cover or by admixing chloride.

The limit values for the corrosion rate presented in FIGS 58 and 59 were obtained through a pickling procedure and a check of the weight loss at varying points in time. The corrosion rate did not, therefore, have the same typical moisture interdependency as that obtained theoretically and by means of corrosion cells.

A rate of corrosion which was independent of the initiating mechanism and the cement type, of approximately a few µm/year was obtained in concrete which was completely saturated with water.

The maximum values were about 5 times higher for chloride-initiated Portland cement concrete than for carbonated Portland cement concrete.

The slag cement with 70% slag had a higher rate of corrosion throughout than did the corresponding Portland cement concrete.

The maximum value agreed with the corrosion cells and the theoretical discussion insofar as it was obtained at 90-95% RH.

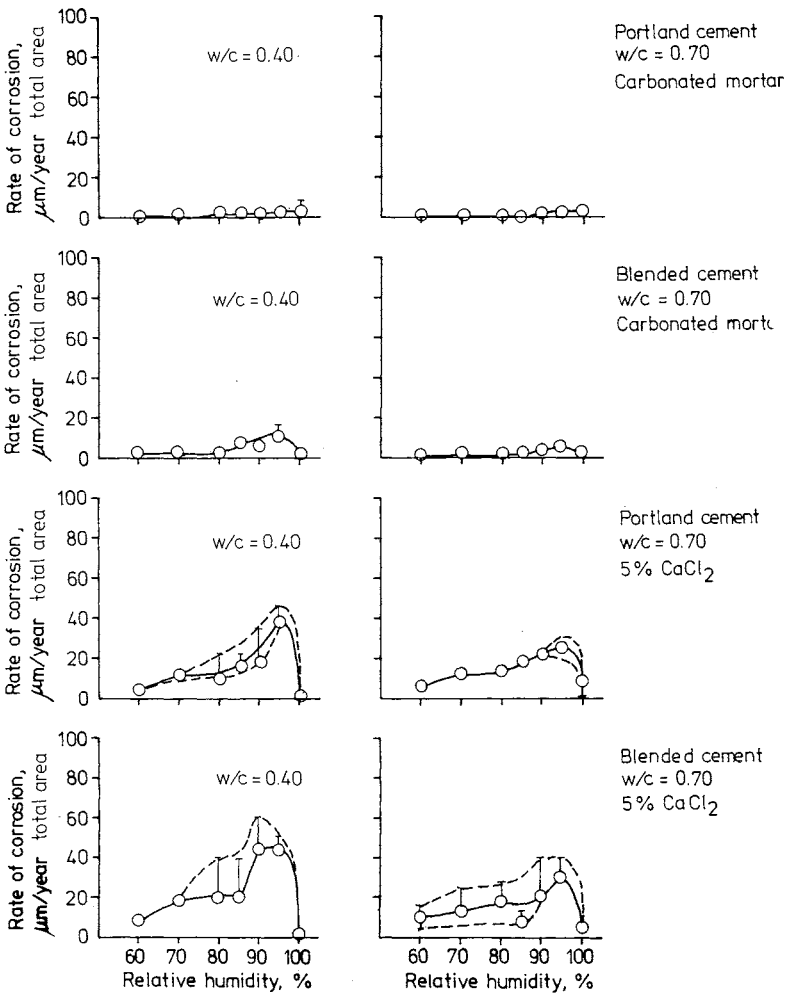

FIG 58. Corrosion rate calculated for entire metal surface as a function of the relative humidity for a number of different types of corrosion cases.

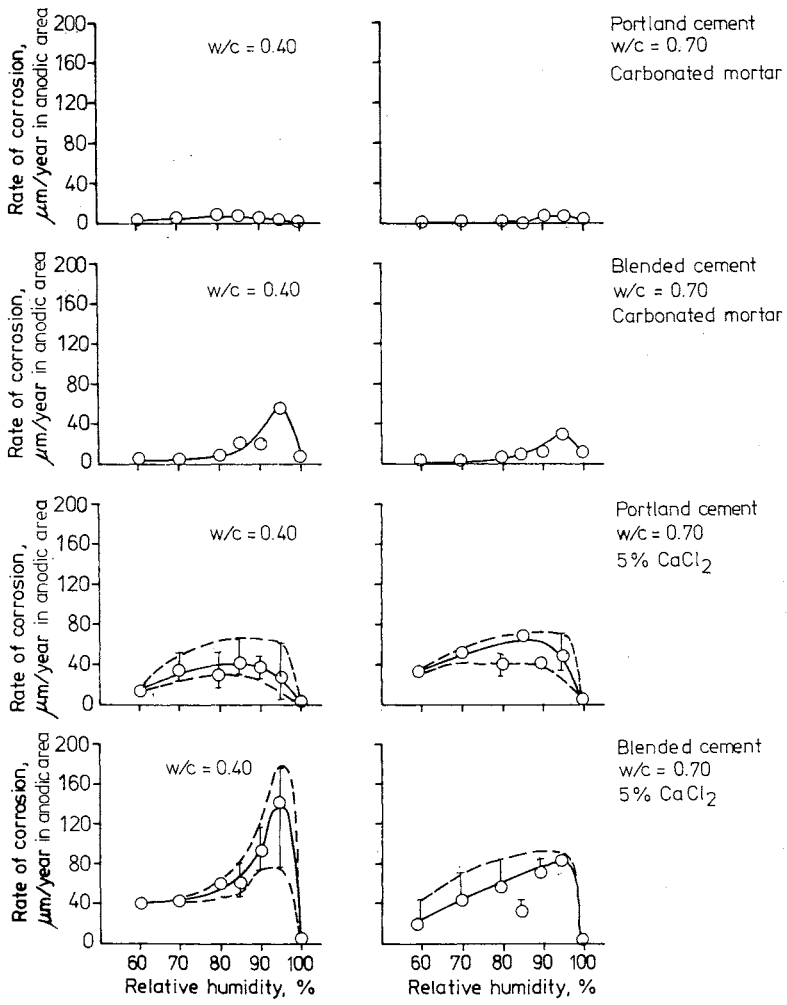

FIG 59. Corrosion rate calculated on the anodic surface as a function of the relative humidity for a number of different types of corrosion cases.

The rate of corrosion for carbonated concrete appears to be no more than insignificant at relative humidities lower than 80%. Admittedly this cannot be clearly seen from the Portland cement figures but the blended cement specimens indicate it.

The figures also show that a low W/C has not given a lower rate of corrosion than a high W/C. The values are at roughly the same level. The reason for this may be that the higher hydroxide ion concentration in the high concrete qualities cause the steel to enter a more active state, see, for example the chart published by Pourbaix for iron at pH 14.0.

The values for chloride-initiationed concrete, approximately 60 µm/year, also agree very closely with measured cell currents in the preceding section, where the maximum value sometimes amounted to about 60 µm/year.

2.6.4 Rate of corrosion - practical case histories

In the corrosion investigations carried out when studying various damage cases at the Swedish Cement and Concrete Research Institute, attempts have sometimes been made to estimate the mean corrosion rate which affected the steel once initiation had taken place. In these cases the initiation time was assessed by making a calculation backwards in time using the models presented here and using the situation when the samples were taken as the starting point.

Balcony slabs

Top reinforcement in a number of balcony slabs with a standard (i.e. according to the applicable code of practice) concrete strength of 25 MPa was found to have corroded an average of about 1 mm in 20 years. The concrete cover was 20 mm. This gives a rate of corrosion of 50 µm/year. The slabs were carbonated only. For further details see Tuutti /1979a/.

Concrete silo

Concrete silos with a standard strength of 25 MPa and which had been cast with material including a chloride admixture had been damaged after 25 years. Salted sand had been stored in the silos. Consequently, high chlo-

ride contents could be measured in the walls. The damage had not occurred to the reinforcement closest to the chloride-rich sand despite the fact that the content in moist concrete was 2.45 $CaCl_2$ of the cement weight. 50%, approximately 5 mm, of the load-bearing steel area on the air side was, on the other hand, lost through corrosion where the chloride content was 1% $CaCl_2$ of the cement weight and the concrete was carbonated. The concrete cover was 25 mm. Clear cracking indicated the damage during an ocular inspection. The rate of corrosion was assessed to amount to 0.2-0.4 mm/year locally. See the report published by Thorsén and Tuutti /1979a/.

Multi-storey car park in indoor climate

Despite the fact that the propagation stage had started about 5 years before the sample was taken, no more than a hint of a corrosion attack was found at several points at a floor slab with a standard compressive strength of 36 MPa in which the carbonation front had passed the reinforcement position and in which salt concentrations of up to 0.2% $CaCl_2$ of the cement weight were measured. 0.6% $CaCl_2$ of the cement weight and carbonation had, on the other hand, led to damage. 10.7% $CaCl_2$ of the cement weight without carbonation had also given rise to major corrosion attacks. A damp indoor climate and carbonated concrete thus gave no more than an insignificant rate of corrosion, Bergström, Thorsén and Tuutti /1980/.

Power line poles

Power line poles with an age of about 50 years were investigated for corrosion damage. The concrete was partly carbonated. No chlorides occurred. The compressive strength of the concrete amounted to about 50 MPa at the testing time. A mean corrosion rate of about 50 µm/year was obtained by calculating backwards in time to the initiation occasion. See Thorsén and Tuutti /1979b/. It should be noted that approximately the same type of structure had been studied the previous year to calculate its possible service life. The minimum service life obtained then, when using the model, amounted to 50 years, in other words precisely the same value as that obtained for the damage case, see Bergström, Rombén and Tuutti /1977/.

Concrete building with chloride admixture

The Swedish Cement and Concrete Research Institute investigated a residential area with an age of about 10 years in Stockholm after reports were received that serious corrosion attacks could be seen. The concrete had a strength of 45-60 MPa at the time of testing. 1.0-1.5% of $CaCl_2$ had been added to the concrete during manufacture. A carbonation depth which was 10-15 mm from the reinforcement had been measured at several points but major attacks had occurred none the less. This is a further proof of the chloride-limiting effect of the carbonates which gives rise to rapid corrosion initiation. The corrosion rate was later estimated to lie on a level of 0.1-0.5 mm/year. See Molin, Klevbo /1981/. The author has seen a parallel case to this in Malmö for a balcony structure. See Hellström /1977/.

Slussen traffic facility - Stockholm

Slussen, which is a 50-year old traffic facility in Stockholm, has been carefully investigated with regard to its durability. Damage had been observed locally and it could be noted that carbonation and chloride-initiation had occurred in the areas which had poor concrete or which were subjected to a considerable environmental load. In order to study if the climate could be so dry anywhere that the corrosion rate became insignificant, extensive moisture measurements were carried out. Personal contact with the investigator, Mr. Steorn, has confirmed the fact that all the outdoor concrete has a sufficient quantity of electrolyte to permit corrosion. The moisture content is increased when the outdoor air temperature suddenly rises with condensation on the concrete as a result.

Fagerlund and Svensson /1980/ came to the same results when studying the moisture state of different types of concrete slab. The relative humidity for this type of structure, which is exposed to rain, was fairly constant around a level of 90-95%, despite the fact that a diffusion-proof barrier had been laid on the top of the balcony.

2.6.5 Discussion and compilation of results

At 100% relative humidity, the rate of corrosion is very low. Measurements with corrosion cells, weight loss measurements and previous investigations

of old concrete structures, see for example Gjörv /1968/, have shown this. In this highly moist state the corrosion process is probably cathodically controlled as a result of a low O_2 flow to the cathodic areas. Measured effective diffusion coefficients showed, on the other hand, a loss of about 20 µm Fe per year as a result of corrosion. The accuracy of the equipment is not, however, sufficiently high for the experiments presented in Chapter 5.1 at the extremely low O_2 quantities which could penetrate through the concrete. A loss of about 0.1-1 µm/year corresponds to an effective diffusion coefficient of approximately 10^{-11} m^2/s.

As far as corrosion rates for steel in carbonated concrete are concerned, the rate loss measurements did not describe reality with sufficient accuracy. In the experiments, all surfaces were in contact with neutralized concrete. In reality only part of the metal surface is in contact with carbonated concrete.

The mean corrosion rate can be set to about 50 µm/year here, using the practical cases as a basis, see Table 8. This value agrees well with the results obtained from the corrosion cell investigation at 95% RH. On the other hand, the weight loss measurements on the carbonated concrete have indicated that incomplete carbonation can retard the corrosion process, i.e. that rapid carbonation can provide a temporary repair alternative since the environmental differences are then equalized along the metal surfaces.

The results from all of the investigations indicated that an indoor climate does not permit corrosion unless high chloride contents occur in the material. An increase in the chloride content probably increases the hygroscopicity of the material.

Chloride-initiated concrete has shown varying corrosion rates. This also agrees with reality. Homogeneous concrete with a low chloride concentration should have a corrosion rate of 50-100 µm/year while non-homogeneous concretes, combinations of carbonation and chloride-initiation etc give values which are 10 times higher.

Table 8. Compilation of estimated corrosion rates for a number of practical cases presented in the preceding section.

Object	Age at investigation (years)	Approx. quality	Corr. mechanism	Estimated Corr. rate µm/year
Balconies	30	25 MPa	Carbonated	50
Power line poles	50	50 MPa	Carbonated	50
Concrete silo for salted sand	25	25 MPa	Carb. + 1% $CaCl_2$	200-400
			2.4% $CaCl_2$	No corr.
Multi-storey car park	15	35 MPa	Carb. + 0.2% $CaCl_2$	No corr.
			Carb. + 0.6% $CaCl_2$	Damage
			10.7% $CaCl_2$	Major damage
Precast concrete elements, outdoors	10-15	45-60 MPa	1-1.5% $CaCl_2$ admixed. Carb. 10-15 mm from reinforcement.	100-500

The temperature effects in FIG 57 provide a fairly accurate description of the problems reported from the Middle East and other hot climates where corrosion-initiation can take place directly due to impurities in the constituents. Damage has appeared within a few years, unlike the cold climate in the Nordic countries where damage cannot be seen until 10-20 years after initiation. Cases have also occurred in Sweden where damage could be seen within a few years but this has been in warm facilities such as indoor swimming pools with a high chloride content, Jönis /1975/, where the damage could be seen after 5 years of corrosion.

In addition, a distinction must always be made between concrete in which liquids flow through the concrete and concrete with a more constant liquid balance. Flowing liquids must always be expected to give a corrosion rate which corresponds to the O_2 flow which the cathodes can receive and the quantity of substances which can be transported away from the anodes. The solubility of iron and ferric hydroxide in the electrolyte is also a determining factor here.

These quantitative assessments can, on the other hand, be difficult to carry out. Consequently, non-homogeneous concrete, pure concrete etc is not accepted, see Nielsen /1976/.

2.7 Final state

2.7.1 Model

The corrosion process of steel in concrete can be considered to function in accordance with one of the following extreme cases or, more likely, as a combination of them.

- The iron dissolves and is transported away from the corrosion area. A final conversion to ferric oxide or ferric hydroxide takes place outside the concrete.

- The iron changes over directly to the final product and is accumulated adjacent to the original metal.

In both of these models, the cross-section area of the steel which has been attacked is reduced. The degree of utilization of the steel - in other words, how close to the yield point limit or the ultimate stress point the stresses lie - is the decisive factor for how large a reduction in area can be accepted. Consequently, no general rules can be provided. The first mechanism occurs very rarely due to the low permeability of concrete. On the other hand, this type of damage can occur in concrete which has varying quality and zones with very poor quality. This is particularly true of structures which have been exposed to a one-sided liquid pressure and in which the liquid contains chlorides or other metal-liberating substances. An assessment of when the final state is reached must, even if the minimum steel area required is known, be made by investigating the status for each individual structure. The damaged sections can, however, be located with the aid of the precipitation of corrosion products which occurs around the anodes.

The most common case is that most or all the corrosion products accumulate around the original metal. The corrosion products also frequently have good adhesion to the steel. An accumulation of corrosion products around

the reinforcement or embedded steel entails an increase in volume which gives rise to stresses in the concrete cover. When the stresses exceed the ultimate load, cracks occur in the concrete cover. The liquid movements in the material cause minor quantities of iron to be transported to the surface, however, where they are coloured brown. Gradually the increase in volume becomes so large that the concrete flakes off and the steel is exposed. The time from the moment when the first crack becomes visible along the reinforcement bars until the damage looks serious and the load-bearing capacity of the structure has been markedly reduced is short. It is assumed here that the most heavily loaded or critical parts have been attacked. The criterium for the final state thus consists of visible cracks along the reinforcement, corresponding to crack widths of about 0.1-0.2 mm. Where the damage occurs in a structure is also of importance from the strength viewpoint. Greater damage can be accepted at points where the reinforcement is poorly utilized or where other structural components can absorb the stresses from the damaged area. Concrete can never be regarded as so homogeneous, however, that the damage or destruction process proceeds uniformly and at the same rate throughout the entire structure. Major variations occur in the quality of the concrete cover, the environment in the immediate surroundings etc. FIG 60 presents an example of precisely this situation. The carbonation depth varies from values around 0 to 50 mm in the same structure. Consequently, it is extremely important to be able to locate the areas which are in a poor condition when carrying out a status investigation. It is not enough to repair damage where it is visible to the naked eye. If repairs are carried out on the basis of an ocular inspection only, the damage will constantly recur in the same structure at points where it was previously considered that the structure did not need repair. We thus have a further reason for following the model when carrying out a status investigation.

2.7.2 Material data for corrosion products

The ferric oxides and ferric hydroxides which can be formed according to Nielsen /1976/ are those presented in FIG 61. The original metal thus increases to about twice its volume when Fe_3O_4 is formed. This has been confirmed by the density determinations carried out on corrosion products, see Chapter 5.6, where the low-porous oxides weighed 3.7 t/m^3 and the porous oxides weighed about 3.0 t/m^3. Rust thus has a density which is less than half the density of iron.

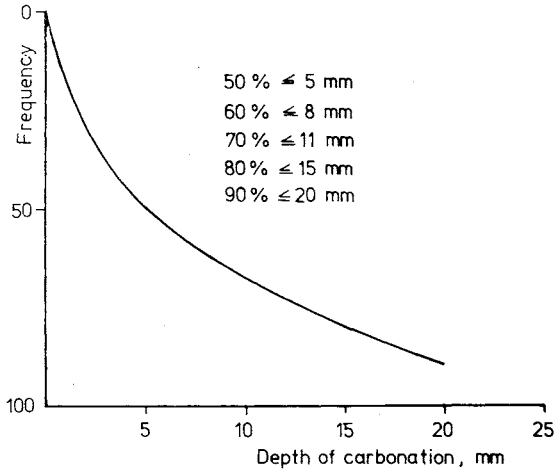

FIG 60. Frequency for measured carbonation depth in Slussen traffic facility in Stockholm. A total of 100 inspections were carried out.

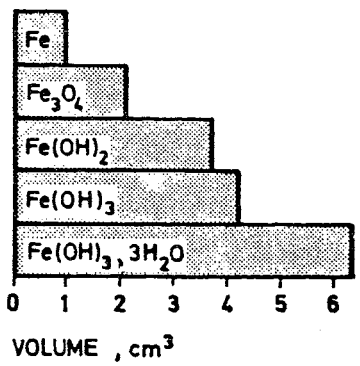

FIG 61. Relative volume for various corrosion products according to Nielsen /1976/.

The corrosion products also have a very low porosity and an impermeable pore structure and can be compared with the the most impermeable cement pastes, see FIG 62. Consequently, the corrosion products should provide an excellent seal against various substances.

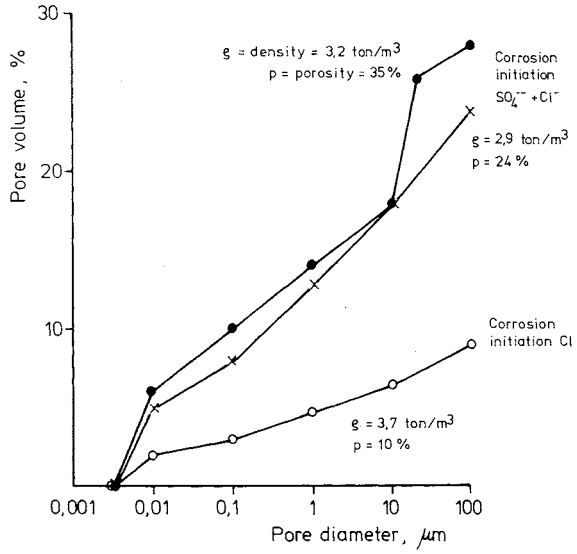

FIG 62. Porosity and pore size distribution measured with a mercury porosimeter for three different corrosion products which consisted of a black, hard and magnetic material.

2.7.3 Final state - laboratory experiments

A number of simple laboratory experiments (see Chapter 5.3.7) were carried out to investigate how much corrosion loss can be accepted on embedded steel of varying dimensions in varying concrete qualities. An accelerated corrosion process was used. The accelerator consisted of an external voltage source, approximately 1 V. Experiments were carried out during a period of two years so as to simulate real conditions as far as possible.

The results are summarized in FIGS 63 and 64 and the following conclusions can be drawn:

- small average attacks, less than 1 mm, are sufficient to cause cracks in the concrete cover.

- if the W/C is high, the bar diameters are small and the concrete cover is thick, the steel can corrode more than is the case when these values are the opposite before damage can be seen in the form of cracks in the concrete cover.

- the maximum pitting depth was about 4-10 times the value for the average attacks.

In the laboratory experiments, magnetite Fe_3O_4 was obtained as a final product around the steel. It should, however be noted that the concrete was relatively moist during the experimental period.

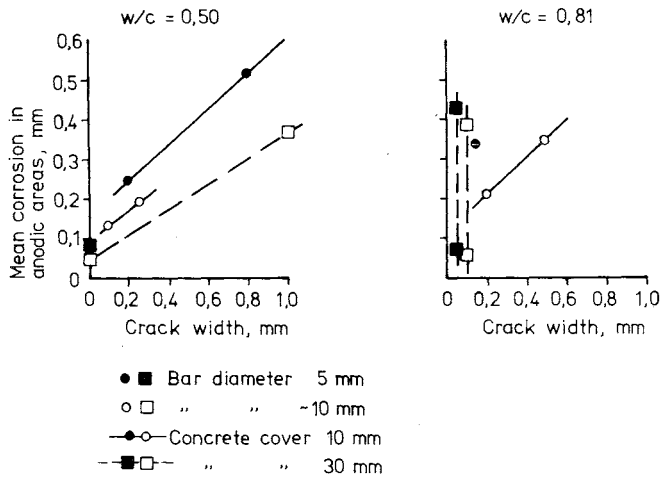

FIG 63. Estimated mean corrosion depth as a function of measured crack width on the concrete surface.

The mean corrosion depth has been calculated by weight-loss measurement and by measured anodic areas.

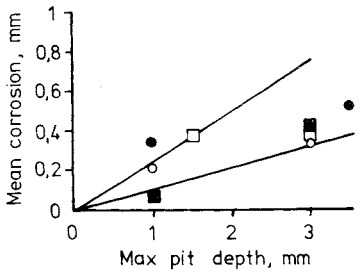

	ϕ mm	Concrete cover mm
●	5	10
■	5	30
○	10	10
□	10	30

FIG 64. Mean corrosion depth as a function of maximum corrosion depth.

2.7.4 Final state - practical case histories

When mapping out corrosion damage on reinforcement in concrete balconies, Tuutti /1979a/ it could be noted that cracks with a width of 0.5-1 mm had occurred in balconies with a concrete cover of 15-20 in cases where the average loss of material due to corrosion amounted to about 1 mm. This estimate of the average corrosion loss was made through measurements with the aid of sliding calipers. The diameter of corroded and non-corroded bars was recorded. The diameter was always larger on corroded bars since the corrosion products had a larger volume than the original metal. Furthermore, the adhesion between the rust and steel was good. The corrosion products were black and were attracted to a magnet. Consequently, it was assumed in these cases that Fe_3O_4 had been formed and that the volume of the rust was twice that of the steel. This was later confirmed by the measurements carried out with the aid of a mercury porosimeter. The time of propagation was in this case about 20 years.

Very old (approximately 50 years) power line poles were investigated as a result of corrosion damage, Thorsén and Tuutti /1979b/.

The poles were subdivided into four classes ranging from no damage to severe damage. The results from this investigation follow the same pattern as the results from the investigation from the Slussen traffic facility, which is also an old concrete structure dating from the 1930s. The damage patterns for the poles varied. Many of them had no corrosion while many others were seriously damaged. This was mainly due to the considerable variation in the concrete cover. About 50 poles were investigated. The thickness of the corrosion products was measured at 21 points. The results are presented in Table 9.

Table 9. Compilation of degree of corrosion in flaked-off material. Estimated W/C for concrete: 0.50. The reinforcement consisted of plain bars with a diameter of 20 mm.

Number of investigated flaking points.	Degree of damage, in percentage of investigated flakes			
	0	I	II	III
21	0	10	52	38
Degree of corrosion	0	0.0 mm rust thickness		
	I	< 0.5 " "		
	II	0.5-2.0 mm rust thickness		
	III	> 2.0 " "		

At the corrosion points investigated, the 3 mm thick wire which acted as stirrup reinforcement was rusted all the way through in many cases. The stirrup reinforcement was more or less corroded all the way through along its entire length in the case of some lengthy corrosion attacks along a principal reinforcement bar.

The result thus shows that the mean corrosion loss varied between 0.2 mm up to a value greater than 1 mm at those points where the concrete cover had been broken off. The variation is probably partly dependent on the time (no information was available indicating when the damage occurred) and partly on the concrete cover since thin covers cannot absorb the same quantity of corrosion as can thick. The maximum concrete cover measured 27 $\pm$ 6 mm and the minimum cover measured 13 $\pm$ 5 mm. The corrosion products had a black colour. When the concrete cover was chipped off, no leaching of iron which was later converted to ferric hydroxide could be seen, see Photos 1 and 2. If, on the other hand, a bar had been exposed for a lengthy period of time a rust-brown colour could be noted along the concrete surfaces, see Photo 3.

The thin 3 mm wire had been completely corroded in certain cases. The maximum corrosion attack can thus be seen to amount to at least this value. Cracks were very seldom noted along the thin wire, however.

Concrete silos, which were used for storing sand for a glassworks, had been damaged by corroding reinforcement, reported by Thorsén and Tuutti /1979a/. The sand had been salted to prevent it from freezing into lumps during the winter. The concrete had a standard strength (10% fractile) according to the regulations of 25 MPa at a 28-day cube test. The reinforcement mainly consisted of 10 mm ribbed bars. The maximum corrosion loss was measured at about 5 mm. This degree of corrosion had not caused the concrete to crack up towards the surface but stratification (i.e. cracking in layers) had, on the other hand, occurred adjacent to the reinforcement. The damage was detected since a cavity was indicated when the concrete was tapped. The chlorides have a metal-liberating effect which a carbonated concrete does not show. The corrosion products had penetrated into the pore system of the concrete and minor cracks had occurred around the reinforcement, see Photo 4.

The thickness of the corrosion products was measured along a vertical crack, i.e. a crack at right angles to the principal reinforcement, see FIG 65 and Photo 5. This silo did not contain salted sand but $CaCl_2$ had, on the other hand, been used during casting. The value measured was 0.7% $CaCl_2$ per weight cement. The vertical crack had occurred as a result of overloading. It could also be seen that corrosion products with a thickness of 2-3 mm had given rise to cracking in layers in the concrete with a concrete cover of 35 mm. Concrete with a cover of 37 mm to the reinforcement had not been damaged in cases where the corrosion products had a thickness of 1 mm. An interdependency can thus be seen between the diameter of the reinforcement bar, the centre-to-centre spacing, the concrete cover and the porosity of the concrete if cracks are to occur towards the surface parallel with the reinforcement or if the concrete is to crack in layers internally. Bazant /1978/ has theoretically dealt with this subject but no material coefficients are yet available.

2.7.5 Summary

Laboratory experiments and practical case studies have shown that the corrosion product for embedded steel normally becomes magnetite, Fe_3O_4, which has a volume of more than twice that of the original metal.

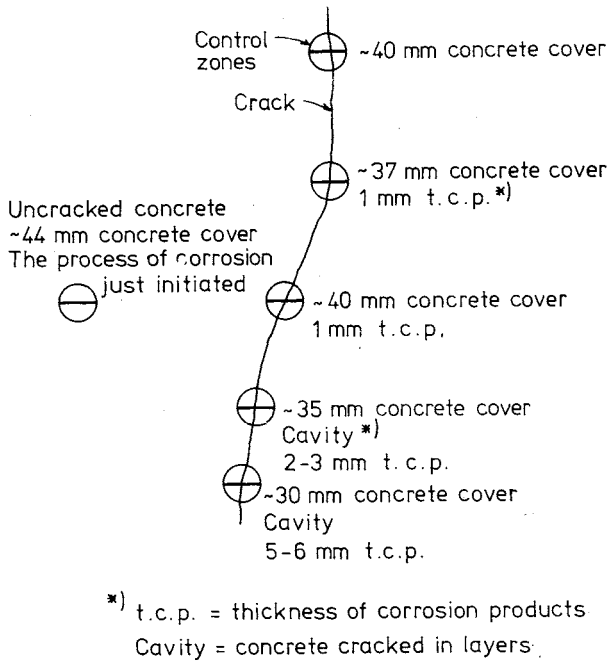

FIG 65. Position of reinforcement. Concrete cover and degree of corrosion in the crack shown in Photo 5.

In the case of CO_2-initiated corrosion, most of the corrosion products are accumulated close up against the steel. Cracks in 10-20 mm concrete covers usually occur when the average corrosion product thickness lies within a few tenths of a millimetre up to one millimetre. If the concrete cover is thicker, for example 40 mm, it is more likely instead that the concrete will crack in layers adjacent to the reinforcement. This form of stratification can be located by tapping the concrete and listening for the hollow sound of the cavity.

In the case of chloride-initiated corrosion, a fairly large quantity of corrosion products can be transported away from the anode and into the pore system of the concrete. Consequently, the mean corrosion product thickness is greater in the chloride case, given the same conditions as for CO_2 initiated corrosion. This problem has not, however, been mapped out with

sufficient accuracy to say more than that the average corrosion product thickness in this case also lies around 1 mm and less when cracks occur in the concrete cover.

The maximum pitting depth is often about 4-10 times greater than the average corrosion attack. Higher concrete quality and an increase in the diameter of the reinforcement gives less corrosion in connection with cracking.

Since pore solution is transported past the reinforcement all the time, for example in connection with one-sided liquid pressure, there is a risk that cracks or cavities do not occur despite the fact that the steel has corroded to more than the extent indicated above. This is particularly so in cases where the chloride content in the pore solution is high. In such cases the damage can, however, be seen in the form of the precipitation of corrosion products on the concrete surfaces. The degree of utilization of the reinforcement is decisive for the final state in these cases.

The principle is thus that visible damage on the surface of the concrete in the form of cracks or discolouration indicates that reinforcement corrosion has advanced so far that repair measures are urgently required, in other words, that the service life of the structure can be regarded as finished.

Damage to existing structures does not, however, express itself instantaneously. The variations which occur in concrete quality, environment and above all in the concrete cover in a structure give rise first of all to damage in critical areas. If the damage is noted at an early stage, repair work can usually be simplified. The other parts of the structure, which have not been damaged, must, however, be protected against decomposition.

3 EFFECT OF VARIOUS FACTORS

3.1 Environment types

3.1.1 General

This report deals only with conditions where the original concrete cover is intact. In those cases in which damage due to frost or chemical attacks also occurs there is generally no reason to calculate the corrosion of the embedded steel since the physical and chemical attacks probably constitute the decisive factors. Weak acids are, however, rapidly neutralised and cannot reach the steel unchanged. Only completely embedded steel is dealt with in the report, in other words the report does not take account of steel which is partly embedded and partly freely exposed.

Steel cast in concrete is provided with highly effective protection against various substances which occur in the atmosphere. Solid airborne pollutants cannot penetrate through the concrete cover. The concrete also protects steel from contact with various minerals in soil. Only particles which are considerably smaller than most of the concrete pores have any possibility of penetrating through the concrete and coming in contact with embedded steel. The following are amongst particles of this type:

- liquids and ions which occur in it
- gases

It is of interest to know how various substances penetrate to the steel in the first stage after casting. Generally speaking, the differences in concentration which occur between the surroundings and the pore system of the concrete strive towards equalization. Substances which occur in greater concentration in the concrete than in the surroundings thus penetrate outwards and vice versa. Such movements of different substances are prevented partly physically by the solid phase in the concrete and partly chemically by the reactions which result from various substances coming in contact with each other. The effect of this resistance depends to a considerable extent on the characteristics of the concrete, the moisture conditions and on which substances are being transported. For example, a considerable time lag occurs in the neutralization of the concrete caused by

penetrating CO_2 while the time lag is a great deal shorter for chloride penetration. The transport laws are, however, linear. This means that doubling the concentration of CO_2, Cl^- etc in the surroundings causes the flow of these substances to be doubled, assuming that other conditions remain the same.

The concentration of CO_2, Cl^- or any other corrosive substance in the surroundings thus consitutes an environmental parameter.

When it comes to the effective CO_2 or Cl^-, conditions are further simplified since noticeable carbonation only occurs in comparatively dry environments while Cl^- is the corrosion activator in moist environments.

Admixing chloride to fresh concrete so as to accelerate the chemical reactions entails an increase in the corrosion rate. Even a moderate admixture of chloride does, however, reduce tolerances for other faults. Pitting attacks occur adjacent to pores, see Halvorsen /1966/. Another example of this consists of cracked concrete with initiated corrosion around the crack as a result of CO_2 penetration. When this has occurred, it is no longer possible to guarantee corrosion-delaying effects such as repassivization, see Chapter 3.2.

The moisture conditions can vary from a dry indoor climate to complete water saturation. No corrosion problems occur in a dry environment or a completely moist environment. Corrosion problems generally occur, on the other hand, in outdoor structures where the moisture content fluctuates. According to the line of reasoning presented earlier, the water saturation of the concrete can be significant both for the initiation stage and for the propagation stage.

Reinforcement in concrete is not, admittedly, affected directly by rain in the same way as exposed steel but rapid moisture fluctuations mean that the concentration differences which occur around the metal and deep in the concrete are rapidly equalized due to rapid liquid movements. A stationary state is never achieved in cases like this.

Furthermore, the temperature is of considerable importance. An increase in temperature means an increase in the mobility of the molecules, in other

words the transport of substances is facilitated. An increase in temperature often increases the solubility of various substances. In extremely cold climates, the liquid which occurs in the pore system of the concrete will freeze to the solid state and the transport of various substances will become more difficult as a result.

3.1.2 Normal CO_2 concentrations

The carbon dioxide concentration varies between 0.033-0.1% by volume in the atmosphere. The lower value applies to a normal atmosphere while the higher value occurs in city atmospheres. Still higher concentrations can occur locally. The relative mean concentration should be checked at sites with a high motor traffic intensity or immediately adjacent to chimney stacks.

3.1.3 Normal Cl^- concentrations

Chlorides occur to a greater or lesser extent in all liquids which surround concrete structures. The following is a suitable subdivision:

- fresh water, in the Nordic countries this normally means groundwater, surface water or rainwater.
- brackish sea water
- salt sea water
- saturated salt solutions
- artificial water accumulations with a special Cl^- concentration

Fresh water is not dangerous from the point of view of chloride effects.

Brackish sea water and salt sea water occur in the Baltic Sea and the North Sea respectively with chloride contents which amount to about 9 and about 20 g/l respectively.

The highest concentration of chloride which can occur around a concrete structure is the concentration of a saturated salt solution. This is, for example, the case when salt is used for de-icing bridge decks. The salt solution which is splashed up on edge beams and columns is practically

saturated. At $0^{o}C$, the solubility counted in Cl^{-} for $CaCl_2$ and NaCl salts is 375 and 215 g/l respectively.

Pools or basins of various types usually contain a certian chloride concentration which can vary from saturation to almost non-existent.

3.1.4 Moisture conditions in Sweden

According to what has been said previously, the moisture state is important in connection with the penetration of CO_2 in the initiation stage and in connection with the penetration of O_2 in the propagation stage. For the approximate calculations which are presented in this report it is quite sufficient to subdivide structures into:

- indoor structures with a constant temperature and humidity < 70%
- outdoor structures sheltered against rain RH = 65-90%, RH_{mean} = 80%
- outdoor structures not sheltered against rain. Number of moistening cycles = 100-200.

Table 10 shows that all of Sweden can be regarded as similar from the point of view of moisture. Numerous rain periods occur. Standard concrete is not capable of drying out to any noteworthy extent during the brief breaks between rainy periods. This is why it is important to distinguish between structures sheltered against rain and structures not sheltered against rain.

Table 10 Moisture state for a number of places in Sweden, 1967

Locality	Relative humidity (%)			Number of days with rain/year
	min	max	mean	
Kiruna	59	87	79	98
Umeå	67	95	83	116
Stockholm	66	88	80	173
Örebro	67	90	80	150
Gothenburg	54	86	78	172
Malmö	66	92	81	216

3.1.5 Temperature conditions in Sweden

The last environmental parameter of major significance is the variation in the ambient temperature. An increase in temperature entails an increase in the rate of corrosion.

Table 11 Mean temperatures measured by SMHI in Sweden 1967

Locality	°C
Kiruna	-1.5
Umeå	+3.0
Stockholm	+7.1
Örebro	+6.4
Gothenburg	+8.4
Malmö	+8.7

No other special environments have been taken into consideration in this report, for example major or minor voids or gaps adjacent to embedded steel etc. The sequence of events in situations like this are likely to be more complicated and should be specially investigated. The main emphasis in this report is on the durability of our normal concrete structures.

3.2 Cracks

3.2.1 General

The description of the model deals with the corrosion of steel in uncracked concrete, i.e. in concrete without visible cracks. Cracks occur, however, in all concrete due to the fact that differences between volumetric changes in the cement base and in the aggregate are greater than the rupture strain of the cement paste. Weak zones or microcracks therefore always occur in the phase interfaces. What is generally meant by cracks are fairly large failure areas in concrete which occur as a result of shrinkage, temperature movements, loads, deformations or environmental influence.

The manner in which a crack has occurred is, in most cases, uninteresting from the corrosion viewpoint. It is important, on the other hand, to know

whether the crack penetrates to the reinforcement or not. Corrosion initiation or a marked increase in the rate of corrosion takes place as a result of various substances penetrating to the steel. A crack in concrete changes the permeability of the material radically in the crack area. Various substances can therefore penetrate through the concrete much faster through cracks than through the pore system of the concrete.

Cracks which run at right angles to the reinforcement and cracks which run parallel with the reinforcement must, on the other hand, be distinguished. Here we shall mainly confine ourselves to cracks which run at right angles to the reinforcement. These have occurred as a result of loads on the structure and entail a small defective area adjacement to the steel. The other cracks, parallel cracks, are normally derived from e.g. settlement during the hardening of the concrete and generally lead to major voids or channels along the steel.

Reference is often made in the literature to the permissible crack width, which varies between 0.1 and 1.0 mm. Rehm and Moll /1964/ carried out an investigation of the effect of the crack width on corrosion in reinforcement in concrete. They noted that when the crack width only was varied, the corrosion attack decreased with the width of the cracks. Schiessl /1976/ later investigated specimens with a longer exposure time than those included by Rehm and Moll in their investigation. Values for both four years and ten years exposure were included in this work, see FIGS 66 and 67. Corrosion always occurred in the uncracked zones as soon as the carbonation front had penetrated to the steel. The thickness of the concrete cover determined the initiation time for the same concrete.

If the exposure time is brief, for example, 5 years, the corrosion process is thus initiated only in cracks which have a width above a critical value. The initiation time increases if the crack width decreases and finally reaches the same value as for the "uncracked" concrete.

Similar experiments were carried out by Tremper /1947/. The specimens were stored outdoors for ten years before the degree of corrosion was determined. The crack width was varied between 0.13-1.3 mm, measured on the surface, W/C 0.40-0.75. When the specimens were inspected corrosion attacks could be seen to have occurred in the cracks and their

immediate surroundings in almost all cases. A significant increase in the size of the corroded area with increasing crack widths could be noted but no effect of the crack width could be found with regard to the maximum corrosion depth. The maximum corrosion depth amounted to 0.4 mm.

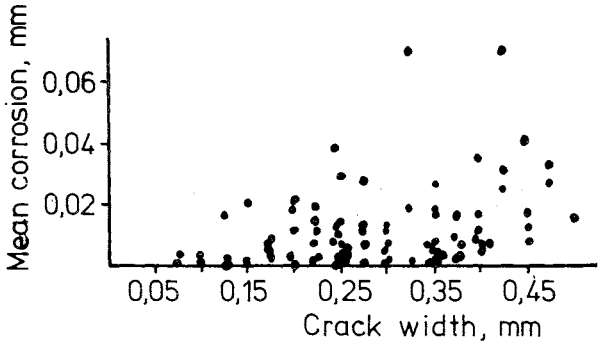

FIG 66. Mean corrosion on reinforcement as a function of the crack width after four years exposure. Schiessl /1976/.

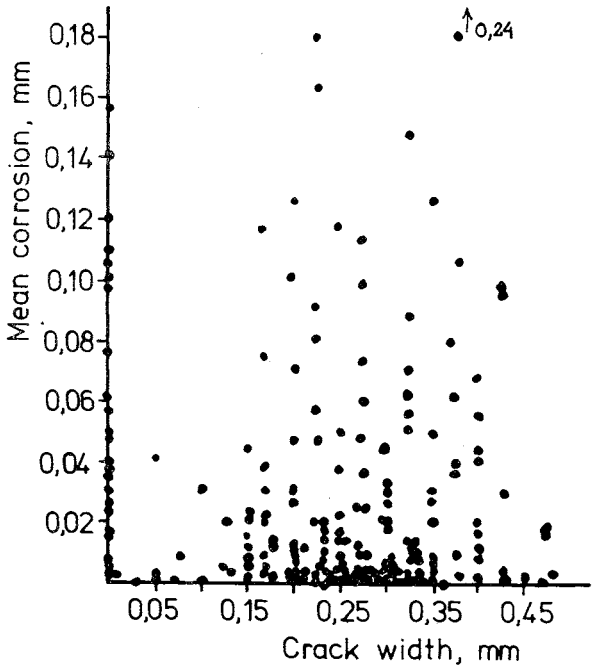

FIG 67. Mean corrosion on reinforcement as a function of the crack width after ten years exposure. Schiessl /1976/

Experiments with chlorides, for example spraying concrete specimens with a 3% salt solution, do not show the same pattern as is the case for CO_2-initiation. Chlorides give rise to a faster penetration and, therefore, an earlier corrosion initiation. Furthermore, the attacks often become deep within a short time and give rise to cracks parallel to the reinforcement due to the volume of the corrosion products, see, for example, Houston, Atimtay and Ferguson /1972/.

It can thus be seen from the experiments mentioned above that the corrosion process is initiated rapidly in crack zones due to an impairment in the permeability of the concrete. When the two different mechanisms are compared, it can be seen that carbonation is somewhat slower than chloride penetration due to the considerable capacity of the concrete for absorbing CO_2. When the crack width is reduced, the convective flows and the diffusion flows etc are reduced due to the dimension factor before finally reaching the same value as for homogeneous concrete. Similarly, a thicker concrete cover gives a longer initiation time due to the dimension factor. An extension of the corrosion attacks in the crack zone could also be noted in all experiments. The extension of the corrosion could also be seen to occur particularly on areas closest to the surface. The same phenomenon occurs if the end faces of the reinforcement do not have a concrete cover. This can only be explained by the fact that in the adhesion between the two phases steel-concrete is impaired and that a crack has been formed.

3.2.2 Model

Cracks which are visible to the naked eye penetrate in most cases all the way into the reinforcement. In such cases the crack width is so large that initiation takes place within a very brief time compared with the life of a concrete structure. Initiation occurs not only in the main crack but also in a smaller area around the crack, for example as a result of the occurrence of a slip zone.

The rate of corrosion after initiation in the crack zone must be low since all concrete structures have visible cracks and yet function satisfactorily after lengthy periods of time. The reason for this, in addition to the fact that the crack is sometimes healed by unhydrated cement etc, is that some substance required for the reactions is often missing.

- Cathodic control caused by low oxygen flows to the cathode reactions. This limitation applies to structures which are completely saturated with water.

- A lack of electrolyte gives rise to a high resistivity and therefore to limited cathodic areas and limited galvanic effect. This applies to structures with a relative humidity < 90% in the pore system, see FIG 68.

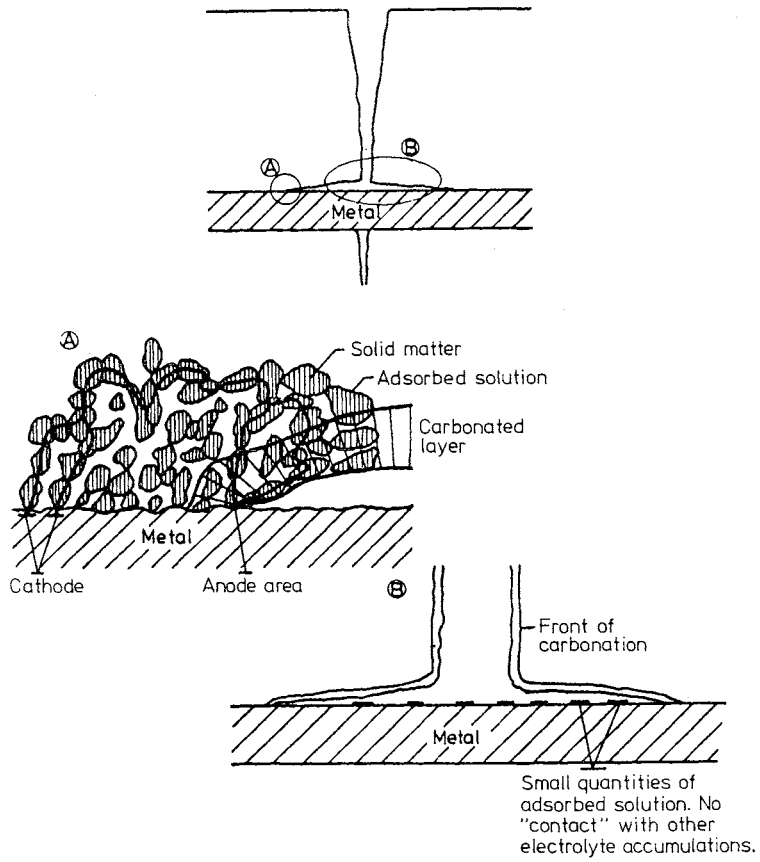

FIG 68. If there is a shortage of electrolyte, the corrosion current is limited by the resistivity of the concrete, and that only adsorbed water and the very small cathodic areas functions as electrolyte.

- Repassivation as a result of the corrosion products seals cracks and voids, whereupon neutralizing substances are kept out and substances which raise the pH value can diffuse to the steel. This applies to initiation through carbonation. This theory has previously been mentioned by other researchers, Schiessl /1976/, see FIG 69.

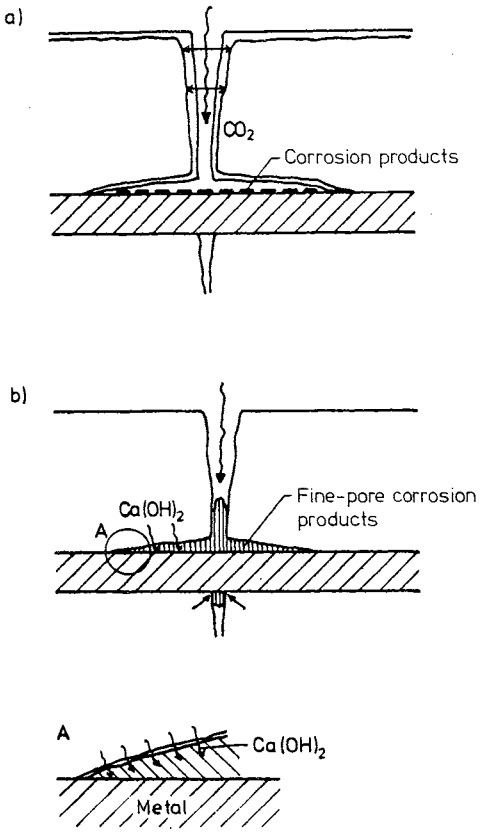

FIG 69. To begin with CO_2 penetrates to the crack and gives rise to a thin carbonation layer. At the same time the moisture is sufficient to cause general corrosion or active-passive cells in the crack zones. Gradually a finely porous non-alkaline corrosion product, which seals the crack, is formed. This phase also binds sufficient quantites of electrolyte to permit an effective ion transport. The concentration differences give rise to re-alkalizing through diffusion.

Cathodic control can be thought of as occurring in connection with chloride initiation since this initiation mechanism occurs in moist environments.

A shortage of electrolyte can be considered to occur in connection with chloride-initiated ($CaCl_2$ admixture) and in connection with carbonation-initiated corrosion.

Repassivation only appears to be possible when no chlorides are present.

The model is summarized in FIG 70.

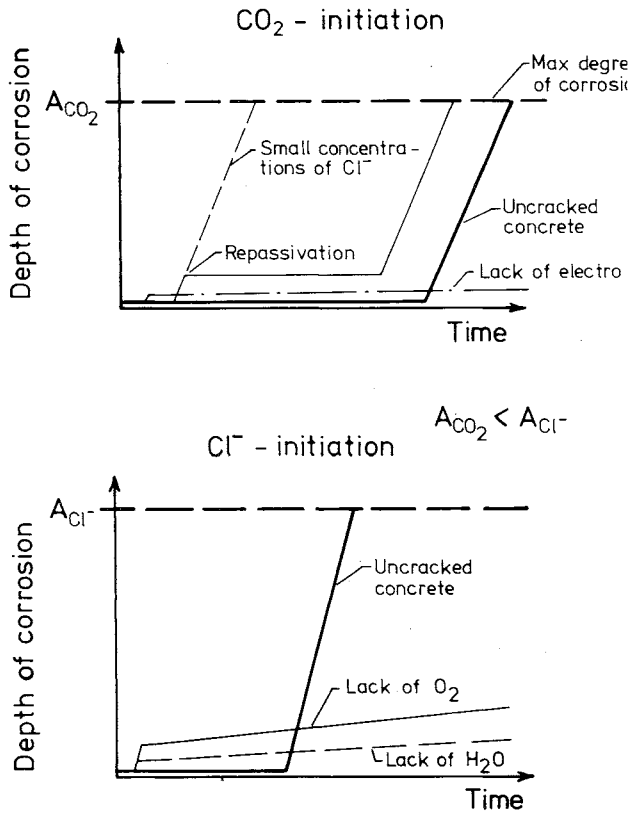

FIG 70. Summary of corrosion model for cracked concrete.

In the case of CO_2 initiation, the steel is repassivated due to the sealing properties of the corrosion products which are increased when the concentration is increased as a result of the diffusion through the rust. Re-

carbonation takes place later on, however, and somewhat earlier than the mean carbonation reaches the steel. The corrosion products only fill part of the crack.

If the concrete is dry, there is no contact between the anode and cathode and, consequently, no corrosion. Carbonation takes place more rapidly, however, in this case.

Note that chlorides can prevent repassivation. If the corrosion process first begins via carbonation, the corrosion current transports chlorides to the anode. This can be sufficient to prevent the retardation of the corrosion process.

In the case of chloride initiation, larger quantities of corrosion products penetrate through the pores than is the case for CO_2 initiation. Consequently, the maximum loss of material due to corrosion is greater in this case, with a reservation however for any reductions in the steel area which are unacceptable from the structural viewpoint. We can also expect the service life of the structure to be shorter in the case of chloride-initiated corrosion partly as the result of the shorter initiation time and partly as a result of the higher corrosion rate.

3.2.3 Cracks - laboratory experiments

Weight loss measurements

Laboratory experiments have been carried out to test if the repassivation theory is possible. At the same time, chloride- initiation corrosion was studied in water-saturated concrete. The experiments were carried out using the previously utilized method of placing two beams against each other and causing cracks in the concrete by means of a bolted joint at either end. The corrosion process was initiated in the largest crack by injecting CO_2. Exposure then began. Samples were taken at various times to check the corrosion area and the mean loss of material due to corrosion. The result can be seen in FIGS 71 and 72.

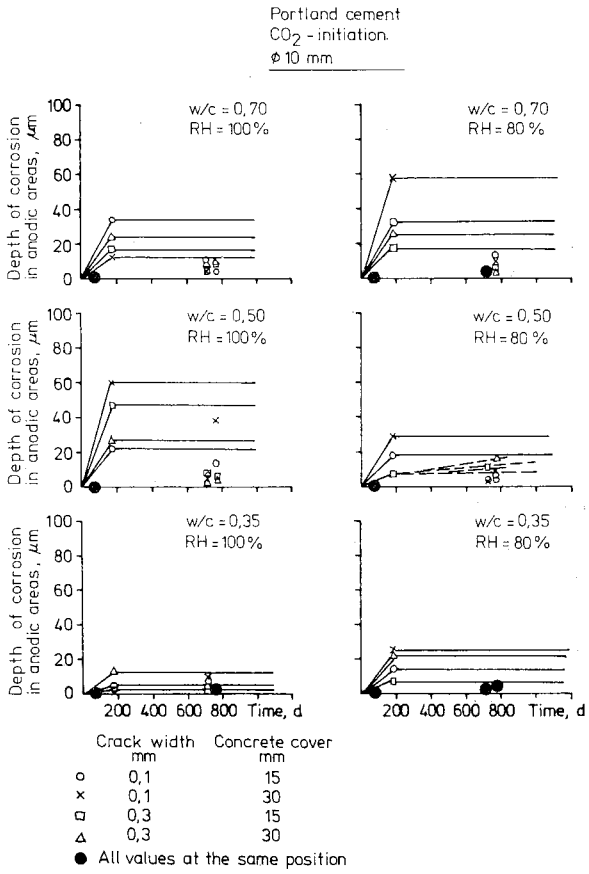

FIG 71. Degree of corrosion as a function of the time for steel embedded in cracked concrete where the time has been calculated from the moment when corrosion initiation took place through carbonation. The curves have been drawn for the maximum corrosion depth, in other words, if a major corrosion attack takes place only at the beginning the curve will, in principle, be horizontal after this time. This makes it possible to see if the process has come to a halt. The accuracy of the measurements is also illustrated in this way.

In a phenolphtalein test it could be noted that the pore solution around the steel and the crack had become basic once again. The weight loss check also indicates that the corrosion process has come to a halt both horizontally and vertically. See also Chapter 5.3.6.

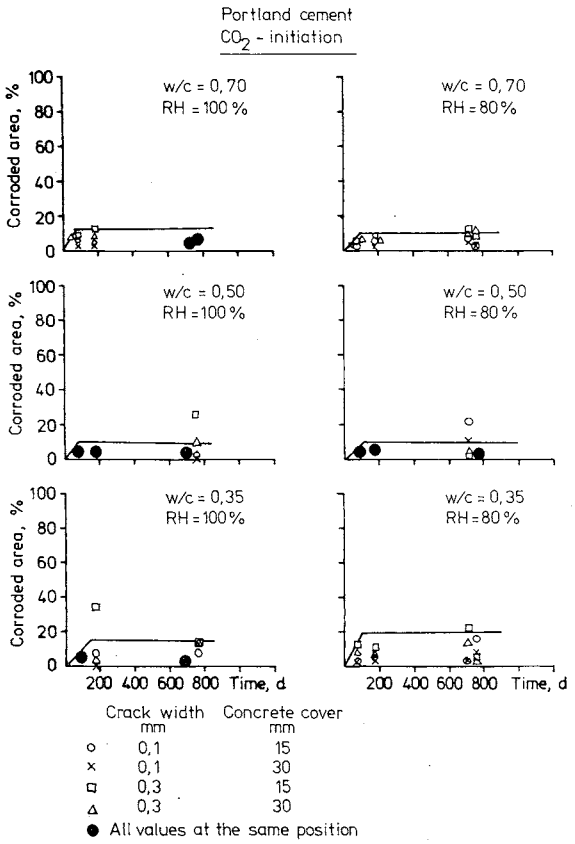

FIG 72 Corroded area as a function of the time for steel embedded in cracked concrete where the time has been calculated from the moment when corrosion initiation took place through carbonation.

Specimens exposed to chloride did not have a sequence which tended to come to a halt. On the other hand the attacks were very small. This makes it difficult to interpret whether the process actually came to a halt or not. The crack width of 0.3 mm also provided a good protection against corrosion.

It should, however, be noted that in addition to the absolute value, the spread of the measured values was particularly large for the specimens in the second batch of measurements. The reason for this could not be determined.

Two years of exposure, however, gave very small attacks compared with the result in Section 2.6.5.

Relative humidities

During simple laboratory experiments it could be noted that the moisture state in the crack zone was roughly the same as that for the homogeneous concrete. Cracks can, however, give rise to higher mean moisture contents due to the fact that they increase the absorption area for concrete during, for example, rain. In the case of small concrete covers for reinforcement, the concrete closest to the steel may dry out more rapidly in the crack zones.

3.2.4 Cracks - practical case histories

Precast concrete elements for balconies, external stairs, columns etc, which had been delivered to a large residential area called Orminge in Stockholm, had been severely damaged (the concrete cover had cracked off) within the course of about 15 years. 0.5 to 1.5% $CaCl_2$ per weight cement had been added to the damaged concrete. The Swedish concrete standards previously permitted this admixture. The concrete cover varied between 12-42 mm. The concrete had a strength between 40-60 MPa. Corrosion damage could be noted at several points despite the fact that the mean carbonation front had not reached the reinforcement. The explanation in this case may be that the carbonation in the surface increased the chloride content at the metal or that a corrosion initiation took place in cracks due to carbonation. No retardation could then take place in the corrosion process since the corrosion content was too high, Molin, Klevbo /1981/.

Hellström /1977/ made similar discoveries for a balcony in Malmö. The chloride content was 1.0% $CaCl_2$ per weight cement. The damage occurred 20 years after the structure had been completed.

The same pattern could be seen in the silo investigation which was presented in Chapter 2.7.4.

Chapter 2.7.4 also included an investigation concerning damaged power line poles. These had a compressive strength of 50 MPa and a concrete cover

of 13-27 mm. They were cracked, and the following observations could be made from the result of the investigation concerning the effects of the cracks. Cracks could be seen on all of the objects involved.

Table 12 below presents a compilation of the crack widths for the cracks which were inspected with regard to carbonation depth.

Table 12. Compilation of crack widths and carbonation depths.

Crack width mm	Carbonation depth mm							Total number of cracks	
	0 5	6 10	11 15	16 20	21 25	26 30	>30	qty	%
0-0.1	1	2	4	5	1	1		14	54
>0.1-0.3	1	1		2		2		6	23
>0.3-0.5	2			1		1	1	5	19
>0.5	1							1	4

No clear interdependency could be noted between the crack width and carbonation depth.

The carbonation depth was measured both in cracks and in undamaged concrete, see Table 13.

Table 13. Compilation of carbonation depth.

Carbonation depth uncracked concrete, mm			Carbonation depth in crack, mm		
Max.	Mean	Spread	Max.	Mean	Spread
19	6.0	4.9	40	15.0	10.1

The carbonation depth in cracks had usually reached the reinforcement or even deeper. Despite this, the reinforcement was not corroded to any noteworthy extent in most cases, see Table 14.

Table 14. Compilation of carbonation and corrosion in cracks

Carbonation depth in crack, mm	Quantity	Distribution of degree of corrosion, quantity			
		0	I	II	III
0-5	4	3	1		
6-10	3	3			
11-15	4	4			
16-20	7	5	1	1	
21-25	1		1		
26-30	3	1	2		
>30	2	1	1		

Degree of corrosion. 0 0.0 mm corrosion product thickness
I < 0.5 " " " "
II > 0.5-2.0 mm corrosion product thickness
III > 2.0 " " " "

No carbonation could be seen in cracks in several of the poles. This was probably due to the fact that water, which was rich in lime and gave rise to lime precipitation as a consequence, ran in the cracks and gave a high pH value. Furthermore, the poles were sometimes washed with lime to remove moss.

Vesikari /1981/ has investigated about 50 bridges in Finland with regard to the danger of cracks from the point of view of corrosion. Very few cracks had given rise to serious corrosion damage despite the fact that many of the structures were 50 years old. The results of this investigation also indicate that the corrosion process is retarded after the first initiation, see Table 15.

Halvorsen /1966/ obtained similar results after an investigation of hydro-electric power plants. These structures were not, however, exposed to chloride-rich water. Instead, extremely pure mountain water was involved.

Table 15. Measured corrosion depth in crack zones Vesikari /1981/. The cracks had a mean width of 0.3 mm.

Corrosion depth at crack (mm)	Number of values (%)
0	89
0-0.1	7
0.1-0.5	3
>0.5	1

3.2.5 Summary

Numerous investigations which have been carried out with the aim of studying the danger of cracks in connection with the corrosion of reinforcement have shown that cracks usually have very little negative effect. One can always feel certain, however, that if the concrete cover around the crack is chipped away corrosion attacks can be seen. These attacks are frequently very small and the corrosion process is dormant until, in principle, the entire concrete cover has changed.

One common denominator can be observed in all the relevant reports and this is that if the concrete pore solution contains chlorides the corrosion process cannot be retarded in the same way as is the case if chloride does not occur. The chloride concentrations involved are not particularly large and quantities as small as 0.5% $CaCl_2$ per weight cement have been sufficient.

Consequently, cracked structures can often be regarded as though they were uncracked. Naturally, this simple rule applies only to a moderate service life for concrete structures, at least 50 years for high-quality concrete and at least 25 years for low-quality concrete located outdoors. Until the opposite has been proved, the rule does not apply to, for example.

- Structures which are exposed to one-sided water pressure in a chloride environment.
  Reason: Different substances are transported at a high rate to the corrosion area, in other words there is no cathodic control, corrosion products are transported outwards and soluble substances are transported out of the concrete. Pure water has not given rise to damage within a reasonable length of time, Halvorsen /1966/.

- Structures which have major movements so that the cracks will vary.
  Reason: The sealing effect and, consequently repassivation, are rendered more difficult due to the movements.

- Structures with cracks larger than 0.3 mm in liquids containing chlorides (Cl^- > 0.5 g/l).
  Reason: A galvanic effect can occur if the environment closest to the steel is neutralized. The alkalinity is retained in very thin cracks.

- Structures which have visible cracks and service life requirements in excess of 50 years.
  Reason: Cracks always reduce the service life of a structure. A more careful assessment is required in these cases.

- Structures in which the concrete cover is less than 20 mm, and particularly structures with porous concrete.
  Reason: Repassivation can be rendered more difficult and take such a long time that damage occurs. Furthermore, several cracks can collaborate

- Cases in which chloride has been added to the concrete or can enter to the reinforcement from the surroundings.
  Reason: The corrosion process is not retarded after re-alkalization. The critical chloride content has not been determined for carbonated concrete.

For obvious reasons the author must make reservations for various special cases. This report is confined to describing how an ordinary concrete structure behaves.

3.3 Cement type - slag

3.3.1 General

An investigation of the properties of slag cement with regard to its capacity for protecting embedded steel against corrosion was carried out at a late stage in the project. Consequently the corrosion model was used when making comparisons between slag cement and Portland cement.

The organization of this subproject can be broken down into four phases, which were intended to provide answers to the following questions:

- do the substances in the cement inititiate corrosion?
- how rapidly is the corrosion process initiated by the usual initiators CO_2 and Cl^-?
- is the propagation time affected by the cement type?
- what effects, if any, does the cement have on the final state?

A comparison, in which the significance of both negative and positive factors have been taken into account, could be carried out by adding the four different phases together.

The following subprocesses have been studied without acceleration so as to avoid erroneous interpretations of the experimental results.

- Initiation
  - carbonation
    permeability - O_2, relation to CO_2 permeability
    bound quantity of CO_2
  - chloride initiation
    permeability - Cl^-
    threshold values - Cl^-
  - sulphide initiation
    threshold values - S^{2-}

- Propagation
  - rate of corrosion in carbonated concrete as a function of the relative humidity
  - rate of corrosion in chloride-initiated concrete as a function of the relative humidity

The final state of the concrete probably has no more than a marginal effect on the service life of the structure when the two cement types are compared. Consequently, no experiments have been carried out with regard to the final state.

It was assumed at the beginning of the project that cracks and sulphides could give rise to accelerated corrosion sequences in the same manner as has been noted in Portland cement concrete which contains cracks and chlorides, i.e. the corrosion initiation is not interrupted when re-alkalization occurs, Tuutti /1978/. The crack effects have been studied in a number of simple experiments in which the relative humidity has been varied.

The experimental methods used in this investigation have been presented in a previous report, see Tuutti /1979b/ or Chapters 5.1.3, 5.2.1, 5.3.2, 5.4.1, 5.5.2.

3.3.2 Initiation - CO_2

Theoretical evaluation

The process of carbonation is simplified by assuming that the pH value profile is discontinuous.

The rate of penetration of the discontinuity point or the carbonation front is affected by

- the ambient concentration of CO_2
- the CO_2 which can be absorbed in the concrete
- the permeability of the concrete with CO_2

When comparing the significance of cement types, the concentration of CO_2 is, of course, the same.

The CO_2 quantity immobilized as a result of the reactions has been measured for both cement types and has been presented in FIG 29. The quantity of bound CO_2 can be set equal to the quantity of hydrated lime which occurs in each layer of the concrete, regardless of the cement type. It can also be seen that the slower rate of reaction of the slag cement leads to very incomplete reactions in the surface layer. This means that about 3 mm of the surface layer of the slag cement concrete does not retard the neutralization to any great extent but merely functions as a diffusion barrier. Furthermore, the carbonation front appears to be less uniform in slag cement concrete.

The permeability of the concrete constitutes the least reliable parameter since the moisture content of the pore system is, in principle, the decisive factor here. The concrete parameters such as W/C are, however, completely decisive in the same environment. An effective O_2 diffusivity has been measured for both slag cement concrete and Portland cement concrete at varying relative humidities, see FIG 73. The slag cement concrete is less permeable than the Portland cement. The diffusitivities used refere to 80% relative humidity when comparing the effects of the cement types on reinforcement corrosion. This value was chosen since initiation through neutralization of the concrete is of interest at a relative humidity of 70-90%. The corrosion rate is limited at lower moisture contents by the lack of electrolyte to such an extent that the attacks are not normally regarded as corrosion. In other words, even if initiation takes place rapidly, the service life of the structure is lengthy due to the very slow rates of corrosion. At very high moisture contents, the neutralization is limited to such an extent that the process is not capable of penetrating a concrete cover of about 15 mm in a period of 50-100 years, in other words the service life of the structure becomes longer than we normally expect.

The rate of penetration of the carbonation front for normal outdoor conditions has been calculated using the measured values as a basis.

The cement contents have been assumed to be 300 kg/m^3 and 450 kg/m^3 for concrete with W/C = 0.70 and W/C = 0.40 respectively.

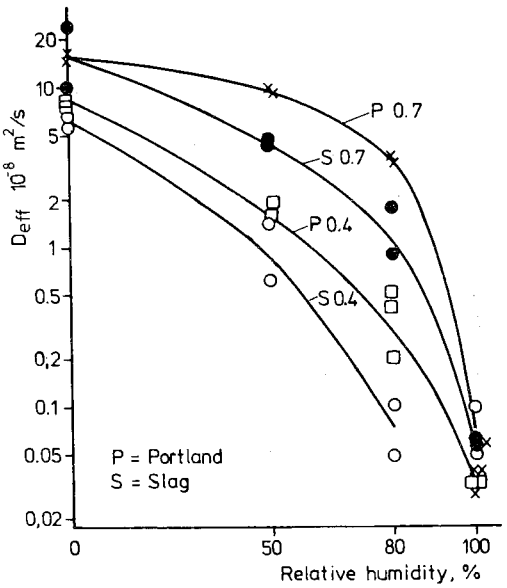

FIG 73. Measured effective diffusivity in slag cement concrete and Portland cement concrete. Age of samples 6-12 months.
The figures indicate the W/C values.
Measured D_{eff} on 10 mm plexiglass = 0.02 10^{-8} m^2/s.
Purity of gas: 4_2ppm 0_2. This gives the lowest measurable D_{eff} as 0.05 · 10^{-8} m^2/s.

The following values have been set for the quantity of CaO included in the reactions; see Table 4 and FIG 29.

80%	of	the	total	quantity	for	Portland cement	W/C = 0.7
60%	"	"	"	"	"	"	W/C = 0.4
70%	"	"	"	"	"	slag	W/C = 0.7
60%	"	"	"	"	"	"	W/C = 0.4

The following diffusivities have been measured for about 80% RH and therefore used in the calculations, see Chapter 5.1.

Portland cement W/C = 0.7; D_{eff} = 3 · 10^{-8} m^2/s
W/C = 0.4; D_{eff} = 0.3 · 10^{-8} m^2/s
Slag cement W/C = 0.7; D_{eff} = 1 · 10^{-8} m^2/s
W/C = 0.4; D_{eff} = 0.1 · 10^{-8} m^2/s

The results are presented in FIG 74. It can be noted there that the negative effects of a generally low lime content and a poorer diffusion barrier in the surface layer of slag cement concrete are balanced by the impermeability of the material if the concrete cover exceeds about 10 mm.

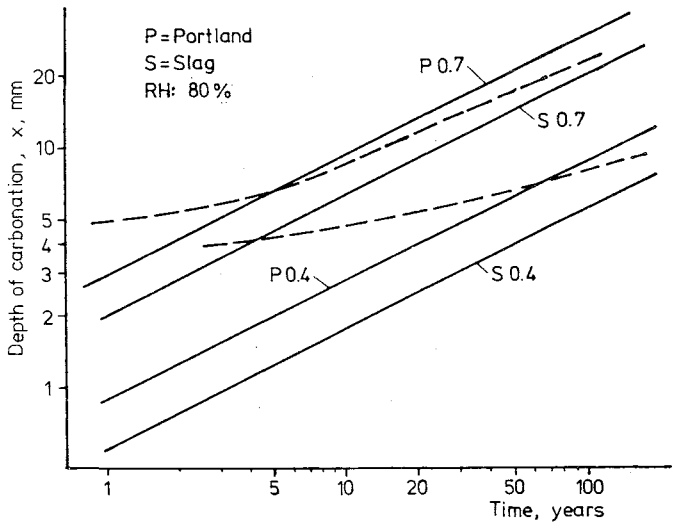

FIG 74. Estimated rate of carbonation in 80% RH. The figures indicate the W/C values.
--- corrected line for slag cement if the first 3 mm are assumed not to participate in the reactions.

Practical evaluation

Theories should always be proved with results from practical case studies. In the same manner as in Chapter 2.5.2, measured carbonation depths for slag cement concretes have been plotted as a function of the time in a log-log chart. In FIG 75 the boundary lines from the Portland cement investigation have also been included. The same pattern as that previously observed can then be noted in this case as well, namely that the values vary within a wide range. The agreement is, however, good for concretes which are sheltered against rain. Carbonation appears to proceed more rapidly, on the other hand, for the concrete exposed to rain with a low W/C ratio.

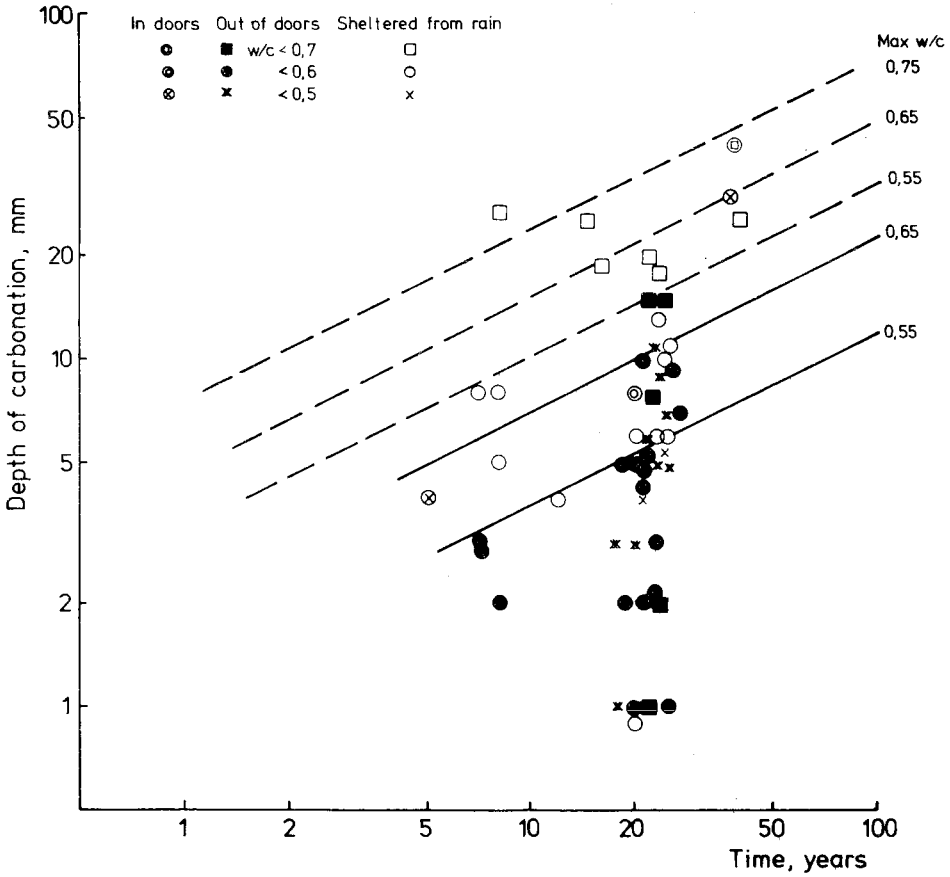

FIG 75. Processed experimental results from DAFS heft 170.

The reason can be a curing effect or the fact that the permeability of the Portland cement concrete at such high moisture contents is still comparable with the permeability of the slag cement concrete, in which case the quantity of lime becomes the decisive factor.

The result thus shows a good agreement with the theory which has been proposed. It should, however, be noted that differences such as slag content, slag composition etc occur between the new Swedish cement which was investigated theoretically and the German cement which dates from the 1950s.

3.3.3 Initiation - Cl^-

It was established in Chapter 2.5.3 that the threshold value increases with increases in the OH^- concentration.

The free OH^- concentration has been determined in the concrete types compared in the presented report by pressing pore solution out of the concrete and by means of microtitration, see Chapter 5.4. The results and, consequently, the threshold values for Portland cement concrete and slag cement are presented in Table 16.

Table 16. Measured OH^- concentrations in pore solution and threshold values for Cl^- calculated with the aid of these concentrations. The OH^- concentrations presented are those measured far from the surface layer where no major leaching of OH^- can be expected.

Cement type	W/C	Concentration OH^- equiv. /l	Threshold value Cl^- g/l
Portland cement	0.4	1.1 ± 0.4	25
	0.6	0.4 ± 0.2	9
Slag cement	0.4	0.3 ± 0.1	8
	0.6	0.1	2

The calculated effective diffusion constants according to Chapter 5.4 are presented in Table 17.

The initiation times for various types of structures can be calculated with the aid of the threshold values and the effective diffusion coefficients. The advantages and disadvantages of different cement types can thus be seen.

Example 1

Assume that a bridge pier with a diameter of 1 m is erected in seawater with a chloride concentration of 19 g Cl^-/l.

Table 17 Effective diffusion coefficients with regard to chloride for different concretes.

Cement type	W/C	$D_{eff}(m^2/s \times 10^{-12})$	Value of D_{eff} used later in various calculations $(m^2/s) \times 10^{-12}$
Portland cement	0.4	0.8 - 5	4
	0.6	4 - 12	7
Slag cement	0.4	0.4 - 1.0	0.7
	0.6	0.6 - 1.0	0.8

The pier can be subdivided into four parts, all of which have different service lives due to different initiation mechanisms:

- The structural part of the pier which is constantly under the lowest water surface is subjected to a gradual leaching of OH^- and penetration of Cl^-. The threshold value for corrosion initiation thus drops due to the reduction in hydroxide concentration. This process can be calculated iteratively with the aid of a computer. Such a calculation has been carried out for a number of different concrete qualities.

  The initiation times become comparatively short, about 10 years, but this has no significance when regarding the entire service life. The corrosion rate is so extremely low in water-saturated concrete that the service life often exceeds 100 years.

- The structural parts of the pier above the water surface are wet so often that one cannot speak of any drying out nor of any leaching of OH^-, although a Cl^- penetration process does occur. The threshold value will not be changed in this case during the period when the chlorides are accumulated. This example has been calculated and the results obtained are presented in FIG 76.

  It can be noted that Portland cement concrete with a low W/C is better in this case due to the high threshold value which occurs. In

fact Portland cement concrete with W/C = 0.40 gives a state in which initiation is impossible due to an insufficient level of surrounding chloride concentration. On the other hand, Portland cement concrete with a high W/C gives poorer results than a corresponding slag cement concrete.

No problem normally occurs, however, with Portland cement concrete or slag cement concrete of good quality; problems occur only when the W/C ratio is comparatively high.

- Structural parts of the pier which occur a step further up, in which a drying-out procedure clearly occurs, will be carbonated and will also absorb water containing chloride by means of capillary suction, although this occurs slowly, whenever the concrete is moistened due to, for example, splashes of seawater. The problem encountered here is extremely complicated particularly if the concrete is cracked to such an extent that a carbonation front can penetrate to the steel in a brief period of time. This particular type of initation is dangerous since chlorides are also present. The re-passivation which normally results when only carbonation occurs in cracks, will not take place in this case. Instead, the corrosion attack will continue unreduced.

- Structural parts of the pier which are located so high that chlorides cannot affect the corrosion process constitute a case which has already been dealt with in connection with the initiation of carbonation.

Finally, all the transition zones between the four sectors dealt with above must also be considered. Case studies have, however, shown that the most dangerous zone occurs just above the water line.

Example 2

The time for the initiation process for a parking deck or a concrete slab with a thickness of 0.5 m, located outdoors and not protected against rain, has been calculated. It has been assumed that road salt has been applied to the slab during the winter season to remove ice, see FIG 77. The chloride concentration can, during many periods, be assumed to be 100 g Cl^-/l, which is about half of the saturation value.

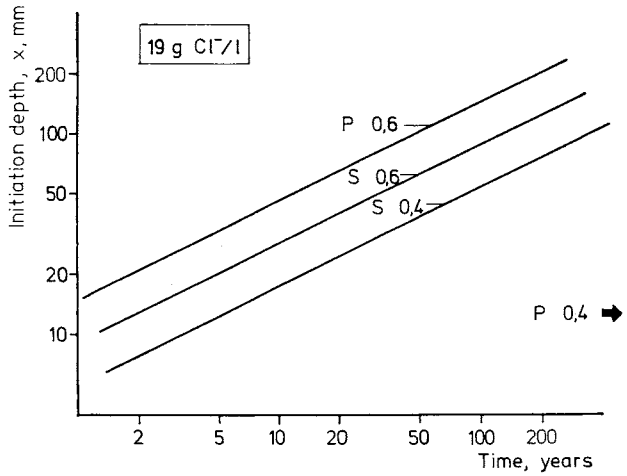

FIG 76. Calculated initiation times with the threshold values indicated in Table 16 and the diffusivities indicated in Table 17 for a concrete which is just above a seawater surface. The chloride concentration has been assumed to be 19 g Cl^-/1. X indicates the depth at which initiation takes place at a certain time, i.e. the thickness of the concrete cover. Note, however, that the threshold value is probably greater for embedded steel in concrete, i.e. the values are, so to speak, on the safe side. The designations P and S mean Portland and slag cement concrete respectively. The figure after this designation specifies the W/C.

This initiation process is more clear-cut than the preceding example since no real carbonation occurs as a result of the constantly high moisture content and the high concrete quality. The rain frequency is so high in Sweden that the slab is moistened at least once every 72 hours.

The conditions become completely different and more dangerous if the slab is located indoors, for example a multi-storey car park in which road salt accompaines the cars when they drive in and in which the concrete is also dry at times. On the other hand, this occurs only during a limited period of the year.

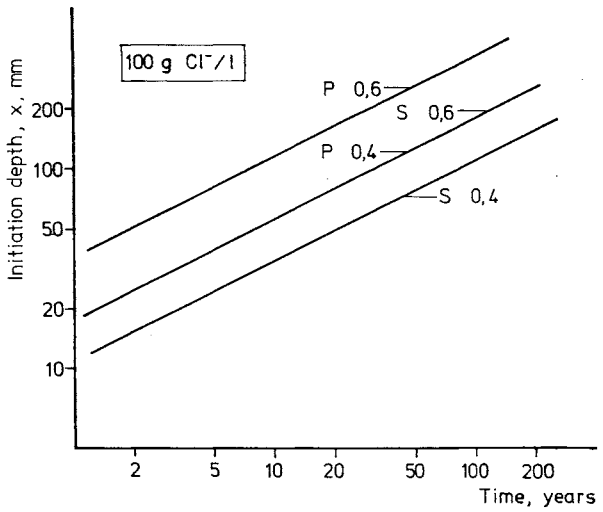

FIG 77 Calculated initiation times with the values indicated in Tables 16 and 17 for a concrete exposed to salt during winter de-icing (NaCl).

In this case, slag cement concrete is a better choice than Portland cement concrete regardless of the W/C value of the concrete.

These two examples show that the corrosion problem is considerably more complicated in chloride environments, since such a large number of factors play a decisive part.

As a result, one cannot draw up any general rule saying that one cement type is better than the other. A careful analysis must be carried out for each individual case.

3.3.4 Sulphide initiation

A simple experiment in a simulated pore solution is presented in Chapter 5.5 with a view to studying the initiation process. In those specimens which contained sulphides with the same concentration as that measured in slag cement concrete, there were no indications that the sulphides had a corrosion initiating effect. Instead, the negative S ions appear to inhibit the decomposing effects of the chlorides.

Possible sulphide initiation has also been studied by means of electrochemical cells which have been developed by the Swedish Corrosion Institute. These cells are particularly useful for recording the initiation time.

In addition to the effects of the sulphides, it is also possible that the chemical contents of the pore system are changed in a manner which differs from that which applies to Portland cement when the material is neutralized.

In order to study this, the specimens were first water cured for 14 days and then conditioned for about 400 days in 50% relative humidity, i.e. the materials were permitted to carbonate.

Before the carbonation front had reached the corrosion cells, the specimens were placed alternately in water and in air. This made it possible to see if the corrosion process had been initiated. The corrosion process was only initiated in the cell which was cast in slag cement concrete with W/C = 0.7 and concrete cover = 15 mm. See Chapter 5.2.3. A carbonation depth of about 10 mm was measured before the corrosion test was started. A carbonation depth of about 2 mm was measured on the same specimen after the first moisture curing period. In other words, the re-alkalizing which can be expected in connection with moistening had occurred. The corrosion process had not, on the other hand, yet been stopped and continued at an unreduced rate. One can speculate about what caused the corrosion initiation. The most likely answer appears to be that the carbonation penetrated to the metal surface through small cracks and gave rise to the attack. An uneven carbonation front of this type is also indicated by the experimental results presented in FIG 29. The chemical composition of the pore

solution which occurs in slag cement concrete will probably stop the corrosion process when the surroundings have become sufficiently basic again, cf. Chapter 3.2 on cracks.

Neither sulphides nor carbonated surface layers proved capable of starting the corrosion process in slag cement concrete with W/C = 0.4.

3.3.5 Propagation state

In FIG 58 the rate of corrosion was up to 5 times higher in slag cement concrete which had been carbonated compared with Portland cement concrete. This means that the corrosion period, which is normally 15-20 years in Sweden in Portland cement concrete, is reduced to about 5 years for slag cement concrete for normal qualities.

No difference could be noted in the corrosion rate between Portland cement concrete and slag cement concrete in connection with chloride initiation. The corrosion rate was, on the other hand, high.

3.3.6 Final state

It is assumed that the final state does not differ in any noteworthy manner between concrete with Portland cement and concrete with slag cement, i.e. the porosity immediately adjacent to the metal surface and the permanent strain after rupture of the concrete cover are assumed to be equal.

It could be noted for Portland cement that small attacks, approximately 0.1 - 1.0 mm Fe, caused cracks in the concrete cover.

3.3.7 The effect of cracks

The description of the model deals with the corrosion of steel in uncracked concrete, i.e. concrete without visible cracks.

Re-passivation in conjunction with carbonation initiation is the factor of primary interest when comparing Portland cement and slag cement. Will this re-passivation occur or will the sulphides or other substances in the pore solution prevent the process?

Specimens were cast and loaded so that cracks occurred and were carbonated. Corrosion attacks were initiated in crack zones. The specimens were then exposed to 50, 80 and 100% relative humidity during a period of 800 days. The corroded area and the quantity of metal consumed due to corrosion were measured during this period. The results in FIG 78 show that the corrosion rate is high locally during a brief period just after initiation and that the corrosion process then comes to a halt until the pore solution adjacent to the metal surface has become neutralized again. The process thus follows the same pattern regardless of which of these two cement types has been used. It should, however, be noted that the investigation embraced concrete with W/C = 0.50 only.

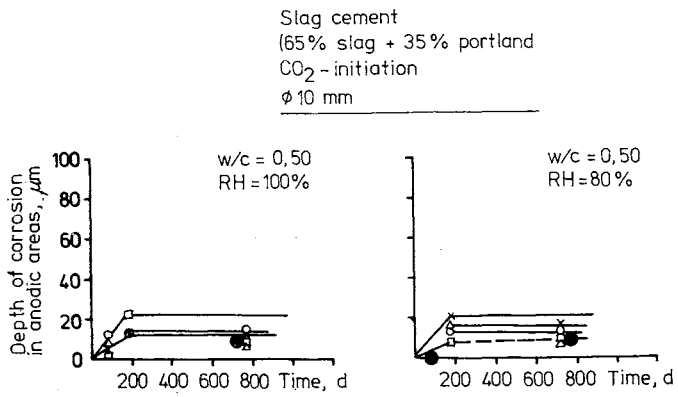

FIG 78. Mean depth of corrosion for smooth bars in cracked slag cement concrete with varying exposure times.

3.3.8 Summary

Slag cement concrete gives the same results as Portland cement concrete when compared with the same W/C, normal concrete covers $\geq$20 mm and old specimens. The higher impermeability of the slag cement concrete compensates for the negative effects of its poorer capacity for binding CO_2 and its low grade of reaction in the surface layer. The carbonation front appears, on the other hand, to become more uneven in this slag cement

concrete, but this is not noticeable in the case of normal concrete covers. It should, however, be noted that slag cement concrete is extra sensitive to carbonation at an early age due to the slow rate of reaction of the cement.

Slag cement concrete is sometimes better than Portland cement concrete in connection with chloride initiation due to its considerably lower permeability. On the other hand, Portland cement concrete may be better than slag cement concrete due to its higher threshold value for Cl^-. The environment closest to the structure is the determining factor.

The sulphides in the cement included in this investigation have not been shown to initiate the corrosion process.

Slag cement concrete is not more sensitive to cracks than Portland cement concrete with regard to reinforcement corrosion. The materials appear to be similar in this regard.

By way of summary we can say that factors other than the cement type determine the service life of a concrete structure. The initiation time is affected by the choice of concrete quality, concrete cover etc, so that the service life lies somewhere within the range 0 - 1 000 years, see FIG 79.

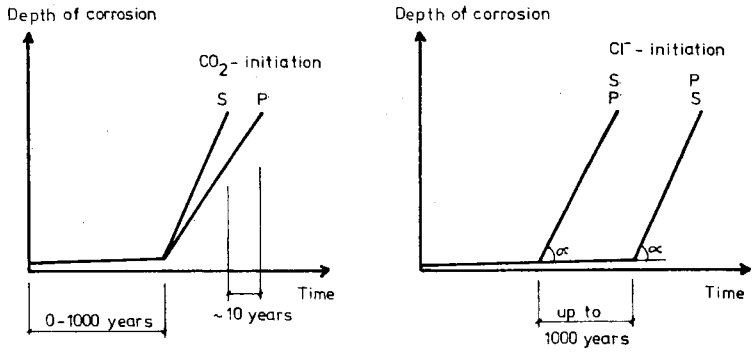

FIG 79. The service life with regard to reinforcement corrosion is mainly influenced by the concrete quality selected and by the concrete cover. The choice of cement type usually has no more than marginal effects. In certain situations Portland cement may be preferable to slag cement and vice versa.

4 RECOMMENDED METHOD FOR PREDICTING SERVICE LIFE

4.1 General

Various comparisons have already been made several times in this report, for example, the effects of the cement type, the effects of the W/C ratio etc. Generally speaking, it is always easier to make comparisons since one can determine, on the basis of published results or by means of measurements, which of the compared objects is best. It is considerably more difficult, on the other hand, to specify precisely how long a structure will be serviceable. A better assessment of the service life of reinforced concrete in various environments than that obtained by means of qualitative guesses only is, however, achieved by subdividing the service life into an initiation stage and a propagation stage, as presented here, and with the aid of the approximate interdependencies which have also been discussed in the report. A repetition of the interdependencies, figures and coefficients which can be used is presented below.

4.2 Method - values for material coefficients

Step 1 Compile the relevant material, structural and environmental data

In order to obtain an overview of the problems and as a use for later calculations it is always valuable to compile the necessary information. Furthermore, better information should be obtained from measurement results for the structure which is to be assessed compared with certain assumptions from previous laboratory experiments, where all the conditions and prerequisites may not have been identical.

Material data:

- W/C
- Concrete cover (min, max, mean)
- Cement type (CaO, Na_2O, K_2O)
- Occurrence of cracks
- Crack width
- Conditioning after casting
- Total chloride content in constituents

Content of other corrosive substances in constituents (SO_4^{2-} Br^{2-} etc)

Comments:

Longitudinal cracks with a greater width than 0.1 mm should not be accepted since uncertainty still prevails concerning how dangerous such cracks are. Cracks at right angles to the reinforcement are also difficult to assess if the width exceeds 0.3-0.5 mm. Cracks of this magnitude are sometimes harmless but sometimes give rise to a rapid corrosion attack. It is difficult to assess conditioning but it can be established if fully satisfactory water curing or membrane curing has been carried out or if the structure has been permitted to dry at an early stage. It has not been possible to define permissible contents of other corrosive substances but their danger should be known.

Structural data:

The dimensions of the structure.
The dimensions of the reinforcement.
Do attacks occur in two or three dimensions for part of the reinforcement.
Beam or slab.
Column, circular or angular.
Protection against the penetration of substances by means of diffusion-proof membrane, brick etc.
Electro-chemical protection.

Comments

Large structures have a higher inertia and are thus often provided with a better protection against various types of attacks.

It is possible that carbonation takes place more rapidly in corners than along a plane surface. Consequently, beams are more sensitive than slabs.

There are many different types of protection. It should, however, be borne in mind that these do not last forever but that they can provide outstanding functions for 20-30 or more years.

In many cases electro-chemical protection means that attempts have been made to eliminate the corrosion risk. Subsequent inspections are, however, recommended.

Environmental data: Content of CO_2 in the surroundings.
Content of Cl^- in the surroundings.
The moisture state (not sheltered against rain, sheltered against rain).
Temperature.
The content of very corrosive substances.
The risk of acid attack or chemical attack.
The risk of frost attack.

Comments

The content of other substances which can give rise to corrosion attacks is not dealt with in this report. If a chemical attack occurs, this mechanism will undoubtedly be decisive unless the quantities of chemicals involved are very small or unless the structure is exposed during no more than a brief period. The chemical resistance of the structure must, however, be investigated first. If there is a risk of frost attack, the concrete must be frost- resistant and this can be documented.

Step 2 Calculate initiation time

Carbonation

Theoretical evaluation with results for laboratory experiments

1. The quantity of bound CO_2 is adjusted to the quantity of reacted CaO. The quantity of CaO is obtained from the analysis of the cement content. The degree of hydration is obtained from Table 4.

Alternatively, laboratory experiments similar to those described in Chapter 2.5.2 in the report are carried out for the cement in question.

2. The permeability of the concrete vis-à-vis CO_2 can be approximated to values in accordance with FIGS 30 and 31.

   Alternatively, the effective diffusion coefficient can be measured.

3. The shortest possible initiation time is obtained if Equation 3 in Chapter 2.5.2 is solved with the aid of the material data provided above.

   In the case of two-dimensional sequences, the rate is increased by a factor of 1.5.

Theoretical evaluation with the aid of practical case studies

The shortest possible initiation time is read off in FIG 23 with the aid of the necessary material data.

Survey of state of structure for which the service life is to be calculated

The absolutely simplest and most reliable method is to measure the carbonation depth in various parts of the structure at any time after an exposure of two years.

The value thus obtained provides a summary of the impermeability of the concrete when all other factors have been in cluded, in other words the result of a non-accelerated test in the relevant environment.

In the case of CO_2 initiation, these items of data are plotted in a figure for CO_2 penetration, for example FIG 23. A curve is then drawn through the plotted value which is parallel to the other curves.

Chloride initiation

Theoretical evaluation with results from laboratory experiments

1. The relation between bound and free chloride is mapped out. A factor of $k_d = 0.7 \frac{\text{free chloride (g/l)}}{\text{bound chloride (g/kg cement)}}$ can be used for Slite Portland cement.

2. The penetration of chlorides and the total chloride content in the concrete are mapped out.

   A. Original chloride content from constituents.
   B. The slowest possible penetration occurs through diffusion. Effective diffusion coefficients are taken from Table 6.

3. The hydroxil concentration in the pore solution is calculated as indicated in Chapter 2.5.3.

4. The threshold value is adjusted to the value obtained from FIG 37.

5. FIG 45 is used to calculate when the threshold value for free chloride is exceeded.

Laboratory experiments can, of course, also be based on other types of materials. It is important to know that the most uncertain factor in this calculation is the threshold value.

Mapping out the state of the structure for which the service life is to be calculated

As was the case for carbonation, this is the best method for measuring the relevant concentrations of OH^- and Cl^- in the pore solution and for measuring, with the aid of potential measurements or some other electrochemical method, any corrosion initiation which may have occurred and determining, if possible, the threshold value.

If the threshold value cannot be determined, FIG 37 is used.

The continued sequence of chloride penetration or reduction in OH^- concentration is then calculated since D_{eff} is known.

Step 3 Calculate the relevant corrosion rate in the propagation stage

The corrosion rate at 20°C can be taken from either FIG 56 or FIG 59. If uncertainty prevails concerning the moisture state, the following values can be assumed (these apply at approx. +10°C):

Indoors = no corrosion

Concrete constantly saturated with water = no corrosion

Other concrete outdoors

CO_2 initiated corrosion approx. 50 µm/year

Cl initiated corrosion approx. 200 µm/year

The maximum attack is about 5-10 times larger than the above mean attacks.

The values must be corrected in accordance with FIG 57 for temperatures other than those specified above.

Step 4 Calculate the maximum corrosion depth

Due to its sensitivity to reductions in area, prestressing reinforcement should not be permitted to corrode, in other words the corrosion depth is 0 and the propagation time is 0.

In the case of non-tensioned reinforcement, the relevant dimensions for the reinforcement and the concrete cover are used for calculating the maximum corrosion depth with the aid of FIGS 63 and 64.

If uncertainty prevails concerning the theoretical background, emperical values can be used for the propagation time until damage can be observed as indicated below (concrete cover $\geq$ 20 mm and temperature approx. + 10°C)

CO_2 initiated corrosion = 15-20 years

Cl initiated corrosion = 5-10 years

These values must be corrected in accordance with FIG 69 for temperatures other than $+10^{o}C$.

Step 5 Compile the initiation time and the propagation time

The service life or the function life consists of the sum of the initiation time and the propagation time. The effects of cracks (if any), special conditions etc must also be added in accordance with the methods indicated previously.

4.3 Comments on above calculation method

It is not the author's intention that the method described above should provide a precise calculation of the service life. The method does, on the other hand, act as an aid which is better than mere guessing. It has also been the author's intention to provide a method which can be used for determining the shortest possible service life, the method provides values on the safe side. The report includes applications of the methods in various forms, see in particular Chapters 2.5.2, 2.5.3 and 3.3.

5 LABORATORY STUDIES

5.1 Measurement of oxygen diffusion coefficient for concrete

5.1.1 General

The pore solution in concrete is highly basic from the beginning and thus provides embedded steel with a good protection against corrosion. Concrete which is, for the most part, in contact with air will, however, gradually become neutralized. As a result, its capacity for providing protection against corrosion will cease. The neutralization of the concrete usually takes place through CO_2 gases penetrating the material and carbonating the concrete. The carbonation process is a combined diffusion process of penetrating CO_2 and OH^- which diffuses outwards due to the difference in concentration on both sides of the front to which carbonation has reached.

The rate of penetration of the carbonation front is dependent on, inter alia, the level of gas tightness of the concrete. The effective diffusion coefficient for O_2 has been measured in a number of different mixes so as to study the effect of various parameters on the gas tightness of the concrete. Major difference do, admittedly, exist between O_2 and CO_2 gases, for example their solubility in fluids, their molecular size etc, but it should be possible to obtain a relative measure of the rate at which the carbonation process proceeds by means of values for the O_2 diffusivity. The CO_2 diffusivity in concrete cannot be measured in the same way since the concrete chemically reacts with large quantities of CO_2 gas.

The effective diffusion coefficient for O_2 in concrete also has a directly decisive effect for the rate of corrosion of steel in concrete. This is so because oxygen is an essential substance for the progress of the cathode process. It has, for example, been established that concrete structures which are always completely saturated with water are not destroyed by reinforcement corrosion, even if corrosion initiation has taken place at an early stage. Consequently, it is of interest to compare the O_2 diffusivity of concrete in a fully saturated state and at different moisture conditions.

5.1.2 Diffusion

General

The flow through a material of a certain quality is directly proportional to the product of the diffusivity and the concentration gradient.

In the case of gas diffusion caused by partial pressure differentials in a hetero-capillary pore system, the complex flow can be subdivided into three different modes of diffusion:

- molecular diffusion
- surface diffusion
- volume diffusion

Molecular diffusion occurs only in material with very fine pores, where the movements of the gas molecules are inhibited more by the pore walls than by the medium which the pores contain. In material such as concrete with pores ranging from a few Å to several mm, the volume diffusion determines the rate for gases which are not adsorbed to the pore walls, while the surface diffusion can be large for gases which are adsorbed. Consequently, care should be observed when converting the effective diffusion coefficient of oxygen to that of other gases.

O_2 diffusion characteristics

The mobility of oxygen in water is determined by the partial pressure in the ambient air and by a constant which is dependent on the temperature. This interdependency is called Henry's law. Similarly, the mobility of the molecules, in other words, the diffusivity, is dependent on the temperature and on the dynamic viscosity of the liquid. Oxygen has a low solubility in water and its mobility is limited by the comparatively high density of the water. The conditions in the gas phase are quite different. The concentration can be high and the diffusivity can be between 10^4 and 10^5 times greater than in liquid.

O_2 in concrete

A covering layer of concrete is comparatively thick compared with, for example, protective paints on steel structures. On the other hand, concrete has a lower level of homogeneity due to, for example, micro-cracks, pores etc. Oxygen must thus diffuse partly through a liquid phase and partly through a gas phase if the concrete is not saturated with water but is in equilibrium with some relative humidity.

The pore system of the concrete can be illustrated approximately in accordance with FIG 81.

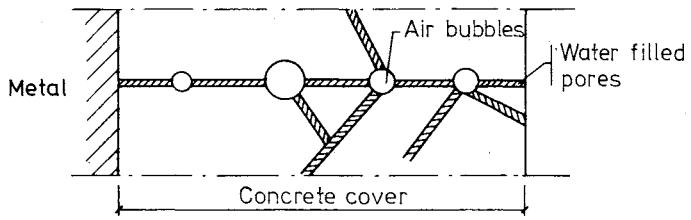

FIG 81. Basic sketch of pore system of the concrete.

Since no noticeable transition resistances occur between the two phases (water versus air under stationary conditions) the water and air phase can be combined to one unit each, see FIG 82.

For normal diffusivities, the mass transfer coefficient, K, for the two phases can be written:

$$K = \frac{D\ c}{\delta}$$

Where D = diffusion constant
c = concentration
δ = distance

$$K_{H_2O} = \frac{10^{-7}}{\delta_{H_2O}} \quad ; \quad K_{air} = \frac{8 \cdot 10^{-7}}{\delta_{air}} \ (kmol/m^2 s)$$

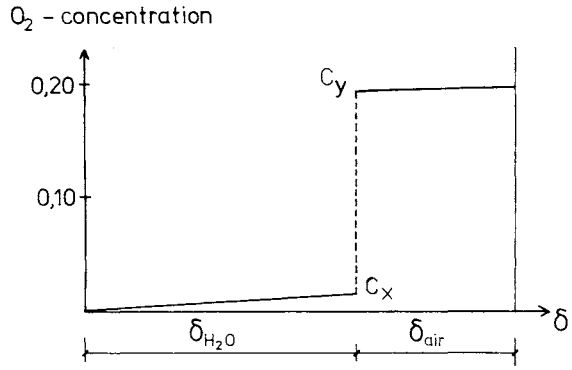

FIG 82. Basic concentration profile of the oxygen contents of the covering layer (Svedberg pers. comm)

Furthermore, Henry's law applies: $c_y = m \cdot c_x$ where m is a temperature-dependent constant. The local diffusion resistance can then be calculated as follows:

$$\frac{1}{K_{total}} = \frac{1}{K_{air}} + \frac{m}{K_{H_2O}} = \frac{\delta_{air}}{8 \cdot 10^{-7}} + \frac{4 \cdot 10^4 \ \delta_{H_2O}}{10^{-7}}$$

The gradient for the concentration is thus considerably greater in the water phase, in other words almost all the resistance occurs in the water phase.

The diffusion resistance of the concrete is thus determined by the water saturation of the concrete cover and by the cross-section of the open pores which are not filled with water. Or, in other words, by the concrete's porosity, pore size distribution, pore form and ambient relative humidity.

A purely theoretical calculation of the permeability of various concrete covers for different concrete qualities etc is not possible due to the complexity of the concrete with regard to pore structure, degree of pore filling etc. Consequently, measurements were carried out on O_2 diffusion through concrete. The principles for this measuring system have previous-

ly been presented by other researchers such as Ludvig and Därr /1973/. The measuring equipment did, however, have a higher degree of accuracy in the experiments referred to here.

5.1.3 Experimental apparatus, specimens

The experimental apparatus consisted of a diffusion cell, a humidifier, extremely clean nitrogen in tubes (maximum 5 ppm O_2 in the gas), air in tubes, a U-tube manometer of glass and an oxygen meter. The equipment was connected as illustrated in FIG 83.

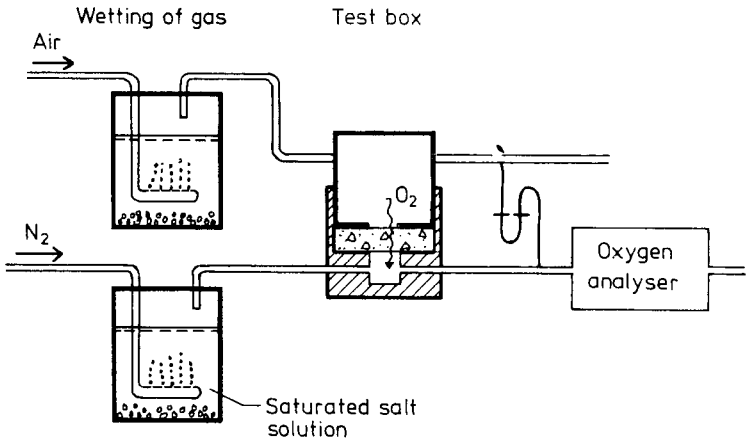

FIG 83. Method to measure the gas diffusion through concrete.

The diffusion cell consisted of a nickel-plated steel vessel illustrated in FIG 84. The concrete specimen was placed in the cell in such a way that it had air on one side and extremely clean nitrogen on the other. The seal was achieved by means of thin rubber gaskets and a jack which created a pressure of 4 MPa on these gaskets.

The tests were carried out with 0.005 MPa excess pressure in both chambers to avoid error sources and leakage. All tubes consisted of stainless steel. A thick PVC hose with the shortest possible length was used at the transition between the glass and the steel.

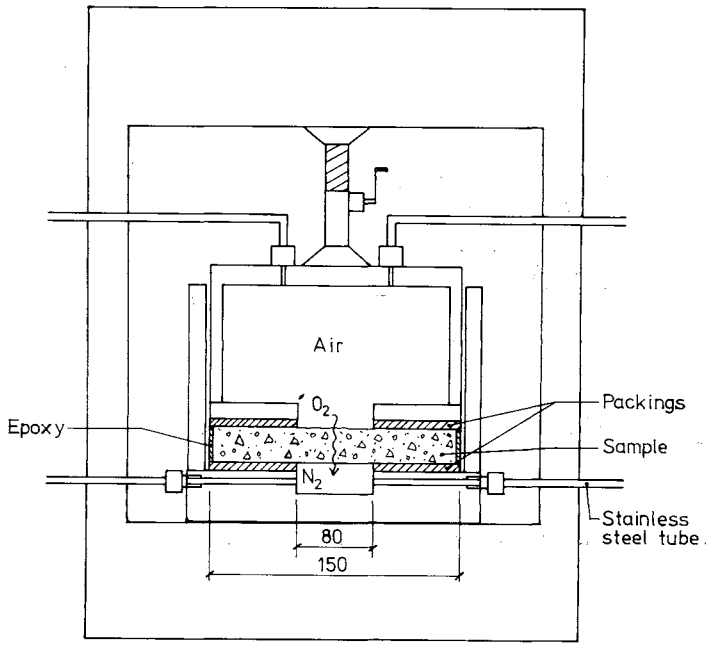

FIG 84. Sketch of diffusion chamber

The analysis with regard to O_2 was carried out with an apparatus in which a constant gas flow passed through a zirconium tube. The measurement accuracy was said by the manufacturer to be at least 0.1 ppm O_2 for the gas which passed through the tube. The apparatus used in these experiments had been tested to ppb level.

The investigation was carried out on concrete slabs of varying thickness but with the same diameter, 150 mm. The concrete slabs were obtained by drilling them from larger specimens then cutting the drilled cores and face grinding the discs thus obtained. The discs were taken in almost all cases from the layer which had been closest to the ambient area. In other words, every effort was made to imitate the treatment and permeability of a concrete cover for reinforcement.

The specimens were conditioned at least 6 months in different climates so that the measurements would represent concrete which had almost reached its final or maximum degree of hydration.

Information on the consituents and concrete is presented in Appendix 1 (Cement analysis), Appendix 3 (Grading curves) and Appendix 4 (Data on fresh and hard concrete).

5.1.4 Results

The measured oxygen flux through the different concrete specimens have been converted to effective diffusion coefficients by means of the following equation according to Fick:

$$J = A\, D_{eff} \frac{dc}{dx}$$

where J = O_2 flow per time unit
A = flow area
D_{eff} = effective diffusion coefficient
$\frac{dc}{dx}$ = concentration gradient

Values for all variables and measured diffusion coefficients are presented in Appendix 5. The effects of the various parameters on the diffusion coefficient are illustrated in FIGS 85 - 89.

5.1.5 Discussion

Varying the composition of the concrete, for example air entrainment, particle size, consistency etc does not have any noteworthy effect on the the concrete permeability, see FIG 86. More permeable concrete is, on the other hand, obtained by means of vacuum treatment. Concrete from the upper surface of a tall wall has a higher diffusion coefficient than parts lower down. These latter effects are mainly due to differences in the porosity of the concrete. This also applies to concrete with 1.5% $CaCl_2$ admitted which gives a minor improvement in the permeability.

Another porosity effect is presented in FIG 85 where the W/C has been varied. The values for the highest and lowest W/C give a difference of a power of 10 with regard to the permeability but a difference of no more than a factor of about 4 with regard to the strength. The improvement in permeability is thus greater than increase in strength for a reduction in the W/C. This is due to the smaller share of capillary and open pores which occurs when the W/C is reduced. It should be noted, however, that the curve is continuous and does not show any marked increase in D_{eff} for W/C = 0.60 as has been indicated by the measured values for the carbonation depth in practical structures, see FIG 34.

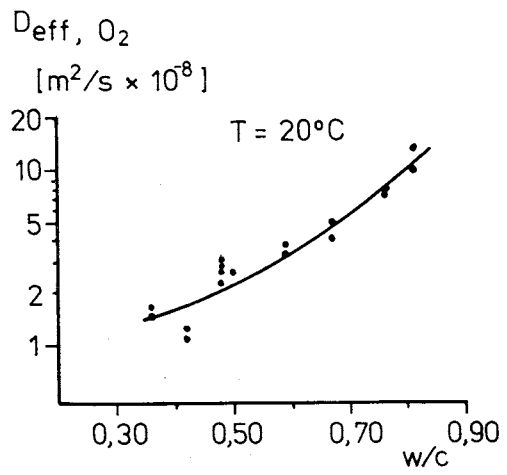

FIG 85. Measured effective diffusion coefficient for O_2 as a function of W/C. The cement type was Slite Portland cement. The measurement was carried out at 20°C and 50% RH. Specimen age approximately 1 year.

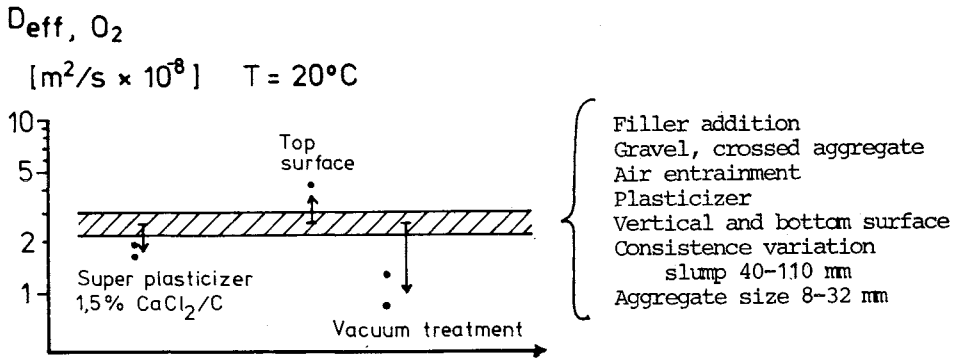

FIG 86. Measured effective diffusion coefficient for O_2 and the influence of different variables. The cement type was Slite Portland cement. The measurement was carried out at 20°C and 50% RH. Specimen age approximately 1 year.

Variations in the thickness of the concrete layer between 10 and 50 mm appear, according to FIG 87, to affect the permeability more than do the W/C variations. One should, however, be aware that variations in the concrete cover entail the following:

- a thicker concrete cover gives better moisture curing and, therefore, a higher degree of hydration.
- the quantity of open pores must decrease when the degree of hydration increases and the thickness increases.
- the degree of pore filling might, perhaps, have been different for thicker concrete covers despite the fact that the specimens were permitted to dry out for about 6 months.
- a thinner specimen would also have been more inclined to crack, particularly at the phase limits between aggregate and paste.

FIG 87 thus presents the combined effect of a large number of different mechanisms on the permeability of the concrete. On the other hand, the same conditions apply to a concrete cover in a normal structure.

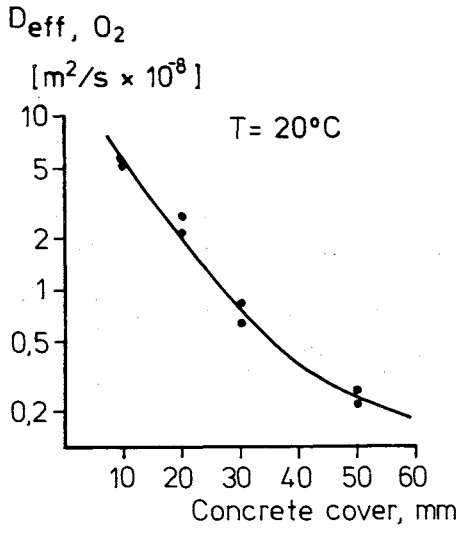

FIG 87. Measured effective diffusion coefficient for O_2 as a function of the thickness of the specimen. The cement type was Slite Portland cement. The measurement was carried out at 20°C and 50% RH. Specimen age approximately 1 year.

The most important parameter with regard to the diffusion of oxygen in concrete is the moisture content or degree of pore filling of the concrete. This agrees with the theoretical discussion presented previously, see FIG 88. The greater the moisture content of the material the more difficult it is for the oxygen to penetrate the concrete. Moisture curing is significant in this context since even as low a value as 80% relative humidity during the conditioning has considerable effects. The moisture curing during the first phase is thus a factor of greater importance for the permeability of the concrete cover and, consequently, for its resistance to penetration against CO_2, than for the strength effects obtained from the moisture curing.

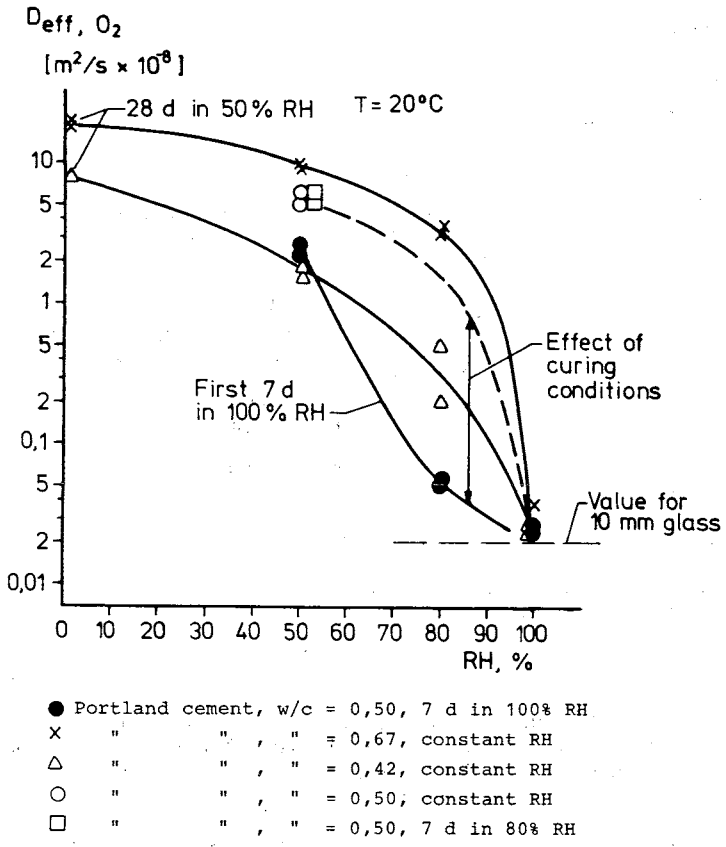

FIG 88. Measured effective diffusion coefficient for O_2 with varying conditioning and moisture state. The cement type was Slite Portland cement. The measurement was carried out at 20°C. Specimen age 6-12 months.

Finally, FIG 89 shows the significance of the cement type for different diffusion coefficients. Slag cement gives a lower value throughout despite the fact that the porosity can be said to be of the same magnitude. The larger hygroscopicity of slag cement probably plays some part in this. Slag cement has a low permeable pore system at a relative humidity as low as 80% and a W/C = 0.40 as a result of pores sealed with liquid. It should also be noted that the strength was considerably lower throughout for the slag cement concrete when compared with pure Portland cement concrete with the same W/C.

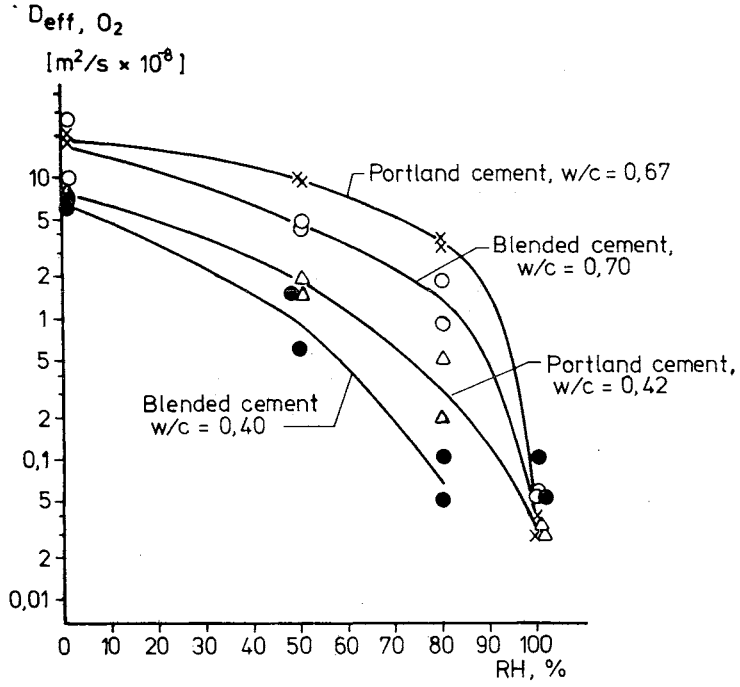

FIG 89. Effective diffusion coefficient for O_2 for Slite Portland cement and slag cement (65% slag + 35% Portland) concrete. Temperature 20°C. Specimen age 6-12 months.

An inititial theoretical consideration of O_2 diffusivity in completely water saturated and completely dry concrete respectively might be expected to result in a difference on an order of size of 3-4 times the power of 10. It has not been possible to establish this in the studies. Despite increased

accuracy in the measurements, the content of nitrogen gas amounting to 5 ppm O_2 may have been too high for the water saturated concrete. Water saturated specimens gave the same values as were obtained from measurements on a 10 mm thick plexiglass sheet. Furthermore, it is possible that a liquid-filled pore system may have less physical effect than a gas-filled pore system since it is more difficult for the gas molecules to pass through the denser liquid medium, in other words the free medium wavelength of the molecules is different in the two media.

5.2 Corrosion investigations with corrosion cells

5.2.1 General

The atmospheric corrosion of various metals has been studied at the Swedish Corrosion Institute. A corrosion cell for measuring the corrosion current under different environmental conditions was developed for this purpose, see Kucera and Collin /1977/. The design of the cell is illustrated in FIG 90.

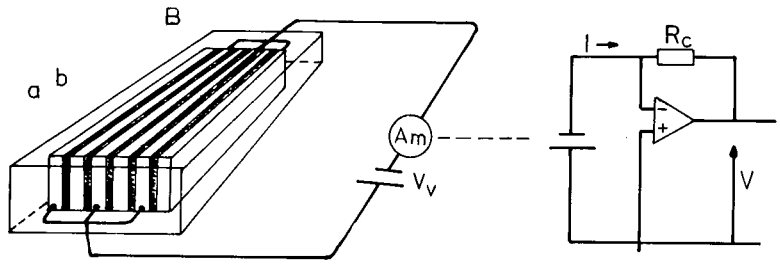

FIG 90. General arrangement of electrochemical device for measurement of atmospheric corrosion:
Am zero resistance anmeter, the circuit of which is shown to the right
B electrochemical cell of electrolytic type
a electrodes b insulators
V_v external emf.

Thin steel plates with a thickness of 1 mm were assembled and insulated from each other by means of a thin plastic film of polycarbonate with a thickness of 0.1 mm. The cell was then cast into epoxy, after which one surface was exposed by means of grinding so that the edges of the steel plates came in direct contact with the corrosion medium. The corrosion process was controlled by means of an external voltage source so that a minor difference in potential occurred between adjacent metal surfaces. During the atmospheric corrosion investigation, the voltage supplied was such that the potential difference amounted to 200 mV. This abnormal difference in voltage was not regarded as having any noteworthy effect on the corrosion process. The corrosion current between the artificial anodic and cathodic areas was regarded as a measure of the actual rate of corrosion in the metal which was studied.

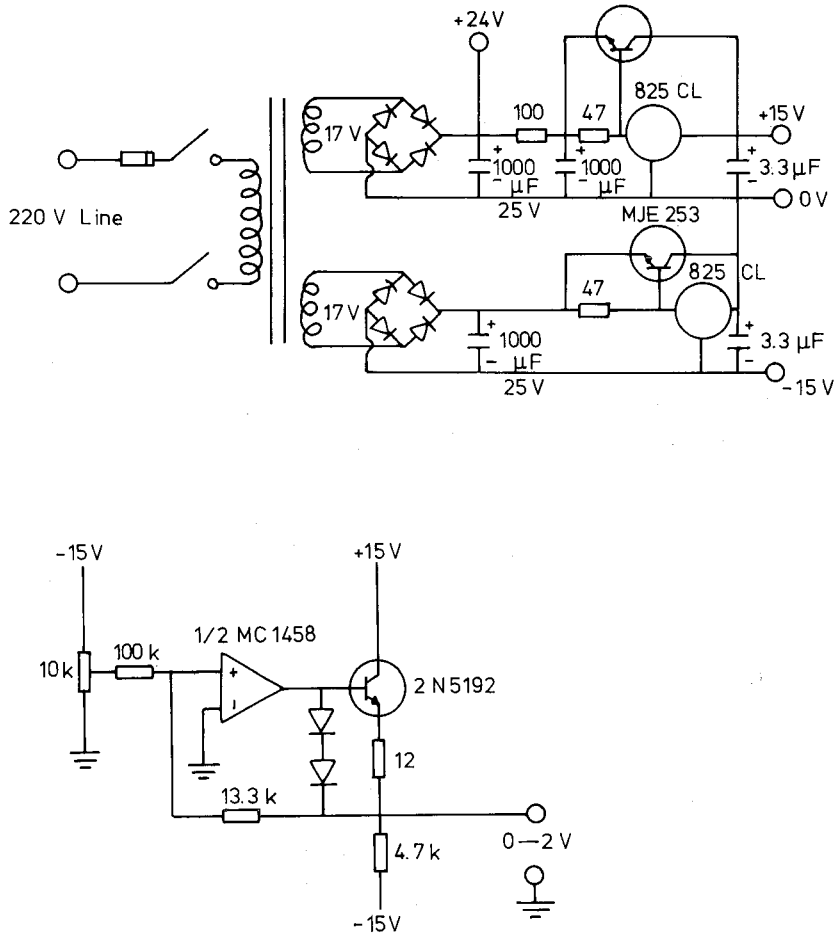

FIG 91.

Diagram showing voltage source for electronic integrator and external voltage source for electrolytic cells (the bottom figure).

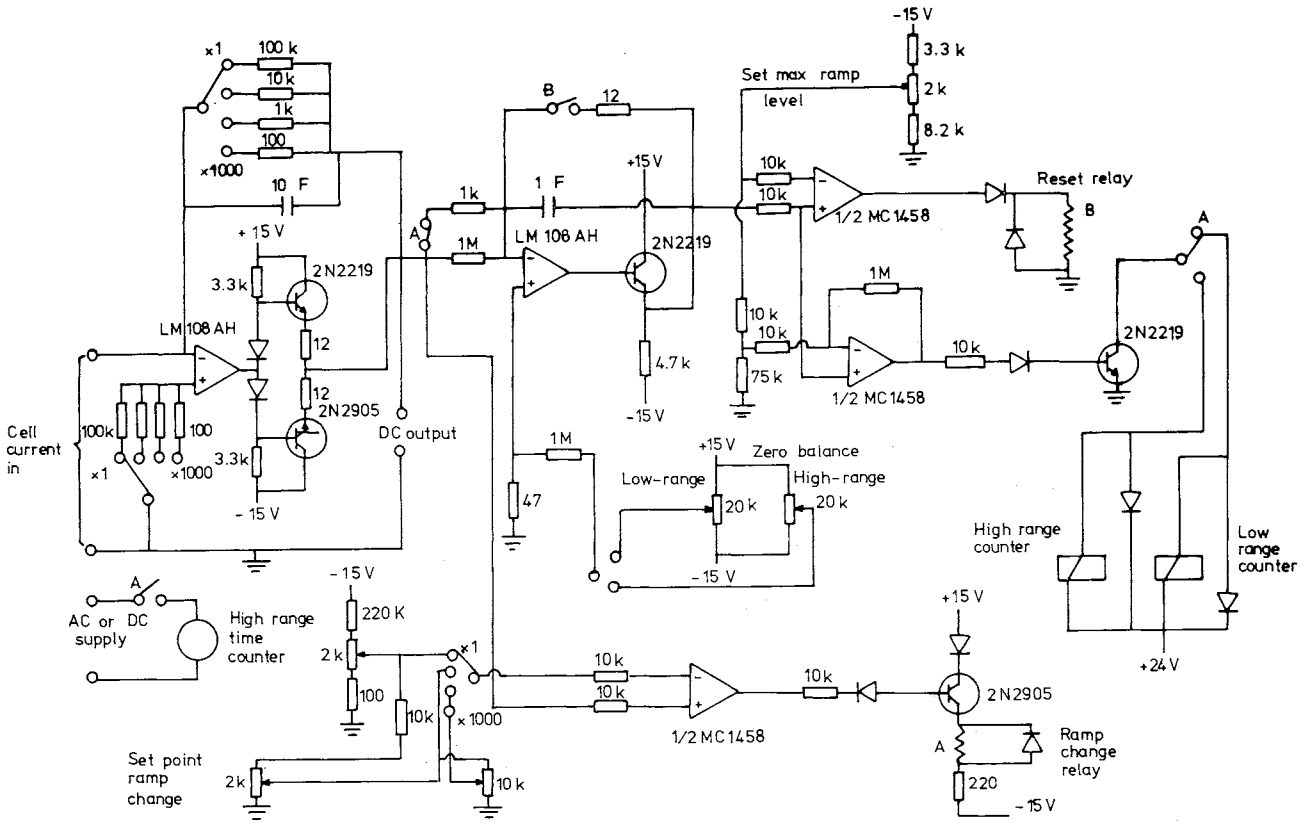

FIG 92. Diagram showing electronic integrator with two current ranges.

The current was measured by means of a special integrator which acted as a zero ammeter, see FIGS 91 and 92. Naturally, not all the current measured corresponded precisely to the weight loss obtained during the comparative investigation. Particularly in the case of dry climates, the distance between the anodic area and the cathodic area became so small that the plastic film could not be bridged over, despite the fact that the areas had a potential difference of 200 mV. On the other hand, a too large potential difference could not be selected since this would have influenced the natural corrosion process to an excessively high degree. Consequently, only part of the corrosion current was recorded. This current, which is known as the cell factor and is the relation between the measured current converted to corrosion rate and the actual corrosion rate, varied between 0.05 and 0.15 in the investigations carried out by Kucera and Collins /1977/. The cell factor increased within increases in the degree of deposit of, for example, SO_2 on the metal surface. This indicated that the cells should function better in concrete in which there is always a thick concrete cover with good conductivity in contact with the exposure surface.

5.2.2 Preliminary investigations and short-term experiments

A number of preliminary investigations were carried out to determine if this type of cell could be used for studying the corrosion of steel in concrete.

First of all, one cell was placed in a saturated $Ca(OH)_2$ solution and another cell was placed in distilled water. The difference in potential between the anodic area and the cathodic area was set at 100 mV. The currents which were recorded from these cells had roughly the same magnitude to begin with. The cell which was placed in water began, however, to corrode immediately. This could be noted during the first inspection after 10 hours. The corrosion current remained at the same level as at the start for this cell. The cell in the $Ca(OH)_2$ solution did not show any corrosion attacks during the time when the environment was strongly basic and did not contain aggresive substances. The corrosion current also decreased gradually so that after an exposure period of 7 days it was approximately 0.02 of the current first measured. This decrease in the current shows that the metal surface was passivated by an oxide layer. NaCl solution was added on the seventh day so that the concentration

around the cell amounted to 1%. The solution was still saturated with $Ca(OH)_2$. A corrosion attack on certain anodic surfaces could clearly be seen after 24 hours in this solution, see Photos 6 and 7. It could also be noted that the corrosion current had increased to the same level as that at the start or to the level which the other cell in water had. The recorded current had thus increased markedly as a result of the fact that the corrosion process had started.

Against this background, this cell type was regarded as suitable for at least providing an indication of when the corrosion process had been initiated.

Four corrosion cells were cast in concrete as illustrated in FIG 93 in the next stage. The aim was to study the characteristics of the cells in standard concrete which not only has an alkaline pore solution but also acts as a physical and chemical barrier for certain substances. One thick and one thin reinforcement bar were placed on either side of each cell. These permitted a visual assessment of the fact that the cells behaved in the same way as the bars. The cover in this case was 7 mm for both cells and the bars. Two different concrete qualities called KC1-76 and KC2-76 were used in the study.

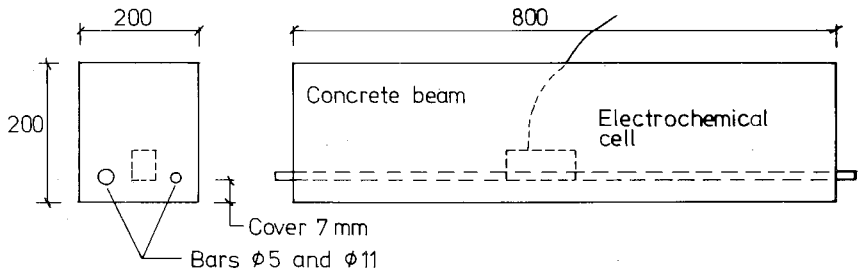

FIG 93. Placing of cells and reference bars in specimens.

After casting, the specimens were moisture cured for 10 days. The experiments then began. Half of the specimens were placed in a 3% NaCl solution and the other half were placed in ordinary tap water. The ambient temperature was $20\pm2^{o}C$. In order to increase the corrosivity of the environment adjacent to the embedded bars, the specimens were alternately dried and

wetted. The currents which flowed into the cells were measured from the moment when the samples were lowered into the vessels at the beginning of the experiment. The applied difference in potential was set at 50 mV in this case. The experiment continued for about 60 days and showed the results which can be seen in FIGS 94 and 95. In the middle of the experimental period, the potential of the embedded reference bars was measured with a saturated calomel electrode. The result is presented in Table 18.

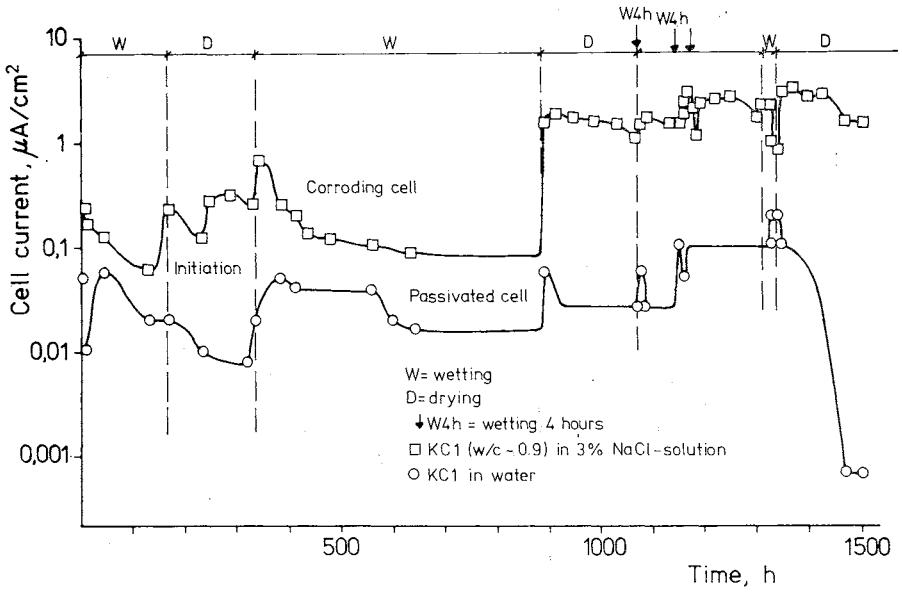

FIG 94. Preliminary experiment with corrosion cells which were cast in concrete with W/C approximately 0.9. One of the specimens was dipped during a number of periods in an NaCl solution while the other was dipped in water. The increase in current from the cell which was exposed to the chloride solution can clearly be seen.

The above values are potentials measured with a saturated calomel electrode. The measurements were carried out 30 days before the experiments were discontinued. All specimens were moist since they were taken up for drying out. The potentials are so low that they indicate that the steel is in an active state.

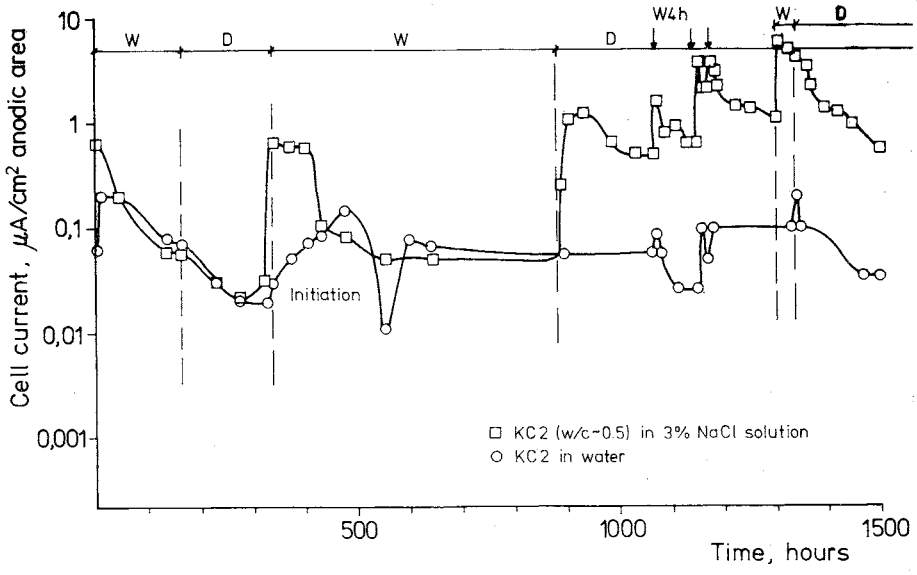

FIG 95. Preliminary experiment with corrosion cells which were cast in concrete with W/C approximately 0.5. One of the specimens was dipped in an NaCl solution during a number of periods while the other was dipped in water. The increase in the current from the cell which was exposed to the chloride solution can clearly be seen.

FIG 94 can be interpreted in the following manner:

During the first period in the salt solution, a sufficient quantity of activated substances - in this case, chloride - penetrate to the cell. The corrosion process is initiated. This can be seen through the marked increase in current at the end of the period.

During the drying procedure, the current intensity continues to increase until it reaches a maximum in conjunction with the next wetting operation. The reason for this may be an increase in or the formation of new anodic areas on the cell.

During the next wetting period, the current intensity decreases assymptotically towards a limit value. The relation between the anodic areas and the cathodic areas has now been stabilized and wetting does not initiate any further corrosion areas. The cathodic areas, on the other hand, con-

sume the O_2 which occurs in the immediate surroundings. The process becomes more and more cathodically controlled.

TAB. 18. Result of measurement of potential on bars exposed adjacent to corrosion cells KC1-KC2. Saturated calomelectrode was used.

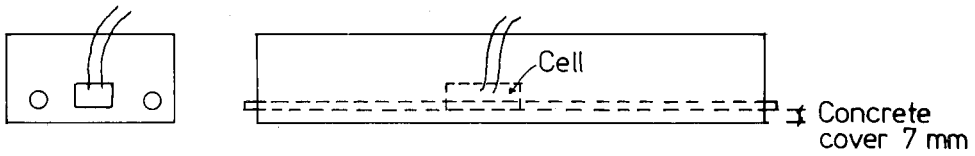

Potentials indicated in volts.

	X mm V						
	100	200	300	400	500	600	700
KC1;H_2O ϕ 5	-0,565	-0,565	-0,565	-0,565	-0,560	-0,565	-0,560
ϕ11	-0,600	-0,600	-0,595	-0,595	-0,590	-0,590	-0,590
KC1;H_2O ϕ 5	-0,600	-0,600	-0,600	-0,600	-0,600	-0,602	-0,603
+ Cl ϕ11	-0,595	-0,596	-0,596	-0,595	-0,596	-0,594	-0,598
KC2;H_2O ϕ 5	-0,385	-0,365	-0,360	-0,360	-0,365	-0,360	-0,360
ϕ11	-0,610	-0,610	-0,610	-0,610	-0,610	-0,610	-0,605
KC2;H_2O ϕ 5	-0,560	-0,560	-0,560	-0,555	-0,552	-0,550	-0,549
+ Cl ϕ11	-0,658	-0,655	-0,655	-0,654	-0,652	-0,650	-0,646

A marked increase in the corrosion current occurs immediately in conjunction with the next drying process and reaches a higher absolute value than before. The drying process causes water to evaporate at the concrete surface. This, in turn, disturbs the entire liquid balance in the specimen. The catodically controlled process ceases since O_2 is no longer forced to diffuse to the corrosion areas. The transport is now mainly carried out by the liquid movement which was started by the drying process. At the same time, further anodic areas are formed since the effectiveness of the cathodic areas has increased at the same time as the chloride concentration around the cell has increased.

Shortly after the drying process was started for the second time, the corrosion process reached its highest value so far. The rate of corrosion then decreased in pace with the drying out of the specimen. The optimum conditions were disturbed by the fact that the electric contact was gradually impaired between the anodic and cathodic areas.

The same development pattern, in principle, was followed during continued cycles of wetting and drying.

The passivated cell, in other words, the specimens which had been exposed to ordinary tap water, showed a small corrosion current throughout the entire experiment. The drying and wetting cycles disturbed the conditions, however. We can assume that the passive state changes over to an active state throughout the second long wetting period but that the rate of corrosion remains very low due to complete water saturation and a lack of O_2. This is also indicated by the results from the potential measurements. When the specimen was later dried, the potential and the rate of corrosion increased to such an extent that the active state changed back to a passive state. The longer the experiment then continued with a satisfactory supply of O_2, the smaller became the recorded current. This indicates a very stable passive state.

The results presented in FIG 95 follow the results presented in FIG 94 to a considerable extent. The better concrete quality, i.e. the less permeable pore systems with all that entails, the higher threshold values, the more difficult transport conditions etc give rise to the following reflections:

During the first wetting process in NaCl solution, the chlorides are not capable of initiating corrosion attacks. A not insignificant quantity of Cl^- has, on the other hand, penetrated to the pore system. This manifests itself during the subsequent drying period. The water evaporation from the concrete surface causes the pore system to be emptied of water. The substances which occur in the pore solution thus increase in concentration. The chemical equilibrium reactions do, admittedly, cause the larger quantities to be fixed in the solid phase when the concentration in the solution increases but the high concentration of activating substances in the solution becomes the decisive factor. In this case, it is chloride which, when the concentration on the surface is increased, causes an increase in the

diffusion rate towards the steel. This transport is, however, inhibited somewhat by the liquid moving in the opposite direction. By way of summary, it can be said that the concentration of chlorides will increase adjacent to the steel surface in conjunction with drying as well as wetting. Consequently, initiation also occurs in this case during the drying period. Another factor which also influences the intiation procedure in this case consists of the mutually changed anodic and cathodic reactions. During the drying, the reaction is displaced, thus entailing an increase in the equilibrium potential. This can also be an accelerating factor. When the corrosion process has been initiated, we can see that the cathodic control in conjunction with wetting becomes more noticeable in a concrete which has a low W/C. This also applies to the current control in conjunction with a shortage of electrolyte or a drying out.

As far as the potential measurements are concerned, the results seem to indicate that all the steel bars are in an active state. The experiment cannot, however, tell us anything about the corrosion rate.

The potential measurements thus support what has been said above concerning the passive cells, i.e. that they alternate between an active and a passive state but that the rate of corrosion is very low all the time.

The experiments were concluded by breaking apart the specimens so that any corrosion attack on the cells or on the reference steel could be studied ocularly. Photos 8-13 are intended to illustrate the results.

All of the reference bars showed small corrosion attacks at the end surfaces due to the minor adhesion failures which always occur around a smooth bar which projects from concrete. The crack had given rise to a local carbonation with corrosion attacks as a result. The fact that the end surfaces of the steel bars were sealed with silicone rubber also contributed in all certainity to the corrosion of the end surfaces.

Apart from that, visible corrosion attacks could only be noted on steel specimens which had been exposed to a chloride solution. This applies both to cells and to reference bars.

Against this background, the corrosion cells were deemed to be suitable for:

- studies of the mechanism involved in conjunction with changes in environmental conditions or other comparative studies
- indications of corrosion initiation

On the other hand, the experiments tell us nothing about the suitability of the cells for absolute measurements of the rate of corrosion.

5.2.3 Long-term experiments and mechanisms studies

General

Three different types of cell were cast in concrete in order to study corrosion mechanisms and the influence of a number of important parameters on the corrosion process. The three types of cell were:

A. The package model which consisted of thin plates in accordance with FIG 90.

B. Cells of smooth, cold-worked reinforcement steel, see FIG 96.

C. Cells of thin plates, in which each plate had a wire connector of its own, see FIG 97.

At the time in question here, moisture measuring equipment which was, in principle, new and which made it possible to record the relative humidity in concrete, had been developed at Lund University of Technology, see Nilsson /1977/. Since the moisture state closest to the corrosion areas is of decisive significance, specimens were also prepared for this measuring procedure, which entailed placing a plastic tube at the same level as that of the corrosion cells. During this latter measurement, a probe could be guided down into the tube for measuring the relative humidity in the pore system which was closest to the tube opening at the bottom. See FIG 98.

All of the material data is presented in Appendix 4.

The concrete specimens were cured in the same manner as that prescribed by the Swedish standards for curing standard cubes: seven days water curing at a water temperature of 20°C with subsequent curing in a relative humidity of 50% at the same temperature. A number of specimens were then conditioned in, for example, an environment which gave a rapid carbonation. Before the actual experiments were started, the concrete specimens had reached an age of at least 4 months.

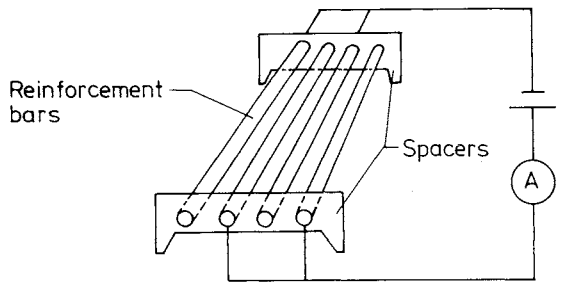

FIG 96. Electrochemical corrosion cell of reinforcement bars.

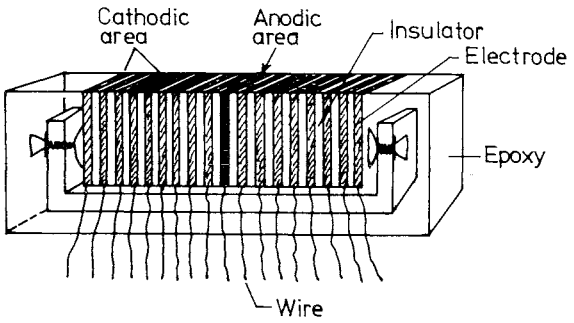

FIG 97. Cross-section of electrochemical cell in which each electrode can be treated separately.

Experiments in Series 1

Cells of type A were used for repeating the procedure in the previous short-term experiments. In this case, the concrete layer was varied. The specimens were placed 4 mm and 15 mm from the surface. The concrete

quality was the same as that used in the preliminary experiment (KC3-77), W/C approx. 0.5 and (KC4-77), W/C approx. 0.8.

The specimens which had been exposed to chlorides had a reference specimen which received similar treatment but in ordinary tap water. For each concrete quality, there was also a specimen which was exposed to the ambient laboratory air only. The concrete cover for the air specimen was 15 mm.

The most important parameters are presented in Table 19.

The results are presented partly in charts in FIGS 99-104 and partly in photographs 14-22 and in Table 20.

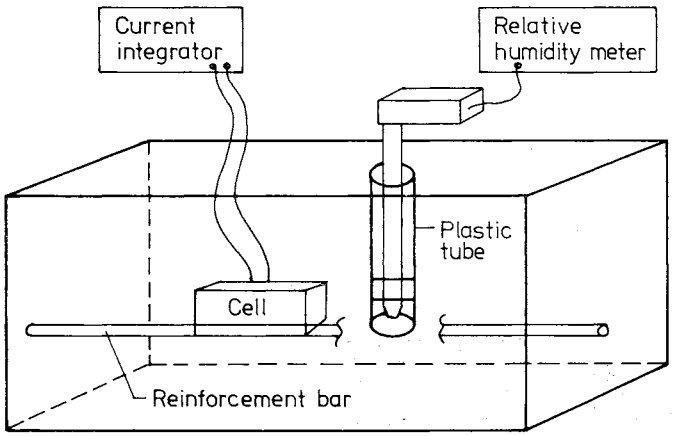

FIG 98. Cells, reinforcement bars and measurement openings for recording relative humidity were placed on the same level in the concrete prisms.

Table 19. Data for corrosion cells in Series 1

Cell nr	Cell type	Concrete quality W/C	Concrete cover mm	Conditioning
1 *	A	0,5 (KC3-77)	4	H_2O
2 *	"	0,5 "	15	"
3	"	0,8 (KC4-77)	4	"
4	"	0,8 "	15	"
5 *	"	0,5 (KC3-77)	4	3% NaCl
6 *	"	0,5 "	15	"
7	"	0,8 (KC4-77)	4	"
8	"	0,8 "	15	"
9 *	"	0,5 (KC3-77)	15	Air
10	"	0,8 (KC4-77)	15	"
11	B, ϕ 11 mm	0,8 "	5	3% NaCl
12	B, ϕ 5 mm	0,8 "	5	"

* In addition to reference specimens of smooth bars, reference specimens consisting of small plates were also embedded.

Table 20. Ocular observations when concrete was chipped away from specimens in Series 1. The experiments were concluded after about 450 days.

Cell No. 1 W/C = 0.5 Concrete cover = 4 mm H_2O	No visible attacks on reference specimens and cell. See photo 14.
Cell No. 2 W/C = 0.5 Concrete cover = 15 mm H_2O	No visible attacks on reference specimens or cell. See photo 15.
Cell No. 3 W/C = 0.8 Concrete cover = 4 mm H_2O	No visible attacks on reference specimens or cell. The metal was considerably more mat than at W/C = 0.5. The colour remained the same, however, i.e. bright metallic. See photo 16.
Cell No. 4 W/C = 0.8 Concrete cover = 15 mm H_2O	No visible attacks on reference specimens or cell. The metal is also more mat in this case than at W/C = 0.5.

Cell No. 5 W/C = 0.5 Concrete cover = 4 mm 3% NaCl	Only approximately 5% of anodic area attacked on corrosion cell. No attacks on reference specimens but may have been discoloured somewhat after concrete was chipped away. See photo 17.
Cell No. 6 W/C = 0.5 Concrete cover = 15 mm 3% NaCl	Approximately 10% of anodic area attacked on corrosion cell. No attacks on reference specimens. Colour varied somewhat, however. See photo 18.
Cell No. 7 W/C = 0.8 Concrete cover = 4 mm 3% NaCl	Approximately 20% attack on anodic area on corrosion cell and reference specimens. See photo 19.
Cell No. 8 W/C = 0.8 Concrete cover = 15 mm 3% NaCl	Approximately 70% attack on anodic areas on corrosion cell. Reference specimens do not show any red or red-brown, black oxides. The colour on all the bar surfaces was, on the other hand, very dark. See photo 20.
Cell No. 9 W/C = 0.5 Concrete cover = 15 mm Air	Approximately 5% of anodic area attacked on corrosion cell. No attacks could be noted on reference specimens. See photo 21.
Cell No. 10 W/C = 0.8 Concrete cover = 15 mm Air	No attacks could be noted on reference specimens or cell.
Cell No. 11 Diameter 11 W/C = 0.8 Concrete cover = 5 mm 3% NaCl	Very marked attacks on corrosion cell, which consisted of smooth bars with a diameter of 11 mm. Reference specimens attacked but not to the same extent as cell.
Cell No. 12 Diameter 5 mm W/C = 0.8 Concrete cover = 5 mm 3% NaCl	Very powerful attacks on corrosion cell, which consisted of smooth bars with a diameter of 5 mm. Reference specimens attack but not to the same extent as cell.

In all cases, the attacks have been concentrated to areas which were linked as anodes. In the case of very powerful corrosion attacks, the cathodes were also attacked but not to the same extent as the anodes.

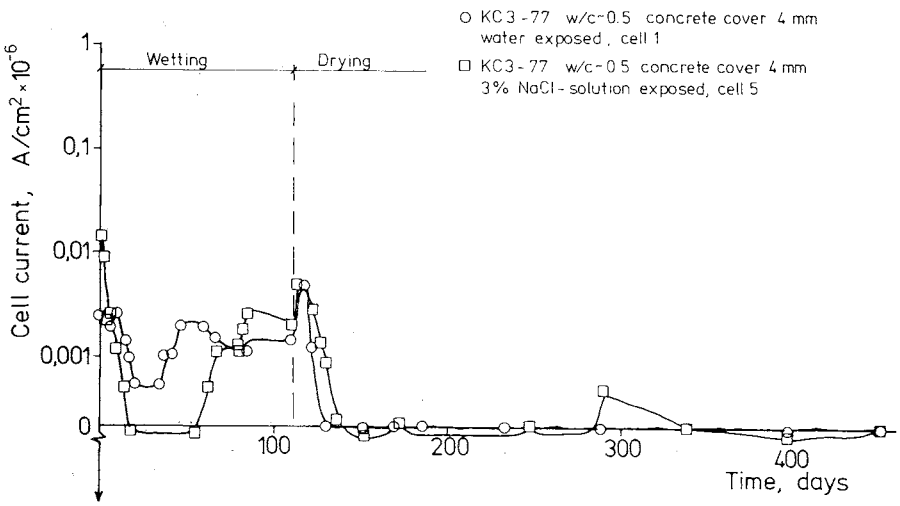

FIG 99. Measured cell current from corrosion cell in Series 1. The cell, which had been exposed to chlorides, gave a negative cell current during a preliminary wetting period. This indicates an unstable state. During the drying stage, the cell current decreased for both samples due to a lack of electrolyte. The lengthy drying period caused the water-exposed specimen to have a negative cell current as well. This derives only from a migration process.

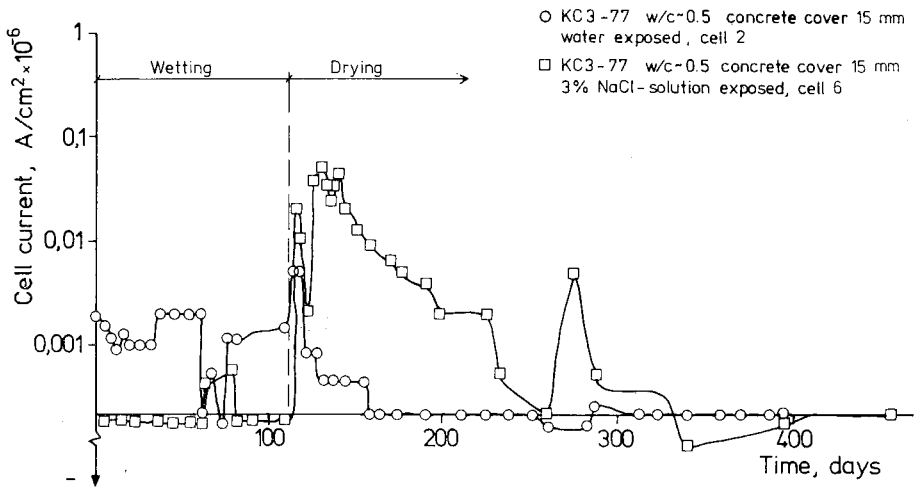

FIG 100. Measured cell current from corrosion cell in Series 1. The concrete covers in FIG 99 were very small. This gave rise to rapid drying-out and small corrosion attacks for the chloride-exposed specimen. The effect of a larger concrete cover can be seen here. It takes about 100 days before the corrosion process comes to a halt as a result of a lack of electrolyte. It should be noted that these experiments were carried out to study the mechanisms in the corrosion stage. In practice, a large concrete cover is preferable, particularly due to the longer initiation times and the more stable environment around the reinforcement which it offers.

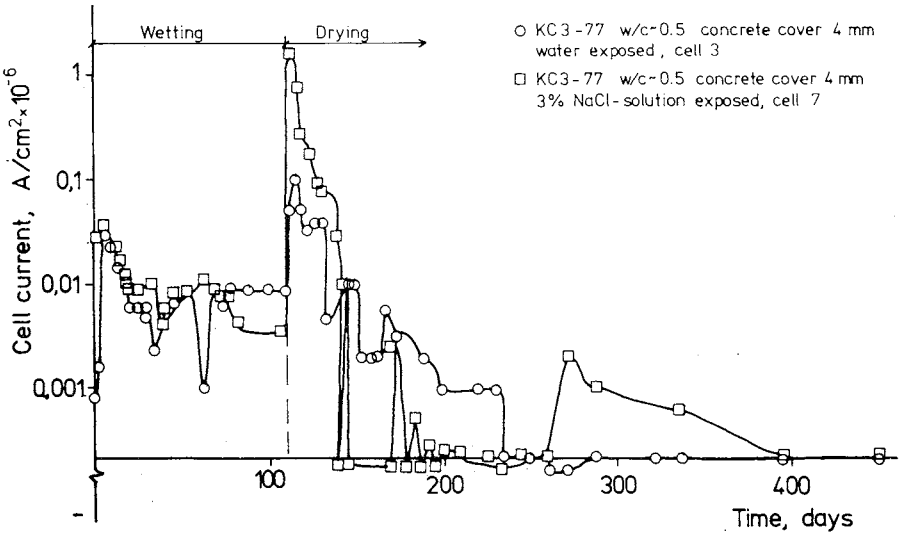

FIG 101. Measured cell current from corrosion cells in Series 1. A poor concrete quality, W/C = 0.8, gave rise to a more marked increase in the current due to corrosion initiation on a larger area than is the case for a less permeable matrix. Once again, we can see that a thin concrete cover rapidly dries out and limits the corrosion process.

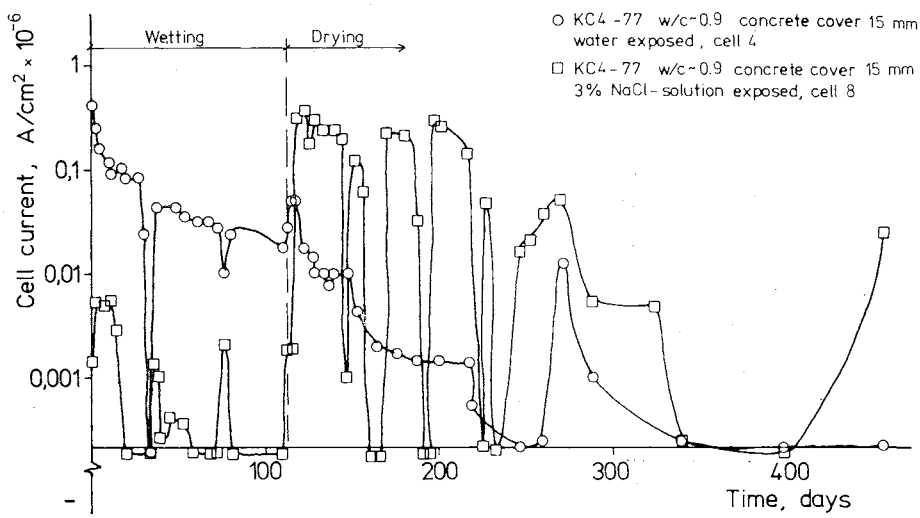

FIG 102. Measured cell current from corrosion cells in Series 1. The cell has a satisfactory supply of O_2 in the water-exposed specimen and acts at the beginning of the exposure as a passive O_2 consumer or, alternatively, changes over from an active state to a passive state. In the chloride-exposed specimen, corrosion initiation mainly takes in the first phase during drying. The corrosion current then decreases as a result of a shortage of electrolyte. This decrease takes place more slowly, however, than is the case for the 4 mm concrete cover. The high chloride concentrations which occur at the electrodes sometimes bridge over the potentials from the measuring equipment, whereupon ions migrate in the opposite direction. This occurs when the negative current values are recorded. A comparison with FIG 100 with a better concrete around the cells shows a greater corrosion current in this case, which does not decrease as easily during drying. The reason for this is probably the longer time which it takes for this concrete to dry out at the cell level. The same tendency occurs in conjunction with small concrete covers, see FIGS 99 and 101.

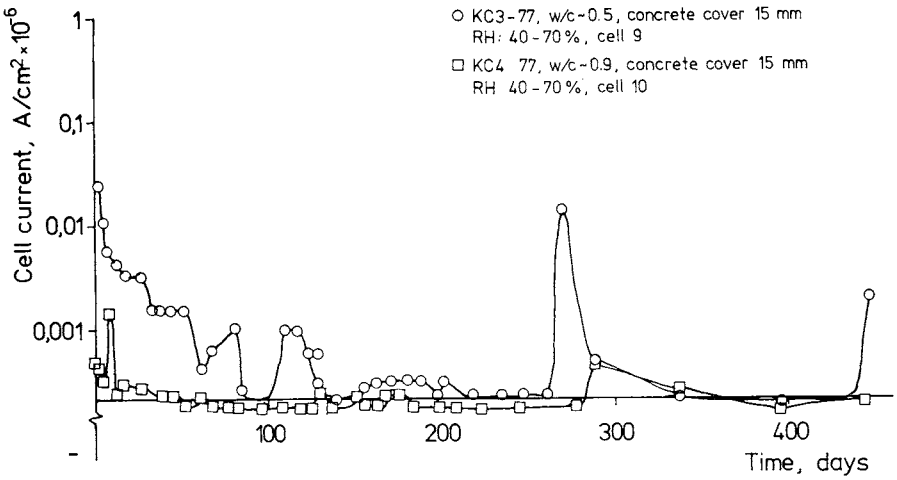

FIG 103. Measured cell current from corrosion cells in Series 1. The specimens which were stored in a dry laboratory environment, i.e. in an indoor climate, give small cell currents regardless of the W/C. This is partly due to the fact that corrosion has not been initiated and partly due to the fact that there is a shortage of electrolyte.

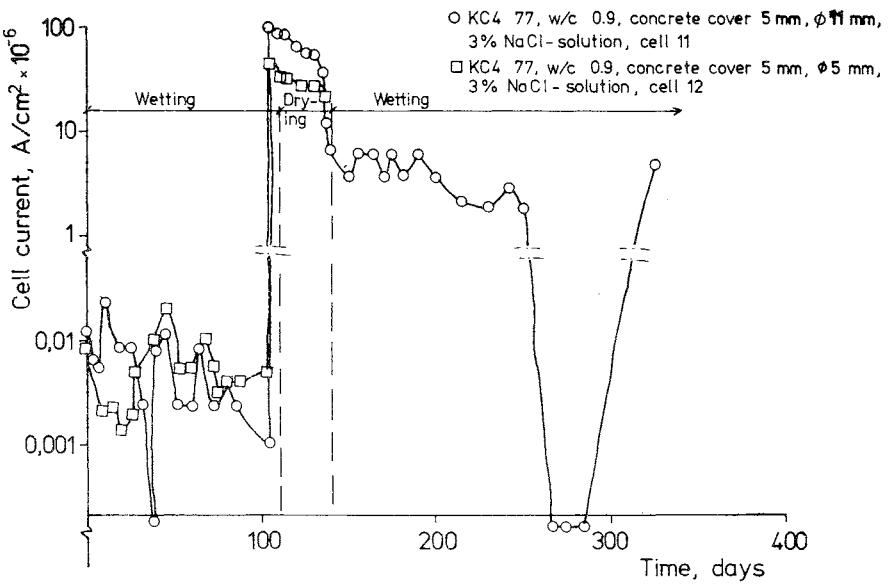

FIG 104. Measured cell current from corrosion cells in Series 1. Cells of reinforcement bars showed the same performance as the package cell but with a larger difference in current when corrosion is initiated. This takes place about a day after the drying-out stage is started.

Detailed discussion of results from Series 1

In a specimen with low permeable concrete and with very small concrete cover, the current curves were almost identical when specimens exposed to a 3% NaCl solution and to ordinary tap water respectively were compared, see FIG 99. After about 55 days, a minor increase in current can be noted. This may be a result of a small anodic formation. The current increase is, however, so small - roughly on the same order of size as that of the reference specimen - that an initiation cannot be predicted solely on the basis of the results presented in FIG 99. When the concrete had been chipped away from the cells, it was, on the other hand, possible to see a very small attack on the specimen which had been exposed to the NaCl solution.

Another phenomenon which was not observed in the short- term experiment, or when the specimens were constantly exposed to moisture changes, was the sudden occurence of a negative cell current. The applied potential of 50 mV was bridged over by a difference in potential in the opposite direction. The reason for this is that a switch in potential gradually takes place due to the state created on the anodic areas by the unnatural drive potential. Concentration differences which have been built up by the current between the anodic and cathodic areas gradually change the corrosion conditions. This can lead to the potential in the cell being changed. Small potential changes of this type can also occur on reinforcement in concrete structures. The result is that the anodic area tends to expand. Otherwise it would be more natural for the pitting which occurs on, for example, reinforcement merely to increase in depth until the material had been completely corroded instead of expanding in area. This does not, of course, normally occur in practice and the anodic areas are usually fairly large.

It is, nevertheless, suprising to note the almost insignificant size of the corrosion attack. A concrete cover as thin as 4 mm normally gives rise to rapid and large attacks but in this case, in which the environment contained only one wetting and one drying cycle, the thin concrete cover reduced the quantity of electrolyte so rapidly that no visible expansion of the anodic areas was possible.

The reference bars also indicate that the chloride concentration was sufficient only for initiating the corrosion process but that the quantity of electrolyte was not sufficient for continuing the process.

It should be noted that an environment as favourable as this very seldom occurs in practice. A rewetting would immediately have resulted in an increase in the attack, as the short-term experiments showed.

For the same concrete quality as in FIG 99 but with a concrete cover which had been increased from 4 mm to 15 mm, a low corrosion current was obtained from the specimen which had been exposed to water, see FIG 100. Exposure to NaCl, on the other hand, gave rise to a large current increase during the beginning of the drying procedure. This indicated the initiation of corrosion. The rate of corrosion was then gradually retarded at an increasingly higher level of drying out. The longer drying period which the thicker concrete cover entailed resulted in a more extensive attack due to the fact that the highly active corrosion period lasted a longer time.

Experience has showed that increased permeability in the concrete cover (an increase in the W/C ratio from 0.5 to about 0.8) increases the risk of corrosion attacks. In FIG 101, which should be compared with FIG 99, this can also be noted. Exposure to water only can also have entailed a higher corrosion current than the corresponding case for a low W/C. The current which was recorded has, admittedly, passed through both the electrodes and given rise to a type of corrosion product. In this case, what we regard as initiation - accelerated attack and the formation of porous oxides - has not taken place. Instead, the passive oxide layer has merely been made less permeable. Here we can thus see another characteristic which the cells provide measured values for, namely the resistivity of the concrete. That was why it was possible to note a more mat surface on the corrosion cells which had been kept in a concrete with a high W/C ratio. When the concrete cover was increased, an increase was also obtained in the corrosion attack, as occured in the parallel case with a low W/C (see FIG 102, photos 19 and 20). The specimen also clearly shows the potential switches.

The specimens which were exposed to laboratory air after the curing process gave rise to very small cell currents, see FIGS 103 and photo 21. The higher quality concrete, on the other hand, gave a higher current. This conflicts with the other measurements. When the concrete had been chipped away, it was possible, however, to note a very small corrosion attack on the cell which had been kept in concrete with a W/C value of approx. 0.5. In this case, the corrosion initiation probably derived from a crack which occurred in the concrete cover during the air curing. The sample with the poorer concrete quality did not have any cracks. Although initiation had taken place locally, the effects of the corrosion limitation due to a shortage of electrolyte could clearly be seen.

Cells built up of reinforcement bars, type B, see FIG 96, reacted far more markedly in conjunction with initiation, see FIG 104. The cell current per area unit was also higher to a power of 10 than it was for the cells embedded in epoxy with a flat exposure surface. One explanation for this is partly that the cathodic areas have better possibilities of obtaining essential substances such as O_2 due to multidimensional transport paths and partly the environmental differences along the exposure surfaces due to the fact that a round bar has a varying concrete cover along its cylindrical surface. The corrosion attacks were also considerably larger for this cell type at the end of the experiments, see photo 22.

In accordance with the previous pattern, cell type B also gave a reduced corrosion rate during both drying and wetting.

As far as the stability of the measured current is concerned, cell type A gave a very stable result while cell type B showed greater instability, see FIG 105. Since the same measuring equipment was used for all cells during the experiment, polarization phenomena occurred in conjunction with the automatic switching during brief periods. The measurement results which are presented here are, however, from the end of each measuring period when the values had been stabilized.

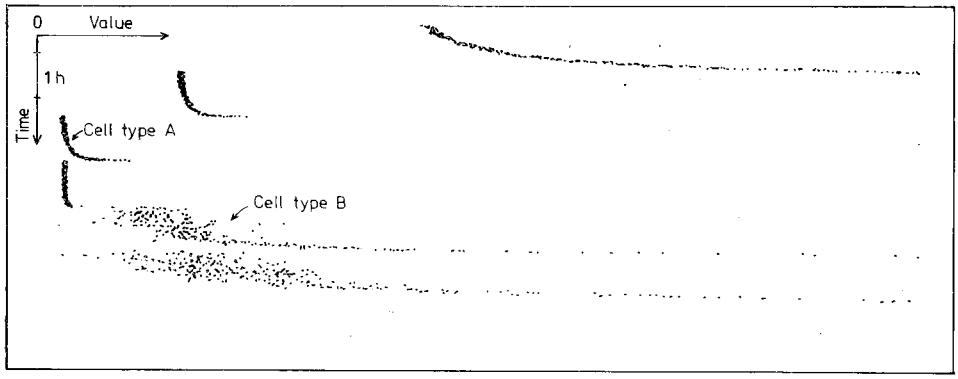

FIG 105. Example of stability in various cell types.

In addition to reference specimens in the form of bars, a steel plate was also embedded in five specimens in order to investigate the possible effects of a flat exposure surface. The result can be seen in photo 23. The corrosion attacks were larger for these plates than for the flat corrosion cells. On the other hand, the plates and cells showed the same relative changes when the effect of the concrete cover and the significance of the environment are studied. Plexiglass sheets, glued with epoxy, had been used as spacers between the plates. This gave rise to differential aeration cells. The corrosion attacks were thus initiated immediately in all cases. In the water-exposed specimens, the metal was, however passivated when the environment had been stabilized whereas the chloride-exposed specimens received an excellent corrosion start which then developed to an increasingly large area.

Differential aeration cells are not common in concrete - i.e. cells with an attack where the O_2 concentration is lowest. Active-passive cells are, on the other hand, common since reinforcement is in both a basic and an almost neutral environment during lengthy periods of time in conjunction with, for example, the initiation of carbonation.

This initiation mechanism has also been noted when pipes have been cast in concrete and have not been completely surrounded by the concrete, see Halvorsen /1966/. In this case the attack is not initiated by the O_2 concentration but by the difference in pH value.

Immediately after the specimens had been taken out of the liquid to which they had been exposed for 111 days, the potentials were measured on the reference bars. The results are presented in Table 21.

All of the bars had a very low potential. This means that the metal was in an active state but had an extremely low rate of corrosion. Further moisture curing would have meant a further drop in the potential until it finally reached values around -1.0V measured with a saturated calomel electrode as has been reported by Arup /1977/ and Fidjestöl and Nilsen /1980/.

Table 21. Potentials in V measured with saturated calomel electrode directly after specimens (series 1) were removed from the exposure bath. Exposure time: 111 days.

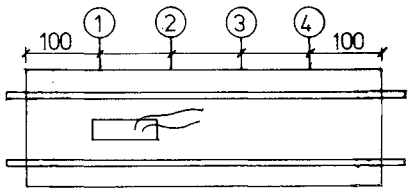

Positions for potential measurements

Cell		1	2	3	4	5	6	7	8
ϕ 5	1	-0,630	-0.630	-0,630	-0,650	-0,700	-0,630	-0,640	-0,690
	2	-0,640	-0,640	-0,630	-0,660	-0,720	-0,640	-0,640	-0,690
	3	-0,630	-0,645	-0,630	-0,670	-0,720	-0,640	-0,650	-0,690
	4	-0,630	-0,630	-0,610	-0,630	-0,720	-0,640	-0,650	-0,690
ϕ 11	1	-0,520	-0,650	-0,610	-0,580	-0,690	-0,770	-0,660	-0,700
	2	-0,520	-0,680	-0,610	-0,590	-0,710	-0,780	-0,660	-0,710
	3	-0,520	-0,670	-0,630	-0,600	-0,710	-0,780	-0,660	-0,710
	4	-0,520	-0,650	-0,620	-0,590	-0,710	-0,780	-0,660	-0,710

In addition to the corrosion current, the air humidity was also recorded at the level in the concrete where the cells were located. It has previously been established that both a drying-out and a wetting can reduce the rate of corrosion counted from a maximum value somewhere around 90% relative humidity.

The cell current has been plotted as a function of the relative humidity in FIG 106. The results are presented more schematically in FIG 107. Different concrete covers and W/C ratios thus give different absolute values for the cell current but it can, however, be seen that the rate of corrosion decreases markedly both at low relative humidity and at complete water saturation. Drying-out also entails immediate high cell currents. These are partly caused by access to the necessary O_2 and partly by an increase in the active anodic area.

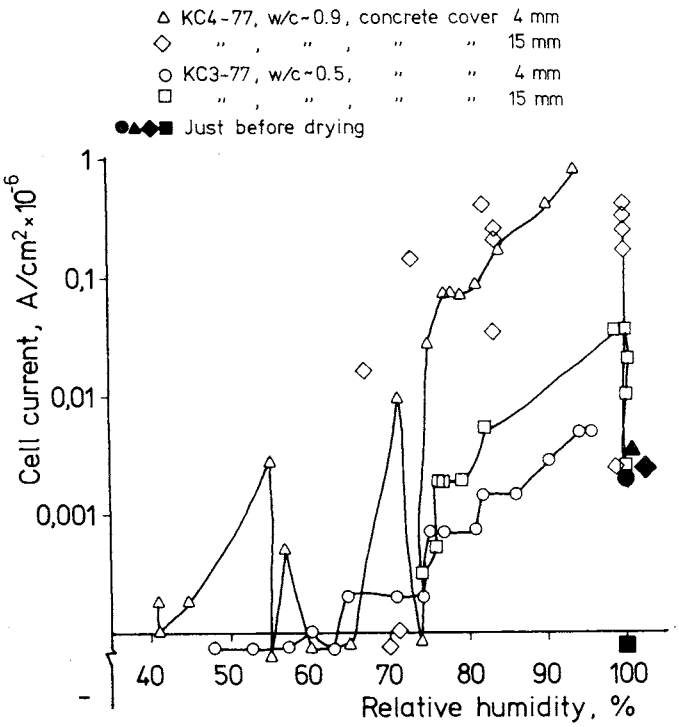

FIG 106. Cell current as a function of relative humidity.

The cell current reached its maximum values somewhere between 90-98% relative humidity. Thin concrete covers gave a poorer electric contact and, consequently, a lower cell current than did thick concrete covers. The cell current thus also provides a measure of the resistivity of the surroundings, thus making it more difficult to interpret the results provided by this measuring method.

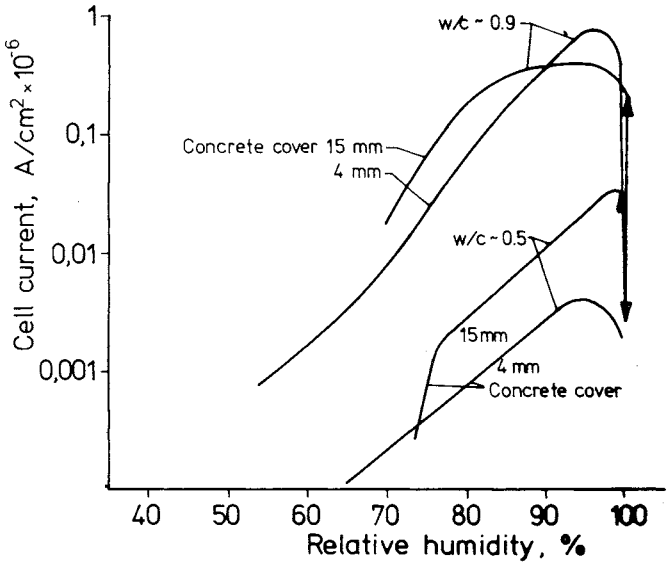

FIG 107. Schematic presentation of FIG 106.

An increase in the concrete cover should reduce the rate of corrosion somewhat due to a reduction in the supply of O_2. Extremely thin concrete covers can, however, limit corrosion if the electric contact is impaired. This effect is not likely to be on an order of size of the type indicated in FIG 107.

Experiments in Series 2

Standards include requirements for concrete covers and concrete qualities. These requirements have, however, always been produced on the basis of normal concrete handling. As a result, an increase in the environmental load also entails an increase in the concrete quality and the thickness of the concrete cover. The standard requirements for concrete quality undoubtedly provide a sufficiently long service life for most structures but inhibit innovative approaches due to the fact that even if extremely high concrete qualities are used, the standards do not permit any reduction in the minimum permissible concrete cover. As a result, the trend is always towards clumsy and massive structures if concrete is to be used in, for example, chloride-rich environments.

The experiments in Series 2 were carried out in order to shed light on the effects of using an extremely low permeable concrete with one-sided fluid pressure on structures, and on the significance of the concrete cover.

Cells of type A and B were cast in concrete with a W/C ratio of approximately 0.32, KC5-78. A PVC tube with a diameter of 150 mm was also cast into six specimens, cells 1-6, to make it possible to apply a fluid pressure corresponding to a head of 4 metres on one of the concrete surfaces at a later stage, see FIG 107.

One of the cells, cell 4, was placed at right angles to the other cells to see what the effects, if any, would be of a variable O_2 concentration or Cl^- concentration along the same metal object.

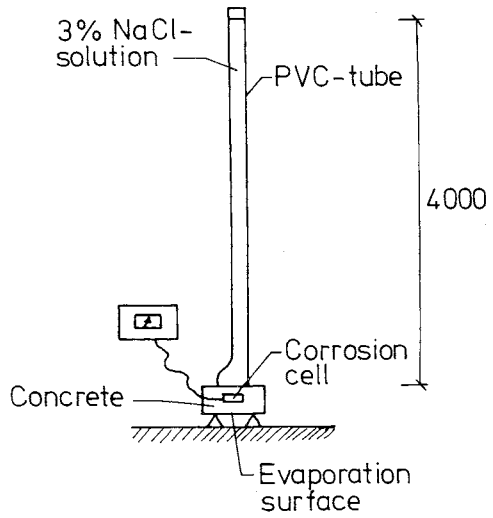

FIG 108. Experimental arrangement for specimen subjected to a head of 4 m. The edge sufaces of the specimen were insulated by means of epoxy plastic so that only the underside acted as a drying-out surface.

All of the edge surfaces of the specimens were sealed by means of epoxy plastic to avoid any end effects.

Reference bars, in the form of ribbed bars with a diameter of 12 mm, were placed in separate specimens.

The specimens, which were exposed to a one-sided pressure from a 3% NaCl solution, were stored in laboratory air throughout the entire experimental period consisting of 1438 days. In the case of these specimens it was not possible to record the relative humidity at the level at which the cells were located.

The other specimens were dried in laboratory air and were moistened alternately in a 3% NaCl solution. The schedule for this procedure is presented partly in the data appendix and partly in charts which have been drawn up to illustrate the results of the experiments.

Table 22 presents the values for the primary parameters whose effects were to be studied, as well as the results of an ocular inspection which was carried out at the conclusion of the experiment.

Other results are presented in the data appendix.

A number of typical pictures have been included in the report - photos 24-30 - with a view to illustrating the degree of attack, the colour differences etc.

Current curves as a function of the exposure time have been drawn for all of the cells, see FIGS 109-113. The aim here is to make it easier to see sudden changes in the measured cell current and thus to indicate the initiation times.

A presentation of the cell current and the relative humidity in the same figure provides an even better understanding of the corrosion problems, see FIGS 114-120.

Table 22 Ocular observations made when specimens in Series 2 were opened. W/C approx. 0.32 for all specimens. Exposure time approximately 4 years.

Cell No. 1 Cell type B Concrete cover$_W$ = 22 mm Concrete cover$_D$ = 50 mm Head = 4 m	This cell was not properly aligned during the casting. Consequently, the concrete cover varied between 20 and 30 mm counted from the wet surface. The corroded area was 15% of the anodic area. The attack was insignificant. The bars had only been slightly discoloured, see photo 24.

Cell No. 2 Cell type B Concrete $cover_W$ = 40 mm Concrete $cover_D$ = 30 mm Head = 4 m	No visible corrosion attacks. Light and dark areas could, however, be seen on the metal.
Cell No. 3 Cell type B Concrete $cover_W$ = 40 mm Concrete $cover_D$ = 55 mm Head = 4m	No visible corrosion attacks. Light and dark areas could, however, be seen on the metal.
Cell No. 4 Cell type B Concrete $cover_W$=10-60mm Concrete $cover_D$=20-70mm The cell had lain at right angles to the exposure surface. Head = 4m	No visible corrosion attacks. Light and dark areas could, however, be seen on the metal. See photo 25.
Cell No. 5 Cell type A Concrete $cover_W$ = 30 mm Concrete $cover_D$ = 40 mm Head = 4 m	Corroded area about 3% of anodic area, of which almost all of the attack had taken place on a steel plate. The corrosion attack had caused no more than a slight brown discolouring on the metal.
Cell No. 6 Cell type A Concrete $cover_W$ = 45 mm Concrete $cover_D$ = 55 mm Head = 4m	Corroded area about 1% of anodic area. The corrosion attack had caused no more than a slight brown discolouring of the metal.
Cell No. 7 Cell type B Concrete $cover_W$ = 20 mm Concrete $cover_D$ = 45 mm Conditioning varied	No visible corrosion attacks. The metal was, however, slightly discoloured.
Cell No. 8 Cell type B Concrete $cover_W$ = 30 mm Concrete $cover_D$ = 30 mm Conditioning varied	Corroded area about 5% of anodic area.The attack had caused no more than a slight brown discolouring of the metal.
Cell No. 9 Cell type B Concrete $cover_W$ = 50 mm Concrete $cover_D$ = 55 mm Conditioning varied	No visible corrosion attacks. The metal had light and dark areas.
Cell No. 10 Cell type A Concrete $cover_W$ = 5 mm Concrete $cover_D$ = 105mm Conditioning varied	The entire corrosion cell was corroded. Maximum pitting depth approximately 0.5 mm. See photo 26.

Cell No. 11 Cell type A Concrete cover$_W$=15-18mm Concrete cover$_D$=72-85mm Conditioning varied	The steel plate closest to the exposure surface was discoloured with a faint brown colour. Total corrosion attack about 10% of anodic area. See photo 27.
Cell No. 12 Cell type A Concrete cover$_W$ = 30 mm Concrete cover$_D$ = 80 mm Conditioning varied	Two steel plates attacked. Weak brown discolouring. Total corrosion attack about 15% of anodic area. See photo 28.
Cell No. 13 type A Concrete cover$_W$ = 45 mm Concrete cover$_D$ = 65 mm Conditioning varied	A total of about 2% of the anodic Cell area was discoloured with a weak brown colour. See photo 29.
Embedded reference bars in separate specimens with the same conditioning as cells 7-13.	
Concrete cover$_W$ = 5 mm Concrete cover$_D$ = 85 mm	A total of about 1% of the cylindrical surface was pitted.
Concrete cover$_W$ = 15 mm Concrete cover$_D$ = 75 mm	A total of about 1% of the cylindrical surface was pitted.
Concrete cover$_W$ = 30 mm Concrete cover$_D$ = 60 mm	A total of about 1% of the cylindrical surface was pitted.
Concrete cover$_W$ = 45 mm Concrete cover$_D$ = 45 mm	A total of about 0.5% of the cylindrical area was pitted, see photo 30.

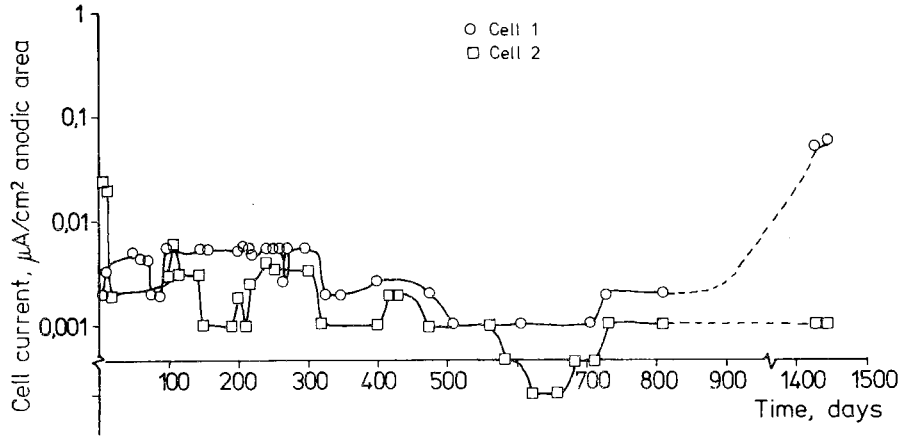

FIG 109. The cell current for these specimens, which were embedded in concrete exposed to a one-sided water pressure, is very low. The current did, however, increase by a power of 10 during the period between 800 days and 1400 days for cell 1. This indicates a corrosion initiation. The curve is broken, however, since no measurement was carried out during this period. Instead, a final reading was taken before the experiment was discontinued.

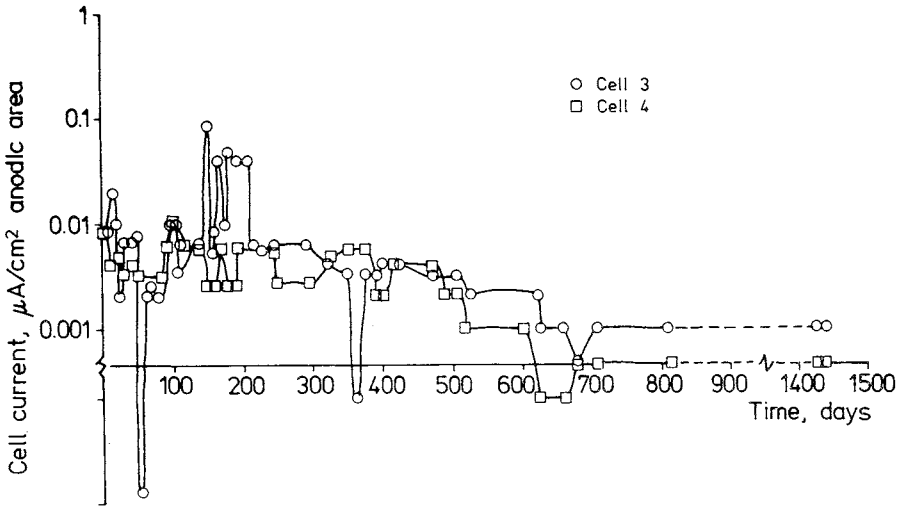

FIG 110. Like FIG 109, the cell current here is constantly decreasing. If corrosion initiation had taken place for cell 3 at 150 days, the cell current would have been unstable later on as well. Consequently, it can be assumed from the current curve that initiation did not take place.

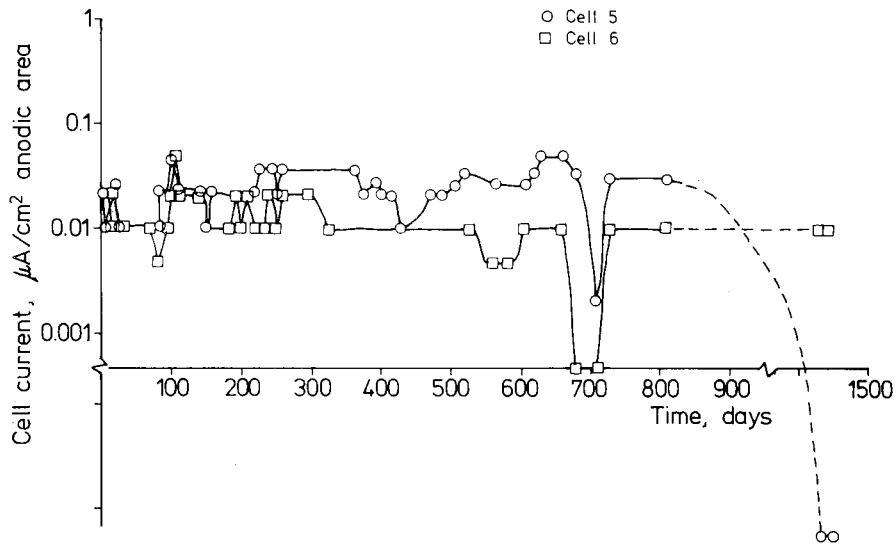

FIG 111. The current curve has become unstable during the final stage for cell 5. This indicates an initiation of corrosion. Cell 6 also showed a similar instability at 700 days exposure. It can, however, be seen that the rate of corrosion was low during this stage due to the low current values.

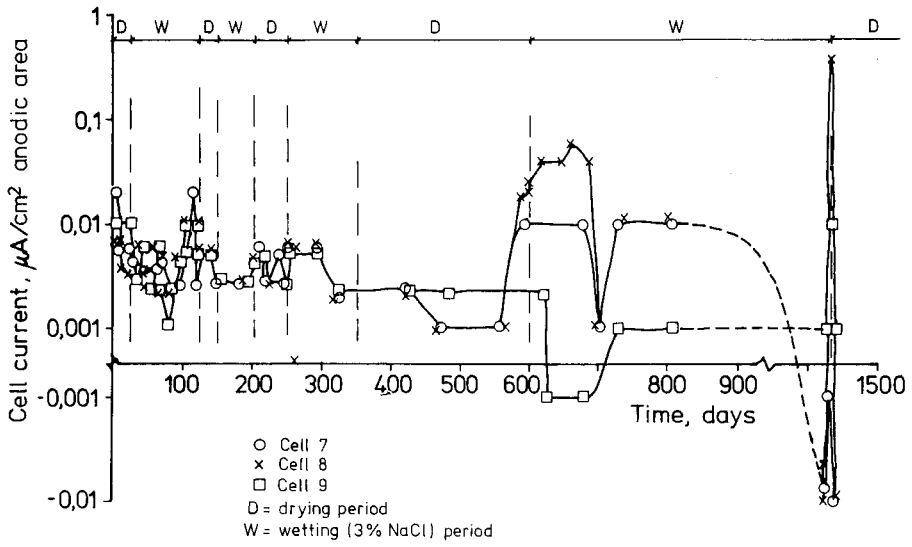

FIG 112. Cells 7 and 8 show a lack of stability in the final stage and cell 9 shows a lack of stability at 650 days exposure. Consequently, initiation should have taken place for these cells. The corrosion rate for cell 9 was likely to be far lower, however, than for the other two cells.

The corrosion rate was probably comparatively high for cell 8, which emitted a very high current intensity during the final stage.

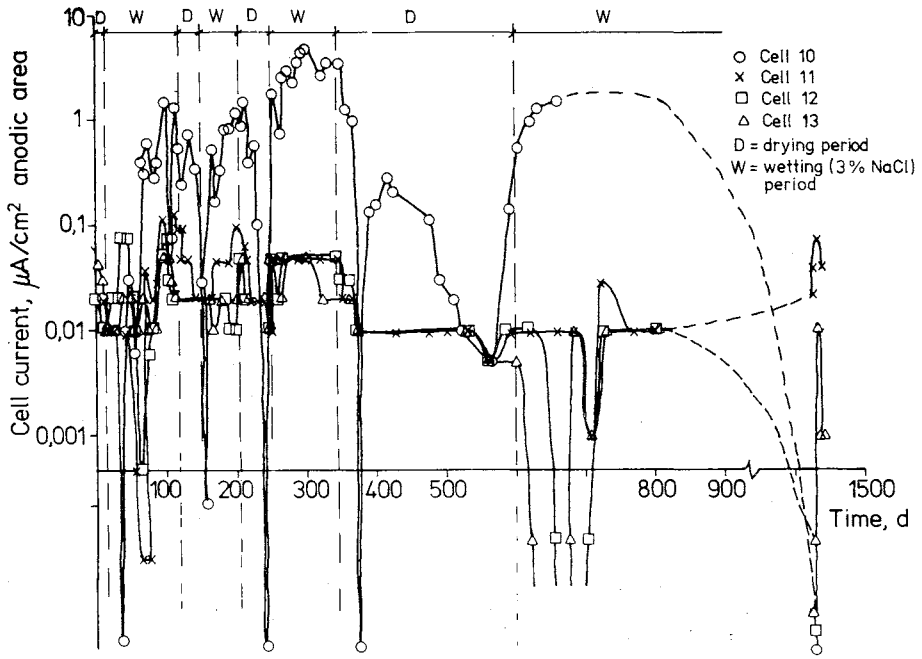

FIG 113. All cells have shown a certain lack of stability throughout the exposure period. This indicates corrosion initiation. A cell current which is twice the power of 10 larger then for the other cells has been measured for cell 10. Consequently, this cell corroded considerably more rapidly than did the other cells.

During the final stage cell 11 also emitted a somewhat higher current. All of the cells except cell 10 had a low rate of corrosion, however.

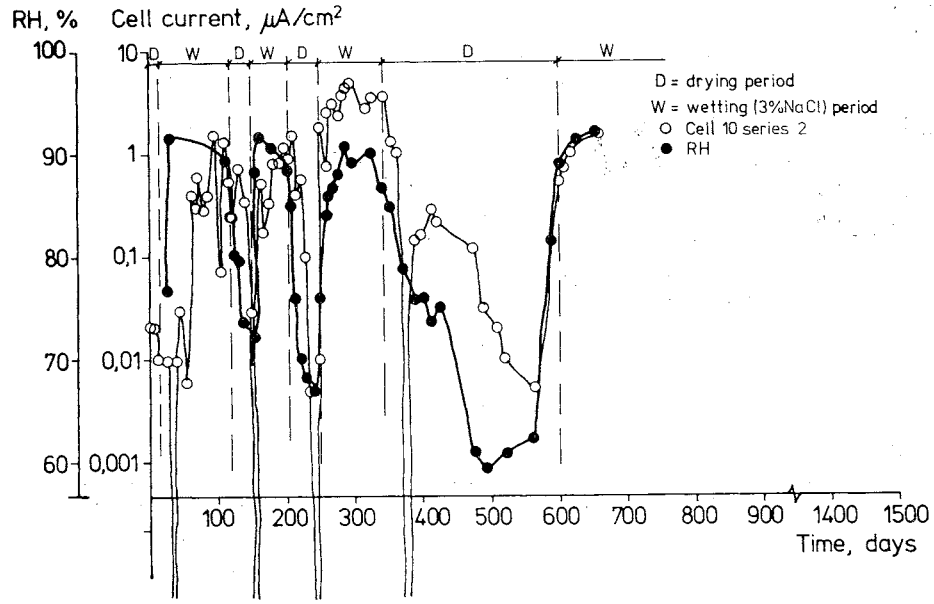

FIG 114. Cell current and relative humidity as a function of the exposure time. In the case of cell 10, for which corrosion initiation took place at an early stage, we can see that the cell current and the relative humidity in the pore system closest to the cell fluctuate in the same direction in conjunction with wetting and drying. Consequently, one can assume with a high level of certainty that the corrosion process is in progress. The cell current is a relative measure of the rate of corrosion.

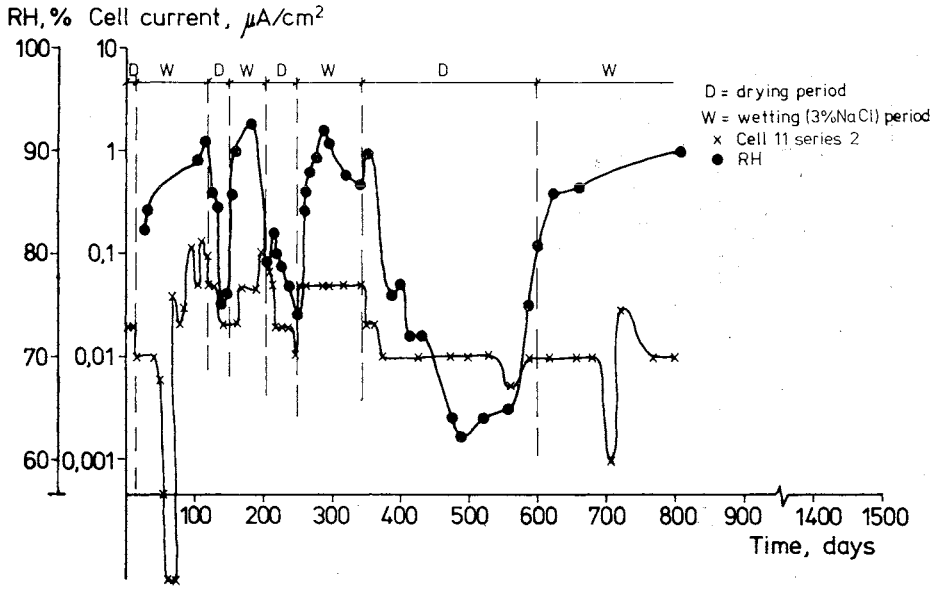

FIG 115. No corrosion initiation took place during the early stage. The current curve lies on a comparatively low level but varies due to variations in the relative humidity. During this time, the cell acted as a O_2 consumer and the moisture state controlled the supply of O_2.

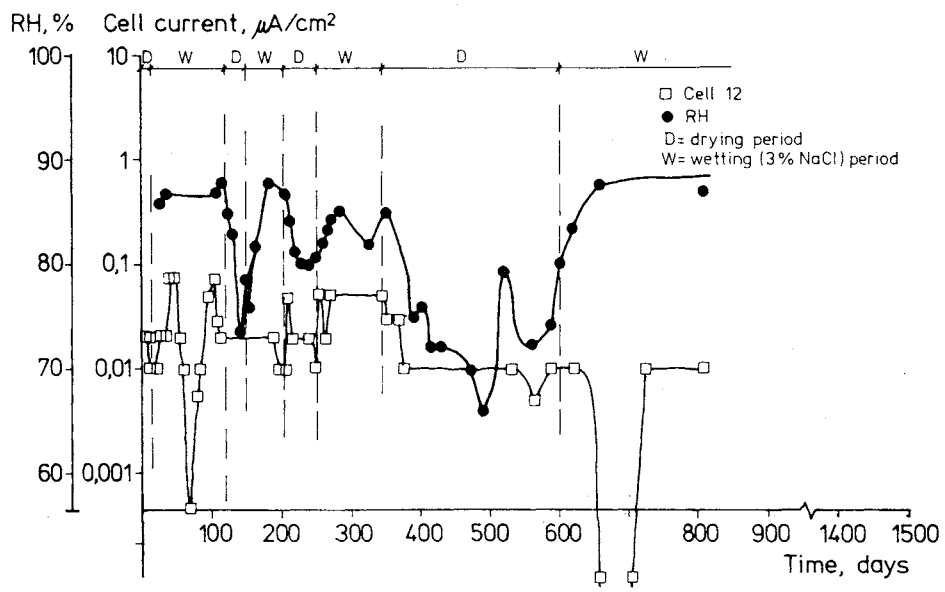

FIG 116. No corrosion initiation took place during the early stage. The current curve lies on a comparatively low level but varies due to variations in the relative humidity. During this time, the cell acted as a O_2 consumer and the moisture state controlled the supply of O_2.

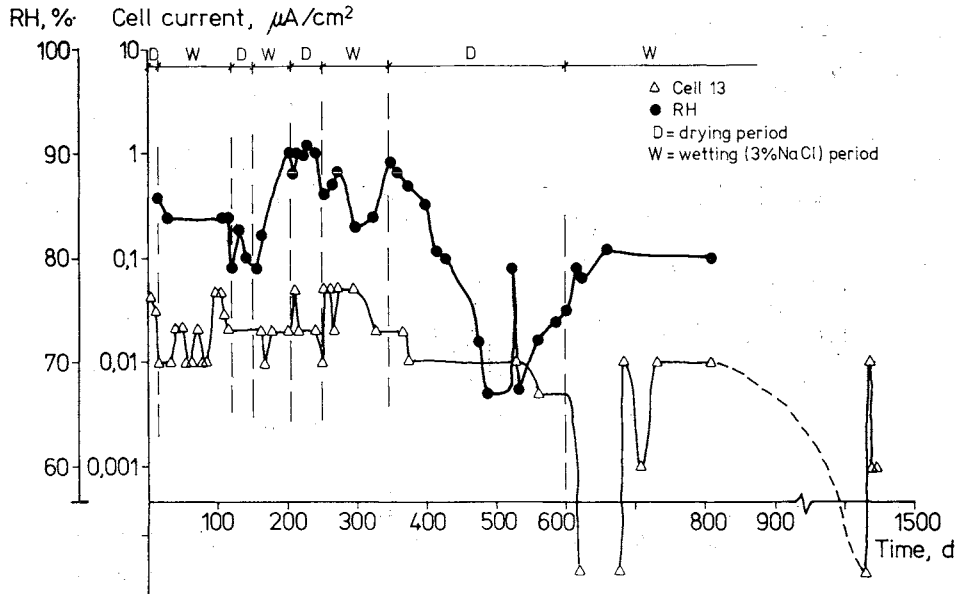

FIG 117. No corrosion initiation took place during the early stage. The current curve lies on a comparatively low level but varies due to variations in the relative humidity. During this time, the cell acted as a O_2 consumer and the moisture state controlled the supply of O_2.

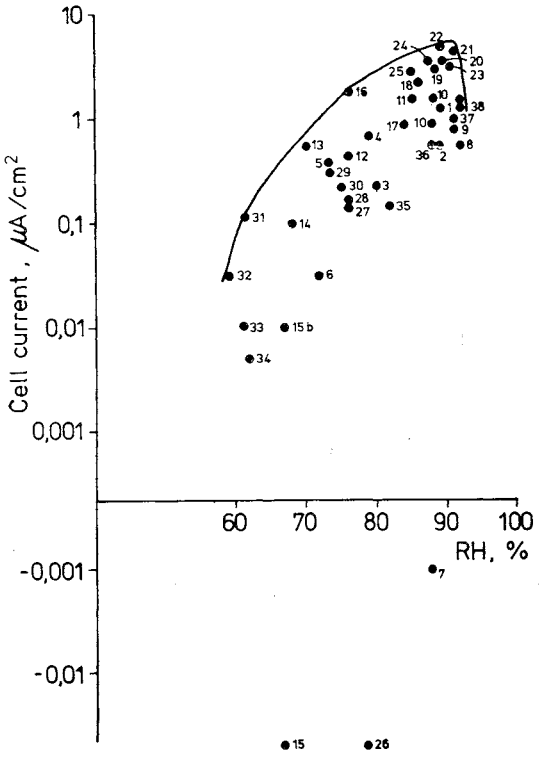

FIG 118. Measured cell current as a function of the relative humidity in a cell which is corroding (cell 10). The values have been plotted in the time sequence in which they occurred.

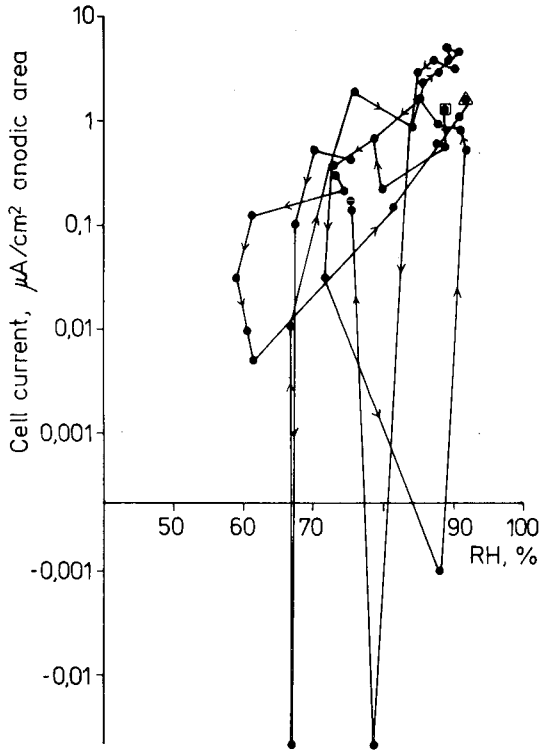

FIG 119. The measured values presented in FIG 118 joined together.

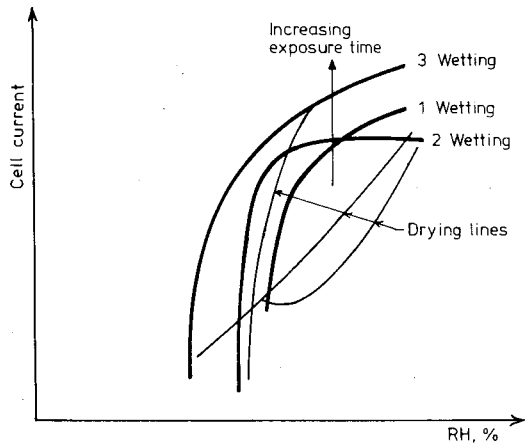

FIG 120. Schematic sketch showing effect of drying and wetting on the corrosion process.

Detailed study of results, series 2

The concrete specimens, which were about 100 mm thick and contained cells of type B and which were kept under a constant fluid pressure of a 3% NaCl solution on the wet side and with laboratory air with a temperature of about 20°C on the other side, gave very low cell currents during the period when the experiment was in progress. When making comparisons with the experiments in series 1, incipient corrosion attacks should have been seen for cells 1 and 3 due to the increase in the current during part of the period. Only cell 1 showed small attacks. In the case of cell 3 the current was, however, very stable after the first increase. This, on the other hand, indicates that inititation did not take place.

The current impulses for cells 2 and 4 in a negative direction and for cell 3 (a current increase to the power of 10 after 150 days exposure) are in this case a displacement of the state between the active and passive areas. It was not possible, however, to break the passivity in such a way that any noticeable corrosion occurred. Some of the current changes may have been migration effects. Cells of type A gave a somewhat higher cell current. This is due, for the most part, to the smaller distance between the electrodes. Nevertheless, small and insignificant corrosion attacks could be seen on these cells.

In this case, the cells have not, consequently, clearly shown that corrosion has been initiated and has been in progress. It can, however, be seen that the rate of corrosion was very low and could, in principle, be regarded as a passive or low-active state although discolouring took place on the metal surface. Photos 24 and 25 also provide an idea of the magnitude of the corrosion attack on a cell which has corroded (photo 24) compared with a cell which has not corroded (photo 25). The differences are scarcely visible.

Samples which had been exposed to a variable climate - i.e. accelerated tests - gave low cell currents in almost all cases except those where the concrete cover was 5 mm.

Minor jumps occur in the current curves for e.g. cell 8 and cells 11-13. Cell 7 also shows a certain lack of stability in the final stage. These variations indicate that something is happening, but once again, the attacks are insignificant.

Approximately the same pattern as that which applies to the cells can be seen on the reference bars. Small local attacks which are of no more than ocular interest occur. Cell 10, which has a concrete cover of 5 mm, shows a marked increase in the current intensity, on the other hand, after an exposure of about 60 days. A rapid corrosion process has thus been initiated in a very early stage.

A study of FIGS 114-117, where both the current intensity and the relative humidity have been plotted, shows the significant sequences of events even more clearly. When insignicant attacks occur or when the cell is in a passive state, the current curve is relatively independent of the moisture state, whereas a corroded cell shows a clear dependency on these two variables, see FIG 114.

Plotting the current intensity of a corroded cell as a function of the relative humidity provides a picture of the product of the resistivity and the rate of corrosion. A figure of this type is useful insofar as it provides information on the critical moisture state when the corrosion is markedly limited as a result of a lack of electrolyte or is reduced as a result of a lack of O_2. No precise value for relative humidity is, on the other hand,

obtained for the maximum rate of corrosion. Instead, this optimum value lies somewhat lower than the value indicated by the cell current curve. This is particularly true in cases where the electrolyte is highly conductive, for example concrete which contains large quantities of chloride.

If the current curve for the corroded cell is studied in more detail, it will be seen that the corrosion areas grow with the exposure time, see FIG 120. Just as a hysterisis sequence is obtained in conjunction with wetting and drying concrete, a hysterisis sequence is obtained if the current curve from a corrosion cell is recorded. The loop thus obtained rises, however, for each cycle due to the increased corrosion areas. A comparison of the point for the maximum rate of corrosion and the critical relative humidity when the W/C ratio is varied shows a displacement of these values to a lower relative humidity for less permeable material (lower W/C) or for material with less capillary pores.

Experiments - Series 3

It is well known that the rate of corrosion is dependent on the magnitude of the anodic and cathodic areas and on their relation to each other. A very large cathode in relation to the anode is obtained if, for example, a steel component is in contact with embedded reinforcement and also projects from a concrete structure. Pitting on an order of size of 10 mm steel per year has been established in cases of this type, Arup /1977/. Approximately the same effect is obtained if the concrete is highly porous locally so that a relatively large flow of water passes parts of the reinforcement, Nielsen /1976/. On the other hand, considerable thought has been devoted to the question of what happens in concrete of fairly uniform quality. Will, for example the cathode grow to such a magnitude that the rate of corrosion increases exponentially?

In order to study questions of this kind, cells of type C were manufactured. These were cast in concrete with a fairly poor but homogeneous quality, W/C approximately 0.8, KC6-78. The concrete cover was carbonated in air with 80% relative humidity and with a CO_2 concentration increased about 100 times compared with the standard atmosphere. When the concrete cover had carbonated (indicated by means of the phenolphthalein method) a number of tests were carried out with increased cathode areas,

with variations in the distance between the anodic and cathodic areas and variations in the potential difference between the anodic and cathodic areas. Since initiation had taken place with CO_2, the experiments were carried out in ordinary laboratory air and using ordinary tap water.

The measured cell current, the conditioning of the specimen and values for the main variables as a function of the exposure time are presented in FIG 121 in the same way as formerly.

During the brief, daily measuring occasions, deviations were made from the schedule presented in FIG 121 with regard to the connection of the electrodes. The results from these measurements have been illustrated in FIGS 122-124. Finally, photo 31 shows the appearance of the cell when the experiment was concluded.

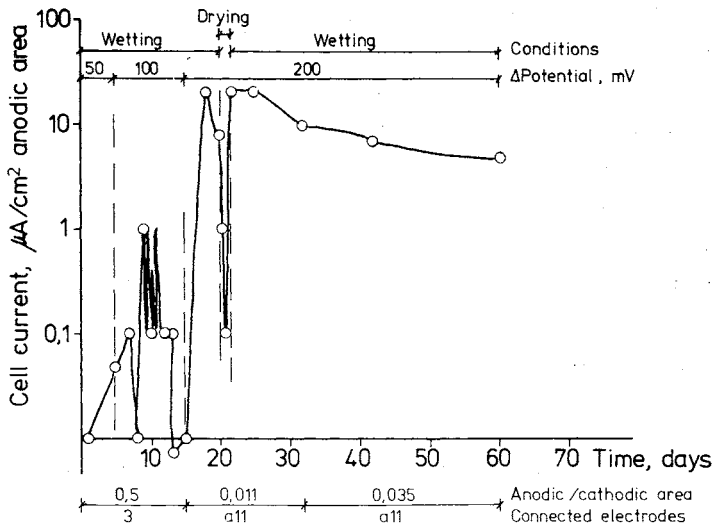

FIG 121. Measured cell current as a function of time, and compilation of specimen treatment, electrode connection and drive potential.

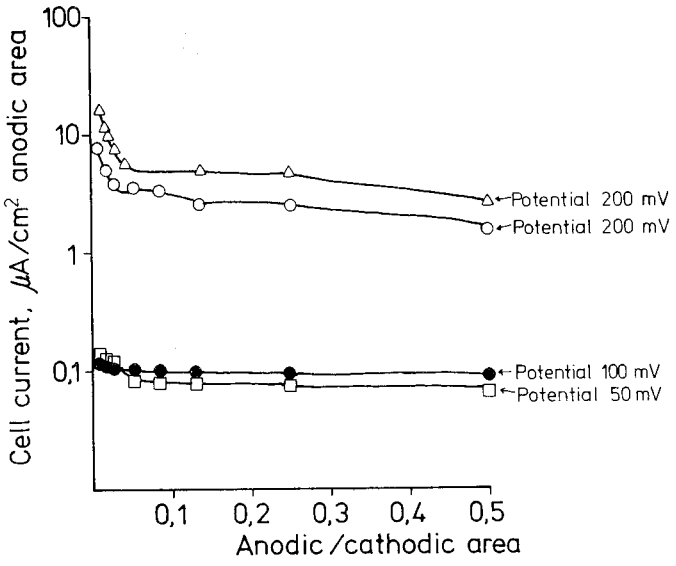

FIG 122. Cell current as a function of anodic/cathodic areas for different drive potentials.

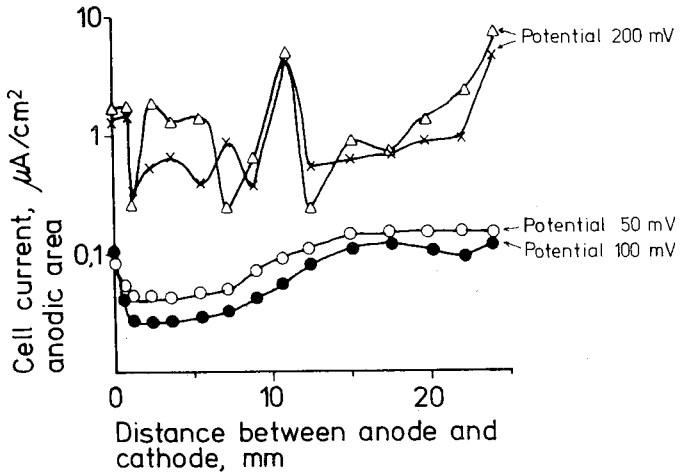

FIG 123. Cell current as a function of the spacing between the anode and cathode electrodes for different drive potentials.

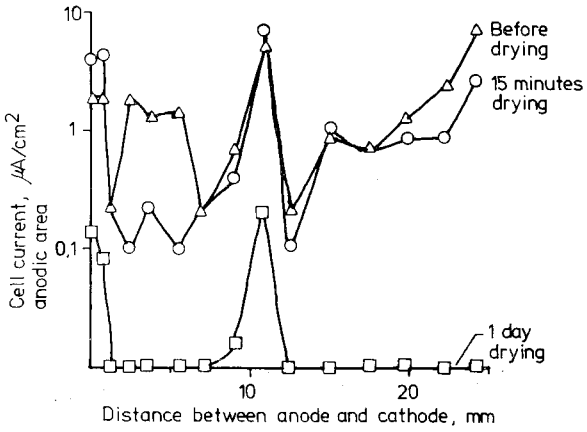

FIG 124. Cell current as a function of the spacing between the anode and cathode electrodes at different stages.

At the same time as the experiment with special cell C was in progress, the corrosion process was also studied with a normal cell A, where the initiation had taken place through carbonation. The concrete quality in this case was also W/C approximately 0.8, KC6-78. The idea was to supplement the previous studies in which only chloride initiation had taken place.

The specimen was gradually moistened in a climate cubicle at a temperature of $+20^{o}C$. In order to achieve high relative humidities in the specimen, it was not always possible to await the penetration of the moisture state of the surroundings to the cell. Instead, the specimen was sprayed with water and the cell current was then permitted to reach an equilibrium state before the next spraying operation was carried out. In the final stage the specimen was placed in a vessel filled with water. The entire apparatus still stored in the climate cubicle throughout these operations.

When the cell current had been stabilized in the water saturated state, the temperature was reduced step by step down to $-25^{o}C$. A stable state was awaited after each change in temperature. The experiment was concluded by increasing the temperature to the original level so as to obtain a check of any changes which might have taken place during the experiment. The cell current is presented in FIGS 125 and 126 as a function of the relative

humidity and temperature respectively. Photo 32 shows the appearance of the cell after exposure.

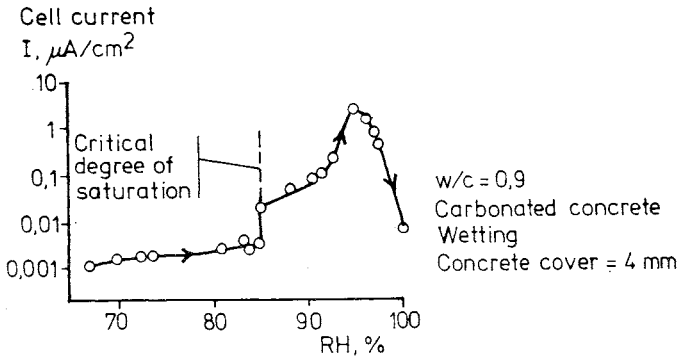

FIG 125. Measured cell current as a function of the relative humidity. The specimen was subjected to gradual wetting. Concrete quality KC6-78.

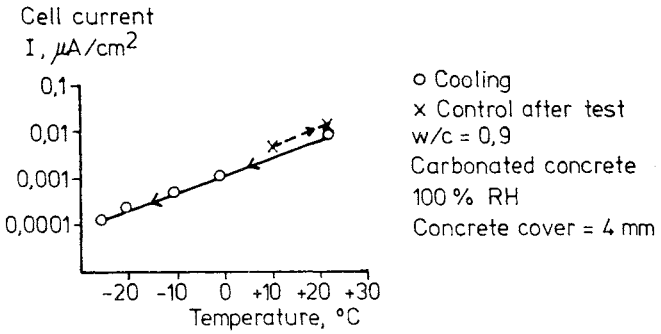

FIG 126. Measured cell current as a function of the temperature. Concrete quality KC6-78.

Detailed discussion of experiments in series 3

Reinforcement which corrodes in concrete structures in cases in which the corrosion initiation took place through carbonation of the concrete cover, has a pH value limit which applies during a lengthy period of time to each individual bar. On one side of this pH value limit, the bar is in a markedly basic environment and on the other side the environment is almost neutral. This relation always occurs at right angles to the longitu-

dinal axis of the bar but, if variations occur in the quality of the concrete cover, it can also occur lengthwise along the bar. The corrosion process will take place at a faster rate under circumstances such as these than would be the case if the entire steel surface was in the same environment.

The cells which have been used in this study have not had a pH value limit of this type. Instead, the entire contact surface has been carbonated. On the other hand, an applied potential of about 200 mV gives rise to a condition which is similar to that which occurs in reality with a pH value difference along the metal. An indication that this is so can be seen in FIG 121. An increase in the potential difference to 100 mV gives an immediate change in the cell current, this change being of an unstable and corrosive nature. A further increase in the supplied potential to 200 mV gives approximately the same result for the cell current as in the case of chloride initiation. The expansion of the cathodic area which took place at the same time as the increase in potential can, however, have contributed to the increase in current.

At a very low potential difference, 50 mV, the current intensity obtained from the cell was almost passive in nature. This may have been caused by a uniformly extended corrosion, in other words a state in which all electrodes are both anodes and cathodes, in which case 50 mV is not capable of redistributing the corrosion areas. This type of corrosion is, however, highly favourable due to the fact that the metal losses proceed slowly when regarded locally, thus extending the service life of the structure.

In cases in which only one small anode occurs, we can also note a higher level of sensitivity to drying-out when the cell current is reduced dramatically after no more than one day of drying-out, see FIGS 121 and 124. The contact mostly takes place along certain paths so that even cathodes which are located a distance from the anode can give the same effect as areas which lie very close. The reason can be cracks or other non-conductive material such as aggregate which limits the contact between the anodic and cathodic areas. The distance between the anodic and cathodic areas is not, consequently, very significant for the corrosion of reinforcement if the distance is roughly the same as the thickness of the concrete cover.

An increase in the cathodic area does not result in an increase in the cell current to the same extent, see FIG 122. In this experiment, the current was increased approximately 5 times when the cathodic area was increased approximately 90 times compared with the original area. The current limitation is derived from the fact that the current must pass through the small channel which is located closest to the anode and since the resistivity is not zero, the current is limited.

If the anodic and cathodic areas are of the same size, the cell current will also be roughly of the same size as it is in the case of chloride initiation. The drive current was, on the other hand, four times larger than that measured in the chloride experiments.

As was the case for the chloride experiments, a critical limit was obtained for the relative humidity at which the cell current became extremely low. This limit agrees fairly well with the limit in which the capillary pore system in the concrete begins to become filled up. Furthermore, a maximum cell current was obtained followed by a current limitation when the moisture content was even greater. The absolute values were of approximately the same size as those obtained in conjunction with the chloride experiments. The electrolyte is thus so highly conductive that the small quantity of chloride which is required for corrosion initiation does not have any noteworthy effect on the resistivity. It has, on the other hand, long been well known that chloride can give rise to pitting. This is in no way connected with the mean corrosion rate, however.

The experiments also showed that the cell current increased markedly and immediately when the specimen was sprayed with water. Climate changes, whether consisting of drying or wetting, thus constitute a factor which has a marked effect on the rate of corrosion.

Although a thick concrete cover protects the reinforcement, wetting or drying disturbs the entire fluid balance in the specimen. If the process before a stage of this type is diffusion controlled, this control ceases immediately in conjunction with, for example, rainfall since the electrolyte begins to move.

Temperature changes in the surroundings affected the cell current in such a way that a lower temperature gave rise to a lower cell current. The relations which were measured agree fairly well with the temperature effect which occurs in conjunction with atmospheric corrosion of steel, Wranglén /1967/. The experiment was, however, carried out in water-saturated concrete. Consequently effects such as condensation with concomitant disturbances in the fluid balance of the concrete were not included. Factors of this type probably influence the rate of corrosion to a far greater extent than does a temperature change in itself.

Experiments in series 4

The influence of the cement type on the corrosion process has been investigated with regard, inter alia, to durability ever since cement brands have been available on the market. How do the sulphides in slag cement influence the corrosion initiation, does initiation take place immediately, how does slag cement concrete behave in chloride-rich environments etc? These are some of the questions which the present investigation aimed at answering, particularly for the cement brand which was to be used in Sweden.

For this purpose, cells of type A were cast in concrete with slag cement and Portland cement respectively. 5% $CaCl_2$/cement content was added to two specimens to ensure that a corrosion attack would take place on the cell in the Portland cement concrete. This would make it possible to compare the cell current from the corroding cells in Portland cement concrete and slag cement concrete, KC7-80 and KC8-80 respectively. The other cells were cast in concrete with W/C approximately 0.7, KC9-80 and KC10-80, and W/C approximately 0.4, KC11-80 and KC12-80.

The concrete cover had a thickness of 30 mm for concretes of quality KC7-80, KC8-80, KC11-80 and KC12-80, and 15 mm for KC9-80 - KC12-80. See also Table 23 in which the appearance of the cells after exposure is presented as well as the primary variables.

The experiment was carried out on specimens which, due to the slower hydration of the slag cement, were cured for 14 days in water directly after casting and then for about 400 days in 50% relative humidity. The

ambient temperature was $20\pm2^{o}C$ both during conditioning and during the experiments.

Throughout this lengthy holding period, the concrete received roughly the degree of hydration which actual structures can be expected to have at the beginning of their service life. Since the pore solution in the slag cement concrete differs in numerous regards from the pore solution in Portland cement concrete, it was possible that unfavourable affects could occur in conjunction with a combined initiation of carbonates and chlorides, even if the neutralization had not reached the steel or cell. The lengthy holding period, which gave a maximum carbonation depth of 5 mm, thus also included this possible combined initiation mechanism.

Varying the concrete cover and concrete quality for both the slag and the Portland cement concretes was intended to provide possibilities for comparing the properties of the slag cement from the durability viewpoint in relation to the properties of the Portland cement.

The experiment was started in a dry state. The specimens were then subjected to the first wetting with ordinary tap water. This made it possible to see if the cell current was already very high, in other words if the corrosion process had been initiated before the start of the experiment by the substances included in the slag cement.

In accordance with the patterns previously established, a number of typical pictures are provided of the cells after exposure in photos 33-37 and the current curves for the cells are presented in FIGS 127 and 128.

Table 23 Main variables and results of an ocular inspection of corrosion cells in series 4. All cells are type A. 200 days exposure.

Cell No. 1 Slite Portland cement W/C = 0.40 5% $CaCl_2$ Concrete $cover_W$ = 30 mm Concrete quality KC7-80	100% of the cell surface attacked by corrosion. Corrosion depth greater locally than for cell No. 2, which is enclosed inside the slag cement concrete.
Cell No. 2 Slag cement, 65% slag W/C = 0.40 5% $CaCl_2$ Concrete $cover_W$ = 30 mm Concrete quality KC8-80	100% of the cell surface attacked by corrosion.
Cell No. 3 Slite Portland cement W/C = 0.70 Concrete $cover_W$ = 15 mm Concrete quality KC9-80	5% of anodic area attacked. A large number of pores under the surface, indicating considerable water separation. See photo 33.
Cell No. 4 Slag cement, 65% slag W/C = 0.70 Concrete $cover_W$ = 15 mm Concrete quality KC10-80	Large pores (diameter 15 mm) gave rise to attacks at an early stage. In the final stage, about 70% of the cell surface was corroded. The attacks were also comparatively deep, reaching a maximum depth of 0.5 mm. See photo 34.
Cell No. 5 Slite Portland cement W/C = 0.40 Concrete $cover_W$ = 30 mm Concrete quality KC11-80	No visible attacks.
Cell No. 6 Slag cement, 65% slag W/C = 0.40 Concrete $cover_W$ = 30 mm Concrete quality KC12-80	No visible corrosion attacks. The metal surface varied in colour from light to dark. Large blisters in contact with cell, not, however, in direct contact with exposure surface. See photo 35.
Cell No. 7 Slite Portland cement W/C = 0.40 Concrete $cover_W$ = 15 mm Concrete quality KC11-80	No visible attacks although a void with a diameter of 6 mm was in direct contact with the cell. See photo 36.
Cell No. 8 Slag cement, 65% slag W/C = 0.40 Concrete $cover_W$ = 15 mm Concrete quality KC12-80	Approximately 15% of anodic area attacked. Fairly dark colour on corrosion product. Corrosion attack probably initiated adjacent to a small void. See photo 37.

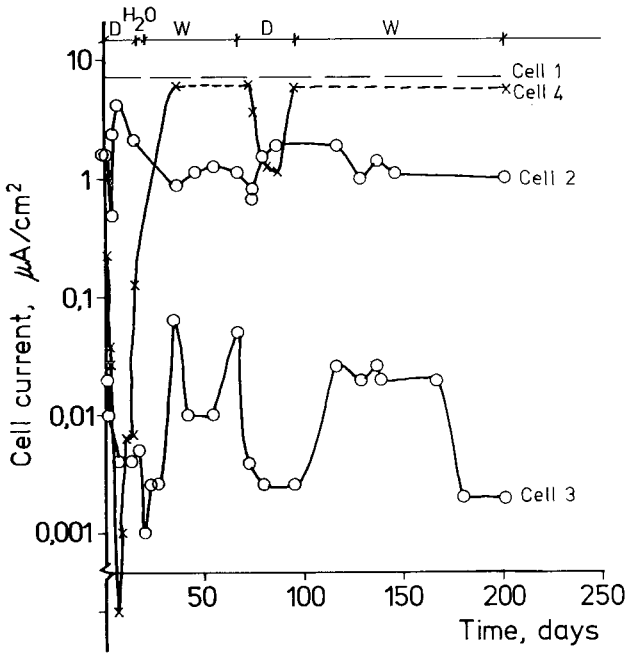

FIG 127. Cell current as a function of exposure time, experiment in Series 4. Cells 1, 2 and 4 show a very high cell current, in other words the corrosion process has been initiated on the cells. Cell 3 is, on the other hand, comparatively stable with a low cell current. This does not indicate initiation which had, nevertheless, taken place, see photo 33.

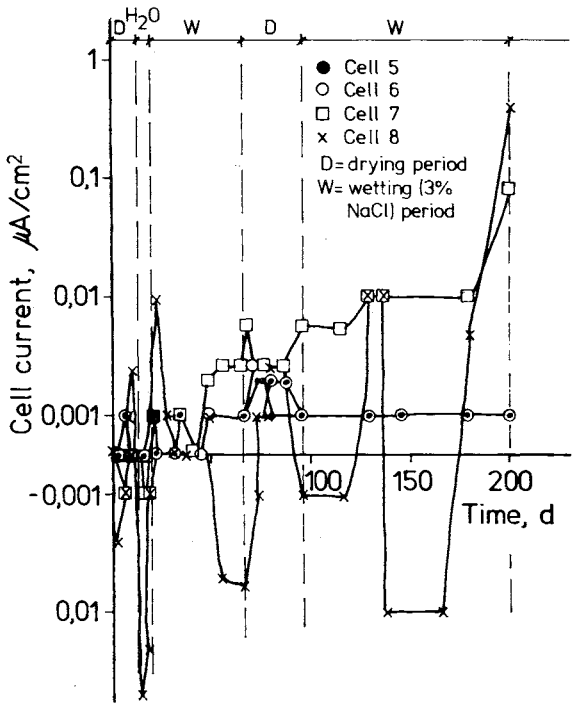

FIG 128. Cell current as a function of exposure time, experiment in Series 4. Cell 8 is highly unstable and fluctuates between positive and negative cell currents. The cell current also increases considerably in the final stage. The corrosion initiation can be seen for this cell. Cell 7, on the other hand, is comparatively stable up to the last 20 days. Whether corrosion initiation had taken place on this cell or not is difficult to say. As far as the other cells in this figure are concerned, it is quite clear, however that no initiation took place during the experimental period.

Detailed discussion of results, series 4

Judging by the cell current, the cells in which the concrete contained 5% $CaCl_2$ of the cement weight corroded. The slag cement specimen showed a lower cell current, however, than did the Portland cement concrete. The reason for this may have been a short circuit on the cell in the Portland cement concrete as a result of the fact that the attack was considerably deeper there. The slag cement concrete thus gave a corrosion attack of general corrosion type, even in conjunction with chloride initiation. Perhaps the more hygroscopic slag gave rise to this affect due to a more uniform and higher moisture state, particularly during the curing period.

During the course of the experiment, corrosion initiation appeared to have occurred for the cell in slag cement concrete and W/C approximately 0.7, in other words there was reason to suspect that the internal, natural substances in this concrete quality were sufficient to give rise to the corrosion attack. Other experiments (the crack experiments) contradicted this hypothesis, however.

When the specimen was opened, it could be seen that the attack had been initiated by a large void which had been formed against the exposure surface. This flat cell surface had thus retarded rising air or water which tends to rise to the surface when subjected to compression and water separation respectively. It should be noted that the cell in Portland cement concrete also had voids but these were smaller in size. The cell in Portland cement concrete had also corroded but to a smaller extent then that in slag cement concrete. Whether or not the current curve indicates an attack cannot be clearly seen in this case.

Concrete of good quality and with a cover of 30 mm provided no indications, however, throughout the experimental period of the occurence of corrosion. This was confirmed when the cells were inspected at the end of the experiments.

It was, on the other hand, possible to establish once again the fact that slag cement concrete involves a greater risk for voids adjacent to the cells. This should, therefore, be taken into consideration when producing concrete products with this type of cement. In the case of a thinner

concrete cover, 15 mm, W/C approximately 0.4, the cell in the slag cement concrete began to corrode, however. The corrosion process had probably been initiated at the start of the experiment since the current curve was irregular from the beginning. No attacks could be seen on the Portland cement specimen despite the fact that the current curve at the end of the experiments indicated that initiation was close at hand.

The reason for the somewhat poorer resistence to cell corrosion of the slag cement concrete in these experiments may be purely accidental due to the considerable porosity which occurred in these particular specimens.

It can, on the other hand, be clearly seen that the substances in the pore solution of the slag cement concrete cannot, in themselves, initiate a corrosion process.

5.2.4 General discussion on the properties of the corrsion cells

The currents which were recorded from the corrosion cells have, in most cases, indicated a possible initiation of the corrosion process. It has always been possible to note the occurence of strong attacks from the currents which run through the electrodes.

In the case of extremely low permeable concrete, the corrosion rate was sometimes so low that the cell current was roughly the same as that from cells in a passive or low-active state. By corrosion is meant in this case the state which occurs when the exposed surface of the cell is discoloured in clear mat brown or mat black.

Furthermore, it was seen that the cell currents could be interpreted more easily if the relative humidity was also recorded at the same level as that occupied by the cell.

When comparisons were carried out of corrosion attacks on cells and on reference steel specimens, the reference specimens of bar type were always much more resistive to corrosion than the corresponding cells. The cells and the reference bars also have different types of surfaces since the cells were flat and the bars were round.

In addition to indicating the initiation time, the cells have also provided a fairly satisfactory measure of the rate of corrosion if the current intensity is compared with an ocular inspection after the end of the experiments.

A later comparison with the weight loss measurements which were carried out showed a good level of agreement for the corrosion rate as a function of the relative humidity for both the methods.

The cells can be used for mechanism studies if one bears in mind the fact that the current which is measured is a combination of the corrosion current and of the resistivity.

By way of conclusion, it should be noted that this part of the investigation was not designed to study cell factors and measuring equipment details but rather to carry out comparative studies, in an inexpensive and simple manner, in conjunction with, for example, variations in environmental parameters, concrete parameters etc. Establishing the occurence of corrosion initiation with the aid of the cells, without breaking off the surrounding concrete, was also considered to be an important objective. The cells also provided better possibilities of interpreting the corrosion mechanisms which control the corrosion process. The cells can, however, be further developed so as to improve their performance. In this case, it would also be desirable to record the resistivity of the concrete and the potential of the individual electrodes.

5.3 Measuring the rate of corrosion by means of the weight loss method

5.3.1 General

Corrosion studies on steel embedded in concrete have been carried out partly with the aid of advanced equipment such as corrosion cells, capacitance measurements, potential measurements etc, and partly by means of simple ocular methods such as weight loss measurements etc.

Corrosion measurements in concrete always entail a complication which does not arise when carrying out studies in liquids, air and other transparent media since the concrete around the embedded steel acts as a barrier and not only protects the steel from various substances but also prevents visual examination and direct contact with measuring equipment. Consequently, problems have arisen in many cases in interpreting the measurement results obtained by means of advanced equipment. One of the reasons for this is that what happens in the concrete layer - both physically and chemically - during the course of the experiments must also be taken into account.

The simpler methods have, on the other hand, entailed problems due, quite simply, to their simplicity. One such method frequently used has been to study the embedded steel ocularly and make a subjective classification of the degree of corrosion. Another problem is that research projects are not normally permitted to continue over a lengthy period of time. Instead, the results of the experiments must be reported within a period which is no more than a fraction of the normal service life of a structure. Consequently, most studies must be accelerated, thus giving rise to even more difficult interpretation problems. The subsequent ocular inspection has sometimes been somewhat more quantitive in nature due to the fact that the corrosion projects have been removed by acid, thus making it possible to measure local attacks.

The classical measuring method for recording the rate of corrosion in general corrosion research is to measure the weight loss. Pickling or cleaning agents, which remove almost nothing except the metal oxide and which give rise to very small attacks on the actual metal have been

developed for this purpose. The attacks which the cleaning agents do, nevertheless, give rise to on non-corroded surfaces are compensated by means of extrapolation or calibration. This method has been described by, inter alia, Mercer, Butler and Warnen /1977/ and has also been described as an ASTM standard, ASTM E1-67. The method has been further developed at the Swedish Corrosion Institute so that it can be applied in studies of atmospheric corrosion of steel. It is also considered to be applicable to studies of the corrosion of steel in concrete.

5.3.2 The cleaning method

This method is based on subjecting the specimen - the steel - to a non-accelerating environment and carrying out the subsequent check, in other words the corrosion measurements, with an extremely high level of accuracy. The corrosion measurement consists of measuring the weight loss after the specimen has been pickled in Clarck's solution. This solution consists of concentrated HCl with the following admixtures per litre: 20 g Sb_2O_3 and 50 g $SnCl_2$. The solution thus obtained rapidly dissolves the corrosion products but causes very little attack on non-corroded steel. In order to correct the minor losses on unattacked steel which the cleaning agent does nevertheless cause, the corroded specimen is pickled several times at regular intervals.

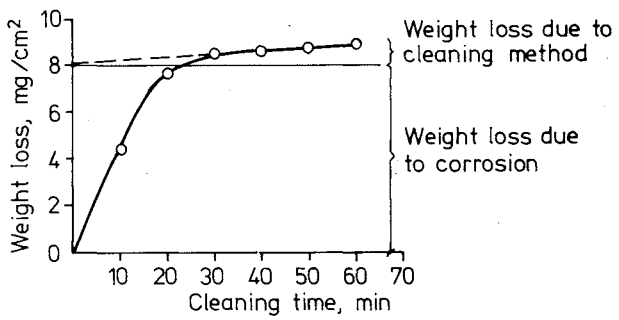

FIG 129. Schematic figure showing how the steel corrosion caused by the cleaning agent is taken into account.

A curve with the appearance of that presented in FIG 129 is obtained if a graph is drawn with the metal loss as a function of the cleaning time. The backward extrapolation of the curve with the smallest slope shows the corrosion caused by the cleaning agent on unattacked steel.

Together with the weighing equipment available today, this method makes it possible to record corrosion attacks of no more than a few tenths of one mg/cm^2.

5.3.3 Control experiments

A number of simple tests were carried out with a view to checking to see if the Clarck's solution also functioned satisfactorily on the steel grades which occurred in the reinforcement steel which was to be used and to see if the method was in any way influenced by the fact that the steel had been embedded in concrete.

The ribbed bar which had been corroded outdoors and smooth bars which had been polished were cleaned first. The result is presented in FIG 130. The cleaning method indicated no corrosion losses for the smooth bars while the corroded bars showed 4.9 mg and 6.7 mg corrosion products/cm^2 steel surface.* The steel grade thus proved suitable for this cleaning method.

The bars which had been cleaned in the first test were weighed and embedded in mortar with Slite Portland cement. The samples were stored in laboratory air - 50-60% relative humidity and 20 $\pm 3^{\circ}C$, for two days. The mortar was then clipped off but could not be completely removed. The bars were pickled again and the remainder of the mortar could then be removed and any weight losses which had occurred could be checked. The results are presented in FIG 131. Embedment in mortar thus entailed a very small metal loss amounting to less than 0.2 mg/cm^2.

---

* A scale with an accuracy of 0.0001 g and a maximum capacity of 200 g was used during these experiments.

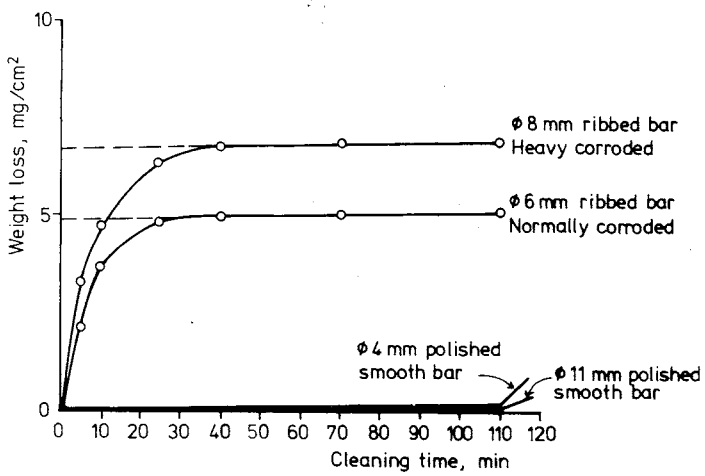

FIG 130. Preliminary investigation to study the suitability of the cleaning method for the reinforcement steel which was to be used.

A further preliminary test was carried out. In this test, the corrosion process was initiated by sprinkling NaCl on the steel which had been embedded in mortar. The specimen was opened and was pickled after a 24-hour exposure in the salty mortar. The results are presented in FIG 132. Although very small attacks could be seen ocularly, in the form of colour variations, no metal losses were recorded in principle.

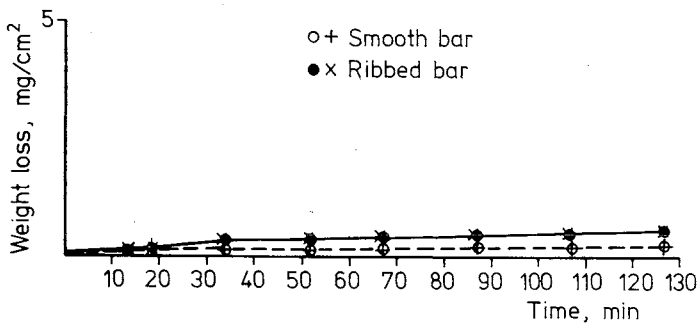

FIG 131. Preliminary test to check if embedding the steel in mortar gives rise to metal losses.

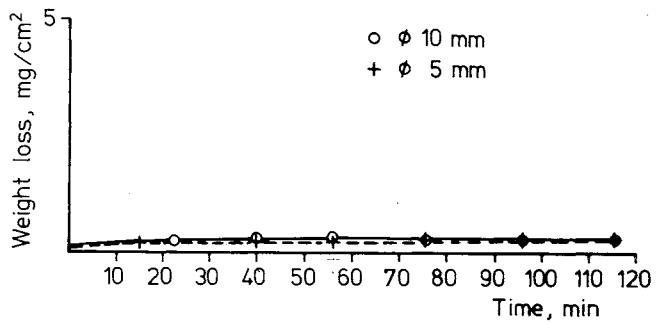

FIG 132. Preliminary test of cleaning method on steel which has been corroded 24 hours.

The above mentioned tests showed that the cleaning method could be used in tests on steel embedded in concrete. The duration of the cleaning time selected for these experiments was 60 + 30 +30 minutes so as to ensure that all mortar which had adhered to the steel would be removed.

It was decided at this stage not only to measure the weight loss but also to determine the visible anodic areas as a percentage of the total steel area. The combination of these two measurements would make it possible to calculate the metal loss in μm on the entire specimen and also the metal loss in the anodic areas.

The size of the anodic areas would be calculated by marking corroded areas on the specimens. A transparent plastic film would then be wound around the bars so that the corroded areas could be traced off. The size of the corroded areas would be assessed by placing the plastic film on a grid, thus making it possible to integrate the areas.

5.3.4 Fields of study with the weight loss method

The corrosion model presented in chapter 2, in which the corrosion process was broken down into an initiation and a corrosion period, showed that most studies in this field had been devoted to the initiation process and its time dependency, see Tuutti /1977/. Initially, the model was no more than a theoretical aid for interpreting the results from various investigations since a large number of material coefficients were missing in the

propagation stage and in the final stage. When carrying out previous assessments of, for example, the corrosion rate, the corrosion volume has been roughly measured for practical cases by means of, measuring-stick, and then extrapolating the end of the initiation process, thus obtaining a mean corrosion rate, see Thorsén and Tuutti /1979b/.

Others have assumed a corrosion rate of the same value, approximately 60 µm/year, as that measured during atmospheric corrosion of fully exposed steel, Schiessl /1976/. Against this background, it was felt important to map out more accurately the parameters which determined the rate of the process and to obtain an absolute measure of the corrosion rate for steel in concrete.

Consequently, the weight loss measurements were regarded as suitable for investigating the corrosion rate after initiation and for determining the depth of corrosion which gave rise to cracks in the concrete cover.

The weight loss measurement method is a method which involves recording that which is sought - namely, metal losses - unlike electrochemical measurements, which usually only provide relative values which must be correlated to the results obtained from weight loss measurements.

At the same time, the results can be compared with those obtained from measurements carried out by means of corrosion cells.

The method was also regarded as suitable for studying the corrosion rate of steel in cracked concrete. This would make it possible to prove or refute the theories concerning re-alkalization and, consequently, repassivation which Schiessl /1976/, Tuutti /1978/ and others have presented.

5.3.5 Mapping out the corrosion rate in the propagation stage

General

The following factors have a marked influence on the corrosion rate.

- The moisture content in the finely porous material which surrounds the steel, expressed by means of the relative humidity in the pore system. The relative humidity is a direct measure of the quantity of

electrolyte which establishes contact between the anodic and cathodic areas. Furthermore, the electrolyte in a finely porous material can restrict to a considerable extent the transport of essential substances to the corrosion areas since convective transports can become diffusive.

- The temperature controls the chemical reaction rates and the physical mobility of the substances which are included in the corrosion process. Fluctuating temperatures can influence the other factors. The moisture content of a material can, for example, increase as a result of condensation.

- The chemical composition of the material which surrounds the steel controls the formation of the corrosion areas. The type of corrosion can either be general or local in character and the quantity of activating substances in the pore solution constitutes the determining factor for this. The hydroscopicity of the material is also influenced by the chemical composition, which affects the equilibrium conditions for e.g. the relative humidity in the material versus its surroundings. The chemical composition is determined partly when manufacturing the concrete through the selection of cement type, additives etc and partly by the substances which can penetrate the material from the surroundings.

- The porosity of the concrete is a physically limiting factor and is thus also of considerable significance for the initiation process. The porosity of the material also affects, to a certain extent, the factors which have previously been mentioned such as sensitivity to external variations in relative humidity, restrictions (of various magnitudes) in transports which occur between corrosion areas etc.

- The concrete cover, like the porosity, is a physical factor and controls the process in a similar manner, i.e. primarily constitutes a parameter which determines the length of the initiation period.

Factors which are more difficult to define, control and record, but which are at least as important as those mentioned above, also exist. Such factors include the environmental variations along the metal which can give rise to differences in potential etc.

The primary objective for the entire project was to develop models. Producing material coefficients which could not be derived from other corrosion research constituted a secondary objective. Consequently, the following factors were selected for inclusion in the investigation:

- relative humidity
- chemical composition
- porosity of concrete cover

The schedule of variations was not exhaustive and a number of values for the abovementioned factors, which were regarded as characteristic for current Swedish concrete technology, were selected.

Basic organization of experiments

The investigation was complicated by the fact that the specimens must first be subjected to an accelerated ageing process and then exposed and broken down under conditions which could be regarded as normal. Furthermore, it was regarded as likely that the corrosion rate in the propagation stage would decline due to the sealing effect of the corrosion products. The anodic area was also expected to increase with increases in the exposure time. Consequently, it was necessary to measure the corrosion rate at various points in time and it was also necessary that each measurement be an individual result for the specimen which had been weighed, since each specimen which had been taken out and pickled could no longer continue its exposure.

This evaluation meant that a number of individual specimens which had been exposed to the same climate for different lengths of time would be compared with each other. Selecting several specimens at the same time lay outside the scope of study for reasons of time and cost.

On the other hand, it was felt that the impaired accuracy in the results due to single tests would be compensated for by the fact that a pattern was obtained of the extent and rate of the corrosion process at various times.

Specimen manufacture, values for variables included, and observations during preliminary treatment

The steel bars which were included in the investigation consisted of cold drawn bars with a diameter of about 10 mm and of a grade presented in Appendix 2. The bars were cut in lengths of about 160 mm. Of this, 10 mm at one end was ground and stamped with a code for later identification.

Considerable importance was attached to ensuring that all of the bars had a similar metal surface when they were embedded. Any oxide layer, patches of grease etc were removed by placing the bars 10 minutes in boiling HCl and then rinsing them under running distilled water, drying them with paper and finally drying them in a heating cabinet at a temperature of 105°C. The bars were then permitted to cool in closed boxes with a very low relative humidity.

The bars were cast in a mortar with 8 different qualities, all of semifluid consistence (see Table 24). The quantities of aggregate were varied to regulate the consistence.

Cement analyses and aggregate reports are presented in Appendix 1 and Appendix 3.

Test tubes of glass with an internal diameter of 17 mm were used as moulds. As a result, the thickness of the concrete cover amounted to about 3.5 mm around the entire bar.

Table 24. Mortar qualities, mix proportions for study of corrosion rate on embedded specimens.

Series	Cement type	W/C	Largest particle size	Mix proportions Cement:filler:sand:water:$CaCl_2$ 0-0.2 :0-1			
0	100% P	0.40	1	1:	-:	1.45:0.40:	-
0	"	0.70	1	1:	0.98:	2.93:0.70:	_
1	70% S + 30% P	0.40	1	1:	-:	1.55:0.40:	-
1	"	0.70	1	1:	1.00:	3.05:0.70:	-
2, 4	100% P	0.40	1	1:	-:	1.45:0.40:	0.05 *
2, 4	"	0.70	1	1:	0.97:	2.93:0.70:	0.05 *
3	70% S + 30% P	0.40	1	1:	-:	1.55:0.40:	0.05 *
3	"	0.70	1	1:	1.00:	3.05:0.70:	0.05 *

P = Slite Portland cement
S = Slag

* The specimens were embedded with cold materials (temperature: +5°C) so that the short binding times would not disturb the casting.

Specimens which did not contain $CaCl_2$ were stripped after 5-7 days and placed in a climate chamber for carbonation. The climate in the conditioning room was adapted in accordance with all recommendations to 50% relative humidity and an increased CO_2 content to about 1% by volume. When the specimens had been subjected to carbonation for 2 months, the following could be noted:

- No direct colour reactions were observed when the specimens were sprayed with phenolphtalein; consequently, the specimens were carbonated all the way through.

- The entire specimen was coloured red when a new check was carried out after 10 minutes, in other words the same specimen as that which was recently carbonated had become basic again.

The specimens were then placed in 85% relative humidity and increased CO_2 content (approximately one percent by volume) to carbonate in an environment in which this process could take place more completely. After four months in this environment, complete carbonation of all mortar qualities

could be noted, even when measurements were carried out after the specimen had been moistened for 15 minutes.

During this time, a number of earlier specimens which had been carbonated in the dry environment (50% RH) had been stored in 100% RH. A check of the carbonation depth by means of a phenophtalein solution showed complete re-alkalization.

These experiments devoted to carbonating specimens thus showed that a 50% relative humidity is by no means the best environment for carbonating concrete. This climate has, admittedly, proved satisfactory when curing large specimens but in these cases the concrete had a considerably higher moisture content in the layer in which carbonation had taken place. It seems likely that a small proportion of the capillary pore system must be filled by liquid if complete carbonation is to occur. If the environment is too dry, only a superficial carbonation takes place. The specimen is then re-alkalized in conjunction with subsequent moistening. This mechanism is important since re-alkalization also repassivates steel which is embedded in concrete. Concrete which is carbonated can have initiated a corrosion process but the environment can be so dry that the corrosion rate is very low. The addition of moisture need not necessary entail a rapid corrosion process in this case but can, instead, mean that a passive state is achieved again. It is thus important to measure the carbonation depth immediately after the concrete surface has been stripped off and immediately after the indicator solution has been sprayed on the exposed surface. This is particularly important when checking thin structures since incomplete carbonation is more frequent there due to rapid drying out.

Specimens with a $CaCl_2$ admixture were stripped after 24 hours and placed in the climates in which they would later be exposed.

The end surfaces on which the code marking had been stamped were not embedded but were first covered with silicon rubber and were, after a month, dipped in a clear epoxy solution since incipient corrosion of the steel under the silicon coating had been noted.

The two initiation methods which were included in the study involved the use of carbonated mortar and chloride-rich mortar respectively.

After initiation, the samples were placed in plastic containers as illustrated in FIG 133 with varying relative humidities. The saturated salt solutions which were used as moisture regulators were as follows for the various relative humidities:

60% RH = NaBr
70% RH = $NH_4Cl + KNO_3$
80% RH = $Na_2S_2O_3$
85% RH = Constant environment chamber in which the RH varied between 83-86% RH
90% RH = $ZnSO_4 \cdot 7H_2O$
95% RH = $Na_2SO_3 \cdot 7H_2O$
100% RH = Constant environment room

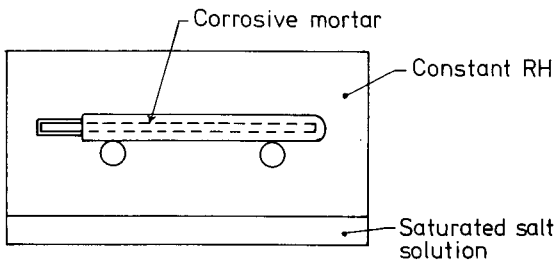

FIG 133. Exposure of samples to different relative humidities.

When the containers in which the specimens had been placed were sealed, they were stored in a constant environment with RH values of 50% and 85% respectively and with a temperature of $20^{\pm}2^{o}C$. The environment around the containers had a maximum relative humidity less or equal to that within the containers.

During the course of the experiments, it was realized that alternating moistening and drying-out of the specimens should also have been included in the study. Consequently, the remaining specimens in series 4, which was a duplicate of series 2, were taken out, as were certain specimens from the other series in which the corrosion rates were seen to be very low.

For comparison purposes, steel specimens which were not embedded in concrete were also conditioned.

The specimens were divided into three groups which were to be treated differently:

- moistening every day
- moistening once a week
- conditioning in laboratory air in which the abovementioned specimens were dried out between the moistenings.

Results

The investigation continued for about two years. All the values obtained and the calculations of basic data such as corrosion rate (µm/year) have been compiled to form tables in Appendix 7. A number of auxilliary figures are also presented in Appendix 7 so as to enable the reader to obtain a better idea of how the absolute numbers presented in this section were approximated and their significance.

The small number of results obtained for specimens which had not been embedded in concrete gave the same results as those obtained previously in a similar environment, see FIG 134 and, for example, Wranglén /1967/. The rate of corrosion was insignificant until a very high moisture state was reached and then increased markedly until it amounted to about 60 µm/year. The rate of corrosion did not increase at a level of 70-80% relative humidity due to the fact that the specimens had been protected from various types of precipitants such as SO_2, soot etc. The maximum rate of corrosion was obtained at a relative humidity of 100%.

All of the main data concerning the rate of corrosion as a function of the relative humidity has been presented in FIG 135 and 136. Each dot corresponds to the development status after six measured values - see the auxilliary figures in Appendix 7. In those cases in which major variations occur in these values, the probable maximum and minimum values have been plotted as bars in the figures.

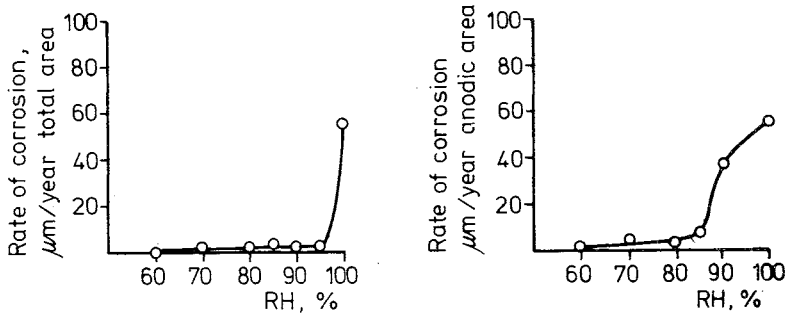

FIG 134. The rate of corrosion on unembedded steel (control-samples). Note that the environment was maintained at a temperature of 20±2°C, that the risk of condensation was small and that the specimens were protected from various types of precipitant such as SO_2, soot etc.

It should be noted that, despite the fact that the figures mention constant conditions, the specimens did not have a constant humidity since the beginning of corrosion. The CO_2 specimens were, for example, conditioned in 85% RH before certain of them were placed in 60% RH. Cl-initiated samples were, admittedly, placed directly in a constant climate but the time taken before the concrete cover achieved equilibrium with the ambient air was, in all certainty, so long that the degree of corrosion had been affected. This can also be seen from the basic material in which the rate of corrosion is always greater during brief exposure times. Not all of the results are derived, however, from the natural reduction in the rate of corrosion with time.

The figures show that slag cement gave rise to a more rapid corrosion after CO_2 initiation. The Portland cement mortar caused an almost insignificant attack.

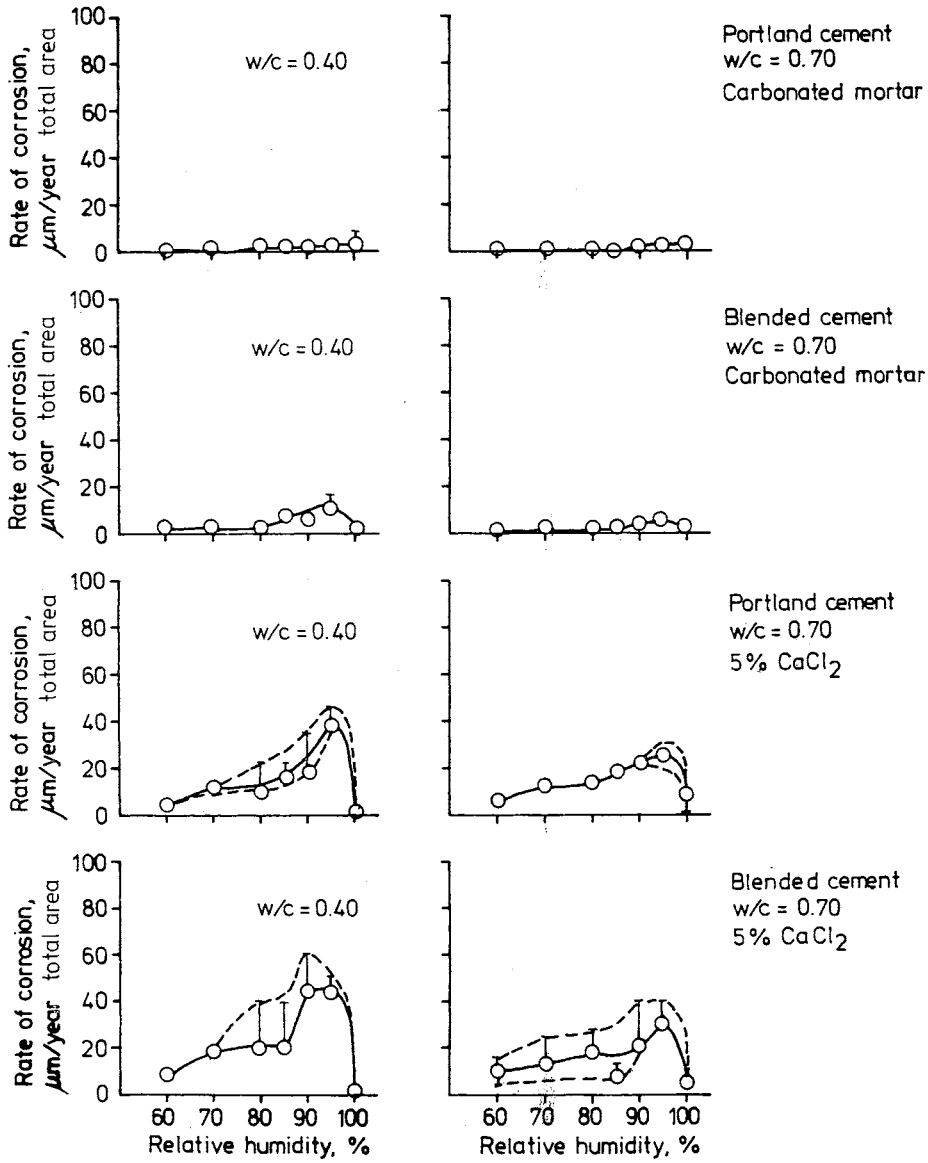

FIG 135. The rate of corrosion calculated on the total metal area as a function of the relative humidity for various types of corrosion cases. The values have been extrapolated from experiments carried out during a period of about 2 years.

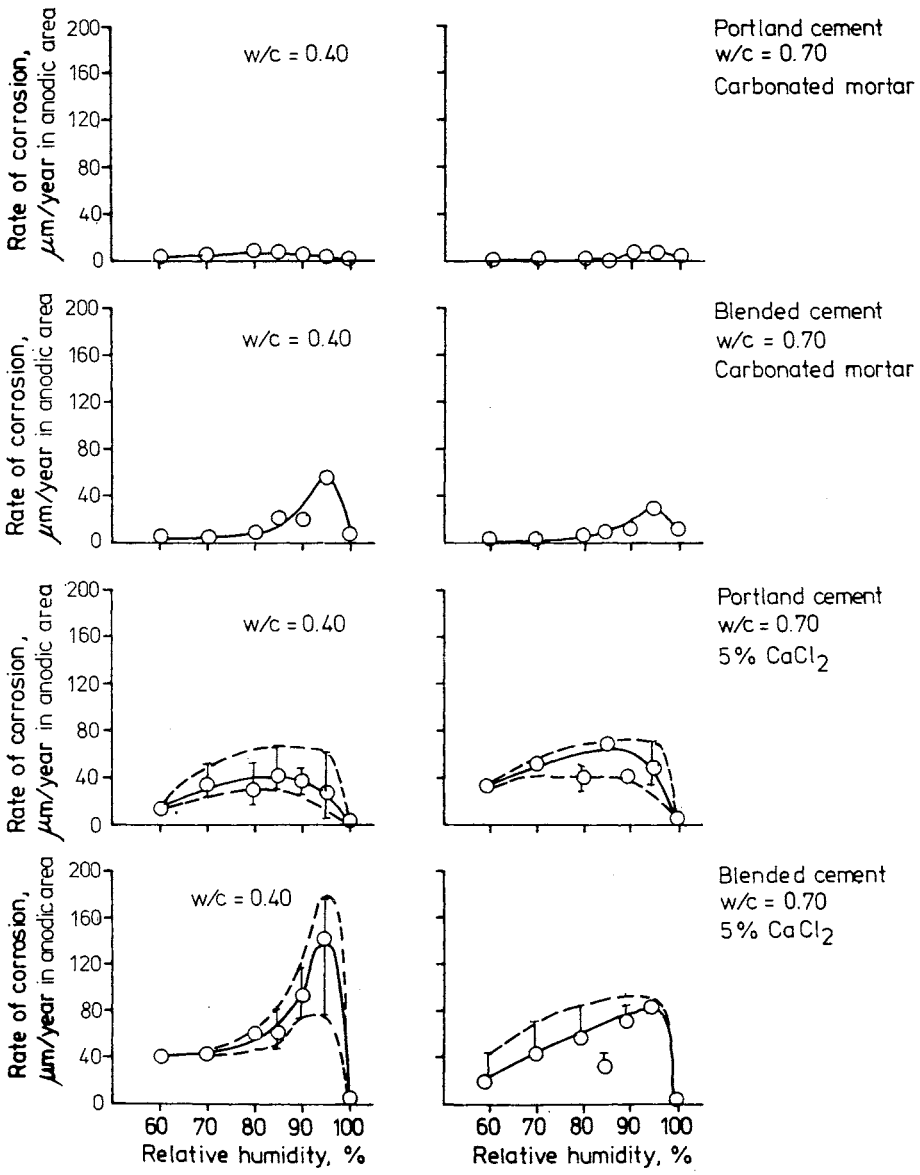

FIG 136. The rate of corrosion calculated on anodic areas as a function of the relative humidity for a number of different types of corrosion cases. The values have been extrapolated from experiments carried out during a period of about 2 years.

What then distinguishes these experiments from a natural corrosion case? Normally, the carbonation process penetrates the concrete structure slowly. This means that only parts of a steel bar are in a carbonated zone during a very long period of time, in other words part of the metal is in a basic environment and another part is in an almost neutral environment. The PH difference gives rise to a difference to potential and, consequently, an acceleration of the decomposition compared with what happened in this experiment. Complete carbonation thus seems to have a positive corrosion-limiting effect. The measurement results can explain the odd phenomenon that cracks parallel to reinforcement do not always give rise to corrosion problems even when the entire steel surface rapidly comes in contact with a carbonated layer. The carbonate ions in themselves can scarcely have any restrictive effect on corrosion. Instead, the corrosion limitation is probably due to the fact that the carbonates form diffusion barriers or limit the electrolyte contact with the steel.

Chloride-initiated samples had a far higher rate of corrosion than CO_2-initiated samples. The slag cement mortar also appeared to give a higher rate of corrosion for the chloride samples then did the Portland cement mortar.

Unlike the case of steel which had not been embedded, the maximum rate of corrosion here was achieved at a relative humidity of about 95%.

The critical moisture state was about 80% RH for CO_2-initiation of both "slag cement mortar and Portland cement mortar, while the rate of corrosion for chloride-initiated specimens was still high at 60% RH. It should, however, be noted that the chloride content was very high. The critical moisture level probably increases when the chloride content is reduced.

The more rapid rate of corrosion after initiation for slag cement can be explained by the chemical composition which gives the material a higher hygroscopicity. Drops of water could be seen on specimens of slag cement mortar which lay in air in a higher relative humidity than 80%, in other words the material was partly saturated with moisture at a relative humidity under 100%.

The effects of the initiation methods (CO_2 and Cl^-) on the extent of the corrosion can be seen in FIG 137.

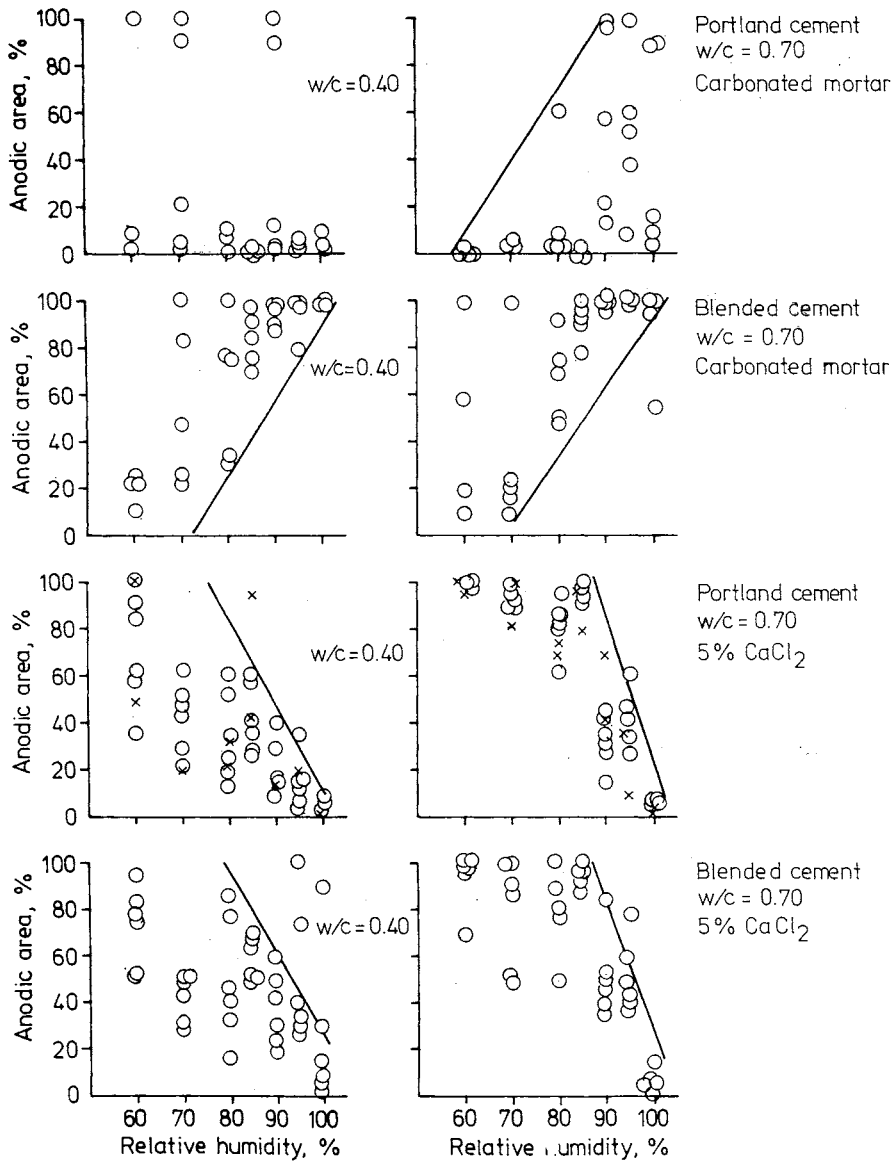

FIG 137. The boundary lines which have been marked in the figures are intended to illustrate the effects of CO_2 initiation and Cl^- initiation. The CO_2 initiation gives rise to general corrosion attacks and the Cl^- initiation gives rise to deeper attacks of the type known as pitting.

CO_2 initiation gives an increase in the corrosion area for increases in the relative humidity. The carbonate distributes the anodic and cathodic areas uniformly across the entire metal surface, thus giving rise to the most favourable general corrosion type which is obtained in conjunction with atmospheric corrosion of, for example, carbon steel.

Cl initiation, on the other hand, gives a smaller corrosion area at higher relative humidities. This entails a larger proportion of local attacks. The reduction in the corrosion area, the anodic area, is probably linked to the difficulty in supplying the cathode reaction with O_2.

The ratio between the anodic area and the cathodic area is balanced for each moisture state. At a relative humidity of 100%, the cathodic area covered a maximum of 90% of the total area. This agrees well with experiments with corrosion cells. The rate of corrosion as a function of the relative humidity also shows a good level of agreement with corrosion cells with regard to optimum and critical RH. Corrosion cells are not, on the other hand, regarded as providing absolute values for corrosion rates with the same accuracy as that obtained from weight loss measurements.

Finally, Table 25 presents the measured rate of corrosion for specimens which had been moistened and dried out in cycles. These values were not, however, the values which had been expected, one of the main reasons being, perhaps, the fact that the specimens had been cured in a large number of different ways, thus giving rise to difficulties with the zero values after calibration. However, the table does show that, for the small mortar covers which the bars had, the rate of corrosion did not become larger compared with the maximum values from constant RH storage.

By way of final comment, it should be noted that the design of the specimens was unsuitable insofar as they did not reflect reality. The uniform mortar cover, which was thin and completely carbonated, gave a lower rate of corrosion than that measured for practical structures in which the pH limit value occurs during a long period of time along the surface of the reinforcement. On the other hand, the chloride specimens had abnormally high chloride contents.

Table 25. Measured rate of corrosion on specimens which were subjected to moistening and drying-out cycles.

Cement	Initiation CO_2	Initiation $CaCl_2$	Drying period (days)	W/C	Corroded area %	Mean corrosion (µm/year) total area	Mean corrosion (µm/year) corroded area
P	X		1	0,40	81 ± 2	4	5
			7	"	67 ± 19	1	1
			1	0,70	99 ± 2	9	9
			7	"	89 ± 8	2	2
		X	1	0,40	84 ± 16	10 ± 5	12 ± 4
			7	"	96 ± 4	6 ± 1	6 ± 2
			1	0,70	68 ± 35	21 ± 10	32 ± 6
			7	"	97 ± 3	8 ± 3	8 ± 3
S	X		1	0,40	100	-	-
			7	"	99 ± 2	1	1
			1	0,70	100	12	12
			7	"	100 ± 0	2	2
P		X	All time	0,40	45 ± 40	3 ± 4	5 ± 6
				0,70	74 ± 43	9 ± 6	36 ± 57

Certain results can also cause some surprise - for example the fact that a high water-cement ratio gave rise to a lower corrosion rate than a low water-cement ratio. When making this comparison it should be borne in mind that the differences are small and that the thin and sometimes cracked mortar cover in these experiments did not have a particularly high capacity for preventing O_2 from reaching the cathodic areas. The quantity of electrolyte was, instead, decisive and the finely porous material was thus more conductive.

The W/C factor is the factor of greatest practical importance for the length of the initiation period and also restricts corrosion due to the fact that a less permeable material gives far more uniform conditions such as RH, chloride etc around embedded steel.

5.3.6 Cracks and corrosion

General

Numerous investigations have been devoted to determining whether or not cracks in concrete are dangerous. At the beginning, it was generally held that a critical crack width of approximately 0.1-0.3 mm existed and that a crack width narrower than this did not affect the corrosion process for embedded steel, see Rehm and Moll /1964/.

Later investigations have indicated that it is the ambient environment and not the crack width which is the decisive parameter for the corrosion process.

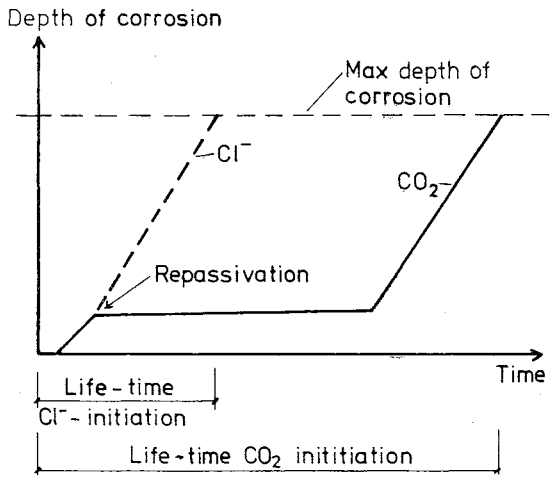

FIG 138. The corrosion attack starts almost immediately in a crack zone but the corrosion products seal the crack and repassivation then takes place. No decomposition of the metal occurs over a lengthy period of time. The attacks start when the entire concrete cover has been destroyed, carbonated.

This means that corrosion attacks can always be seen in crack zones but what is more important is to determine the stage which the process has reached. Note that this applies to cracks at right angles to reinforcement and to structures in air.

No pause occurs in a chloride-initiated corrosion process. Instead, the corrosion attacks continue uninterrupted until the concrete cover has cracked. The attacks are then accelerated.

Regardless of the crack width, cracks in concrete always increase the risk for corrosion damage. The width of the crack merely affects the time factor when the first corrosion attack is initiated, see FIG 138, Schiessl /1975/ and Tuutti /1978/. In many cases, cracked concrete can be regarded as though it did not have any cracks, see FIGS 138 and 139. Cracks in concrete submerged in water, for example, are sealed, see Fidjestöl and Nilsen /1980/. Concrete in air is sealed by corrosion products, see Tuutti /1978/ and chapter 5.6.

The pickling method was regarded as suitable for a more detailed study of the effects which cracks entail on the corrosion process, such as repassivation, cathodically controlled corrosion etc. This method makes it possible to check whether the attacks are reduced or cease when the cracks have been almost completely sealed.

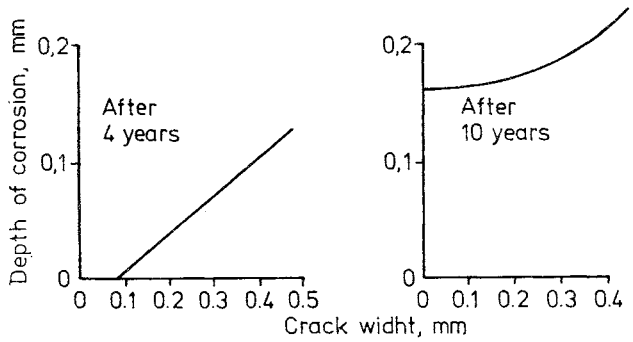

FIG 139. Depth of corrosion as a function of crack width. Processed data from Schiessl /1976/.

Production of specimens, values for component variables, conditioning

Three types of reinforcement - smooth bars with diameters of 10 mm and 5 mm respectively and ribbed bars with a diameter of 8 mm - were used in this experiment. The length of the bars was adapted to 250 mm, 750 mm and 300 mm respectively due to the weighing equipment. The quality of the smooth bars is presented in the chemical analysis in Appendix 2. The ribbed bar has not been investigated in closer detail than to establish that it had type designation Ks 40 and was manufactured at Halmstad Iron Works. The smooth bars were filed at both ends to give them a wave-

shapped profile so as to improve their adhesion to the concrete. All of the steel was pickled and processed in the same way as the specimens in the preceding chapter.

The bars were cast in the beam in accordance with FIG 140 and four different concrete qualities with a semi-fluid consistency were used, see Table 26 and Appendix 4. Two bars were embedded in each beam to permit the weight loss to be checked. These bars have two different concrete covers. The reinforcement bars which were to be checked with regard to weight loss were, in most cases, so short that they were overlapped with the ribbed bar. In the preliminary experiments, extensive shear cracking occurred. Consequently, 10 stirrups with a diameter of 6 mm were inserted in each beam. After casting, the beams were conditioned for 7 days in 100% relative humidity and then in 50% relative humidity to an age of about 30 days. The beams were cracked by laying two beams against each other with a 10 mm round bar in the centre and then creating cracks by means of two bolted joints at the end of the beams.

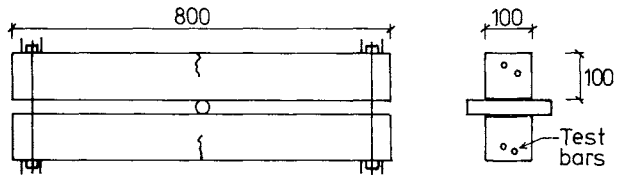

FIG 140. Test beam for crack experiments. Two reinforcement bars with two different concrete layers were placed in each beam. The bars were so short that they were overlapped with the ribbed bar. Each beam had bend-up bar reinforcements consisting of 10 smooth bars with a diameter of 6 mm.

When applying stress, the aim was to obtain cracks in the concrete surfaces with widths of 0.1 mm and 0.3 mm. The values obtained are presented in Appendix 7.

In most of the specimens, the corrosion process was to be initiated by means of CO_2. This was done locally by connecting a plastic dish to a crack and releasing air with a CO_2 content of about 1% through a hose system into the dish, see photo 38. After about a month it could be noted that all cracks had carbonated past the level where the reinforce-

ment was located. Exposure in different relative humidities was then started for the specimens.

In a number of specimens salty water with a 3% NaCl solution was to be used as an initiator for the corrosion process. Specimens of this type were laid directly in the solution after the beams had cracked.

The different variables and values for these are presented in Table 26.

Four beams of each type were used for all series with reinforcement consisting of 10 mm diameter smooth bars. This meant that tests could be carried out on four different occasions. The longest exposure time amounted to 760 days. Other series had only two specimens.

Table 26. Variables in investigation of effect of cracks on corrosion process

CEMENT TYPE	Slite Portland	Slag cement * 35% Slite Portland 65% slag
WATER CEMENT RATIO	0.35; 0.50; 0.70	
CRACK WIDTH (mm)	0.1; 0.3	
AMBIENT ENVIRONMENT	80% RH; 100% RH;	Varying 50 $\rightleftarrows$ 100% RH ** The RH value was changed every 7 days by wetting in 3% NaCl solution
REINFORCEMENT	smooth bars, 10 mm dia: smooth bar 5 mm dia. *** ribbed bar 8 mm dia. ***	
CONCRETE COVER (mm)	15; 30 for smooth bars 5 mm dia. 10 and 25	

* Only W/C = 0.5, reinforcement 10 mm dia., 80 and 100% RH.
** Only Slite Portland cement W/C = 0.5, reinforcement 10 mm dia.
*** Only Slite Portland cement, W/C = 0.5, 80 and 100% RH

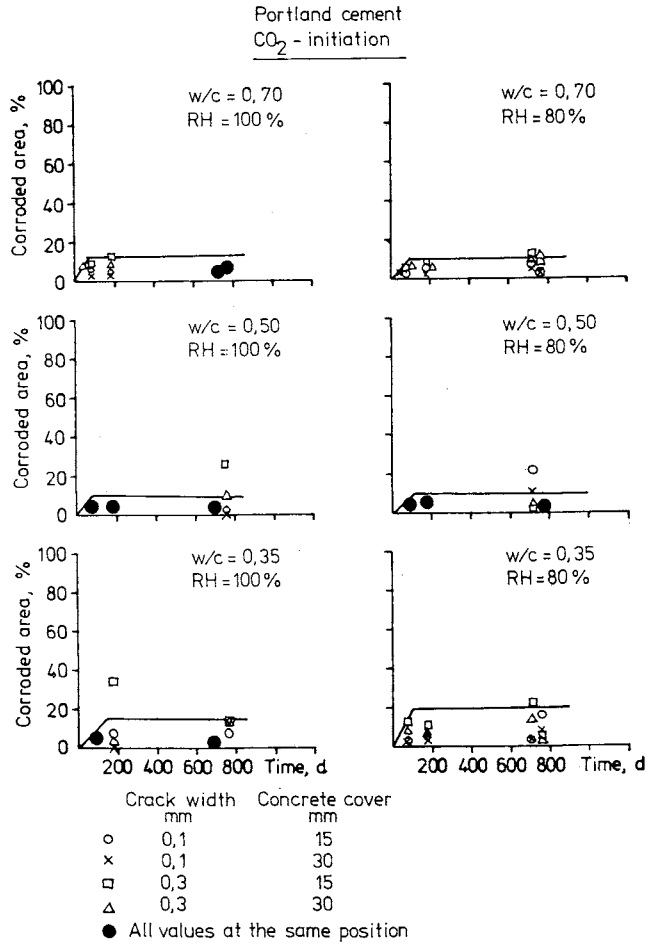

FIG 141. This figure is intended to illustrate the halt in growth of the corrosion area after the corrosion products have sealed the crack. A curve which deflects at about 100 days has been inserted to illustrate this. The values from exposure in excess of 100 days have very seldom exceeded the limiting curve. A number of points have, however, come high above the limiting curve. This may be due to the fact that more than one crack caused initiation. Only the largest crack was subjected to rapid initiation with CO_2. The entire steel surface was included in this processing. The binder consisted of Slite Portland cement. The temperature was $+20^{\circ}C$.

Tests

In addition to pickling, weighing and measuring of corroded areas, tests were carried out with phenolphthalein solution to check whether the steel surface in the crack zone was basic or not.

Results

When the specimens were broken open, it could be seen that about 90% of them with a bar diameter of 10 mm and CO_2 initiation had visible corrosion attacks. Only about 25% of the specimens with Cl^- initiation had visible corrosion attacks.

The corrosion area measured as a function of the time is presented in FIGS 141 and 142. The size of the corrosion area appears in this case to be independent of the exposure time, relative humidity, W/C, concrete cover and crack width. The blended cement, on the other hand, gives a larger corrosion area at 80% RH. Note that unlike the results presented in FIG 139, the measurements in these experiments were not started until the corrosion process was initiated.

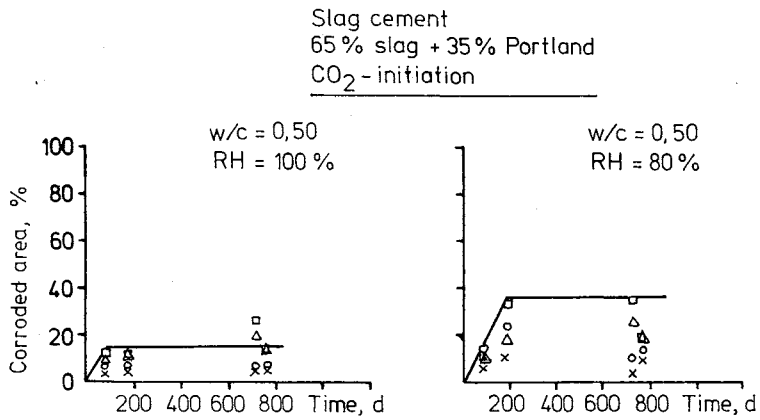

FIG 142. Corrosion area as a function of the exposure time for slag cement specimens. For other details, see FIG 141.

The depth of corrosion in anode-rich areas has been calculated and plotted for all specimens in FIGS 143-146. Specimens with a 10 mm diameter bar

had considerably smaller corrosion attacks than had specimens with a 5 mm diameter bar.

Theoretically speaking, a lower W/C should entail less corrosion when compared over the same period of time. This agrees with the results presented in FIG 143 except for W/C 0.50 and RH 100%.

For all CO_2-initiated corrosion processes, the corrosion process appears to have come to a halt after an exposure of about 200 days. This was also indicated by the phenophthalein test. All of the specimens had a strong mauve colour which then rapidly disappeared in the air. The colour disappeared after about 10 seconds in the crack zone. This was faster than for surfaces which were in zones free from cracks. The re-alkalization theory was also tested on an old drilled core of concrete which had first been permitted to carbonate to a depth of 1-2 mm. This specimen was then placed in a liquid for 10 days and a new phenophthalein test then showed that the surface had become basic again.

Specimens exposed to chloride did not have a corrosion sequence which came to a halt with time. On the other hand, the corrosion areas were very small for the specimens.

The specimens, which lay in liquid throughout the entire experimental period, had undergone autogenous healing in the cracks, in other words the cracks were sealed not only by the corrosion products but also by unhydrated cement or lime in the concrete.

All the relevant data is collected in Appendix 7.

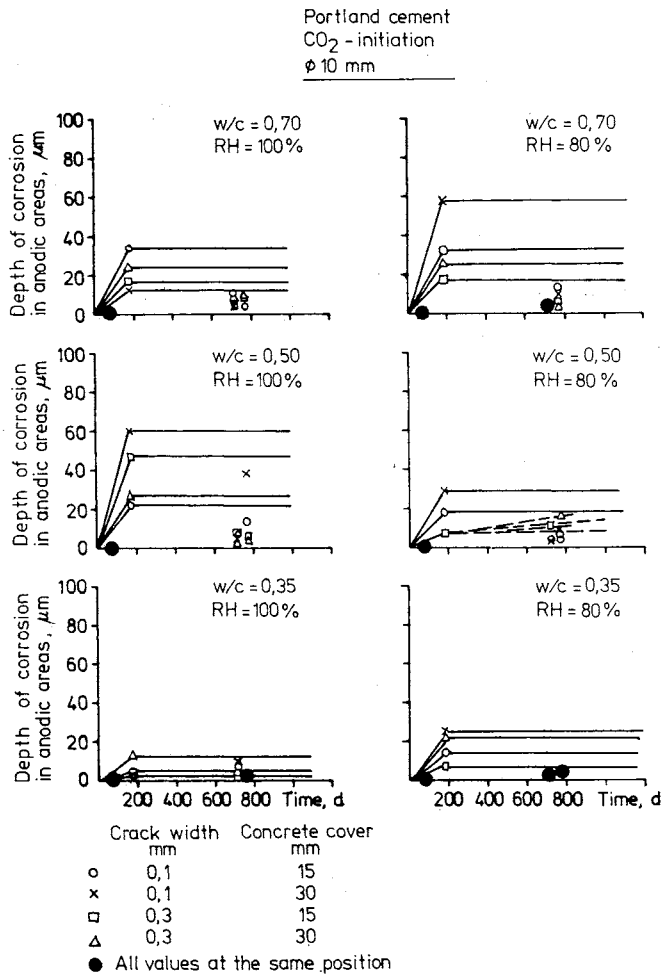

FIG 143. Mean depth of corrosion as a function of the time for steel contained in cracked concrete where the time has been counted from the initiation of corrosion through carbonation. Unbroken curves have been plotted if the experimental values agreed with the model that the corrosion process comes to a halt after a certain period of time. Broken curves have been plotted for increases in the degree of corrosion with time.

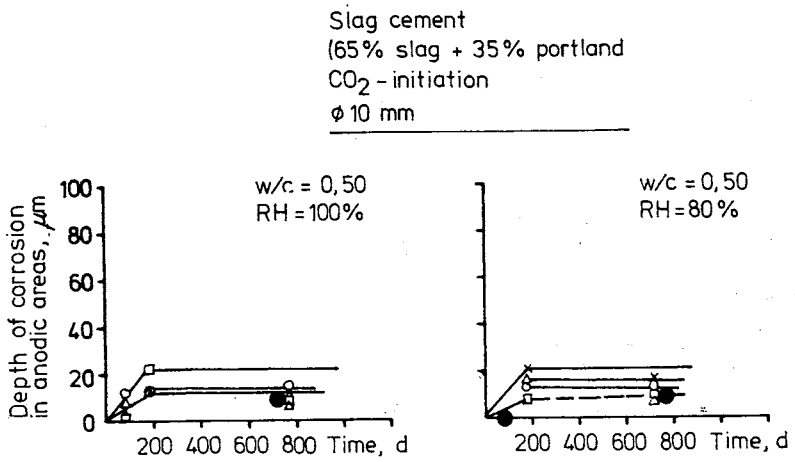

FIG 144. Mean depth of corrosion for smooth bars in cracked slag cement concrete with varying exposure times.

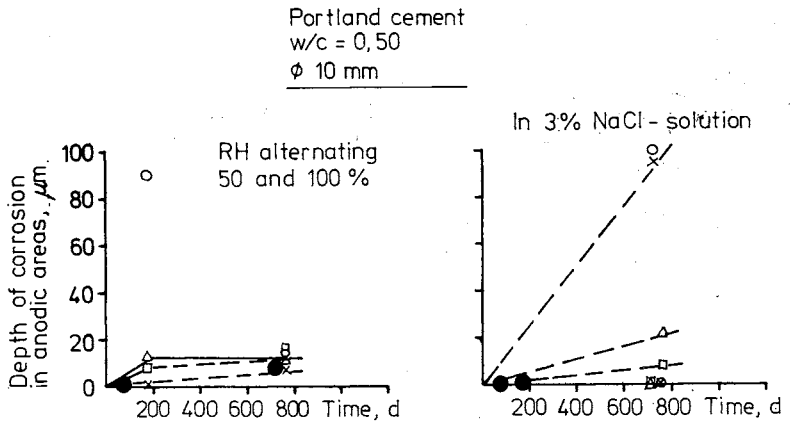

FIG 145. Mean depth of corrosion for steel in crack zones where the environment was either varied between 50 and 100% RH or consisted of a 3% NaCl solution.

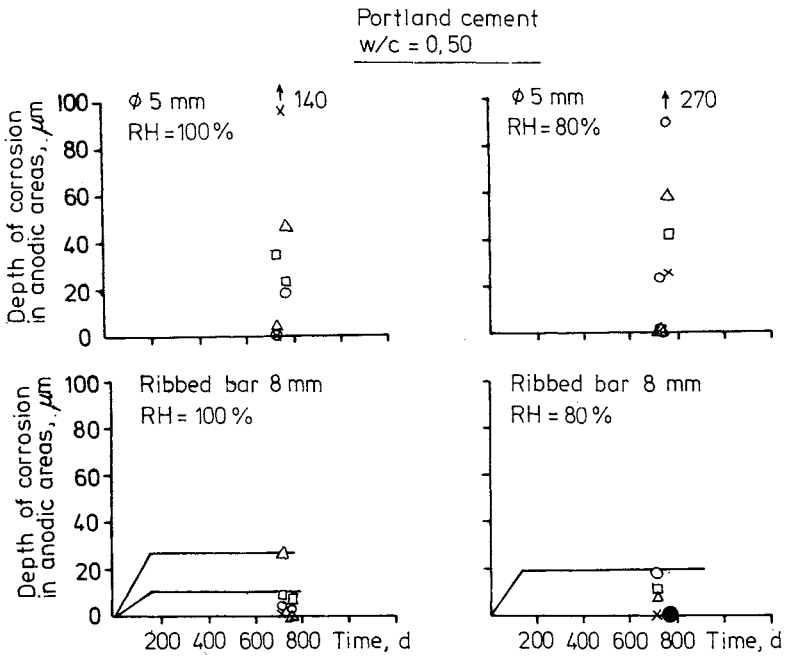

FIG 146. Mean depth of corrosion in crack zone for narrow smooth bars and for ribbed bar approximately two years after initiation of corrosion.

Discussion of results

The tests which were carried out with a view to studying the effects of cracks on the corrosion process differ from the practice applied in the CO_2 case insofar as only a limited surface was exposed to rapid carbonation. Consequently, it might be expected that the corroded area would not increase with time in the same way as in experiments where the entire surface receives the same treatment. The carbonation front thus penetrates to the steel only if air with an increased CO_2 content is sprayed on this specimen. This has made it possible to study the effect of a crack on the growth of the anodic areas. The experiment shows that the corrosion products sealed the crack, thus preventing an increase in the anodic area. In

practice, however, one can expect an increase in the corrosion area with an increase in the exposure time but this is achieved through the carbonation front reaching the steel via a constantly increasing number of cracks. Consequently, no effect was noted from the cover layer, crack width or W/C, which naturally affected the length of the first initiation period.

Slag cement, on the other hand, appears to give larger anodic areas in the same manner as was shown in the investigation of the rate of corrosion after initiation. The reason may be that the conditioning, consisting of artificial initiation, gave a deeper initiation for the blended cement specimen. Another explanation is that when the prerequisites for corrosion exist for steel in blended cement concrete, a rapid corrosion sequence takes place giving a larger corrosion area and, perhaps, also a deeper corrosion depth before re-passivation.

What is important here, however, is that both the Portland cement and the blended cement specimens indicate that the corrosion process comes to a halt when the corrosion products have sealed the crack zone and when realkalization has taken place. This claim can be made despite the fact that the test at 180 days for certain specimens appears to have suffered from a systematic error. Excessively high corrosion values have been read off due to the fact that poorer accuracy was obtained as a result of using oxidized Clarck's solution by mistake. The two-year specimens have very small attacks, measuring less than 10 µm. This is lower for the blended cement and roughly of the same size for the Portland cement specimens compared with the corrosion rate tests carried out with completely carbonated concrete surfaces in contact with steel. In this case, the potential difference should have caused considerably larger attacks as a result of the difference in pH values between the crack zone and the remainder of the surface, if the process had not been stopped.

The experiment also shows that samples which have lain in an NaCl solution, in other words those with a 0.3 mm crack width, did not show high corrosion rates but rather extremely small pitting. Since the corrosion areas for these samples were so small, considerable uncertainty can also be expected for the estimated corrosion depth. One error may, to a considerable extent, have been caused by the fact that the large steel surface which did not have any corrosion products nevertheless contributed to a

significant weight loss. The reliability of the results increases with increases in the corrosion area and corrosion depth.

The same line of reasoning as that presented above can also be applied to the bars with a diameter of 5 mm which also showed small corrosion areas in relation to their overall area.

The degree of corrosion was roughly the same for ribbed bars as for smooth bars.

5.3.7 Final state

General

The corrosion of the reinforcement causes the metal Fe to be converted in various stages to ferric hydroxides and ferric oxides. Depending on the prevailing conditions, such as the supply of electrolyte, O_2 etc, the conversion takes place at a varying rate and to varying corrosion products. FIG 147 presents a sketch of what can happen around the steel and a little away from the focal point of the corrosion.

The corrosion products always have a larger volume than does the original metal. The supply of oxygen around the steel determines the type of corrosion product which is formed and thus also the increase in volume which takes place at points where the corrosion products are deposited, see FIG 148.

The most common case in concrete is that the corrosion products are accumulated tight up against the reinforcement. The nearest pores are also usually filled with corrosion products. The increase in volume around the reinforcement leads to cracks in the concrete cover. These cracks are expanded in pace with the progress of the process until they finally expose the reinforcement. The result of this type of corrosion is that the reinforcement cross-section is reduced with time and that the reinforcement's interaction with the concrete for absorbing tensile stresses ceases. When the capacity of the concrete for absorbing the loads is exceeded, its service life can be said to have come to an end. It is, however, difficult to calculate the final state precisely. The reinforcement can corrode

locally, in which case the reduction in area becomes decisive. Another alternative is that the reinforcement can corrode along its entire length, in which case the interaction between the two materials becomes the decisive factor.

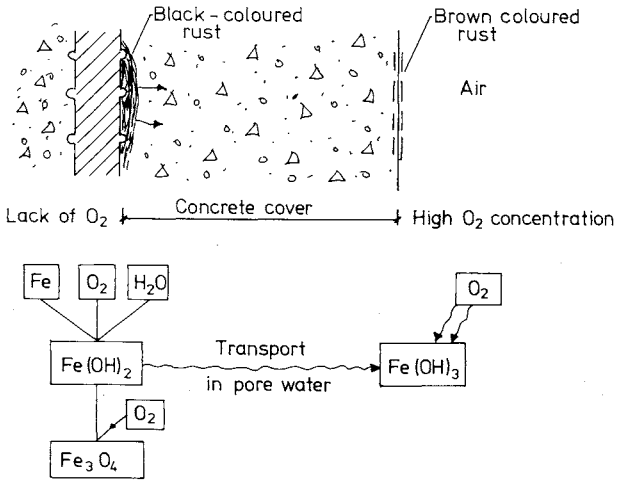

FIG 147. Sketch of possible corrosion products for steel in concrete

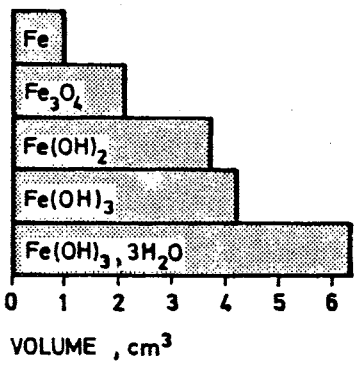

FIG 148. Relative volume for various corrosion products according to Nielsen /1976/.

Because of this, a criterium which says that the service life has come to an end when damage can be seen as a result of the entire structure having become deformed or when cracks can be seen in the concrete cover, has often been set up.

In order to study how much steel can corrode before the concrete cover breaks, experiments were carried out in which the mean degree of corrosion was measured at the time when small crack widths occurred above the reinforcement.

It should be noted that cracks need not occur despite the fact that the reinforcement has corroded to a considerable extent. When the mechanisms are of the latter type, the ferric ions are transported away from the reinforcement before they have precipitated in the form of rust. This type of corrosion is particularly common when water containing chloride flows past the steel.

Organization in principle of the experiments

The purpose was to cast bars in concrete and to get them to corrode in as natural a manner as possible. The maximum length of the experimental period was set at about 2 years. Consequently, some type of acceleration was required. Practical investigations had shown that the propagation time could become about 20 years in the case of CO_2-initiated corrosion. Two possibilities were available for accelerating the process, one was by means of an externally applied voltage and the other was by admixing a large quantity of chlorides and conditioning the samples so that they were permitted to dry out and to absorb water alternately. It was decided to use both these methods, see FIGS 149 and 150.

It should be pointed out here that the attempt to use a salt admixture was unsuccessful due to the fact that urea was used by mistake instead of $CaCl_2$. After two years of exposure, no corrosion attacks could be seen on the embedded steel. The content of urea was 5% by weight of the cement content. Consequently, only the experiments involving an external voltage source as a corrosion accelerator will be dealt with here.

It is, however, valuable to know that urea, which is sometimes used as a de-icing salt, does not entail an initiation of corrosion.

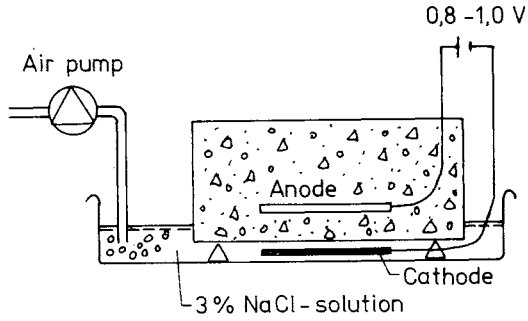

FIG 149. Sketch of test method in which an externally applied voltage source drives the corrosion process on steel in concrete.

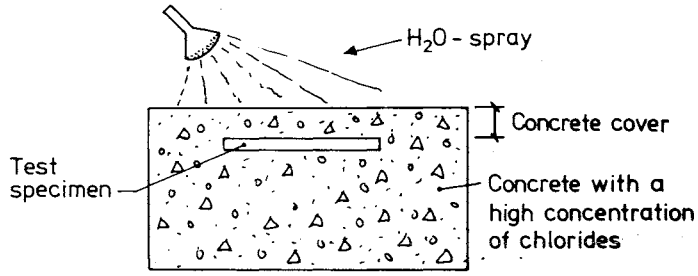

FIG 150. Sketch of test method in which the corrosion process has been initiated with a high chloride admixture during casting. The propagation is accelerated by alternately drying out and moistening the sample.

Manufacture of specimens, values for constituent variables

Plain bars with a chemical composition in accordance with Appendix 2 were cut in lengths of 150 - 300 mm. The bars were weighed and insulated wiring was then soldered to them. The soldering was carried out on a small area so that the tin could be removed without affecting the result of the weight loss measurements. Control experiments confirmed this. Before the bars were embedded in the concrete, they were dried clean from grease etc with the aid of rags soaked in spirits.

Two different concrete covers - 10 and 30 mm - were to be studied with regard to their capacity for dealing with corrosion products. The bars

were fixed at a certain distance from the bottom of the mould by means of plexiglass frames.

Two bar diameters were included in the investigation, 5 and 10 mm respectively. The thicker bars had two different diameters around the value 10 mm, namely 9.5 and 10.5 mm.

The effect of the porosity and permeability of the concrete was to be studied by selecting a low and a high W/C, 0.50 and 0.81 respectively. The concrete composition, the properties of fresh and hardened concrete for the constituents included in the investigation, can be seen in Appendix 4.

After casting the specimens were moisture cured for 7 days and the experiments were then started. The external voltage source was set at a value of 0.9 V. The voltage was checked throughout the course of the experiment and it could be noted that it varied between 0.8 and 1.0 V.

Results and discussion

The concrete surfaces of the specimens were checked at regular intervals for any discolouring and cracks.

After a period of no more than a month of the experiment, the 3% salt solution had been coloured a rust brown colour, indicating that ferric hydroxide had been liberated and had oxidized in the solution, in which the O_2 content was probably higher than in the concrete. After another month the concrete surface had also been discoloured in a number of small areas. No other external signs of damage to the embedded steel could be noted during the first year.

After an exposure of $1\frac{1}{2}$ years, a small crack appeared parallel with the reinforcement on the specimens in which damage could first be noted, W/C = 0.81 and concrete cover 10 mm. The experiments continued, however, for a further period of 6 months. At the end of this time, almost all the other specimens had cracked.

The experiments were discontinued and the cracks were measured with the aid of a crack microscope. The reinforcement was then chipped free to

permit an estimate of the corrosion area, pickling and a check of the weight loss. The maximum pitting depth was estimated by means of sliding calipers. The results are presented in Table 27 in which the weight losses have also been converted to a mean degree of corrosion in the anodic areas. It should be noted that the corrosion area has been estimated for half of the specimens. This has been marked with the sign ∿.

Table 27 Measured crack width on concrete surface above corroded bars after a test period of two years. The pores of corrosion was accelerated with an external voltage source.

W/C	Bar Φ (mm)	Concrete cover (mm)	Crack width (mm)	Total area (cm^2)	Corrosion area (%)	Pitt depth (mm)	Weight loss (gram)	Mean corrosion (mm) Total area (mm)	Anodic area (mm)	
0.50	5	10	0.05-0.20	27	∿30		1.57	0.07	0.25	*
"	"	10	0-0.8	42	34	∿3,5	6.37	0.19	0.52	*, **
"	"	30	0	27	∿10		0.16	0.01	0.08	*
"	9.5	10	0-0.10	82	12		0.98	0.02	0.13	*
"	"	30	0.2-1.0	82	32	∿3	7.53	0.12	0.37	*
"	10.5	10	0.05-0.25	48	∿30		2.17	0.06	0.19	*
"	"	30	0	48	∿30		0.55	0.01	0.05	*
0.81	5	10	0.1-0.15	27	∿50	∿1	3.60	0.17	0.34	*
"	"	30	0-0.05	26	∿50	∿3	4.37	0.21	0.43	*
"	"	30	0-0.05	46	57	∿1	1.54	0.04	0.07	*
"	9,5	10	0-0.50	82	19	∿3	4.29	0.07	0.35	*
"	"	30	0-0.10	82	7		0.27	<0.01	0.06	*
"	10.5	10	0.10-0.20	49	∿30	∿1	2.38	0.06	0.21	*
"	"	30	0.05-0.10	48	∿30	∿1.5	4.38	0.12	0.39	*

Remarks: * Black coloured rust
** Surface level discontinues

The results are summerized in FIG 151.

It can be seen that small average attacks are sufficient to cause cracks in the concrete cover. The process of corrosion was in other respects accelerated by an external voltage source. Normal time of propagation could become about 20 years as practical investigations had shown, see Tuutti /1979a/. An increasing propagation time could result in an increasing amount of corrosion products which could penetrate into pores and therefore increase the maximum degree of corrosion. In this special test the corrosion current, however, caused a greater liberation of ferric ions as

could be possible in processes where both anodic and cathodic areas are located in the concrete.

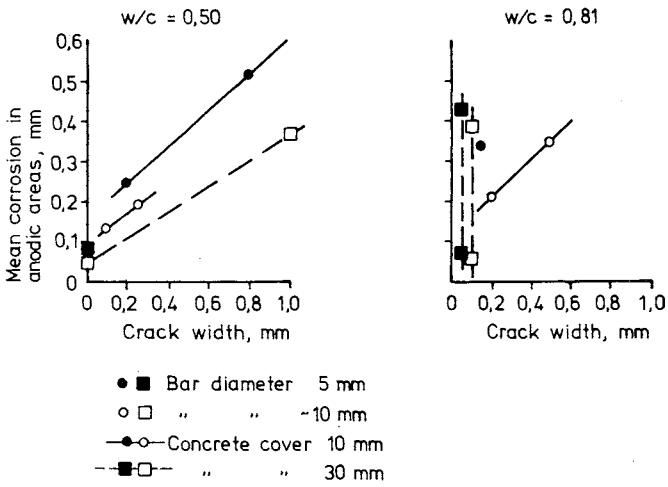

FIG 151. Estimated mean corrosion depth as a function of measured maximum crack width on the concrete surface.

The mean corrosion depth has been calculated by weight-loss measurements and by measured anodic areas.

Concrete with a high porosity, a small bar diameter and a thick concrete cover shoved the best capacity of storing corrosion products without cracking of the concrete cover.

The effect of the dimensional parametres was mostly by a change of the stress situation from a one- to a two-dimensional character.

Most of the corrosion products had formed to magnetite, Fe_3O_4. The rust was coloured black and it had magnetical properties.

The maximum pitting depth was about 4-10 times the value for the average attacks, see FIG 152.

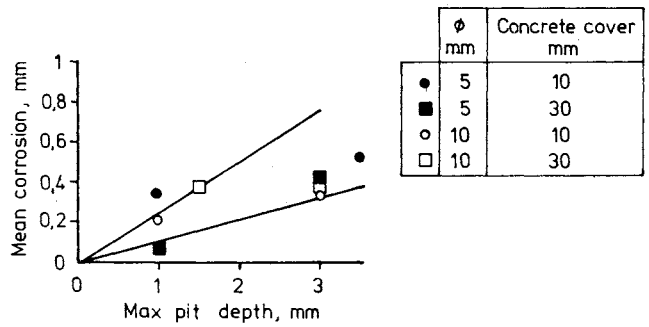

FIG 152. Mean corrosion depth as a function of maximum corrosion depth.

5.4 Analysis of pore solution squeezed out of cement paste and mortar

5.4.1 General

A common cause for the initiation of corrosion in reinforcement in concrete is that the solution which surrounds the steel contains excessively high chloride concentrations. As a result of this, numerous researchers have studied how rapidly chlorides are transported into the concrete, which chloride concentrations have occurred in concrete damaged by corrosion etc. A study of the literature shows, for example, that widely varying values have been given for the maximum chloride content in concrete. These areas lie within a range of 30-30 000 mg/l, converted to concentration in pore solution. A closer study of the maximum values which can be tolerated shows that the minimum value specified comes from laboratory experiments where the corrosion study was carried out in saturated $Ca(OH)_2$ solution. The largest values come from practical experience in cases where chloride has been mixed with the concrete, which has been surrounded by an indoor climate during the function period.

No uniform system for specifying chloride concentration in concrete has yet been established. The method most commonly adopted is to specify the chloride content as Cl^-/cement content, $CaCl_2$/ cement content or Cl^-/concrete weight. The reason why these measuring systems are used is that the values can be obtained through a purely chemical analysis. This is not, however, the chloride content which surrounds the embedded steel since a considerable proportion of it is bound chemically and physically in the concrete. For a specific chloride quantity per m^3 concrete, the concentration in the pore solution will vary not only with the bound quantity but also with the porosity and the degree of filling of the pore system. A high level of porosity offers increased possibilities for dilution compared with a low level of porosity. When concrete is dried out, the concentration of all soluble substances in the pore solution is increased due to the lower degree of dilution. Furthermore, it seems reasonable to assume that the quantity of chloride bound in concrete is a function of the concentration in the pore solution, in other words the free chloride. The chemical composition for cement and aggregate, and the ageing of the concrete are also likely to play an important part here.

Consequently, the chloride quantity should be determined in such a way that the concentration in the solution which surrounds the embedded steel can be specified.

Measurements of the free chloride concentration in cement paste, mortar and concrete can be carried out, in the case of fully saturated specimens, by means of a pressure method which Lonquet /1976/ and others have made use of. This method has been further developed by Rombén at the Cement and Concrete Research Institute in Stockholm in such a way that small mortar specimens (approx. 1 g) can be analyzed.

The method cannot be used for squeezing out the pore solution in partially saturated specimens. In these cases, the specimen must first be saturated with a solution before the method can be applied. The concentration in the original can then be calculated with the aid of the measurement results obtained. Alternatively, the free chloride concentration can be estimated with the aid of an equation, in which the free chloride concentration is a function of the total chloride content, after a conventional chemical analysis. Since no such interrelations were available during the course of the project, an investigation was started in which the free chloride concentrations and the total chloride contents were measured, partly after chloride ions had penetrated the pore system and partly on specimens in which chlorides had been admixed during the casting. In order to shed light on the effects of the considerably more dangerous situation when chlorides not only diffuse into the material but are also transported convectively in the evaporation zone, experiments were arranged in which one surface of the specimen was in contact with a 3% NaCl solution and the other surface was in contact with laboratory air.

In addition to Cl^-, OH^- and, in the case of slag cement, S^{--} also were considered to be important with regard to the threshold values which initiated the corrosion process. Consequently, the pore solution which had been squeezed out was analyzed for these substances.

5.4.2 Preliminary experiments

The equipment used for squeezing out pore solution from cement paste and mortar consisted of a tablet press in which a hole had been drilled in the lower mould unit to permit the pore solution to run out when the specimen

was subjected to pressure, see FIG 153. Squeezing out pore solution from paste and mortar was relatively simple as long as the material had a capillary pore system which was filled with solution. It was difficult, on the other hand, to guide the solution along the correct path to the cup used for collecting the solution. All the seals, which consisted of teflon packing, consequently constituted important components in the equipment.

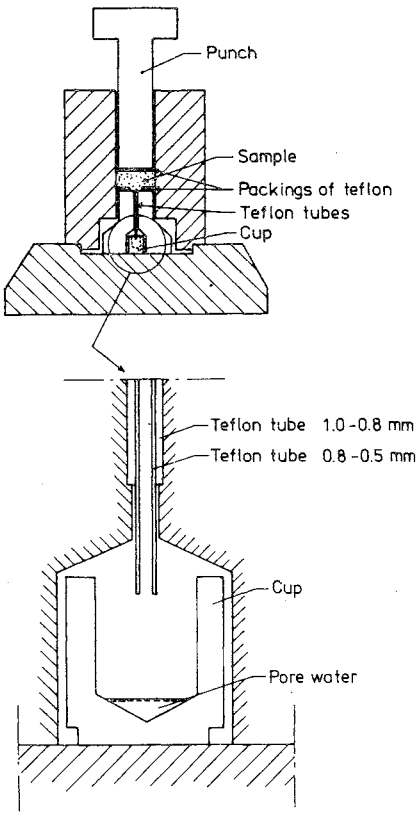

FIG 153. Equipment used for pressing out pore water in concrete.

The quantity of pore solution obtained from each pressing, from about 1 g paste or mortar, varied between 0 and 15 µl.

Consequently, it was not possible to carry out the chemical analysis in the conventional manner by means of titration. Microtitration would, admittedly, have been possible but it was considered far too time-consuming. After various preliminary experiments, it was established that ion-selective chloride electrodes and sulphide electrodes could be used, see FIG 154.

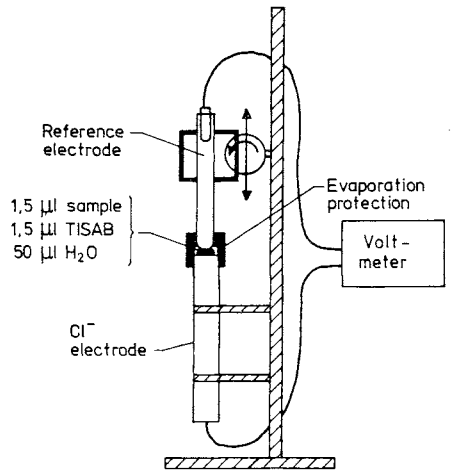

FIG 154. Analyzing equipment.

The chloride electrode gave the same result as was obtained with microtitration and a colorimeter. In each case, each of the measurements was calibrated with a known solution which had roughly the same composition. The analysis quantity varied between 1.5-3 µl.

The specimens were cut by means of a guillotine to avoid disturbances in connection with sampling. Sawing out discs might have entailed a redistribution of the substances which occurred in the pore system due to the heat developed during sawing and a possible dilution of the pore solution with the cooling water. When the specimens had been cut, they were placed in small, tightly sealed plastic boxes to prevent them from drying out and carbonating.

An important question was whether or not the pressing operation would entail squeezing out more than the free chlorides only. Consequently, the

concentration of chloride was measured in one specimen with a known chloride content after the solution had been squeezed out at a pressure varying between 100-800 MPa. No marked difference could be noticed in the chloride concentration during these measurements. Consequently, the method involving the squeezed out chloride solution was considered to be useful in this investigation of the pore solution in cement-based materials.

5.4.3 Production of specimens, values of component variables and conditioning

Bars with a diameter of 19.5 mm and a length of about 70 mm, made of mortar and paste, were cast with different W/C and cement types in accordance with Table 28. The casting was carried out in teflon moulds and with intensive external vibration.

All of the specimens were placed in a slowly rotating container directly after casting to avoid separation effects, particularly for the paste specimens.

All of the specimens were conditioned between 2 and 4 months in a saturated $Ca(OH)_2$ solution. During this time, specimens were sawn from the bars.

The experiments were subdivided into two main groups: diffusion experiments and evaporation experiments. For the diffusion experiments, the specimens were cut into lengths of 30 mm and 50 mm. For the evaporation experiments the specimens were cut into lengths of 20 mm and 40 mm.

After the first curing period in saturated $Ca(OH)_2$ solution, the specimens were placed in three different humidity climates:

- continued curing in saturated $Ca(OH)_2$ solution
- 80% relative humidity, air free from CO_2.
- 50% relative humidity, air free from CO_2

This conditioning continued for about a year. The specimens which had been subjected to drying out before the test were weighed both before and after the conditioning.

After this lengthy conditioning, the Portland cement and the slag cement specimens were regarded as having a similar degree of hydration for the various climates. This meant that the slower slag cement would not be less favoured in the experiments.

Table 28. Mix proportions and measured porosity for different mixes. The porosity was measured by means of weighing and drying out at 105°C on 5 specimens which had lain in a saturated $Ca(OH)_2$ solution for about 2 years. The consistence of these mixes varied from fluid to harsh. The compaction applied was, consequently, varied until fully satisfactory compaction had been obtained.

Cement type	Cement content kg/m^3	Paste	Mortar C: Sand (0-4 mm)	W/C	Porosity * %
Portland	1390	P	-	0.40	38.4 ± 0.4
"	1090	P	-	0.60	50.3 ± 0.5
"	540	-	1 : 3	0.40	15.1 ± 0.8
"	480	-	1 : 3	0.60	22.5 ± 0.4
Slag **	1370	P	-	0.40	44.9 ± 0.4
"	530	-	1 : 3	0.40	16.8 ± 0.3
"	480	-	1 : 3	0.60	24.1 ± 0.6

* The theoretically calculated porosity agreed with the real porosity within ±2% units.
** (70% slag, 30% Portland cement)

The specimens were thoroughly insulated with epoxy and with an external protection as illustrated in FIGS 155 and 156. They were then exposed to a 3% NaCl solution and the experiments were started.

Specimens in which chlorides were added to the fresh cement paste were also cast for comparison purposes with the values obtained from the diffusion and evaporation experiments. The chloride quantity was varied from 0-2.5% Cl^-/weight cement. Two different salts were used, KCl and $CaCl_2$.

It should be noted that experiments with specimens which had been dried out and included in the diffusion test consisted of a combined transport as a result of capilliary suction and diffusion. These experiments are, however, called diffusion tests.

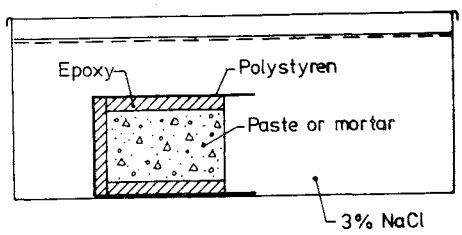

FIG 155. Sample for diffusion test

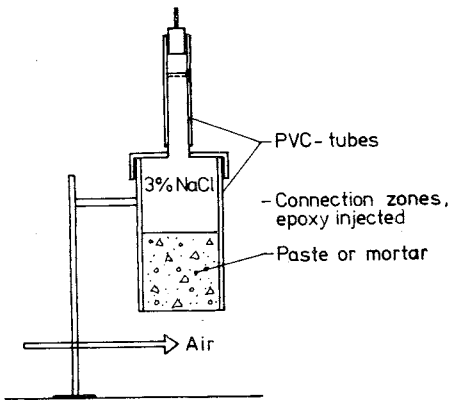

FIG 156. Sample for evaporation test.

5.4.4 Results of diffusion test.

Free, bound and total chloride concentration

Test cores were taken from the 3% salt solution at various times. These cores were cut into discs as described in Chapter 5.4.2. The pore solution which was squeezed out was analyzed for both Cl^- and OH^- in cases where the pore fluid was sufficient and for Cl^- only in cases where the quantity of pore fluid was small. Double determinations were carried out for most of the Cl^- measurements. The total chloride content was also measured in relation to the CaO quantity in most of the specimens. The quantity of chloride per cement quantity could thus be calculated in a conventional

manner. All of the measured values for free chloride and hydroxide in the pore solutions and for total chloride in relation to the quantity of cement are presented in Appendix 8.

In order to be able to calculate the quantity of bound chloride with the aid of the test results, the porosity was determined by means of weighing and drying out at $105^{o}C$ on specimens which had the same age and had been taken from the same concrete batch as that used for the specimens in the tests. These values have already been presented in Table 28.

Appendix 8 also presents the total and bound quantities of Cl^{-} in mg/l. These values have been calculated by means of the following equation.

$$c_{tot} = \frac{C_{cement} \cdot c_{\%}\ 1000}{p}$$

where c_{tot} = fictitous concentration in pore solution where all chloride is assumed to be dissolved in the pore solution (mg/l) when the pores are saturated.

C_{cement} = cement content (kg/m^3)

$c_{\%}$ = measured Cl/cement (%) ordinary chemical analysis

p = measured porosity (%)

The bound choride was calculated in accordance with the following formula:

$$c_{bound} = c_{tot} - c_{free}$$

where c_{bound} = bound chloride (mg/l)

c_{free} = measured free chloride according to pressure method (mg/l)

FIGS 157-161 present c_{free} as a function of c_{tot} for those specimens which were measured in diffusion tests. FIG 162 makes a similar presentation of the results obtained from specimens in which chlorides had been admixed during the casting.

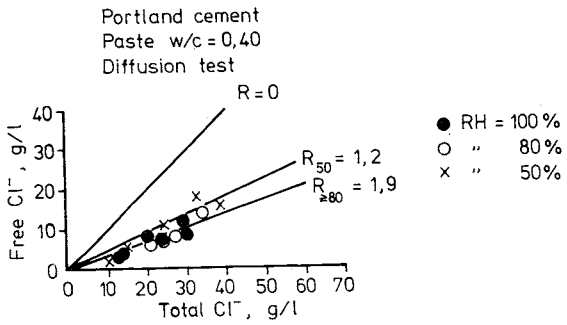

FIG 157. Measured free chloride concentration as a function of the calculated fictitious total chloride concentration. The exposure time varied between about 65 and 550 days.

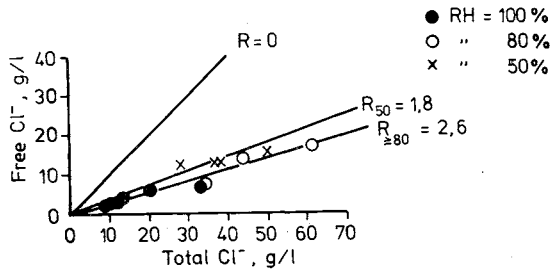

FIG 158. Measured free chloride concentration as a function of the calculated fictitious total chloride concentration. Exposure time approximately 450 days.

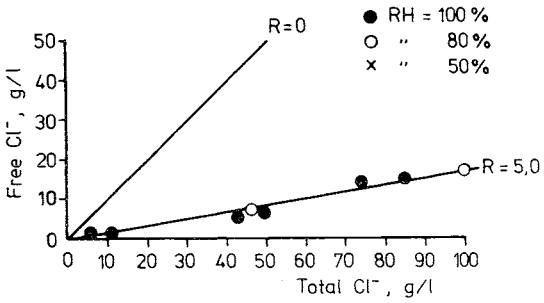

FIG 159. Measured free chloride concentration as a function of the calculated fictitious total chloride concentration. The exposure time varied between 510-540 days.

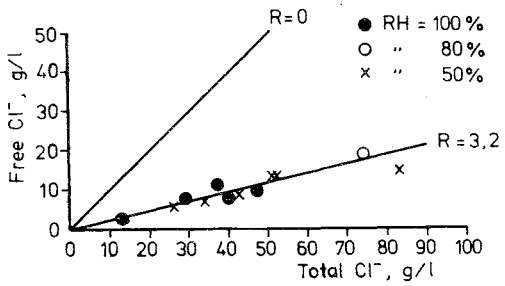

FIG 160. Measured free chloride concentration as a function of the calculated fictitious total chloride concentration. The exposure time varied between 510-550 days.

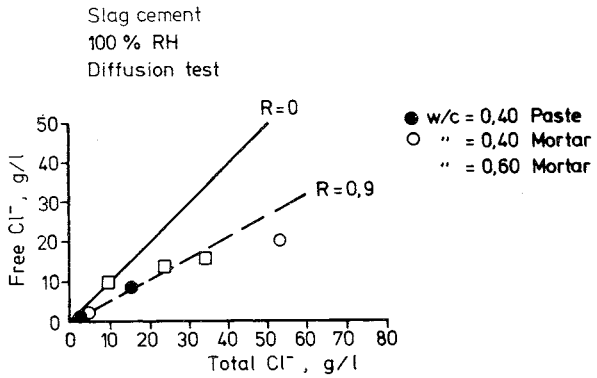

FIG 161. Measured free chloride concentration as a function of the calculated fictitious total chloride concentration. Exposure time approximately 450 days.

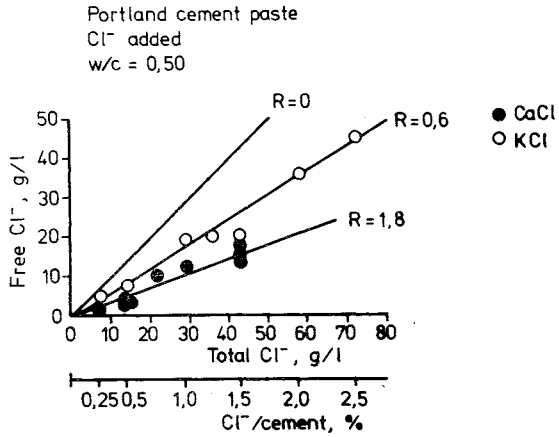

FIG 162. Measured free chloride concentration as a function of the calculated fictitious total chloride concentration. Exposure time approximately 400 days.

The factor R is a constant which specifies the quantity of bound chlorides in relation to the quantity of free chloride.

$$c_{bound} = R \cdot c_{free}$$

FIGS 163-167 show an alternative mode of presentation where free chloride has been plotted as a function of the bound chloride per weight unit cement.

The factor k_d is a constant which specifies the quantity of free chloride in relation to the quantity of bound chloride per weight unit cement.

$$k_d = \frac{c_{free} \cdot 10^{-4}}{\frac{c_{bound}}{c_{tot}} \cdot c_{\%}} \qquad \frac{g\ Cl^-_{free}/l}{g\ Cl^-_{bound}/kg\ cement}$$

A factor which must be noted at this stage is that certain difficulties were encountered in squeezing out the pore solution from specimens with W/C = 0.40 which had been hydrated during a lengthy period of time. This was particularly true of specimens which had already dried, in other words, in cases where the degree of water saturation was not maximum. It was probably possible to squeeze out only the water in the capillary pore in these specimens.

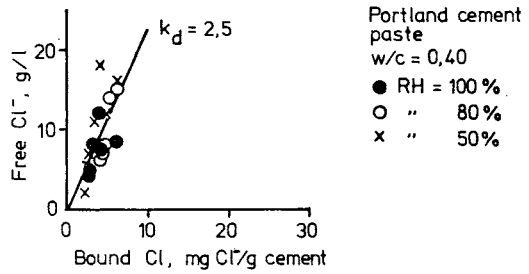

FIG 163. Measured free chloride concentration as a function of the bound chloride per weight unit cement.

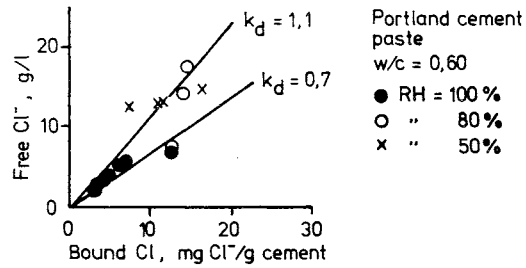

FIG 164. Measured free chloride concentration as a function of the bound chloride per weight unit cement.

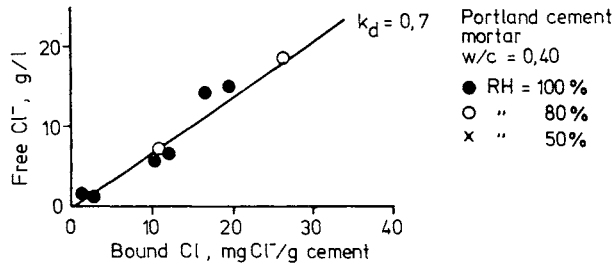

FIG 165. Measured free chloride concentration as a function of the bound chloride per weight unit cement.

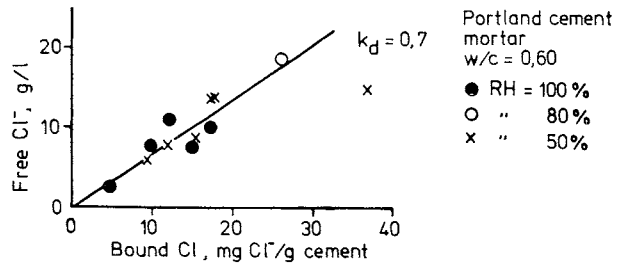

FIG 166. Measured free chloride concentration as a function of the bound chloride per weight unit cement.

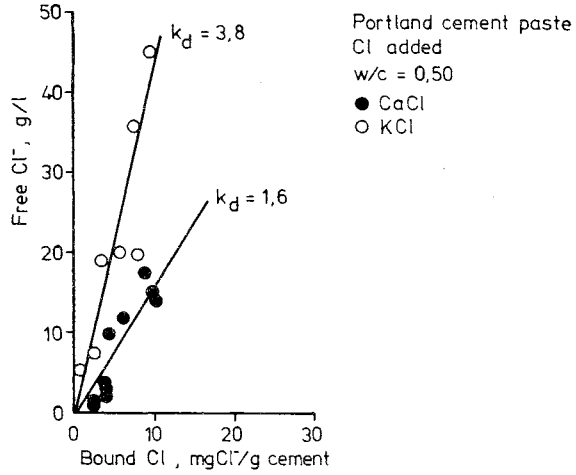

FIG 167. Measured free chloride concentration as a function of the bound chloride per weight unit cement.

Diffusion with chemical reaction

It was assumed in the introduction that chlorides are, in some way, partly eliminated from the diffusion process. In the simplest case, where a chemical reaction and a physical adsorption consume chlorides immediately and where the free concentration, c_{free}, is directly proportionate to the bound concentrations, c_{bound}, according to the following equation:

$$c_{bound} = R \cdot c_{free}$$

where R is a constant.

The diffusion equation becomes, in one dimension:

$$\frac{\partial c_{free}}{\partial t} = D \frac{\partial^2 c_{free}}{\partial x^2} - \frac{\partial c_{bound}}{\partial t}$$

where t = time

x = distance

This equation is the same as the pure diffusion equation if D is constant:

$$\frac{\partial c_{free}}{\partial t} = \frac{D}{R + 1} \frac{\partial^2 c_{free}}{\partial x^2}$$

where the constant $D/(R + 1) = D_{eff}$, effective diffusion coefficient.

In these tests and in the processing of the results, it has been assumed that the transport has followed the abovementioned equation in those cases in which the specimens were conditioned at 100% RH.

The effective diffusion coefficient has been calculated with the aid of concentration profile curves in accordance with FIG 168, where the measurement results have been plotted.

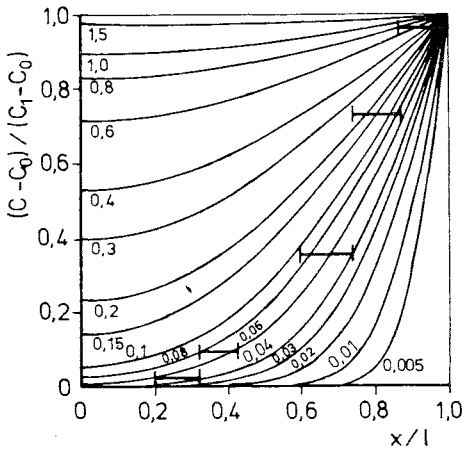

FIG 168. Concentration distributions at various times in the sheet $-1<x<1$ with initial uniform concentration c_0 and surface concentration c_1. Numbers on curves are values of Dt/l^2.

It can be seen from this figure that $D_{eff} \cdot t/l^2 = 0.05$ to 0.07 for the plotted specimen, Portland cement mortar, W/C = 0.16 and 71 days exposure. The effective diffusion coefficient lies between the values 7 to $10 \cdot 10^{-12}$ m^2/s.

Sometimes the specimens which have been taken have been so thick that the effective diffusion coefficient was difficult to determine. Consequently, the limits where the coefficient should lie have been specified for all the measurement batches.

Since several specimens were taken from the same quality but at different points in time and since the specimens have a different lengths, several values were received for the same test unit.

The results have been compiled in Table 29, which also indicates the varying ranges.

A concentration profile was obtained in a number of specimens which did not agree with the relation which had been assumed, Fick's diffusion with a bound chloride quantity which was directly proportionate to the free chloride concentration. In cases of this type, the innermost parts of the specimens have been used when calculating D_{eff} since the coefficient became greatest there. Sometimes too low a concentration was obtained in the surface layer in relation to the mathematical calculation. This was probably due to a measuring error, perhaps as a result of an error in the sampling volume during the analysis. It should be noted in this context that the concentration in the surface layer became higher in a number of cases than the value which was theoretically possible.

Table 29. Calculated effective diffusion coefficients from measured free chloride concentrations in mortar and paste.

Cement type	Paste/Mortar	W/C	Porosity (%)	D_{eff} ($m^2/s \cdot 10^{-12}$)
Portland	Paste	0.40	38	1 - 10
"	"	0.60	50	3 - 14
"	Mortar	0.40	15	0.8 - 5
"	"	0.60	23	4 - 12
Slag	Paste	0.40	45	0.3 - 0.7
"	Mortar	0.40	17	0.6 - 1
"	"	0.60	24	0.5 - 1

In order to shed light on the effects of capillary suction on chloride solution, FIGS 169 and 170 present measured concentration profiles for specimens which were partly permitted to dry out compared with specimens which were kept saturated with moisture all the time.

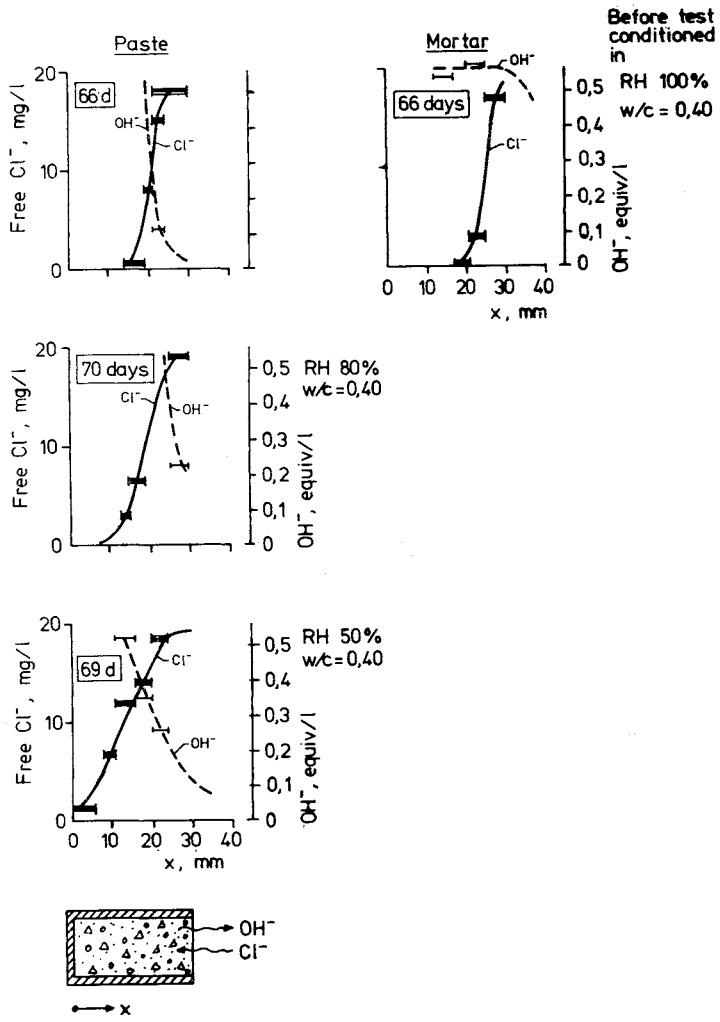

FIG 169. Measured Cl^- and OH^- concentration in squeezed out pore solution

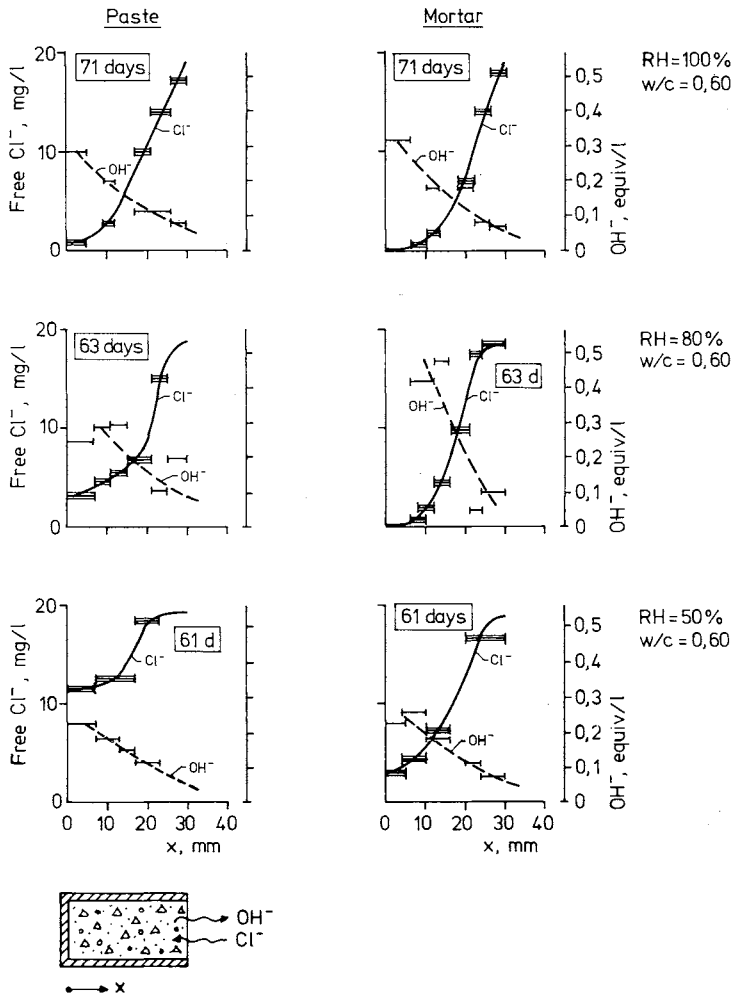

FIG 170. Measured Cl^- and OH^- concentration in squeezed out pore solution

FIG 171 presents measured concentration profiles for specimens of Portland cement and slag cement mortar respectively so as to shed light on the importance of the cement type in a diffusion test.

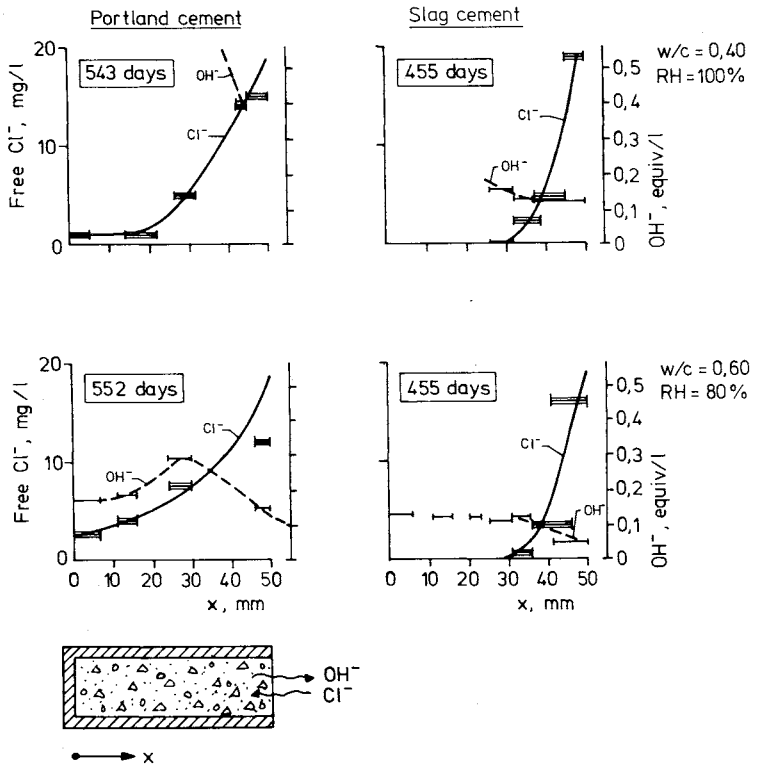

FIG 171. Measured Cl^- and OH^- concentration in squeezed out pore solution

5.4.5 Discussion of diffusion tests

Free, bound and total chloride

The results have been processed in two different ways in the groups of figures numbered 157-162 and 163-167. In the first group, the different quantities in the same units are compared, in other words g Cl^- per volume unit pore solution. In the second group, the comparison is made with the solid phase which binds chlorides, in other words g Cl per weight unit cement. The reason for using these two systems in the presentation is that the first group of figures provides the reader with a possibility of assessing the free chloride concentration around the steel in connection

with, for example, a drying-out procedure. The quantity of pore solution can then be calculated from the absorption and drying-out isotherms, whereupon the free chloride concentration can be calculated from the total concentration. The second group of figures is a conventional method for presenting chemical binding of the substance, particularly chloride binding, in the field of concrete material technology. The results can be summarized as follows:

- Chlorides were bound to a greater extent in the mortar which was used compared with the cement paste, for example, FIGS 163 and 165. This applied particularly to the less permeable paste with W/C = 0.40. The reason may have been that the less permeable paste did not have the same accessibility for chlorides as mortar had. A lengthier exposure time might have entailed a higher degree of binding in the low permeable paste.

- The quantity of chlorides bound in Portland cement products is, in the case of lengthy exposure times, independent of whether the chlorides were added during mixing or if they were later transported into the material, see, for example, FIGS 157 and 162. This can be regarded as correct since the chemical equilibriums are gradually stabilized, unless the reactions are irreversible and possible only during the hydration of the cement - assumptions not supported by the test.

- The quantity of bound chloride is dependent on which salt the concrete is exposed to, see FIG 167. $CaCl_2$ gives a larger quantity of bound chloride than does KCl. This can also be explained chemically. The positive ion Ca changes over on release from $CaCl_2$ to $Ca(OH)_2$ and is precipitated due to the fact that the solution is already supersaturated. KCl changes over to KOH, which is not precipitated and which therefore counteracts continued chloride binding.

- The slag cement also showed a markedly poorer capacity for binding chlorides, see FIG 161. This, on the other hand, is remarkable, since the slag contains more aluminates and should, consequently, have a better capacity for binding chloride. On the other hand, Traetteberg /1977/ has obtained results which show that the quantity of bound chloride was independent of the quantity of C_3A.

- Bound chloride in relation to free chloride can be independent of the W/C for mortar if the bound chloride is counted per weight unit cement, see FIGS 165 and 166. A higher cement content per m^3 concrete would thus give increased corrosion protection in chloride environments. This has been well known since concrete of a higher quality has always been selected in environments of this type.

Chloride diffusion in concrete

The values measured for the effective diffusion coefficient for chloride in concrete are between 3 and 5 times the power of 10 lower than for chloride in pure water. This can be regarded as theoretically correct since the solid phase in concrete prevents chlorides from being transported through the material. Furthermore, the channel system which exists in concrete is complex and gives a meandering path for the transport of the chlorides. These two factors should reduce the transport rate by about 3 times the power of 10. This has also been measured for many different substances in concrete. The permeability of the material is further increased by its ion-changing capacity. It should be noted here that although the slag cement specimens appear to have a lower absorption capacity of chlorides compared with Portland cement, the material is up to 10 times less permeable than the Portland cement specimens. The pore system is probably so designed that the large chloride ions can only utilize a small part of the pore system during their transport in the slag cement specimens or else the chemical composition is such that the chlorides are weakly repellent to the material.

Furthermore, the slagcement specimens were not as sensitive to W/C with regard to the value of the effective diffusion coefficient, see also chapter 5.4.7.

In other respects, the measured values can be said to correspond to expectations and to show satisfactory agreement with previous experience, see, for example, Short and Page /1981/.

Tests with specimens which had partly dried out show that a capillary suction rapidly transports chlorides into concrete. A marked effect is obtained as the result of drying out in 50% relative humidity compared with drying out in 80% relative humidity. The exposure time is, however, very

short, approximately 70 days, and only one moistening operation, in a salt solution, occured in the experiment. This is very different from practical structures which may be constantly moistened and dried out.

As was the case for the absorption results, a cement mortar gave lower chloride concentrations compared with the paste specimens. The explanation is that paste binds smaller quantities of the mortar according to the results in the preceding section.

The hydroxide concentration in the specimens after the experiments was affected very little, on the other hand, by drying out. It should be noted, however, that the specimens were dried out in air free from CO_2. The explanation for this may be that the liquid which flowed in at the start of the test had the opposite direction to the OH^- which was diffusing out. Furthermore, it should be mentioned that the solution in which the specimens were stored became basic fairly rapidly.

The measured values for the OH^- concentration which are presented have the same order of size as the theoretically calculated values if one assumes that all the K and Na which occurs in the cement is dissolved in the pore solution.

Numerous OH^- values in Appendix 8 show considerable differences, however, in concentration even at a large depth. Since the titration was carried out in an acid solution, any carbonation which may have occurred cannot have affected the result. It may, however, be that alkali, which was not dissolved and which was enclosed in unhydrated cement, became dissolved when the pore solution was squeezed out. The concentration may, as a result of this, have become higher than it was originally.

The results show quite clearly that the slag cement samples have a lower OH^- concentration in their pore solution when compared with the samples which have been cast with alkaline Slite Portland cement.

5.4.6 Results from evaporation tests

The evaporation tests were checked regularly with regard to the quantity of water which had evaporated. This provided a measure of the permeability of the specimens, see Table 30 and FIG 172 where the values are illustrated after one year of evaportation tests.

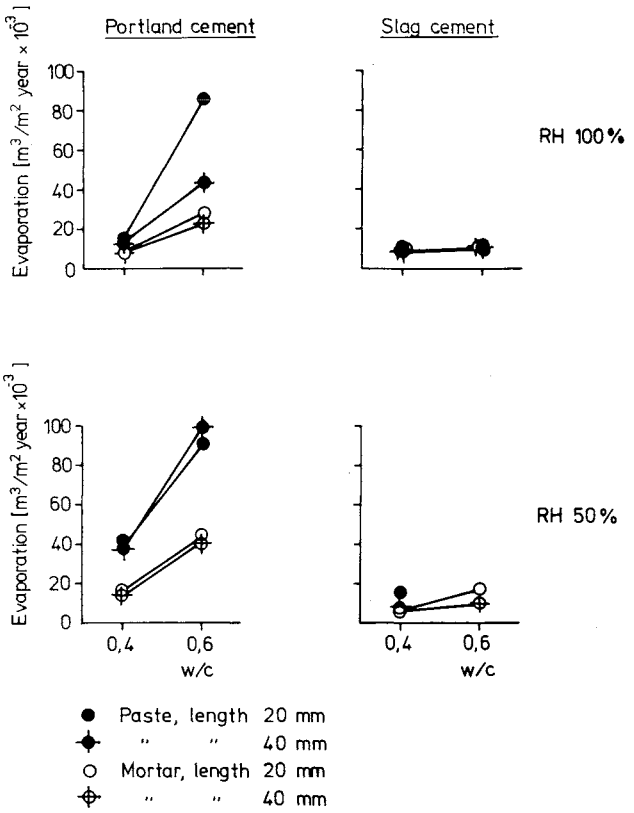

FIG 172. Measured evaporation after about 1 year from specimens with a diameter of 19.5 mm and with different lengths and compositions. The specimens had been in contact with the 3% NaCl solution on one side and laboratory air on the other.

As was the case for the diffusion tests, samples were taken for cutting into discs and for later analysis for chloride and hydroxide. When taking samples, a check was first made to ensure that the quantity of water

which had evaporated did not differ to any noteworthy extent from comparison samples of the same sort.

Table 30 Quantity of water which had evaporated from samples in the evaporation tests.

Cement type	Paste/ Mortar	W/C	Curing RH (%)	Length (mm)	Time (days)	Evaporation (gram)	Remarks
P	P	0.4	100	20	124	1.56 ± 0.03	
				40		1.42 ± 0.06	
			50	20	123	4.41 ± 0.11	
				40		4.21 ± 0,21	
P	P	0.6	100	20	126	9.30 ± 0.78	
				40		4.59 ± 0.68	
			50	20	123	9.85 ± 0.88	
				40		10.75 ± 1.98	3 samples cracked
P	M	0.4	100	20	124	0.93 ± 0.10	
				40		0.90 ± 0.08	
			50	20	124	1.77 ± 0.10	
				40		1.50 ± 0.25	
P	M	0.6	100	20	126	2.98 ± 0.09	
				40		2.46 ± 0.22	
			50	20	124	4.67 ± 0.24	
				40		4.36 ± 0.26	
S	P	0.4	100	20	126	1.27 ± 0.02	
				40		1.35 ± 0.04	
			50	20	123	1.69 ± 0.27	
				40		1.00 ± 0.02	
S	M	0.4	100	20	123	0.83 ± 0.10	2 samples
				40		1.17 ± 0.51	1 sample cracked
			50	20	123	0.73 ± 0.04	
				40		0.77 ± 0.01	
S	M	0.6	100	20	123	1.04 ± 0.04	
				40		1.08 ± 0.01	
			50	20	123	1.90 ± 0.13	
				40		1.12 ± 0.07	

P = Slite Portland cement
S = Slag cement (70% slag + 30% Slite Portland cement)

The same type of processing as that applied in the diffusion tests were carried out in the evaporation test for free, bound and total chloride quantities. The results are presented in Appendix 8. FIGS 173-175 show the effects for varied W/C, conditioning, cement type and whether the

specimen consisted of paste or mortar. Note that the quantities of liquid which penetrated the samples varied from one case to another. FIG 176 presents a compilation of a number of values for slag cement and Portland cement specimens where the total evaporation was roughly the same.

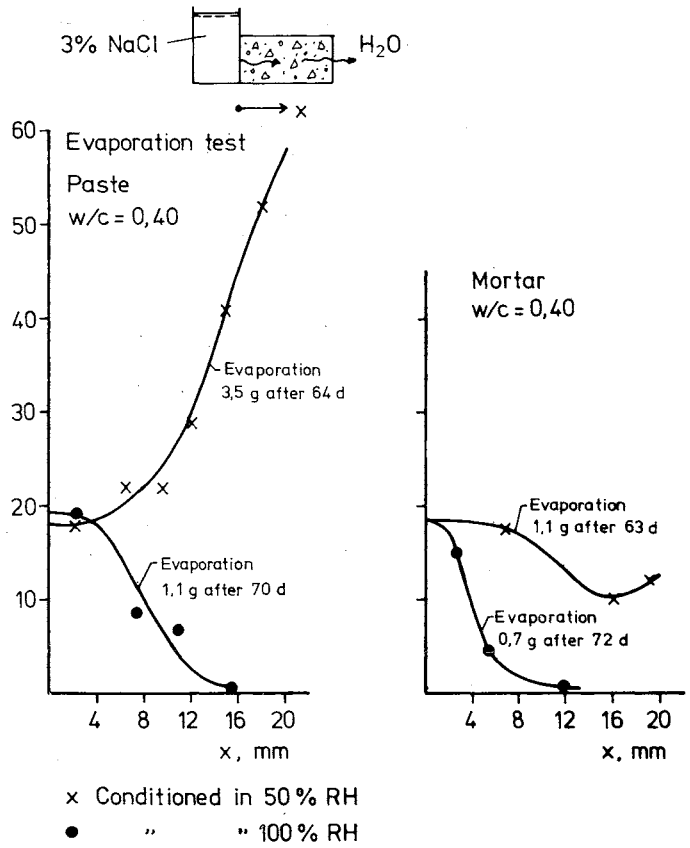

FIG 173. Measured free chloride concentrations. The aim is to present the differences between different conditioning cases and between paste and mortar.

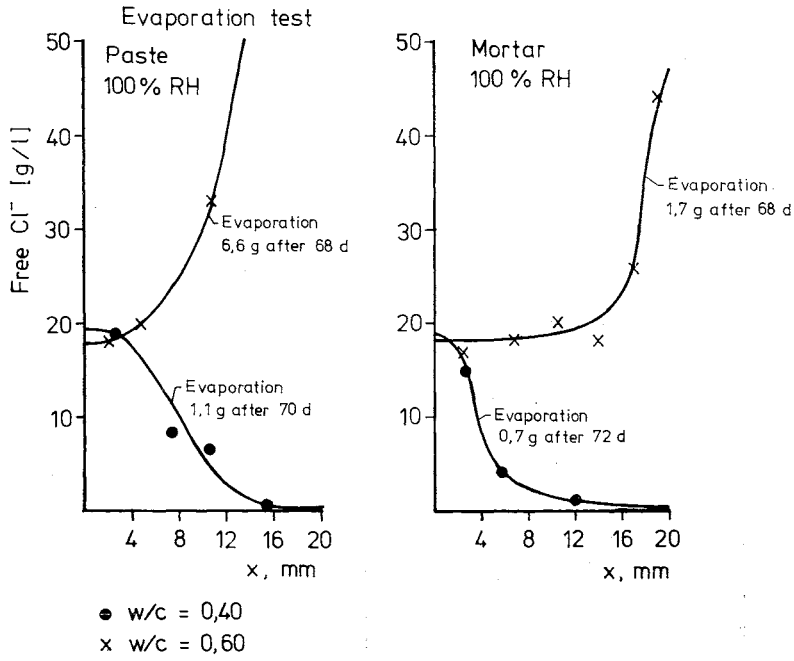

FIG 174. Measured free chloride concentrations. The aim is to present the effects of W/C and conditioning for paste and mortar.

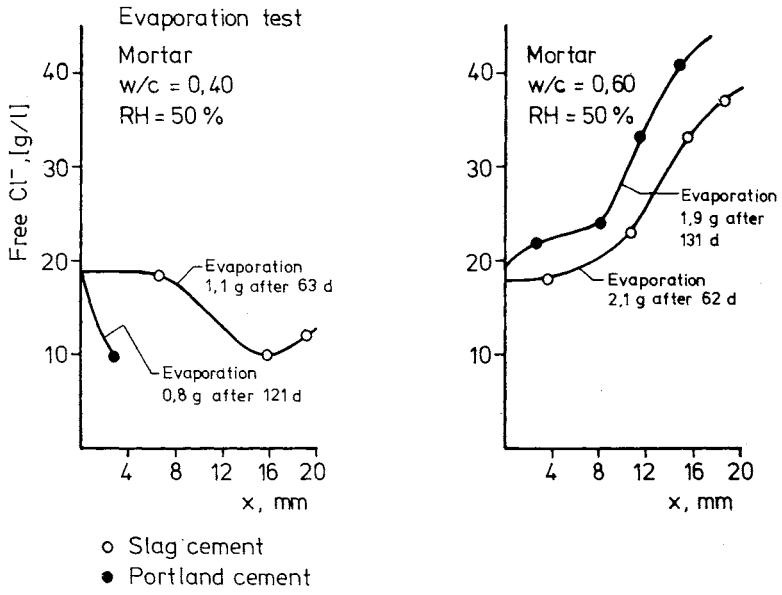

FIG 175. Measured free chloride concentrations. The figure is mainly intended to illustrate the effects of the cement type.

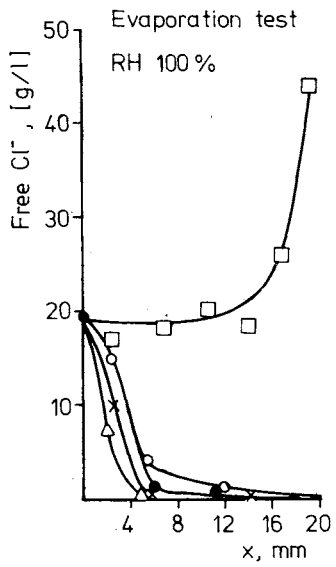

X	Slag cement,	mortar, w/c=0,40,	evaporation	0,7 g	after 69 d
●	" "	" , " =0,60,	"	0,6 g	after 73 d
o	Portland cement,	mortar, " =0,40,	"	0,7 g	after 72 d
□	" "	" , " =0,60,	"	1,7 g	after 68 d
Δ	Slag cement,	paste , " =0,40,	"	0,8 g	after 69 d

FIG 176. Measured free chloride concentrations. The figure is intended to show that even if the water transport through the specimen is the same, the chloride concentrations can become different.

FIGS 177 and 178 present the relation between free and fictitious total chloride concentrations in pore solution for paste and mortar cast with Portland cement. The results in these figures have been obtained after a much shorter exposure time than that used for the diffusion test.

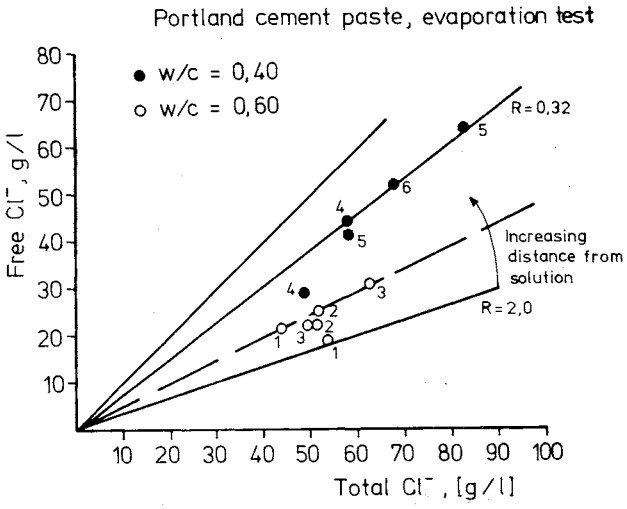

FIG 177. Measured free chloride concetration as a function of the calculated fictious total chloride concentration. Exposure time approximately 70 days. The figures illustrates the position from the wet surface where the tests were made. A higher number means an increasing distance from the solution.

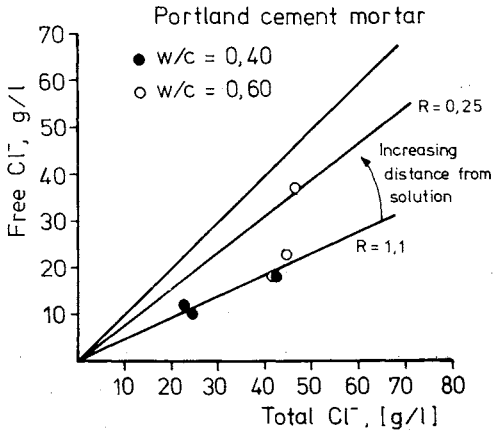

FIG 178. Measured free chloride concetration as a function of the calculated fictious total chloride concentration. Exposure time approximately 70 days. The figures illustrates the position from the wet surface where the tests were made. A higher number means an increasing distance from the solution.

5.4.7 Discussion of evaporation tests

As can be seen from FIG 172, the slag cement specimens had a very low water permeability. These specimens were not so dependent on W/C or drying out before tests, compared with the Portland cement specimens, as to give a low permeability. It should be noted, however, that all specimens were cured in water for several months before they were dried out. Measured diffusion coefficients also showed almost identical values at W/C = 0.40 and 0.60. The reason for this effect thus appears to be a purely physical permeability. Since the slag proved to be more hygroscopic than Portland klinker, storing slag cement specimens in a somewhat drier environment should not cause the same damage as for the Portland cement specimens.

As far as chloride concentration profiles are concerned, the results obtained from varying different parameters mainly follow the physical laws.

- an increase in the water penetration increases the chloride content. Note that this applies to the same specimen mix.
- the permeability increases with increases in the W/C and reduced thickness in the specimen.
- the concentration gradually becomes greatest at the evaporation surface. This applies to all substances which cannot evaporate.
- specimens dried out before the test absorb the liquid more rapidly, including the substances contained in the liquid, compared with moisture cured specimens.

It can be seen, however, in FIG 176 that even if the quantity of water transported through the specimens is equal and if the porosity is roughly the same (W/C = 0.4) for both cement types, the concentrations nevertheless become different. The slag cement appears to function better as a chloride filter than does the Portland cement. No direct comparison is possible between the other specimens since their porosities are different. A large porosity permits a greater degree of dilution.

It can be seen from FIGS 177 and 178 that the quantity of bound chlorides is dependent on the time which a solution with a certain chloride concentration is in contact with the cement's hydration products until a certain

level is reached. The longer the exposure time, the higher the degree of binding. In those parts which lie close to the evaporation zone, the chloride concentrations increase all the time more rapidly than is the case for the chemical equilibrium reaction between free and bound chloride in the pore solution. Another effect which influences the binding of the chloride in the hydration products is the carbonation of the lime. The surface specimens, which have a very small quantity of bound chloride, may have been influenced by carbonation in the surface layer.

5.4.8 Sulphide in slag cement specimens

Separate specimens had been cast to examine the sulphide content in the pore solution of slag cement paste. The paste specimens were stored in glass tubes which had a slightly larger internal diameter than that of the specimen, in other words a very small volume of lime solution was in contact with the specimen during the storage time. The tubes were sealed until the tests were carried out.

The mortar specimens were taken from the regular specimens for the chloride investigations, in other words these specimens were stored in large vessels surrounded by a 3% NaCl solution.

The variables included in the investigation and the measured sulphide contents are presented in Table 31.

The sulphide content amounted to a maximum of 300 ppm with the cement which was used in this investigation. Oxidation occurred for specimens which were exposed to large quantities of oxygen so that the sulphide content in the pore solution became very low after a time (see the results from the mortar specimens). This could also be observed by subjecting the specimens to ocular inspection. After a period of storage, the dark colour which the specimens had at the beginning disappeared, in other words the sulphide which caused the dark colour was probably oxidized to sulphate.

Table 31. Measured sulphide content in pore solution squeezed out of slag cement specimens.

Paste/Mortar	W/C	Cl^--addition % Cl	Age (month)	S^{--}_{max} (ppm)
Paste	0.50	0	0.8	160
"	"	"	15	160
"	"	1.25	15	300
"	"	"	"	250
"	"	1.50	0.8	160
"	"	"	"	160
"	0.40	0	15	300
"	"	"	"	250
"	"	"	"	270
"	0.40	1.50	"	150
"	"	0	21	300
"	"	"	"	160
"	"	"	"	300
Mortar	0.40	0	21	6
"	"	"	"	20
"	"	"	"	3
"	"	"	"	10
"	0.60	"	21	3
"	"	"	"	5
"	"	"	"	2
"	"	"	"	2
"	"	"	"	3
"	"	"	"	2
"	"	"	"	2

5.5 Chloride concentrations which initiate the corrosion process

5.5.1 General

Hausmann /1967/ has indicated critical chloride concentrations which initiate the corrosion process for steel in basic solutions. According to Hausmann, this threshold value is a function of the hydroxide concentration.

$$\frac{c_{Cl^-}}{c_{OH^-}} \leq 0.61$$

Where c_{Cl^-} and c_{OH^-} are the concentrations for Cl^- and OH^- in equiv./ /litre.

Bearing in mind the service life of a structure, this relation should give values on the safe side since embedded steel is surrounded by a pore system which prevents locally large concentrations of a substance around the steel to a greater extent than would be the case if the steel were freely exposed to a solution.

Furthermore, it has sometimes been reported that slag cement is more dangerous than Portland cement; the opposite has also sometimes been reported. It has been claimed that the sulphide in slag cement constitutes a factor which could initiate the corrosion process.

A number of very simple experiments, which are described below, were carried out with a view to studying whether or not the sulphides in the concentration which occurs in pore solution in concrete were dangerous and whether Hausmann's equation could be reproduced.

5.5.2 Experimental methods

In principle, the experiment was based on an ocular inspection of polished steel bars with regard to incipient corrosion attacks in a simulated pore solution, see FIG 179.

The concentration of hydroxide ions was varied by adding different quantities of NaOH and KOH in the solution. Trace elements such as S^{--}, Cr^{-} and SO_4^{--} were added by mixing the following salts in the solution: Na_2S $9H_2O$, K_2CrO_4 and K_2SO_4 respectively. Chloride was added with different concentrations of NaCl.

The sulphide content of the slag cement investigated here (70% slag) was approximately 1%. The pore solution concentration was measured at approximately 300 ppm for sealed samples which were 1 year old. The sulphide concentration had been reduced to approximately 5 ppm after 1 year from non-sealed samples. Consequently, the sulphide concentrations used in these tests were selected at 500 ppm S^{--}.

The significance of the metal surface was tested by polishing half of certain steel bars while leaving the mill scale on the remaining half.

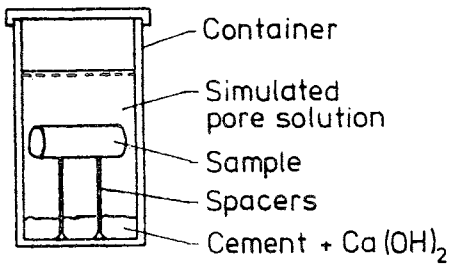

FIG 179. Test method for studying the effect of Cl^{-}, OH^{-} and S^{--} on steel corrosion concrete.

5.5.3 Results and discussion

After certain periods of time, the specimens were subjected to ocular inspection to see if any local attacks had occurred. The results can be seen in Table 32.

Observations have shown that increases in the OH^{-} (calculated from OH^{-} = 0.05 equiv/l) and Cl^{-} concentrations result in an increase in the general corrosion. If the chloride concentration becomes excessively high in relation to the OH^{-} concentration, more severe local attacks occur.

The results presented in Table 32 show a good degree of agreement with the threshold values reported by Hausmann /1967/.

Small concentrations of S^{--} have not shown any negative effects; instead, the sulphides appear to prevent the occurrence of pitting in high alkaline solutions.

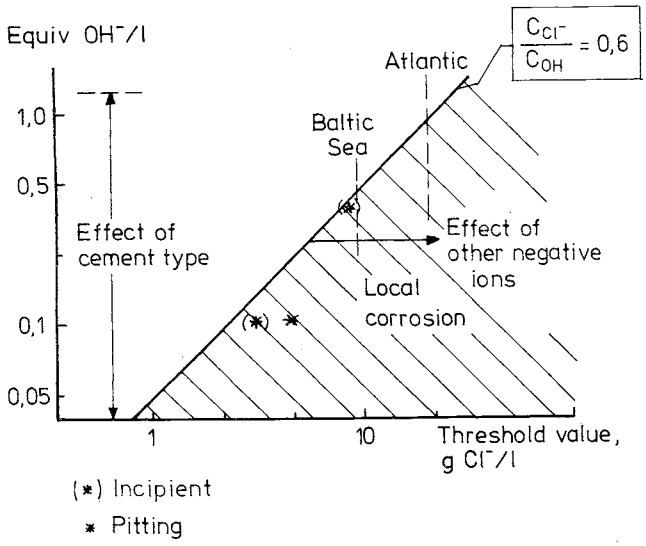

FIG 180. Threshold values.

The threshold value is not, however, dependent solely on the OH^- concentration in the solution but can also be affected by other negative ions which prevent the chlorides from coming in contact with the metal surface. See FIG 180 where the measured values have also been plotted for pure Portland cement pore solution.

The pore solution in the Portland cement concrete which was used in these tests has a high OH^- concentration. This concentration is mainly determined by the fluid content of the concrete. Concrete made with Slite Portland cement with a water-cement ratio of 0.6 - 0.4 has a free OH^- concentration of 0.3 - 1.0 equiv/l. The corresponding values for slag cement are approximately 0.1 - 0.5 equiv/l.

Table 32 Observed local corrosion (pitting) after 60 days exposure.

- = no local corrosion
(Corr) = indistinct local corrosion
Corr = distinct local corrosion

Cement type	OH^- equiv/l	Admixture or metal type	Cl-concentration in simulated solution mg/l						
			0	500	1000	3000	5000	7000	9000
P	0.04		Corr	Corr	Corr	Corr	Corr	Corr	Corr
P	0.1		-	-	-	(Corr)	Corr	Corr	Corr
P	0.32		-	-	-	-	-	-	(Corr)
P	1		-	-	- *	--	-	-	-
P	0.1	O	-	-	-	Corr	Corr	Corr	Corr
P	0.32	O	(Corr)	-	-	-	-	-	-
P	1	O	-	-	-	-	-	-	-
P	0.32	SO_4+Cr	-	-	-	-	-	-	-
P	0.32	$Cr^{}$	-	-	-	-	-	-	-
P	0.32	SO_4	-	-	-	-	-	-	(Corr)
P	0.32	10xCr	-	-	-	-	-	-	-
P	0.32	SO_4+10xCr	-	-	-	-	-	-	-
S	0.1		-	-	-	(Corr)	Corr	Corr	Corr
S	0.1	S	-	-	-	-	-	-	-
S	0.32	S	-	-	-	-	-	(Corr)	-

CODE

Cement type

P = Slite Portland cement
S = Slag cement
(70% slag + 30% Portland)

Admixtures

O = Oxide scale
S = 500 ppm S^{--}
SO_4 = 100 ppm SO_4^{--}
$Cr^{}$ = 22 ppm CrO_4^{--}
10 x Cr = 220 ppm CrO_4^{--}

* Darker surface with increasing chloride concentration

The critical chloride concentrations would then, according to FIG 180, be 6-21 g Cl/l for Portland cement and 2-11 g Cl/l for slag cement.

It should be noted that the interrelationship in FIG 180 is the result of a simple measurement in simulated pore solution. Further research is required in this sector to provide a better investigation of the threshold values when corrosion initiation takes place. The penetration of chlorides is, on the other hand, more clearly established than these threshold values and both parameters must occur for a reliable assessment of service life in a chloride environment.

5.5.4 Method for calculating OH^- concentration

The OH^- concentration can be measured for various types of concrete in accordance with the methods presented in Chapter 5.4 or can be calculated approximately as follows:

If the K and Na contents of the cement are known and if the constituents of the concrete are known, the concentration in the pore solution can be calculated as follows:

$$p = \frac{C}{10} (W/C - 0.19\ \alpha) + l_o \quad \text{(Bergström /1967/).}$$

where p = porosity of concrete in volumetric percentage
C = cement content kg/m^3
W/C = water-cement ratio
α = degree of hydration, see Table 33
l_o = air content of fresh concrete

Since almost all Na and K are dissolved, the maximum concentration is calculated as follows:

$$c_{OH^-} = \frac{\frac{C \cdot (Na)}{23} + \frac{C \cdot (K)}{39}}{p} \cdot 100$$

where c_{OH^-} = OH^- concentration in equiv/l
C = cement content kg/m^3
(Na), (K) = proportion of Na and K respectively by weight in cement

Table 33. Maximum degree of hydration as a function of W/C, Byfors /1980/.

W/C	Degree of hydration
0.4	0.60
0.6	0.70
0.8	0.80

Pressing out pore solution and titration with regard to OH^- is an other method for determining the OH^-concentration.

5.6 Porosity and pore size distribution in corrosion products

5.6.1 General

The O_2 supply is often limited when steel corrodes in concrete so that the most porous corrosion products cannot be formed. The normal development is that the corrosion products accumulate close up against the metal and/or that a solution or ion flow transports precipitated ion away from the corrosion area. Iron leaching occurs to a limited extent in all corrosion cases but can be of decisive significance in highly porous concrete where activating substances initiate the corrosion process. Concrete in air, on the other hand, has very little iron leaching although more or less rusty concrete surfaces can always be seen on corrosion-damaged reinforcement of this type.

The corrosion products always have a larger volume than the volume of the original metal. Consequently, it is important to determine the expansion a corrosion process entails for the reinforcement. Excessively large increases in volume result in cracks and cause the concrete cover to flake off.

Whether or not the corrosion products seal the concrete has also been discussed, in other words whether they cause a reduction in the rate of corrosion when the corrosion depth increases. The crack theory, which postulates re-alkalization after a local attack, is based on the fact that the corrosion products provide efficient sealing against CO_2.

The permeability properties are dependent not only on the chemical composition of the material but also on its porosity and pore size distribution. For these reasons, pore investigations were carried out on corrosion products from a number of practical damage cases.

5.6.2 Tests

Numerous damage cases have been studied, within the terms of reference of the present project and on a consultancy basis, during the course of the project. It has proved possible to distinguish three different types of corrosion product by appearance:

- red rust, which appears to be a finely grained, porous material and which is formed on reinforcement before casting or in dry environments where corrosion is, nevertheless, possible.

- black rust, which is firmly attached to the reinforcement and is compact and magnetic. Black reinforcement flakes off in the form of discs when the steel is mechanically cleaned.

- red-brown rust which is formed on concrete surfaces after iron has been liberated deeper in the concrete.

A porosity investigation has been carried out with a mercury porosimeter on the first two corrosion types.

5.6.3 Results and discussion

The results of the measurements which were carried out are presented in FIGS 181 and 182. Three different samples were taken of the black corroded. Two samples were taken from corrosion floor reinforcement where the corrosion had been initiated by chemicals, particularly Cl^- and SO_4^{--}, from a photographic laboratory. One sample was taken from a traffic facility called Slussen in Stockholm where chlorides from road salt had initiated the corrosion process, see the photograph 39.

Measurements which have been carried out show that the larger the supply of oxygen, the more porous the corrosion products become. The red powder is highly porous in cases where the pores are, for the most part, larger than 1 μm.

The rust from the floor slab, which was considerably drier than the traffic facility, also showed a greater porosity compared with the rust from the traffic facility. This also applied to the ratio between the densities. The black rust did, however, have a pore structure in which about half of the pores were smaller than 1 μm. Furthermore, the porosity of the rust was smaller than or of the same size as for Portland cement paste, W/C = 0.40.

Rust from outdoor structures have a very low degree of porosity and a large number of small pores.

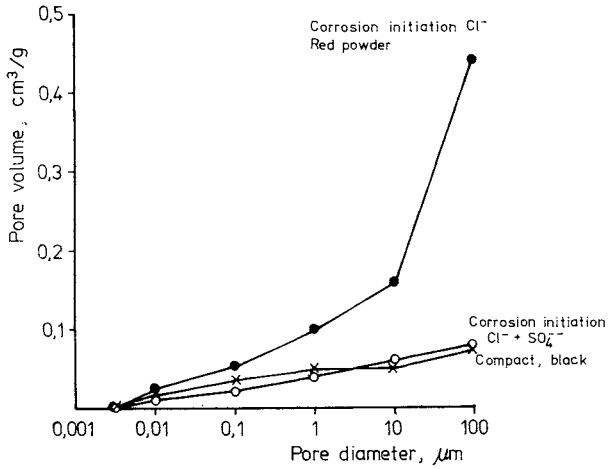

FIG 181. Measured porosity per weight unit with mercury porosimeter. One of the materials consisted of a red powder which had been scraped off a pipe which had corroded in an environment with a high O_2 content. The other specimen is a double specimen which was taken from a concrete floor slab where photographic chemicals had penetrated the concrete and initiated corrosion attacks. Chlorides have been an initiating factor in all the samples.

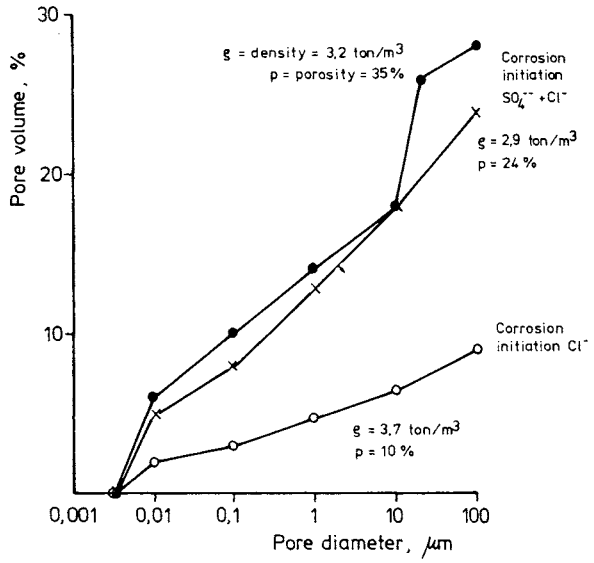

FIG 182. Measured porosity and pore size distribution with mercury porosimeter for three different corrosion products which consisted of a black, compact and magnetic material. The two top curves are the two bottom curves in FIG 181 which have been converted to volumetric units.

The results thus confirm the claims discussed concerning the sealing affect of the corrosion, partly for the rate of corrosion after initiation and partly for the retardation of CO_2 and the re-alkalization possibility for cracked concrete.

The measured densities show a good level of agreement with the theoretical density for Fe_3O_4. Consequently, there is reason to expect that the black corrosion consists of a magnetite, possibly with one or two complex bindings with Cl, SO_4 or the like.

5.7 Relative humidity in cracks

5.7.1 General

The moisture state in concrete has been mapped out fairly thoroughly. We know that the material sucks water through capillary action and that the drying- out process is a diffusion process which is considerably slower than the wetting process when the concrete is in direct contact with water. One of the factors which controls the corrosion process is the quantity of electrolyte in the concrete, in other words the water content in the concrete pores. This means that, when considering corrosion, concrete structures can be distinguished with regard to the humidity of the surroundings and the possibilities of wetting and drying the concrete.

A subdivision of this type has already been applied in many cases:

- concrete indoors
- concrete outdoors, protected from rain
- concrete outdoors, exposed to rain.

The subdivision can be made as rough as this since the rain frequency is large and the drying-out period is long. The question arises, however, of what happens in a crack zone. Does the abovementioned subdivision suffice or must a finer subdivision be made since the cracks dry out more rapidly etc?

The aim of the present investigation was to provide an answer to this question.

5.7.2 Experiments

150 mm cubes were cast to simulate a crack. One of the faces was cast against a 10 mm thick sheet of plexiglass. PVC tubes had been inserted in the cubes so as to provide future channels for measuring the relative humidity. These channels lay at different depths, see FIG 183. The cubes were water cured for 7 days and then dried for 100 days at 50% RH. The plexiglass sheets against which the cubes had been cast were placed against the previously cast surfaces but with a spacer, which varied in

thickness, between them. The gap which was formed between the plexiglass sheet and the concrete surface would thus constitute an artificial crack. A perfect fit was obtained since that face of the cube had previously been cast against the plexiglass sheet. All surfaces and gaps, except one side, were insulated with three layers of epoxy.

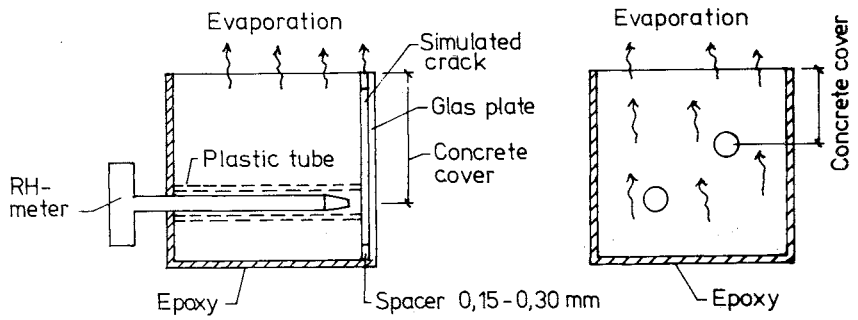

FIG 183. Sketch of specimens for check of moisture state in cracks.

Tests could now begin by spraying all of the specimens with water for 10 minutes. The water could run down into the cracks but not into the channels where the measuring equipment would later be placed. The channels were sealed with plastic covers. 24 hours after this wetting operation, recording of the relative humidity in the various channels was started by puncturing the plastic covers against the cracks.

5.7.3 Results and discussion

The measured relative humidities can be seen in FIG 184.

It can be seen from these figures that the moisture state around reinforcement in cracks is normally approximately the same as in "homogeneous" concrete, except when the concrete cover becomes extremely thin, 10 mm and thinner, or when the crack width is larger than 0.3 mm. Note that the crack width in FIG 184 must be regarded as half the width in a real crack since the plexiglass does not absorb water.

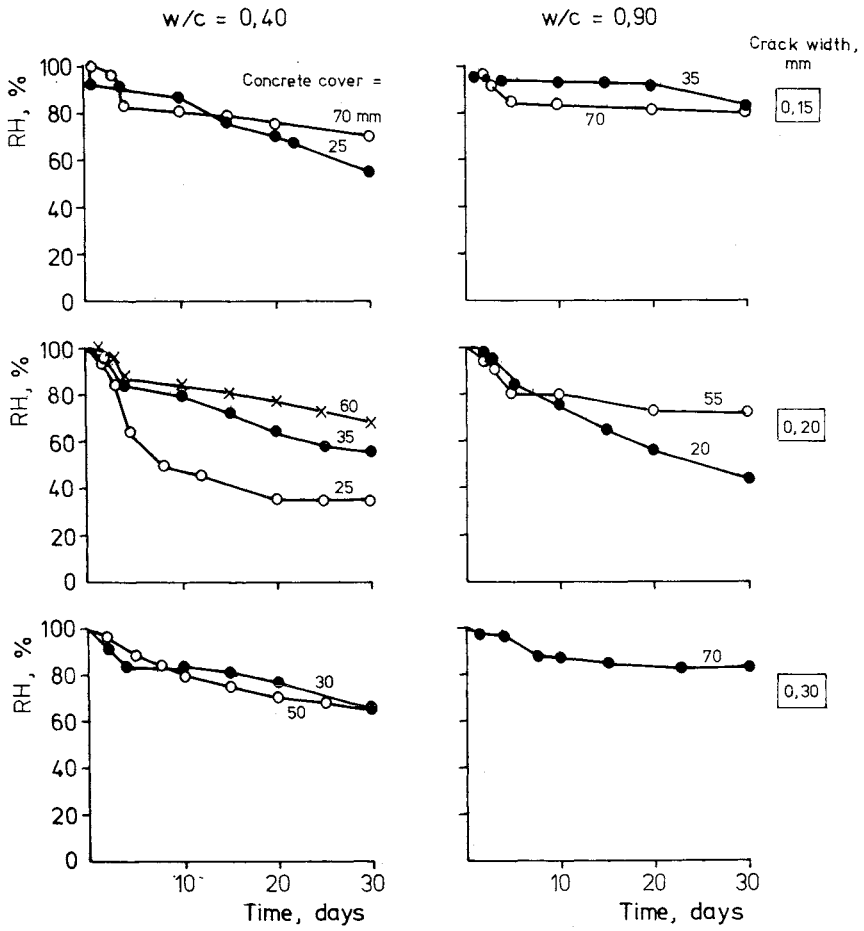

FIG 184. Measured relative humidity in crack after 10 minutes spraying with water day 0, followed by drying out in 50% RH.

It should, however, be noted that the cracks mainly act as very rapid transport paths for water when the concrete is subject to wetting. Cracked concrete should thus have a higher moisture content compared with the same type of concrete which is uncracked in the same environment, see FIG 185.

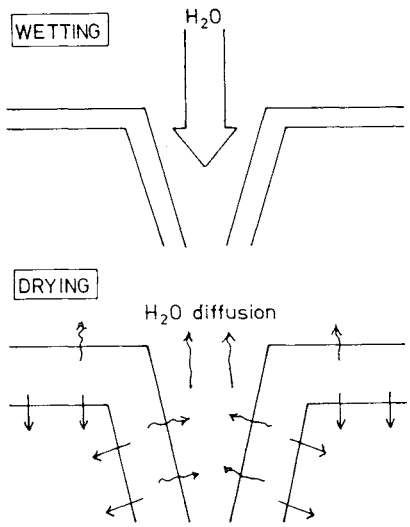

FIG 185. Cracks are rapidly filled when the concrete surface is sprayed with water. The water is transported in by means of capillary action from all surfaces which have been in contact with the water. The water transport into the concrete continues during drying out since the drying-out process is so slow.

5.8 Potential measurements

5.8.1 General

A corrosion process consists of two reactions, an anode reaction and a cathode reaction. The rate of corrosion is, consequently, determined not by one reaction but by two. The anode reactions increase in speed with increases in the potential while the cathode reactions increase in speed with reductions in the potential. When the systems are connected together, the corrosion potential lies on a level where the same number of electrodes is liberated at the anode as is consumed at the cathode. Since the cathode reaction consumes O_2, it was considered of interest to measure potentials as a function of the O_2 supply. Consequently, a number of measurements were carried out on reinforcement which had corroded and on reinforcement which had not corroded respectively in concrete with different relative humidities.

5.8.2 Tests

Specimens (100 x 150 x 800 mm) of concrete with a W/C = 0.50 were cast, partly with 5% $CaCl_2$ in relation to the cement weight and partly without salt, see FIG 186. Reinforcement was inserted in the specimens in such a way that the concrete cover became 4 mm. The reinforcement consisted of smooth bars with diameters of 5 mm and 10 mm respectively. The specimens were water cured for 7 days and were then placed in 3 different climate chambers with 50, 80 and 100% RH. At an age of about 6 months the potential of the reinforcement bars was measured in relation to a saturated calomel electrode.

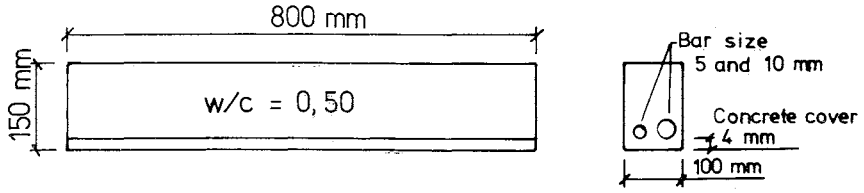

FIG 186. Specimens for potential measurements.

5.8.3 Results and discussion

The results of the potential measurements are presented in Table 34.

Table 34 Measured potentials on reinforcement at different RH, measured with saturated calomel electrode. The concrete surrounding the reinforcement contained 0 and 5% respectively of $CaCl_2$/cement weight, which was added during the casting.

Chloride admixture CaCl/C (%)	Potentials (V) 50% RH ϕ5 mm	ϕ10 mm	80% RH ϕ5 mm	ϕ10 mm	100% RH ϕ5 mm	ϕ10 mm
0	+0.04 -0.07	+0.05 -0.07	-0.03 -0.04	-0.02	-0.36	-0.47
5	-0.23 -0.30	-0.23 -0.27	-0.15 -0.16	-0.19 -0.25	-0.38	-0.50 -0.58

All of the bars in concrete containing chloride corroded at the time of measurment, whereas the 0 specimens only had attacks at the transition from concrete to air.

To begin with, we can see that there is no interdependence between the rate of corrosion and the potential. Generally speaking, the potentials are, however, lower in the bars in which corrosion was initiated with $CaCl_2$.

An increase in the moisture content entails a lower potential, in other words the corrosion process became more and more cathodically controlled. This also applied in the case of what is known as non-corroding steel. Here, the potential change must be regarded as a consequence of the fact that the passivated steel consumes O_2 (oxygen electrode) or that the steel entered an active state but with an extremely low rate of corrosion (cf. the measurements with corrosion cells).

The conclusions reached here are the same as those reached by other researchers who have found that the corrosion potential in a highly active area lies around -0.3-0.6 V, measured with a saturated calomel electrode.

A careful mapping system must be used for carrying out more advanced assessments with potential measurements as a basis, see Arup and Grönvold /1979/. It is, however, always difficult to take account of the equalizing influence of the concrete cover on the potentials when measurements are carried out against concrete surfaces and not directly against steel.

REFERENCES

Abeles, F, 1965: Corrosion of steel in finely cracked reinforced and prestressed concrete. PCA, Vol 10, No 2, pp 36-41. Skokie.

Andrade, C, 1974: The inhibitive action of different quantities of NO_2Na on the corrosion of reinforcements in prestressed concrete beams using the polarization resistance as technique of measurment. Research Working Papers, Instituto Eduardo Torroja. Madrid.

Arup H, 1977: Galvanic Action of Steel in Concrete. Korrosionscentralen ATV, Denmark.

Arup and Grönvold, 1979: Localisation of corroding reinforcement by electrochemical potential surveys. RILEM Quality control of concrete structures, June 17-21, Stockholm 1979, pp 251-258, Vol I.

Atimtay and Ferguson, 1973: Early Chloride Corrosion of Reinforced Concrete - Test Report. ACI Journal, September, nr 9, pp 606-610. Detroit.

Auskern and Horn, 1973: Capillary porosity in hardened cement paste. Journal of Testing and Evaluation, ITEVA, vol 1, nr 1.

Backstrom, T E, 1975: Use of coatings on steel embedded in concrete. ACI Separate Publication SP-49, pp 103-114. Detroit.

Bazant, Z, 1978: Physical model for corrosion of steel in concrete. Research report Fo 5:78 Cement- och Betonginstitutet. Stockholm.

Beijer, O, 1976: Temperatur- och fuktrörelser i fasadskivor av betong. Forskningsrapport 8:76. Cement- och Betonginstitutet. Stockholm.

Benninghoff and Grunau, 1971: Korrosionsverhalten und Korrosionsschutz von Stahl im Beton. Köln-Braunsfeld.

Bergström, S G, 1959: PM angående korrosion på värmerör i bostadsområdet Norra Biskopsgården, Göteborg. Cement- och Betonginstitutet, Kontaktavdelningen, Rapport 85. Stockholm.

Bergström, S G, 1967: Kompendium i Byggnadsmateriallära FK I. Lunds Tekniska Högskola. Lund.

Bergström, S G, 1973: Färsk och hårdnad betongs egenskaper. Cement- och Betonginstitutets Kursverksamhet, Betongkurs A. Stockholm.

Bergström and Holst, 1960: Korrosionsrisken vi användning av kalciumklorid i betong. Statens nämnd för byggnadsforskning, Rapport 60. Stockholm.

Bergström and Lundström, 1959: Korrosion på ingjutna värmeslingor i Åsaområdet. Cement- och Betonginstitutet, kontaktavdelningen, Rapport 95. Stockholm.

Bergström, Nielsen, Ahlgren and Fagerlund, 1970: Kompendium i Byggnadsmateriallära, Allmän Kurs. Lunds Tekniska Högskola. Lund.

Bergström, Rombén and Tuutti, 1977: Bedömning av beständighet hos kraftledningsstolpar av betong. Uppdragsrapport 7755. Cement- och Betonginstitutet. Stockholm.

Bergström, Thorsén and Tuutti, 1980: Korrosion på armering i garagebjälklag, Göteborg. Uppdragsrapport 8011. Cement- och Betonginstitutet. Stockholm.

Berman, H A, 1974: The effect of sodium chloride on the corrosion of concrete reinforcing steel and on the pH on calcium hydroxide solution. NTIS, PB 228 679. Springfield.

Bernhardt and Sopler, 1974: An experimental study of the corrosion of steel in reinforced concrete in marine enviroment. Nordisk Betong 2-1974.

Bernard and Verbeck, 1975: Corrosion of metals in concrete-needed research. ACI Separate Publication SP-49, pp 39-46. Detroit.

Bird and Strauss, 1967: Metallic coatings for reinforcing steel. Materials Protection, Vol 6, nr 7, pp 48-52.

Boulware, R L, 1973: Field electrical measurments for bridge deck membrane permeability and reinforcing steel corrosion. NTIS, PB 234 569. Springfield.

Brand, H, 1971: Korrosion von Stahl im Beton, Dissertation, Rheinisch-Westfälische Technische Hochschule. Aachen.

Brocard, I, 1958: Corrosion des aciers dan le béton armé. Annales de l' Institut Technique du Batiment et des Travaux Publics, nr 126. Paris.

Brown, R D, 1979: Testing & testing design for durability of concrete structures, RILEM Symposium Quality Control of Concrete Structures. Stockholm, June 17-21, 1979. Proceedings, Volume 1, pp 231-242.

Bryden, J E, 1974: Laboratory and field evaluation of plasticcoated dowel bars. NTIS, PB-235 984. Springfield.

Byfors, J, 1980: Plain concrete at early ages. Researchreport Fo 3:80, Cement- och Betonginstitutet. Stockholm.

Bäumel and Egnell, 1959: Korrosion von Stahl in Beton. Archiv für das Eisenhüttenwesen 30, nr 7.

Clear, K C, 1974: Time to corrosion of reinforcing steel in concrete slabs. Transportation Research Record 500, pp 16-24. Washington.

Clear, C, 1975: Rebar corrosion in concrete: effect of special treatments. ACI Separate Publication SP-49, pp 71-82. Detroit.

Clear and Hay, 1973: Time-to-corrosion of reinforcing steel in concrete slabs. NTIS, PB-224 655. Springfield.

Clifton, Beeghly and Mathey, 1975: Protecting reinforcing bars from corrosion with epoxy coatings. ACI Separate Publication SP-49, pp 115-132. Detroit.

Collepardi, Marcialis and Turriziani, 1972: Penetration of Chloride Ions into Cement Pastes and Concretes. Journal of the American Ceramic Society - Discussion and Notes, vol 55, no 10.

Craig, W, 1970: Effectiveness of corrosion inhibitors and their influence on the physical properties of portland cement mortars. Highway Research Record, nr 328, pp 77-88. Washington.

Crank, J, 1975: The mathematics of diffusion. Oxford.

Crowley, Francis X, 1975: Shotcrete covercoats for prestressed concrete tanks. ACI Separate Publication SP-49, pp 11-20. Detroit.

Czernin, W, 1964: Cementkemi för byggare. Svenska Cementföreningen. Malmö.

Dana, A W, 1957: Stress corrosion cracking of insulated austentitic stainless stell. ASTM-bulletin, 1957:226, pp 46-52.

Dietrich, W F, 1967: Corrosion test program. NTIS, PB-192496. Springfield.

Därr and Ludwig, 1973: Determination of permeable prosity, Matériaux et Constructions, Vol 6, nr 33. Paris.

El-Busaidy, 1975: Factors affecting corrosion behaviour of steel in concrete exposed to marine enviroments. University of Trondheim. Norway.

Evans, U R, 1968: The corrosion and oxidation of metals. First supplementary volume. London.

Fagerlund, G, 1973: Determination of pore size distribution by suction porosimetry. Matériaux et Constructions, Vol 6, nr 33. Paris.

Fagerlund, G, 1974: Non-Feezable Water Contents of Porous Building Materials. Inst. för Byggnadsteknik, Lunds Tekniska Högskola. Lund.

Fagerlund, G, 1980: Influence of slag cement on the frost resistance of concrete - a teoretical analysis. Cement- och Betonginstitutet, Rapport 1:80. Stockholm.

Fagerlund and Svensson, 1980: Beständighet hos lagningssystem för betongbalkonger. Fo 2:80, Cement- och Betonginstitutet. Stockholm.

Fidjestøl and Nielsen, 1980: Field test of reinforcement corrosion in concrete. ACI Publication SP-65, Performance of concrete in marine environment, pp 205-222.

Fontana and Greene, 1967: Corrosion Engineering, McGraw-Hill.

Forschungsinst. der Zementind. des Vereins Deutscher Zementverke e.V., 1965: Tiefe der carbonatisierten Schicht alter Betonbauten Untersuchungen an Betonproben. Dusseldorf, DAfS, Heft 170. Berlin.

Frazier, K S, 1965: Value of Galvanizied Reinforcing in concrete struct. Materials Protection, Nr 5. New York.

Friedland, R, 1950: Influence of the quality of mortar and concrete upon corrosion of reinforcement. ACI Journal, Vol 22, Nr 12. Detroit.

Gewertz, M W, 1958: Causes and repair of deterioration to a California bridge due to corrosion of reinforcing steel in a marine environment, Part I: Method of repair, Highway Research Board, Bulletin 182, pp 1-17. Washington.

Gjörv, O E, 1968: Durability of Reinforced Concrete Wharves in Norwegian Harbours. Ingengörsförlaget A/S, 208 pp. Oslo.

Gjörv, O E, 1972: Korrosionsbeskyttelse av armeringstål. Nordisk Betong, årgång 16, nr 1. Stockholm.

Gjörv, O E, 1975: Control of steel corrosion in concrete sea structures. ACI Separate Publication SP-49, pp 1-10. Detroit.

Gjörv, Vennesland, El-Busaidy, 1976: Diffusion Of Dissolved Oxygen Through Concrete. Corrosion/76. Int. Corrosion Forum March 22-26.

Gjörv, Vennesland and El-Busaidy, 1977: Electrical Resistivity of Concrete in the Oceans. The 9th Annual Offshore Technology Conference in Houston May 2-5 1977, pp 581-588.

Griffin, D F, 1964: The effect of salt in concrete on compressive strength, water wapor transmission, and corrosion of reinforcing steel. U.S. Naval Civil Engineering Laboratory. Port Hueneme, California.

Griffin, D F, 1975: Corrosion inhibitors for reinforced concrete. ACI Separate Publication SP-49, pp 95-102. Detroit.

Grimer, F I, 1967: The durability of steel embedded in lightweight concrete. Concrete No 4. London.

Gouda, V K, 1970: Corrosion and Corrosion Inhibition of Reinforcing Steel. British Corrosion Journal Vol. 5, Sept, 1970.

Gouda, Mikhail and Shater, 1975: Hardened Portland blast-furnace slag cement pastes, III. Corrosion of steel reinforced versus port structure of the paste matrix. Cement and Concrete Research, Vol 5, pp 99-102.

Göhring and Riedel, 1974: Gasdurchlässigkeit von Betonen und ihr Einfluss auf die Korrosionsbeständigkeit in Salzlösungen. Wissenschaftliche Zeitschrift der Hochschule für Architektur und Bauwesen Weimar, Heft 2. Weimar.

Halvorsen, U, 1962: Beträffande ingjutna värmeslingor, Råsebäcksskolan. Cement- och Betonginstitutet, Kontaktavdelningen Rapport 159. Stockholm.

Halvorsen, U, 1963: Kalciumklorid som tillsatsmedel till betong. Cement- och Betonginstitutet, Utredning nr 6. Stockholm.

Halvorsen, U, 1964: Undersökning av sprickors inverkan på korrosion av värmerör ingjutna i slipbruk. Cement- och Betonginstitutet, Kontaktavdelningen Rapport 255a. Stockholm.

Halvorsen, U, 1966: Korrosion och kalkurlakning vid sprickor i betongkonstruktioner, Bulletin 1. Institutionen för Byggnadsteknik, Tekniska Högskolan i Lund. Lund.

Hamada, M, 1968: Neutralization (carbonation) of concrete and corrosion of reinforcing steel. V-ISCC. Tokyo.

Hannant and Edgington, 1975: Durability of steel fibre concrete. RILEM Symposium, Fibre reinforced cement and concrete, pp 159-169. Leeds.

Hausmann, D A, 1967: Steel corrosion in concrete. Materials protection. November, pp 19-23.

Hebberling, H, 1953: Die Rostschutzwirkung des Zements. Werkstoffe u. Korrosion 4, Nr 7.

Hellström, B, 1977: Bedömning av skador på fasadelement kv 37 Lorensborg, Malmö. Uppdragsrapport 7735. Cement- och Betonginstitutet. Stockholm.

Hermann, P, 1932: Uber Mörtel und Beton. Allgemeiner Industriverlag. Berlin.

Houston, Atimtay and Ferguson, 1972: Corrosion of Reinforcing Steel Embedded in Structural Concrete. Center for Highway Research, University of Texas at Austin, Research Report 112-IF. Austin.

Ivanov, Chernomordik and Akimova, 1971: Diffusion of Salt in Cement Mortars. Zhurnal Prikladnol Khimit, vol 44, no 12, pp 2727-29, Dec. 1971.

Johansson, A, 1973: Betongtillsatsmedel. Byggforskningens informationsblad B8:1973. Stockholm.

Johansson, L, 1976: Skador hos betongbalkonger. Cement- och Betonginstitutet, Fo 3:76. Stockholm.

Jung, M, 1969: Beiträge zur Gütebewertung korrosions- und wasserdichter Betone. Hochschule für Architektur und Bauwesen. Weimar.

Jönis, P, 1975: Rost- och kalkutfällningar på bassäng, Enskede. Uppdragsrapport 7561, Cement- och Betonginstitutet. Stockholm.

KB5, 1966: Kommentarer till 1965 års material- och utförandebestämmelser för betong. Stockholm.

Keeton, J R, 1970: Permeability studies of reinforced thin-shell concrete, NTIS, AD-711841. Springfield.

Kleinschmidt, H-J, 1965: Untersuchung über das Fortscheiten der Carbonatisierung an Betonanverken. DAfS, Heft 1970. Berlin.

Kosaka, K, 1961: Durability (especially carbonation) test of concrete. RILEM-symposium, Durability of Concrete. Prag.

Kucera and Collin, 1977: Atmospheric Corrosion with Special Regard to Short-Term Variations - An Investigation Using Electrochemical and Weight Loss Methods, 6th European Congress on Metallic Corrosion, 19-23 September 1977. London.

Lewis, D A, 1962: Some Aspects of the Corrosion of Steel in Concrete. Proceedings of the First International Congress on Metallic Corrosion, London, 1962, pp 547-555.

Locher and Sprung, 1970: Einwirkung von salzäurehaltigen PVC-Brandgasen auf Beton. Beton nr 3. Düsseldorf.

Longuet, P, 1976: La protection des armatures dans le béton armé élaboré avec des ciments de laitier. Silicates Industriels 1976-7/8 pp 321-328.

Martikainen, O, 1968: Metallien sähkökemiallisesta käytäytymisestä sementtiliimassa. Valtion Teknillinen Tutkimuslaitos, Tiedotus Sarja III - Rakennus 125. Helsingfors.

Martin, H, 1975: Zeitlicher Verlauf der Chloridionenwanderung in Beton, der einem PVC-Brand ausgesetzt war, Teil 2. Betonsteinwerk und Fertigteil-Technik, Nr 2. Wiesbaden.

Materialprüfungsamt für das Bauwesen der TH München, 1961: Versuche zur Frage der pH-Wert-Abminderung von Beton. Interner Bericht Dec 1961, bearbeitet von H Moll.

Mattsson, E, 1970: Elektrokemi och korrosionslära. Korrosionsinstitutet, Bulletin nr 56. Stockholm.

Mercer, Butler and Warren, 1977: Cleaning of Corroded Test Specimens, British Corrosion Institute, 1977, Vol 12, No 2.

Meyer, Wierig and Husmann, 1967: Karbonatisierung von Schwerbeton. Deutscher Ausschuss für Stahlbeton, Heft 182. Berlin.

Molin and Klevbo, 1980: Skador på pelare, trappor, Orminge, lägesrapport. Uppdragsrapport 8061, Cement- och Betonginstitutet. Stockholm.

Molin and Klevbo, 1981: Skador på utvändiga betongelement. Förslag till åtgärder, Orminge. Uppdragsrapport 8146, Cement- och Betonginstitutet. Stockholm.

Moll, H L, 1964: Über die Korrosion von Stahl in Beton. DAfS, Heft 169. Berlin.

Monfore and Verbeck, 1960: Corrosion of prestressed wire in concrete. PCA Bulletin 120. Detroit.

Moore, R T, 1972: Penetration resistance tests of reinforced concrete barriers, NTIS, COM-73-10867. Springfield.

Nevander, Bankvall and Sandberg, 1968: Fukt. Kompendium i byggnadsteknik I, Allmän kurs I, Lunds Tekniska Högskola. Lund.

Nielsen, A, 1976: Hvid grön og sort rust, Nordisk Betong, nr 2-76.

Nilsson, L-O, 1977: Fuktproblem vid betonggolv, Lund Institute of Technology, Report TVBM-3002. Lund.

Nordisk Förzinkningsförening, 1967: Varmförzinkning som korrosionsskydd. Informationskontoret. Stockholm.

Odén, S, 1965: Aspects of the atmospheric corrosion climate. IVA's korrosionsnämnd, Bulletin 45.

Peterson, O, 1979: Sätt att följa betongens karbonatisering som funktion av djupet under ytan. Report from CEMENTA Research and Development Section, Stockholm.

Petersons, N, 1965: Korrosion av värmelednings- och luftcirkulationsrör ingjutna i betong. Cement- och Betonginstitutet, Utredning nr 7. Stockholm.

Plum and Jessing, 1965: Behov for en debat om statistisk forsögsanlägning og verdering. Ingeniörens Ugeblad nr 42, 1965.

Pourbaix, M, 1963: Atlas d'Equilibres Elechtrochimiques à 25°C. Gauthiers-Villars & Cie. Paris.

Powers, T C, 1962: A Hypothesis on Carbonation Shrinkage. PCA Journal, Vol 4, Nr 2. Skokie.

Powers, Copeland and Mann, 1959: Capillary continuity or discontinuity in cement pastes, PCA Journal, Vol 1, Nr 2, May 1959, pp 38-48. Skokie.

Rehm and Nürnberger, 1972: Spannungsrisskorrosion hochfester Spannstähle, Cement XXIV Nr 3, p 106-115. Amsterdam.

Rehm and Moll, 1964: Versuche zum Studium des Einflusses der Rissbreite auf die Rostbildung an der Bewehrung von Stahlbetonbauteilen. DAfS, Heft 169. Berlin.

Reinsdorf and Dippel, 1971: Permeabilität von Beton und Mörtel, Schriftenreihen der Bauforschung, Reihe Stahlbeton Nr 19, pp 41-71. Berlin.

Richartz, W, 1969: Die Bindung von Chlorid bei der Zementerhärtung. Zement-Kalk-Gips, Vol 22, Nr 10, pp 447-456.

Rieche, G, 1973: Mechanismen der Spannungskorrosion von Spannstählen in hintblick auf ihr verhalten in Spannbetonkonstruktionen. Von der Fakultät für Bauwesen der Techn. Universität Carolo-Wilhelmina zu Braunschweig.

RILEM CRC Committee, 1975: Steel in concrete: Corrosion of reinforcement and prestressing tendons.

Roberts, N P, 1970: The resistance of reinforcement to corrosion, Concrete, Vol 4, Nr 10, pp 383-387. London.

Robinson, R C, 1975: Cathodic protection of steel in concrete. ACI Separate Publication SP-49, pp 83-94. Detroit.

Rombén and Tuutti, 1978: Slutförvaring av aktiverade ståldetaljer i betong. Uppdragsrapport 7853. Cement- och Betonginstitutet. Stockholm.

Roshore, E C, 1971: Durability and behaviour of prestressed concrete beams, Report 3, Laboratory tests of weathered pretensioned beams, NTIS, AD 732442. Springfield.

Rouen, A, 1970: Investigations of the corrosion behaviour of galvanized steel reinforcement in concrete. Internationale Verzinkertagung Düsseldorf.

Rounsley, R R, 1961: Multimolecular absorption equation. Journal of Am. Inst. Chem. Eng., 7 1961.

Ruettgers, Vidal and Wing, 1935: An investigation of the Permeability of Mass Concrete with Particular Reference to Boulder Dam. Journal of American Concrete Institute, Vol 6, No 4, March-April 1935.

Saarima, J, 1971: Metalliputkien syöpyminen lattiarakenteissa, Rakennustekniikka, (1971):8, pp 415-418. Helsingfors.

Saarima and Sivhonen, 1970: Korrosion av armering i konstruktioner av vanlig betong och lättklinkerbetong. Stencil. Tekniska Högskolan i Otnäs.

Schiessl, P, 1975: Zusammenhang zwischen Rissbreite und Korrosionsabtragung an der Bewehrung. Betonwerk und Fertigteil-Technik, Nr 2. Wiesbaden.

Schiessl, P, 1976: Zur Frage der zulässigen Rissbreite und der erforderlichen Betondeckung im Stahlbetonbau - unter besonderer Berücksichtigung der Karbonatisierung des Betons. DAfS, Heft 255. Berlin.

Schröder, Smolezyk, Grade, Vinkeloe and Roth, 1967: Einfluss von Luftkohlensäure und Feuchtigkeit auf die Beschaffenheit des Betons als DAfS, Heft 182. Berlin.

Schulze and Günzler, 1968: Corrosion protection of the reinforcement in lightweight concrete. Proceedings, First International Congress on Lightweight Concrete, Vol 1. London.

Schwiete, L, 1966: Über die Bestimmung der offenen Porosität im Zementstein, Tonindustrie Zeitung Nr 12. Goslar.

Schwiete, B, 1970: Bestimmung der effektiven Porosität von Beton durch Glasdiffusionsmessungen, Zement-Kalk-Gips, Nr 3. Wiesbaden.

Scott, G N, 1965: Corrosion Protection Properties of Portland Cement Concrete. Journal American Water Works Ass. 57 (1965), pp 1038-52.

Shalon and Raphael, 1959: Influence of sea water on corrosion of reinforcement. ACI Journal, Vol 30, Nr 12, pp 1251-68. Detroit.

Short and Page, 1981: The diffusion of chloride ions through Portland and blended cement pastes. Paper presented at International Conference on Slag and Blended Cements, Mons, Belgium, Sept. 7-11, 1981.

Skarendahl, Å, 1973: Lättballast och lättballastbetong. Svenska Forskningsinstitutet för Cement och Betong vid KTH i Stockholm, Handlingar nr 47. Stockholm.

Sneck, T, 1959: Kontaktkorrosion - metallers korrosion vid kontakt med fast byggnadsmaterial. VVS-tidskriften (1959), pp 219-227.

Sneck, T, 1961: Korrosion av järn och stål ingjutet i betong. Valtion Teknillinen Tutkimuslaitos, Tiedotus sarja III - Rakenus 49. Helsingfors.

Soda and Yamazaki, 1958: Long time study on the neutralization of Concrete and the Rusting of Reinforcement in Concrete. Japan Cement Engineering Association. Review of the twelfth General Meeting. Tokyo.

Soretz, S, 1966: Korrosionsschutz im Stahlbeton und Spannbeton. Zement und Beton Nr 36. Wien.

Soretz, S, 1967: Korrosionsschutz im Stahlbeton und Spannbeton. Betonstein-Zeitung Nr 2. Wiesbaden.

Spellman and Stratfull, 1973: Concrete variables and corrosion testing, Highway Research Record Nr 423, pp 27-45.

Steinour, H H, 1964: Influence of the Cement on the Corrosion Behaviour of Steel in Concrete. PCA, Bulletin 168. Skokie.

Stratfull, R F, 1972: Half cell potentials and the corrosion of steel in concrete. NTIS, PB-218 720. Springfield.

Stratfull, R F, 1972: Corrosion autopsy of structurally unsound bridge deck. NTIS, PB-218 843. Springfield.

Stratfull, R F, 1974: Experimental cathodic protection of a bridge deck. Transportation Research Record 500, pp 1-15. Washington.

Stratfull, Jurkovich and Spellman, 1975: Corrosion testing of bridge decks. Transportation Research Record 539, pp 50-59. Washington.

Szilard, Rudolph, Wallevik and Oddmund, 1975: Effectiveness of concrete cover in corrosion protection of prestressing steel. ACI Separate Publication SP-49, pp 47-70. Detroit.

Sällström, S, 1973: Ballast. Cement- och Betonginstitutets Kursverksamhet, Betongkurs A. Stockholm.

Timofeev, D P, 1960: The mechanism of transport of matter in porous sorbents. Russiona chemical reviews, Vol 29, Nr 3, pp 180-192.

Traetteberg, A, 1977: The mechanism of chloride penetration in concrete, report No A77070, The Norwegian Institute of Technology. Trondheim.

Tremper, B, 1947: The corrosion of reinforced steel in cracked concrete. ACI Journal, June 1947.

Tremper, Beaton ans Stratfull, 1958: Causes and repair of deterioration to a California bridge due to corrosion of reinforcing steel in a marine corrosion, Highway Research Board, Bulletin 182, pp 18-41. Washington.

Thorsén, A, 1978: Kloridhaltsbestämning, Korsnäsverken, Gävle. Uppdragsrapport 7880, Cement- och Betonginstitutet. Stockholm.

Thorsén, A, 1979: Betongkvalitet i bjälklag, Sveriges Radios filmlaboratorium. Uppdragsrapport 7956, Cement- och Betonginstitutet. Stockholm.

Thorsén and Tuutti, 1979a: Bedömning av skador hos silos, Hammars Glasbruk. Uppdragsrapport 7947, Cement- och Betonginstitutet. Stockholm.

Thorsén and Tuutti, 1979b: Skadade kraftledningsstolpar av betong. Uppdragsrapport 7916, Cement- och Betonginstitutet. Stockholm.

Tuutti, K, 1975: Sprickor i prefabpelare, Korsnäsverken. Uppdragsrapport 7596, Cement- och Betonginstitutet. Stockholm.

Tuutti, K, 1977: Stålets korrosionsförlopp i osprucken betong - en hypotes. Cement- och Betonginstitutet, Fo 4:77. Stockholm.

Tuutti, K, 1978: Cracks and corrosion. Cement- och Betonginstitutet, Rapport Fo 6:78. Stockholm.

Tuutti, K, 1979a: Korrosionsskador på armering i betongbalkonger. Cement- och Betonginstitutet, Rapport Fo 2:79. Stockholm.

Tuutti, K, 1979b: Service life of concrete structures - corrosion test methods. Studies on concrete technology. Dedicated to Professor Sven G Bergström on his 60th anniversary December 14, 1979. Cement- och Betonginstitutet. Stockholm.

Tuutti, K, 1979c: Service life of structure with regard to corrosion of embedded steel. RILEM Quality control of concrete structures, June 17-21, Stockholm, pp 293-301 Vol I, 1979.

Uhlig, H H, 1963: Corrosion and Corrosion Control. John Wiley & Sons. New York.

Verbeck, G J, 1975: Mechanism of corrosion of steel in concrete. ACI Separate Publication SP-49, pp 21-38. Detroit.

Vernon, W H J, 1935: IBID 31, 1668, 1935.

Vesikari, E, 1981: Corrosion of reinforcing steels at cracks in concrete. Research report 11/1981, Technical Research Centre of Finland.

Warris, B, 1965: Korrosionsskador på värmerör ingjutna i betonggolv i villor belägna i Skene kommun. Cement- och Betonginstitutet, Kontaktavdelningen, Rapport 275. Stockholm.

Warris, B, 1966: Korrosionsskador, sporthall i Malmö. Cement- och Betonginstitutet, Kontaktavdelningen, Rapport 313. Stockholm.

Weigler and Segmüller, 1973: Einwirkung von chloriden auf Beton. Betonwerk und Fertigteil-Technik, Nr 8, pp 577-584. Wiesbaden.

Wesche, K, 1973: Baustoffe für hagende Bauteile, Band 3, Stahl Aluminium, Wiesbaden.

Woods, H, 1966: Corrosion of embedded material other than reinforcing steel. PCA, Bulletin 198. Detroit.

Woods, H, 1968: Durability of Concrete Construction. American Concrete Institute. Detroit.

Wranglén, G, 1967: Metallers korrosion och ytskydd, Almqvist & Wicksell. Uppsala.

Zagar and Ludwig, 1955: Die Grundlagen zur Ermitteilung der Gasdurchlässigkeit von feuerfesten Baustoffen. Archiv für das Eisenhüttenwesen. Nr 12. Düsseldorf.

Personal communications

Arup, H:	Korrosioncentralen ATV, Denmark
Bergman, E:	The Swedish Cement and Concrete research Institute

Bergström, S G:	The Swedish Cement and Concrete Research Institute
Fagerlund, G:	Cementa AB
Grønvold, F:	Korrosionscentralen ATV, Denmark
Kucera, V:	The Swedish Cement and Concrete Research Institute
Rombén, L:	The Swedish Cement and Concrete Research Institute
Sneck, T:	Technical Research Centre of Finland
Svedberg, G:	The Royal Institute of Technology, Stockholm

APPENDIX 1

Cement analysis

Chemical compounds	Slite Portland Cement /%/	100% Slag /%/
CaO	62.6	42.0
SiO_2	19.5	36.4
Al_2O_3	4.6	9.7
Fe_2O_3	2.2	0.6
Mg O	3.8	6.6
$SO_{3,tot}$	3.4	3.2
K_2O	1.5	0.8
Na_2O	0.5	0.7
Cl^-	< 0.01	< 0.1
S^{2-}	-	1.04
loss of ignition	1.9	1.2

spec surface 370 m^2/kg

Steel analysis

Chemical compounds	Smooth bars /%/	Plates te, electrochemical cells /%/	Reference plates in series 1 corrosion cells /%/	K_s 40 Normal values /%/
C	0.048	0.053	0.15	0.35-0.55
Si	0.00	0.02	0.33	0.15-0.60
Mn	0.20	0.29	0.38	0.45-0.90
F	0.10			
S	0.02	0.28	0.039	0.04
N	0.003	0.12		
Cn	0.01	0.01	0.34	0.10-0.50
Al_{tot}	0.054	0.029		
P		0.22	0.013	0.04
Cr		0.01	0.07	0.05-0.25
Ni		0.02	0.10	0.05-0.25
V			0.007	
Mo			0.01	

GRADING CURVES ACCORDING TO CONCRETE RECIPES IN APPENDIX 4

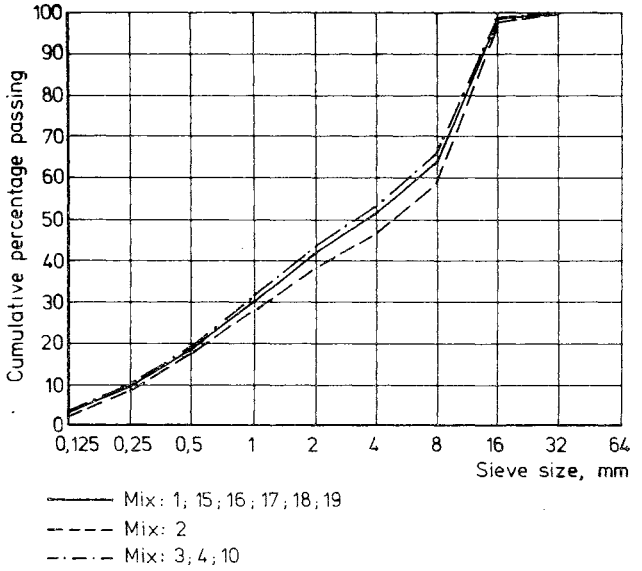

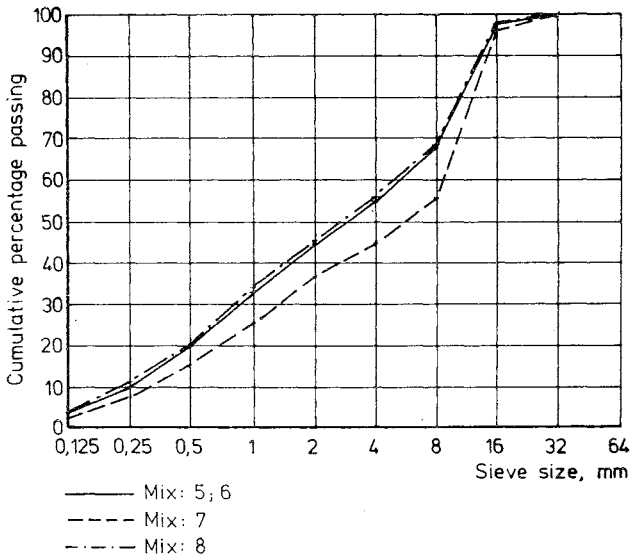

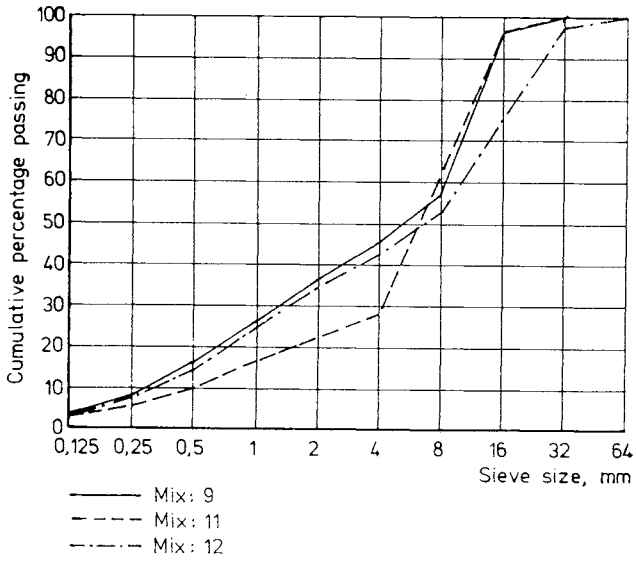
Cumulative percentage passing
100
90
80
70
60
50
40
30
20
10
0
0,125 0,25 0,5 1 2 4 8 16 32 64
Sieve size, mm
Mix: 9
Mix: 11
Mix: 12

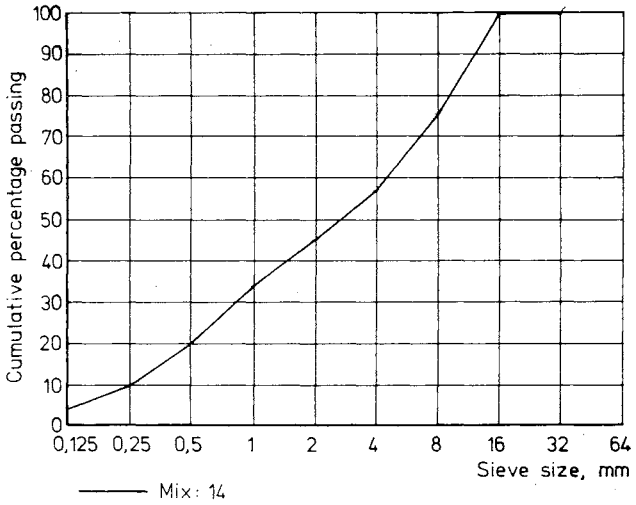
Cumulative percentage passing
100
90
80
70
60
50
40
30
20
10
0
0,125 0,25 0,5 1 2 4 8 16 32 64
Sieve size, mm
Mix: 14

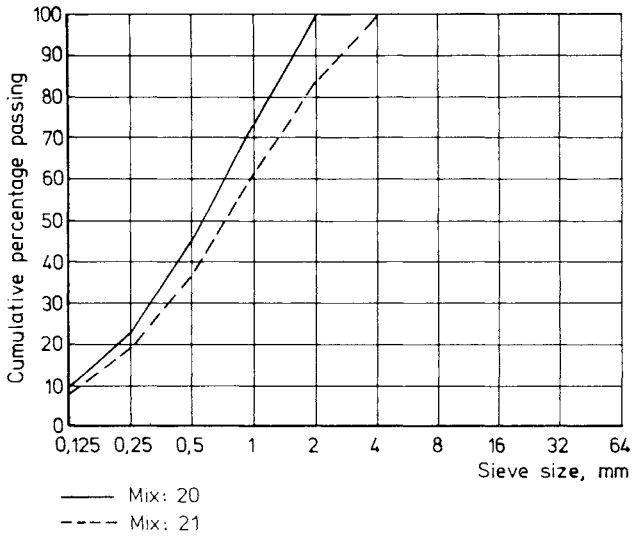
Cumulative percentage passing
100
90
80
70
60
50
40
30
20
10
0
0,125 0,25 0,5 1 2 4 8 16 32 64
Sieve size, mm
Mix: 20
Mix: 21

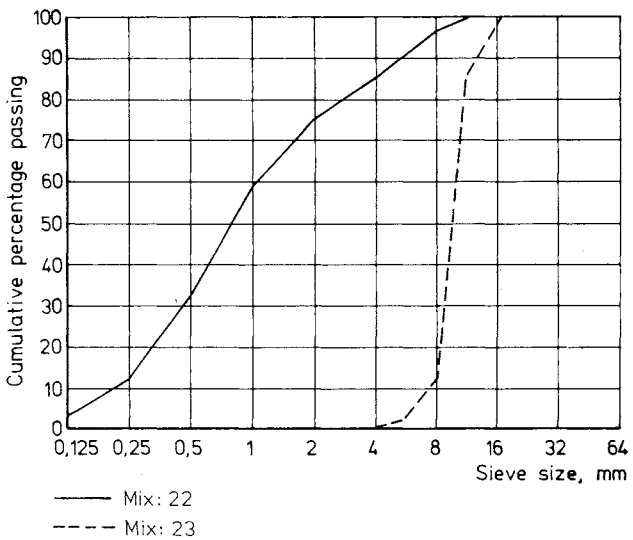
Cumulative percentage passing
100
90
80
70
60
50
40
30
20
10
0
0,125 0,25 0,5 1 2 4 8 16 32 64
Sieve size, mm
Mix: 22
Mix: 23

TABLE A. Concrete of mix proportions in 0_2 diffusion measurements.

Mix proportion	Cement content /kg/m^3/	w/c	Aggregate				Admix-tures	Air content /%/	Slump /mm/	Bulk density /ton/m^3/	Compressive strength 28 d /MPa/
			0-8 /kg/m^3/	8-16 mm /kg/cm^3/	16-32 mm /kg/cm^3/	Grading curve					
1	405	0.50	1092	620		1		2.1	110	2.37	60 ± 2
2	530	0.42	935	654		2		2.4	75	2.35	64 ± 5
3	335	0.59	1183	599		3		2.2	100	2.34	49 ± 1
4	288	0.67	1207	613		4		2.7	80	2.33	40 ± 1
5	259	0.76	1255	569		5		2.5	120	2.33	34 ± 1
6	235	0.81	1268	575		6		2.6	110	2.32	30 ± 1
7	760	0.36	721	559		7		1.6	85	2.33	69 ± 4
8	420	0.50	1180	503		8		2.0	85	2.35	59 ± 1
9	392	0.50	1003	738		9		2.0	70	2.37	56 ± 1
10	433	0.50	1097	559		10		1.8	110	2.34	57 ± 1
11	378	0.50	1074	677		11		2.5	40	2.36	57 ± 1
12	374	0.50	948	428	436	12		1.5	65	2.39	56 ± 2
13	458	0.51	1551			13		3.8	70	2.28	55 ± 2
14	431	0.50	1132	504		14		2.4	85	2.34	56 ± 1
15	400	0.49	1092	620		15	Air	4.0	85	2.32	52 ± 1
16	369	0.47	1145	649		16	Wetting	2.6	5	2.39	57 ± 1
17	408	0.49	1092	620		17	1.5$CaCl_2$	2.1	95	2.38	72 ± 4
18	410	0.53	1092	620		18	Super p	0.2	265	2.39	55 ± 1
19:1	410	0.48	1092	620		19		-	110	2.37	50 ± 2
19:2	407	0.50	1092	620		19		2.1	85	2.35	56 ± 3
20-23	280	0.67	1210	610		4		2.8	85	2.30	33 ± 1
24-27	530	0.42	940	650		2		2.5	75	2.35	69 ± 2
28-31	280*	0.67	1210	610		4		2.1	110	2.28	24 ± 1**
32-35	530	0.42	940	650		2		2.0	85	2.32	52 ± 1**

* Slagg cement
** 90 days

TABLE B. Concrete mix proportions in measurements with corrosion cells.

Mix proportion	Cement content /kg/m^3/	w/c	Aggregate				Admix-tures	Air content /%/	Slump /mm/	Bulk den-sity /ton/m^3/	Compres-sive strength 28 d /MPa/
			0-8 /kg/m^3/	8-16 mm /kg/cm^3/	16-32 mm /kg/cm^3/	Grading curve					
KC-76	235	0.82	1265	570		6			110	2.27	26 _ 1
KC-76	405	0.51	1090	620		1			125	2.33	49 _ 2
Series 1											
KC3-77	405	0.50	1090	620		1			110	2.34	50 _ 2
KC4-77	235	0.81	1265	570		6			65	2.25	27 _ 2
Series 2											
KC5-78	470	0.32	600	1200		22.23	Superplast		20	2.45	82 _ 3
Series 3											
KC6-78	235	0.83	1265	570		6			120	2.25	26 _ 1
Series 4											
KC7	530	0.39	935	650		2	5%CaCl$_2$	2.2	90	2.35	90 _ 1
KC8	530*	0.39	935	650		2	"	2.0	110	2.31	58 _ 1**
KC9	280	0.68	1205	615		4		2.9	150	2.30	36 _ 1
KC10	280*	0.68	1205	615		4		2.9	95	2.28	30 _ 1**
KC11	530	0.39	935	650		2		1.7	75	2.35	78 _ 1
KC12	530*	0.39	935	650		2		1.7	160	2.33	60 _ 1**

*Slag
**(90 d)

TABLE C. Mix proportions of concrete in weight loss measurements.

Mix proportion	Cement content /kg/m^3/	w/c	Aggreg			Admix-tures	Air content /%/	Slump /mm/	Bulk den-sity /ton/m^3/	Compres-sive strength 28 d /MPa/
			0-8 /kg/m^3/	8-16 mm /kg/cm^3/	Grading curve					
Rate of corrosion, chapter 5.3.5										
w/c=0.4	540	0.40	1620		20					
w/c=0.70	360	0.70	1700		20					
Some proportions for mortar made by slag cement (70% slag+30% with 5% $CaCl_2$ by weight of cement.							Slite portland cement and mortar			
Cracks and corrosion, chapter 5.3.6										
w/c=0.35	770	0.35	720	560	7		2.1	90	2.32	71 _ 1
w/c=0.50	405	0.49	1090	620	1		1.9	85	2.37	56 _ 2
w/c=0.70	280	0.66	1200	610	4		2.7	85	2.34	39 _ 1
w/c=0.50	390*	0.48	1100	630	1		2.0	80	2.35	37 _ 1
Final state, chapter 5.3.7										
w/c=0.50	405	0.47	1090	620	1		2.5	65	2.34	52 _ 2
w/c=0.81	230	0.85	1250	575	6		3.2	65	2.29	26 _ 1

*Slag

TABLE D. Mix proportions of concrete in relative humidity in cracks and in potential measurements.

Mix proportion	Cement content /kg/m^3/	w/c	Aggregate			Admix-tures	Air content /%/	Slump /mm/	Bulk density /ton/m^3/	Compressive strength 28 d /MPa/
			0-8 /kg/m^3/	8-16 mm /kg/cm^3/	Grading curve					
Potential measurements, chapter 5.8										
pot 1	400	0.50	1090	620	1		2.1	90	2.36	56 _ 2
pot 2	400	0.50	1090	620	1	5%$CaCl_2$	2.3	45	2.36	79 _ 2
Relative humidity in cracks, chapter 5.7										
w/c=0.40	530	0.41	930	650	2		2.6	70	2.34	63 _ 3
w/c=0.90	235	0.82	1260	570	6		2.5	90	2.30	28 _ 2

TABLE A. Results, oxygen diffusion measurements, chapter 5.1.

Sample number	Cement-type	w/c	Thick-ness /mm/	Max aggr size /mm/	Slump /mm/	Admixtures	Relative humidity, %			D_{eff,O_2} /x10^{-8} m^2/s/
							0-7 days	8-28 days	28 days - 7 months	
1:1	Portland	0,50	20	16	110	-	100	50	50	2,7
1:2	"	"	"	"	"	-	"	"	"	2,1
2:1	"	0,42	"	"	750	-	"	"	"	1,1
2:2	"	"	"	"	"	-	"	"	"	1,2
3:1	"	0,59	"	"	100	-	"	"	"	3,3
3:2	"	"	"	"	"	-	"	"	"	3,7
4:1	"	0,67	"	"	80	-	"	"	"	4,0
4:2	"	"	"	"	"	-	"	"	"	5,0
5:1	"	0,76	"	"	120	-	"	"	"	7,3
5:2	"	"	"	"	"	-	"	"	"	7,8
6:1	"	0,81	"	"	100	-	"	"	"	10
6:2	"	"	"	"	"	-	"	"	"	14
7:1	"	0,36	"	"	85	-	"	"	"	1,6
7:2	"	"	"	"	"	-	"	"	"	1,5
8:1	"	0,50	"	"	85	-	"	"	"	3,7
8:2	"	"	"	"	"	-	"	"	"	3,1
9:1	"	0,50	"	"	70	-	"	"	"	3,0
9:2	"	"	"	"	"	-	"	"	"	2,2
10:1	"	0,50	"	"	110	-	"	"	"	4,1
10:2	"	"	"	"	"	-	"	"	"	3,1
11:1	"	0,50	"	"	40	-	"	"	"	2,7
11:2	"	"	"	"	"	-	"	"	"	2,3
12:1	"	0,50	"	"	65	-	"	"	"	2,9
12:2	"	"	"	"	"	-	"	"	"	1,9
13:1	"	0,51	"	"	70	-	"	"	"	2,8
13:2	"	"	"	"	"	-	"	"	"	2,7

Table A, continued

Sample number	Cement-type	w/c	Thick-ness /mm/	Max aggr size /mm/	Slump /mm/	Admixtures	Relative humidity, %			D_{eff,O_2} /x10^{-8} m^2/s/
							0-7 days	8-28 days	28 days - 7 months	
14:1	Portland	0,50	20	32	85	-	100	50	50	2.5
14:2	"	"	20	"	"	-	"	"	"	2,5
15:1	"	0,49	20	16	"	air en-	"	"	"	2,8
15:2	"	"	20	"	"	trainment	"	"	"	2,5
16:1	"	0,47	20	"	50	plastic-	"	"	"	2,2
16:2	"	"	20	"	"	izer	"	"	"	2,0
17:1	"	0,49	20	"	95	1,5%$CaCl_2$/	"	"	"	1,7
17:2	"	"	20	"	"	C	"	"	"	1,9
18:1	"	0,53	20	"	55	Superplas-	"	"	"	1,7
18:2	"	"	20	"	"	ticizer	"	"	"	1,9
19:1:11	"	0,40	20	"	110	-	"	"	"	2,7
19:1:22	"	"	20	"	"	-	"	"	"	3,1
19:1:21	"	"	20	"	"	-	"	"	"	2,8
22	"	"	20	"	"		"	"	"	2,3
19:1:31	"	"	20	"	"	-	"	"	"	2,3
19:1:41	"	"	20	"	"	-	"	"	"	2,3
19:1:51	"	0,50	20	"	"	-	"	"	"	2,7
19:1:61	"	"	20	"	"		50	"	"	5,1
62	"	"	20	"	"	-	"	"	"	6,7
19:1:71	"	"	20	"	"	-	80	"	"	6,5
72	"	"	20	"	"	-	"	"	"	6,3
19:1:81	"	"	20	"	"		100	80	80	0,050
82	"	"	20	"	"	-	"	"	"	0,050
19:1:91	"	"	20	"	"	-	"	100	100	< 0,03
92	"	"	20	"	"	-	"	"	"	< 0,03

Table A, continued

Sample number	Cement-type	w/c	Thick-ness /mm/	Max aggr size /mm/	Slump /mm/	Admixtures	Relative humidity, %			D_{eff,O_2} /x10^{-8} m^2/s/
							0-7 days	8-28 days	28 days - 7 months	
19:2:11	Portland	0,50	10	16	85	-	100	50	50	5,3
12	"	"	10	"	"	-	"	"	"	5,9
19:2:21	"	"	30	"	"	-	"	"	"	0,67
22	"	"	30	"	"	-	"	"	"	0,80
19:2:31	"	"	50	"	"	-	"	"	"	0,27
32	"	"	50	"	"	-	"	"	"	0,21
19:2:41	"	"	20	"	"	-	"	"	"	2,1
42	"	"	"	"	"	-	"	"	"	2,7
19:2:51	"	"	"	"	"	-	"	"	"	2,3
52	"	"	"	"	"	-	"	"	"	4,1
19:2:61	"	"	"	"	"	-	"	"	"	1,3
62	"	"	"	"	"	-	"	"	"	0,85
20:1	"	0,67	"	"	80	-	50	50	0	17,2
20:2	"	"	"	"	"	-	"	"	"	16,6
21:1	"	"	"	"	"	-	"	"	50	9,9
21:2	"	"	"	"	"	-	"	"	"	9,9
22:1	"	"	"	"	"	-	80	80	80	3,3
22:2	"	"	"	"	"	-	"	"	"	3,5
23:1	"	"	"	"	"	-	100	100	100	0,04
23:2	"	"	"	"	"	-	"	"	"	0,03
24:1	"	0,42	"	"	"	-	50	50	0	7,7
24:2	"	"	"	"	"	-	"	"	"	8,3
25:1	"	"	"	"	"	-	"	"	50	1,5
25:2	"	"	"	"	"	-	"	"	"	1,9
26:1	"	"	"	"	"	-	80	80	80	0,2
26:2	"	"	"	"	"	-	"	"	"	0,5

Table A, continued

Sample number	Cement-type	w/c	Thick-ness /mm/	Max aggr size /mm/	Slump /mm/	Admixtures	Relative humidity, %			D_{eff,O_2} /x10^{-8} m^2/s/
							0-7 days	8-28 days	28 days - 7 months	
27:1	Portland	0,42	20	16	75	-	100	100	100	0,03
27:2	"	"	"	"	"	-	"	"	"	0,03
28:1	Blended	0,70	"	"	110	-	50	50*	0	10,2
28:2	cement	"	"	"	"	-	"	"	"	26,8
29:1	"	"	"	"	"	-	"	"	50	4,8
29:2	"	"	"	"	"	-	"	"	"	4.3
30:1	"	"	"	"	"	-	80	80*	80	0,9
30:2	"	"	"	"	"	-	"	"	"	1,9
31:1	"	"	"	"	"	-	100	100*	100	0,06
31:2	"	"	"	"	"	-	"	"	"	0,06
32:1	"	0,40	"	"	85	-	50	50*	0	6,1
32:2	"	"	"	"	"	-	"	"	"	7,0
33:1	"	"	"	"	"	-	"	"	50	1,5
33:2	"	"	"	"	"	-	"	"	"	0,6
34:1	"	"	"	"	"	-	80	80*	80	0,05
34:2	"	"	"	"	"	-	"	"	"	0,10
35:1	"	"	"	"	"	-	100	100*	100	0,05
35:2	"	"	"	"	"	-	"	"	"	0,10

*8-90 days in this climate.

TABLE A. Measured cell current in pilot test.

Cell number	Cell current /μA/cm^2 anodic area/				Remarks
Time, hours	1	2	3	4	
	0.006	0.003	0.01	0.01	
0	0.05	0.25	0.06	0.7	Wetting
18	0.01	0.18	0.2	0.6	
48	0.06	0.13	0.2	0.2	
139	0.02	0.06	0.07	0.06	
168	0.02	0.22	0.03	0.06	Drying
233	0.01	0.12	0.12	0.03	
240	0.01	0.30	0.03	0.03	
288	<0.01	0.36	0.02	0.02	
328	<0.01	0.28	0.02	0.03	
336	0.02	0.70	0.03	0.70	Wetting
384	0.05	0.30	0.05	0.65	
408	0.04	0.20	0.07	0.60	
432	0.04	0.15	0.09	0.10	
480	0.04	0.13	0.15	0.08	
552	0.04	0.10	0.01	0.05	
600	0.02	0.10	0.08	0.05	
640	<0.01	0.09	0.07	0.05	
893	0.06	1.5	0.06	0.3	Drying
917	<0.03	1.9	0.06	1.1	
941	<0.03	1.8	0.06	1.2	
989	<0.03	1.6	0.06	0.7	
1037	<0.03	1.5	0.06	0.5	
1070	<0.03	1.1	0.06	0.5	Wetting
1074	0.06	1.5	0.09	1.8	Drying
1085	<0.03	1.6	0.06	0.8	
1109	<0.03	1.6	<0.03	0.9	
1138	<0.03	1.5	<0.03	0.7	
1140	<0.03	1.5	<0.03	0.7	
1144	<0.03	1.5	<0.03	0.7	Wetting
1148	0.1	1.8	0.1	3.8	Drying
1158	<0.05	2.7	<0.05	2.5	
1165	<0.05	2.9	<0.05	2.1	
1168	0.1	2.0	0.1	3.8	Wetting
1172		1.2		3.0	Drying
1181		2.3		2.3	
1229		2.5		1.6	
1253		2.6		1.5	
1301		1.9		1.1	
1312		2.2		6.0	Wetting
1325	0.2	2.3	0.1	5.0	
1335	0.2	1.0	0.2	4.2	Drying
1339	0.1	0.8	0.1	3.9	
1349		3.0		3.4	
1363		3.0		2.4	
1397		2.7		1.6	
1421		2.8		1.4	
1469		1.6		1.0	
1477	0.008		0.04		
1493		1.6		0.7	
1501	0.008	1.6	0.04	0.6	

TABLE B . Measured cell current from corrosion cells in Series 1. /$\mu A/cm^2$/.

Time /days/	Cell number											
	1	2	3	4	5	6	7	8	9	10	11	12
1	0.00275	0.0019	0.0008	0.46	0.0135	-	0.0365	0.00135				
2	0.0025	0.00175	0.0018	0.34	0.0096	-	0.04	0.005	0.025	0.0005	0.0132	0.0075
6	0.002	0.0015	0.035	0.16	0.0022	-	0.022	0.005	0.011	0.0003	0.0074	
9	0.003	0.0012	0.022	0.13	0.0013	-	0.017	0.006	0.0062	0.0017	0.0059	
14	0.0015	0.0009	0.015	0.09	0.0005	-	0.013	0.003	0.0045	-	0.029	0.002
17	0.001	0.0014	0.01	0.1	-	-	0.014	-	0.003	0.0001	0.0059	0.0025
20	0.0006	0.001	0.006	0.08	-	-	0.009	-	0.003	0.0002	0.0088	0.0015
23	0.0006	0.001	0.006	0.08	-	-	0.009	-	0.003	0.0002	0.0088	0.0015
27	0.0006	0.001	0.006	0.08	-	-	0.009	-	0.003	0.0002	0.0059	0.002
34	0.0006	0.001	0.002	0.029	-	-	0.01	0.0015	0.0016	0.0001	0.0029	0.0005
38	0.001	0.002	-	-	-	-	0.004	0.001	0.0015	0.00005	-	0.005
39	0.001	0.002	0.004	0.045	-	-	0.006	0.0002	0.002	0.00005	0.0088	0.01
45	0.002	0.002	0.006	0.045	-	-	0.007	0.0004	0.0017	0.00005	-	0.022
54	0.002	0.002	0.009	0.032	-	-	0.0085	0.0003	0.0015	-	0.0029	0.005
61	0.002	0.0001	0.0011	0.03	0.0005	0.0004	0.012	-	0.0004	0.00003	0.0029	0.005
67	0.0016	0.0006	0.008	0.03	0.0012	0.0005	0.009	-	0.0007	-	0.0088	0.01
74	0.0015	-	0.006	0.029	0.0012	0.0003	0.0075	-	0.0004	-	0.0029	0.005
77	0.0015	0.0012	0.008	0.01	0.0012	0.0006	0.0075	0.002	0.0003	-	0.0029	0.003
81	0.0012	0.0011	0.008	0.027	0.0017	-	0.004	-	0.0011	-	0.0044	0.004
84	0.0012	0.0011	0.008	0.021	0.0031	-	0.004	-	0.0002	-	0.002	0.004
111	0.0015	0.0015	0.008	0.0185	0.002	-	0.003	-	0.001	-	0.08	0.0005
112	0.0015	0.0015	0.05	0.03	0.002	-	1.5	0.0002	0.001	-	100	0.0001
115	0.005	0.005	0.10	0.05	0.015	0.02	0.75	0.0002	0.001	-	90	4.00
117	0.005	0.005	0.05	0.05	0.015	0.01	0.35	0.3	0.001	-	90	4.00
122	0.00013	0.0008	0.025	0.018	0.0033	0.0024	0.19	0.43	0.0006	-	80	3.00
126	0.00013	0.0008	0.03	0.015	0.0015	0.039	0.098	0.18	0.0006	-	70	3.00
129	0.00013	0.0008	0.03	0.011	0.0015	0.039	0.08	0.325	0.0006	-	60	3.00

Table B, continued

Time /days/	Cell number											
	1	2	3	4	5	6	7	8	9	10	11	12
130	0.00002	0.0004	0.028	0.011	0.0008	0.052	0.083	0.29	0.0003	0.00004	60	3x10
133	0.00002	0.0004	0.004	0.01	0.0008	0.036	0.085	0.26	0.0003	-	52	2.7x10
136	0.00002	0.0004	0.004	0.01	0.0008	0.025	0.025	0.17	0.00007	-	40	-
137	0	0.0004	0.004	0.007	0.0002	0.038	-	0.20	-	-	13	-
138	0	0.0004	0.004	0.007	0.0002	0.026	-	0.175	0.0004	-	7.5	
139	0.0002	0.0004	0.01	0.01	0.0002	0.04	0.01	0.22	0.0004	0.00001	6.1	
143	0.0002	0.0004	0.01	0.01	0.0002	0.02	-	0.18	0.0004	0.00001		
147	0.0002	0.0004	0.01	0.01	0.0002	0.02	-	0.001	0.0004	0.00001	6.1	
151	-	0.0004	0.002	0.004	-	0.015	-	0.13	0.0004	0	4.5	
155	-	0.0004	0.002	0.004	-	0.015	-	0.09	0.0003	-	6	
158	-	0	0.002	0.004	-	0.009	-	0.06	0.0003	-	6	
162	-	0	0.002	0.002	-	0.007	-	-	0.0004	-	6	
166	-	0.0005	0.006	0.002	-	0.007	-	-	0.0004	0.00002	4	
170	-	0.0005	0.006	0.002	0.00001	0.007	-	0.23	0.0004	-	4	
171	0	0.0005	0.006	0.002	0	0.007	0.003	0.25	0.0004	0	6	
176	-	0.00004	0.0036	0.0018	-	0.005	-	0.25	0.0004	0	4	
183	-	0.00004	0.0036	0.0018	0.000001	0.004	0.0005	0.2	0.0004	-	4	
185	0				-		-	-		-	5.3	
187	-	0.00004	0.002	0.0015	0.00001	0.0038	-	0.035	0.0004	-	4.2	
190	-	0.00004	0.002	0.0015	-	0.0038	0.0003	-	0.0004	-	5.8	
197	-	0.00004	0.002	0.0015	-	0.002	-	0.39	0.0001	-	4.2	
200	-	0.00004	0.001	0.0015	-	0.002	0.0002	0.3	0.0004	-	4.2	
219	-	0.00004	0.001	0.0005	-	0.002	0.0002	0.15	0.00019	-	2.7	
225	-	0.00004	0.001	0.0005	-	0.002	0	0	0.00019	-	2.1	
232	-	0.00004	0.001	0.0005	-	0.0005	-	-	0.00019	-	2.4	
234	0	0	0	0.0005	-	0.0005	-	0.05	0.00019	-	2.0	

Table B, continued

Time /days/	Cell number											
	1	2	3	4	5	6	7	8	9	10	11	12
247	-	0	0	0	0	0.00026	0.00002	0.018	0.00015	-	3.8	
253	-	0	0	0.0003	-	0.00018	0.00003	0.024	0.00018	-	2.1	
260	-	-	-	0.0002	-	0	0	0.04	0.00018	-	-	
274	-	-	-	0.015	-	0.005	0.0025	>0.05	0.015	-	-	
288	0	0.0001	0.0001	0.001	0.0005	0.0005	0.001	0.006	0.0005	0.0005	-	
325								0.005	0.005	0.005		
339	0	0	0	0.0002	0	-0.0002	0.0007	0	0	0		
396	0.00003	0.00003	0.00002	0	-0.00002	-0.00005	0	-0.0008	-0.00003	-0.00008		
457	0	0	0	0.0001	0	0	0.0025	>0.05	0.002	-		
	0.001	0.001	0	0.005	0	0.001	0	0.015	0.002	0.0001		

Table B, continued

Time /days/	Cell number											
	1		3		5		6		7		8	
	RH	I	RH	I	RH	I	RH	I	RH	I	RH	I
115					95.5	0.005	100	0.02	93.5	0.75	100	0.0002
117					94.0	0.005	100	0.01	90.0	0.35	100	0.30
122					90.0	0.0033	100	0.0024	84.0	0.19	100	0.43
123					89.0		100		83.0		100	
124					87.0		100		82.0		100	
125					86.0	0.0015	100	0.039	81.0	0.098	100	0.18
129					82.0	0.0015	99	0.039	79.0	0.08	100	0.325
130					81.0		99		78.0		100	
131	93	0.00002	93	0.028	81.0	0.0008			78.0	0.083		
133	91	0.00002	90	0.004	80.0	0.0008			77.0	0.083		
136	89	0.00002	87	0.004	77.0	0.0008			75.0	0.025		
137	88	0	86	0.004	77.0	0.0002			74.0	-		
140	87	0.0002	83	0.01	75.0	0.0002			71.0	0.01		
145	84	0.0002	75	0.01	69.0	0.0002			65.0	-		
151	77	-	70	0.002	67.0	-			63.0	-		
155	75	-	67	0.002	65.0	-			60.0	-		
177					60.0	0.000001	82	0.005	55.0	-	83	0.25
184					61.0	0	82	0.004	57.0	0.0005	83	0.2
190					59.0	-	81	0.004	55.0	0.003	83	0.035
196					59.0	-	79	0.002	53.0	-	82	0.39
219					52.0	-	77	0.002	45.0	0.0002	73	0.15
225					49.0	-	76	0.002	41.0	0	71	0
229					49.0	-	76	0.0005	41.0	-	70	-
247					48.0	0	74	0.0003	40.0	0.0002	67	0.018

TABLE C. Measured cell current /μA/cm^2/ and relative humidity /%/ in series 2.

Time /days/	Cell number															
	1	2	3	4	5	6	7	8	9	10		11		12		13	
	I	I	I	I	I	I	I	I	I	I	RH	I	RH	I	RH	I	RH
5*	0.002	0.03	0.008	0.008	0.02	0.02	0.02	0.008	0.01	0.02		0.02		0.02		0.04	
9	0.004	0.02	0.008	0.008	0.01	0.02	0.008	0.008	0.01	0.02		0.02		0.02		0.03	
14	0.004	0.002	0.02	0.004	0.02	0.01	0.006	0.004	0.01	0.01		0.01		0.01		0.01	
21	0.004	0.002	0.01	0.005	0.03	0.02	0.006	0.004	0.01	0.01		0.01		0.01		0.01	
26**	0.004	0.002	0.002	0.003	0.01	0.01	0.004	0.003	0.01	0.01	77	0.01	82	0.02	86	0.01	86
34	0.004	0.002	0.007	0.003	0.01	0.01	0.003	0.003	0.003	-0.03	92	0.01	84	0.02	87	0.01	84
41***	0.004	0.002	0.007	0.004	0.01	0.01	-0.02	0.006	0.006	0.01		0.01		0.08		0.02	
48	0.005	0.002	0.008	0.004	0.01	0.01	0.004	0.003	0.006	0.03		0.006		0.08		0.02	
55	0.004	0.002	-0.008	0.003	0.01	0.01	0.002	0.003	0.006	0.006		0		0.02		0.01	
63	0.004	0.002	0.002	0.003	0.01	0.01	0.004	0.006	0.006	0.44		-0.006		0.01		0.01	
65	0.004	0.002	0.003	0.003	0.01	0.01	0.003	0.002	0.004	0.36		0.006		0.01		0.01	
70	0.004	0.002	0.003	0.003	0.01	0.01	0.005	0.005	0.002	0.62		0.04		0		0.02	
79	0.002	0.002	0.002	0.003	0.01	0.005	0.002	0.002	0.001	0.30		0.02		0.006		0.01	
85	0.002	0.002	0.002	0.003	0.01	0.005	0.002	0.002	0.002	0.38		0.03		0.01		0.01	
98	0.006	0.003	0.01	0.006	0.02	0.02	0.003	0.005	0.005	1.5		0.12		0.05		0.05	
106	0.006	0.006	0.01	0.01	0.05	0.05	0.01	0.01	0.006	0.08		0.05		0.08		0.05	
109***	0.006	0.003	0.003	0.006	0.02	0.02	0.01	0.01	0.01	1.3	89	0.13	89	0.03	87	0.03	84
116*	0.006	0.003	0.006	0.006	0.02	0.02	0.02	0.01	0.01	0.55	89	0.1	91	0.02	88	0.02	84
119	0.006	0.003	0.006	0.006	0.02	0.02	0.003	0.01	0.01	0.25		0.1		0.02		0.02	
123	0.006	0.003	0.006	0.006	0.02	0.02	0.006	0.006	0.006	0.25	80	0.05	86	0.02	85	0.02	79
133	0.006	0.003	0.006	0.006	0.02	0.02	0.006	0.006	0.006	0.72	79	0.05	84	0.02	83	0.02	83
141	0.006	0.003	0.006	0.006	0.02	0.02	0.006	0.006	0.006	0.38	73	0.02	75	0.02	73	0.02	80
149**	0.005	0.001	0.09	0.003	0.01	0.01	0.003	0.003	0.003	0.03	72	0.02	76	0.02	78	0.02	
156	0.005	0.001	0.005	0.003	0.02	0.01	0.003	0.003	0.003	-0.001	88	0.02	86	0.02	76	0.02	79
162	0.005	0.001	0.008	0.003	0.02	0.01	0.003	0.003	0.003	0.51	92	0.02	90	0.02	82	0.02	82
165	0.005	0.001	0.04	0.006	0.02	0.01	0.003	0.003	0.003	0.18		0.02		0.02		0.02	
173	0.005	0.001	0.01	0.003	0.02	0.01	0.003	0.003	0.003	0.35		0.05		0.02		0.01	
179	0.005	0.001	0.05	0.003	0.02	0.01	0.003	0.003	0.003	0.86	91	0.05	93	0.02	88	0.02	

Table C, continued

Time /days/	Cell number															
	1	2	3	4	5	6	7	8	9	10		11		12		13	
	I	I	I	I	I	I	I	I	I	I	RH	I	RH	I	RH	I	RH
190	0.005	0.001	0.04	0.006	0.02	0.02	0.003	0.003	0.003	0.86		0.05		0.02		0.02	
198	0.005	0.002	0.04	0.006	0.02	0.01	0.003	0.003	0.003	1.1		0.1		0.01		0.02	
205	0.005	0.001	0.04	0.006	0.02	0.02	0.003	0.005	0.005	0.95	88	0.1		0.01	87	0.02	90
208	0.006	0.001	0.04	0.006	0.02	0.02	0.003	0.005	0.005	1.5	85	0.07	79	0.05	84	0.05	88
215	0.006	0.003	0.006	0.006	0.02	0.02	0.006	0.006	0.006	0.45	76	0.05	82	0.02	84	0.02	90
222	0.005	0.003	0.005	0.006	0.02	0.01	0.003	0.003	0.003	0.59	70	0.02	80	0.02	81	0.02	90
231	0.003	0.003	0.005	0.006	0.04	0.01	0.003	0.003	0.003	0.1	68	0.02	79	0.02	80	0.02	91
241	0.005	0.005	0.006	0.006	0.04	0.02	0.005	0.003	0.003	-0.05	67	0.02	77	0.02	81	0.02	90
249**	0.003	0.002	0.006	0.003	0.02	0.01	0.003	0.003	0.003	0.01		0.01		0.01		0.01	
251	0.006	0.004	0.006	0.003	0.04	0.02	0.006	0.006	0.006	1.9	76	0.05	74	0.05	81	0.05	86
259	0.006	0.004	0.006	0.003	0.04	0.02	0.006	0	0.006	0.88	84	0.05	84	0.05	82	0.05	86
265	0.003	0.004	0.006	0.003	0.04	0.02	0.006	0.006	0.006	2.4	86	0.05	86	0.02	83	0.02	87
269	0.006	0.004	0.006	0.003	0.04	0.02	0.006	0.006	0.006	3.0	87	0.05	88	0.05	84	0.05	88
277	0.006	0.004	0.006	0.003	0.04	0.02	0.006	0.006	0.006	2.3		0.05		0.05		0.05	
283	0.006	0.004	0.006	0.003	0.04	0.02	0.006	0.006	0.006	3.5	88	0.05	89	0.05	85	0.05	
290	0.006	0.004	0.006	0.003	0.04	0.02	0.006	0.006	0.006	4.2	91	0.05	92	0.05		0.05	
294	0.006	0.004	0.006	0.003	0.04	0.02	0.006	0.006	0.006	4.9	89	0.05	91	0.05		0.05	83
326	0.002	0.001	0.004	0.005	0.04	0.01	0.002	0.002	0.002	3.0	90	0.05	88	0.05	82	0.02	84
333	0.002	0.001	0.004	0.005	0.04	0.01	0.002	0.002	0.002	3.5		0.05		0.05		0.02	
346*	0.002	0.001	0.004	0.005	0.04	0.01	0.002	0.002	0.002	3.5	87	0.05	87	0.05		0.02	89
356	0.002	0.001	0.003	0.006	0.04	0.01	0.002	0.002	0.002	1.3	85	0.02	90	0.03	85	0.02	88
364	0.002	0.001	-0.001	0.006	0.04	0.01	0.002	0.002	0.002	1.0		0.02		0.03		0.02	
375	0.002	0.001	0.003	0.006	0.02	0.01	0.002	0.002	0.002	-0.05	79	0.01		0.01		0.01	87
393	0.002	0.001	0.003	0.002	0.03	0.01	0.002	0.002	0.002	0.14	76	0.01	76	0.01	75	0.01	85
400	0.003	0.001	0.004	0.002	0.02	0.01	0.002	0.002	0.002	0.15	76	0.01	77	0.01	76	0.01	85
417	0.003	0.002	0.004	0.004	0.02	0.01	0.002	0.002	0.002	0.31	73	0.01	72	0.01	72	0.01	81
427	0.003	0.002	0.004	0.004	0.01	0.01	0.002	0.002	0.002	0.22	75	0.01	72	0.01	72	0.01	80

Table C, continued

Time /days/	Cell number															
	1	2	3	4	5	6	7	8	9	10		11		12		13	
	I	I	I	I	I	I	I	I	I	I	RH	I	RH	I	RH	I	RH
474***	0.002	0.001	0.003	0.004	0.02	0.01	0.001	0.001	0.002	0.12	61	0.01	64	0.01	70	0.01	72
489	0.001	0.001	0.003	0.002	0.02	0.01	0.001	0.001	0.002	0.03	59	0.01	62	0.01	66	0.01	67
508	0.001	0.001	0.003	0.002	0.03	0.01	0.001	0.001	0.002	0.02		0.01		0.01		0.01	
523	0.001	0.001	0.002	0.001	0.04	0.01	0.001	0.001	0.002	0.01	61	0.01	64	0.01	79	0.01	79
532	0.001	0.001	0.002	0.001	0.04	0.01	0.001	0.001	0.002	0.01		0.01		0.01		0.01	
562	0.001	0.001	0.002	0.001	0.03	0.005	0.001	0.001	0.002	0.005	62	0.005	65	0.005	72	0.005	72
587	0.001	0	0.002	0.001	0.03	0.005	0.01	0.02	0.002	0.16	82	0.01	75	0.01	74	0.005	74
601**	0.001	0.001	0.002	0.001	0.03	0.01	0.01	0.02	0.002	0.54	88	0.01	81	0.01	80	0.005	75
621	0.001	-0.001	0.002	-0.001	0.04	0.01	0.01	0.04	0.002	1.0	91	0.01	86	0.01	83	-0.01	79
625	0.001	-0.001	0.001	-0.001	0.05	-0.01	0.01	0.04	-0.001	1.2	92	0.01	86	0.01	83	-0.01	78
660	0.001	-0.001	0.001	-0.001	0.05	-0.01	0.01	0.06	-0.001	>1.4	92	0.01	87	-0.01	88	-0.01	81
680	0.001	0	0	0	0.03	0	0.01	0.04	-0.001	>1.4		0.01		-0.01		0.01	
707	0.001	0	0.001	0	0.002	0	0.001	0.001	0	>1.4		0.001		-0.001		0.001	
729	0.002	0.001	0.001	0	0.03	0.01	0.01	0.01	0.001	>1.4		0.03		0.01		0.01	
769	0.002	0.001	0.001	0	0.03	0.01	0.01	0.01	0.001	>1.4		0.01		0.01		0.01	
810	0.002	0.001	0.001	0	0.03	0.01	0.01	0.01	0.001	>1.4	93	0.01	90	0.01	87	0.01	80
1430	0.05	0.001	0.001	0	-0.09	0.01	-0.008	-0.01	0.001	-0.16		0.02		-0.02		-0.01	
1434	0.05	0.001	0.001	0	-0.1	0.01	-0.001	-0.005	0.001	-0.3		0.05		0		0.01	
1436*	0.06	0.001	0.001	0	-0.1	0.01	-0.01	0.41	0.01	-0.3		0.08		+1.3		0.001	
1438	0.06	0.001	0.001	0	-0.02	0.01	-0.01	-0.01	0.001	-0.3		0.05		0.01		0.001	

*Cell 7-13 drying
** Cell 7-13 wetting in 3% NaCl
***RH-cells calibrated

TABLE D. Measured cell cements in series 3. Carbonated concrete, w/c∿ 0.8, concrete cover 4 mm. Cell type C.

Anode area chanel	Cathode area chanel	Anode area / Cathode area	Cell cement /μA/m² anodic area/ Potential differences, time							REMARKS
			50 mV 6 days	100 mV 7 days	200 mV 14 days	200 mV 20 days	200 mV 20 days dried 30 min	200 mV 21 days dried 1 day	200 mV 24 days rewetted 3 days	
0	1	0,50	0,070	0,095	0,055		3,5	0,10	3,2	Increase of cathodic area
0	1+2	0,25	0,080	0,095	0,070		4,0	0,13	5,0	
0	1→3	0,13	0,084	0,098	0,075		3,7	0,13	5,6	
0	1→4	0,083	0,087	0,098	0,072		3,5	0,12	5,7	
0	1→5	0,056	0,093	0,100	0,075		3,5	0,12	6,0	"
0	1→6	0,042	0,094	0,100	0,070		3,4	0,12	6,2	
0	1→7	0,033	0,098	0,100	0,070		3,3	0,35	6,3	
0	1→8	0,028	0,105	0,103	0,072		3,2	0,25	7,2	
0	1→9	0,024	0,110	0,107	0,078		3,9	0,24	10,5	
0	1→10	0,021	0,120	0,110	0,075		3,9	0,24	11,0	
0	1→11	0,018	0,125	0,116	0,082		3,8	0,24	11,5	
0	1→12	0,016	0,128	0,116	0,080		3,7	0,24	12,8	
0	1→13	0,014	0,128	0,116	0,080		3,7	0,24	13,6	
0	1→14	0,013	0,128	0,116	0,080		3,6	0,24	14,6	
0	1→15	0,011	0,128	0,116	0,060	7,0	3,5	0,13	16,5	
0	1→14	0,013	0,128	0,116		6,0				Decrease of cathodic area
0	1→13					5,8				
0	1→12					5,8				

Table D, continued

Anode area chanel	Cathode area chanel	Anode area / Cathode area	Cell cement /μA/m² anodic area/						
			Potential differences, time						
			50 mV 6 days	100 mV 7 days	200 mV 14 days	200 mV 20 days	200 mV 20 days dried 30 min	200 mV 21 days dried 1 day	200 mV 24 days rewetted 3 days
0	1→11	0.018	0.128	0.116		5.8			
0	1→10	0.021	0.122	0.110		5.3			
0	1→9	0.024	0.113	0.105		5.1			
0	1→8	0.028	0.101	0.105		3.3			
0	1→7	0.033	0.100	0.103		3.2			
0	1→6	0.042	0.098	0.102		3.0			
0	1→5	0.056	0.093	0.100		2.9			
0	1→4	0.083	0.095	0.100		2.7			
0	1→3	0.137	0.096	0.100		2.6			
0	1+2	0.25	0.094	0.100		2.5			
0	1	0.5	0.087	0.098		1.7			

Table D, continued

Anodic area chanel	Cathodic area chanel	Anodic area / Cathodic area	Cell cement /μA/m² anodic area/ Potential differences, time							Distance between anode and cathode
			50 mV 6 days	100 mV 7 days	200 mV 18 days	200 mV 20 days	200 mV 20 days 15 min drying	200 mV 21 days	200 mV 24 days rewet 3 days	
0	1	0,5	0,087		1,8	1,3	4,0	0,14	3,2	0,1
0	2	0,5	0,058		1,9	1,7	4,3	0,08	3,7	0,7
0	3	0,25	0,046		0,2	0,3	0,20	0,005	1,5	1,3
0	4	0,25	0,043		1,9	0,6	0,10	0	0,2	2,5
0	5	0,167	0,044		1,3	0,7	0,20	0	0,8	3,7
0	6	0,167	0,049		1,4	0,4	0,10	0	0,5	5,5
0	7	0,167	0,056		0,2	0,9	0,20	0,003	0,4	7,3
0	8	0,167	0,070		0,7	0,4	0,40	0,015	2,0	9,1
0	9	0,167	0,091		5,1	4,7	7,0	0,20	7,5	10,8
0	10	0,167	0,110		0,2	0,6	0,10	0	2,5	12,6
0	11	0,125	0,135		0,9	0,7	1,0	0,006	2,4	15,0
0	12	0,125	0,135		0,8	0,8	0,70	0,009	2,0	17,4
0	13	0,125	0,135		1,3	0,9	0,90	0	4,4	19,8
0	14	0,125	0,120		2,5	0,9	0,90	0	6,2	22,2
0	15	0,125	0,135	0,116	7,0	5,8	3,0	0	12,2	24,6
0	14	0,125	0,125	0,095						22,2
0	13	0,125	0,135	0,105						19,8
0	12	0,125	0,135	0,115						17,4
0	11	0,125	0,130	0,112						15,0
0	10	0,167	0,115	0,080						12,6

Table D, continued

Anodic area chanel	Cathodic area chanel	Anodic area / Cathodic area	Cell cement /μA/m² anodic area/ Potential differences, time							Distance between anode and cathode
			50 mV 6 days	100 mV 7 days	200 mV 18 days	200 mV 20 days	200 mV 20 days 15 min drying	200 mV 21 days	200 mV 24 days rewet 3 days	
0	9	0,167	0,088	0,060						10,8
0	8	0,167	0,074	0,045						9,1
0	7	0,167	0,060	0,035						7,3
0	6	0,167	0,053	0,030						5,5
0	5	0,167	0,047	0,025						3,7
0	4	0,25	0,045	0,025						2,5
0	3	0,25	0,047	0,025						1,3
0	2	0,50	0,060	0,040						0,7
0	1	0,50	0,110	0,105						0,1

Table D, continued

Anode area chanel	Cathode area chanel	Anode area / Cathode area	Distance between electrodes /mm/	Time 18 days	Time 24 days	RH %
0	15	0.130	24.6	7.0	12.0	100
0	15+14	0.063	22.2	7.2	12.0	"
0	15→13	0.042	19.8	7.3	13.9	"
0	15→12	0.031	17.4	7.3	14.6	"
0	15→11	0.025	15.0	7.3	14.8	"
0	15→10	0.022	12.6	7.3	15.8	"
0	15→9	0.019	10.8	8.2	17.8	"
0	15→8	0.017	9.1	8.4	18.6	"
0	15→7	0.016	7.3	8.5	18.6	"
0	15→6	0.014	5.5	8.5	18.6	"
0	15→5	0.013	3.7	8.4	19.0	"
0	15→4	0.013	2.5	8.4	19.0	"
0	15→3	0.012	1.3	8.3	19.5	"
0	15→2	0.011	0.7	9.0	20.2	"
0	15→1	0.011	0.1	9.0	21.5	"

Anode area chanel	Cathode area chanel	Anode area Cathode area	Time 32 days	Time 42 days	Time 60 days	RH %
0+1	2→15	0.035	2.7	2.6	1.3	100
0+1	2→14	0.038	2.3	2.4	1.3	"
0+1	2→13	0.043	2.0	2.2	1.3	"
0+1	2→12	0.048	1.8	1.9	1.2	"
0+1	2→11	0.056	1.7	1.7	1.1	"
0+1	2→10	0.065	1.5	1.5	1.1	"
0+1	2→9	0.075	1.3	1.4	1.0	"
0+1	2→8	0.088	0.9	0.9	0.77	"
0+1	2→7	0.11	0.7	0.8	0.63	"
0+1	2→6	0.14	0.7	0.7	0.53	"
0+1	2→5	0.19	0.6	0.6	0.47	"
0+1	2→4	0.30	0.6	0.5	0.37	"
0+1	2+3	0.50	0.5	0.4	0.30	"
0+1	2	1.50	0.4	0.3	0.23	"
0+1	2→15	0.035		3.2		"
0	2→15	0.012		6.4		"

Table D, continued

Anode area chanel	Cathode area chanel	Anode area / Cathode area	Cell cement /μA/m² anodic area/		Distance between anode and cathode
			Pot difference= 200 mV 42 days	Pot difference= 100 mV 60 days	
0+1	2	1,5	0,4	0,22	0,1
0+1	3	0,75	0,2	0,13	0,6
0+1	4	0,75	0,1	0,10	1,8
0+1	5	0,50	0,1	0,17	3,6
0+1	6	0,50	0,1	0,17	5,2
0+1	7	0,50	0,3	0,20	7,2
0+1	8	0,50	0,3	0,40	9,0
0+1	9	0,50	1,2	0,77	10,8
0+1	10	0,50	0,4	0,33	12,6
0+1	11	0,38	0,4	0,50	15,0
0+1	12	0,38	1,7	0,57	17,4
0+1	13	0,38	1,3	0,70	19,8
0+1	14	0,38	1,7	0,90	22,2
0+1	15	0,38	2,7	1,07	24,6

Anodic area chanel	Cathodic area chanel	Anodic area / Cathodic area	Cell cement /μA/cm²/anodic area
			Pot difference= 200 mV 42 days
0+1	2 →15	0,035	1,6
0+1	3 →15	0,036	1,6
0+1	4 →15	0,038	1,6
0+1	5 →15	0,039	1,6
0+1	6 →15	0,043	1,6
0+1	7 →15	0,047	1,6
0+1	8 →15	0,052	1,5
0+1	9 →15	0,058	1,5
0+1	10→15	0,065	1,4
0+1	11→15	0,075	1,4
0+1	12→15	0,094	1,3
0+1	13→15	0,125	1,3
0+1	14→15	0,188	1,2

Table D, continued

Exp. time /days/	Potential difference /mV/	Andoic area / Cathodic area	Cell current /μA/cm² anodic area/	REMARKS
1	50	0.50	0.01	
5	50	0.50	0.05	
7	100	0.50	0.1	
8	100	0.50	0.01	
9	100	0.50	1.0	Cell current instable (1.0-0.1)
10	100	0.50	0.1	" (0.1-0.5)
11	100	0.50	0.3	" (0.1-1.0)
12	100	0.50	0.1	
13	100	0.50	0.1	Cell current periodically negative
15	200	0.011	0.00	
18	200	0.011	20	"
20	200	0.011	8	Drying procedure
20	200	0.011	1	
21	200	0.011	0.1	In water
21	200	0.011	20	
25	200	0.011	20	
32	200	0.035	10	
42	200	0.035	8	
60	200	0.035	5	

Results from measurements in series 3, w/c 0.8, concrete cover 4 mm, carbonated concrete, cell type A.

Time	Box		Sample		
	Temp C°	RH %	RH %	Cell current A/cm²	
780905	20	70	61	0.0011	
06, 0800	20	72	64	0.0007	
06, 1500	20	84	65	0.0010	
07, 0800	20	90	70	0.0013	
07, 1200	20	98	72	0.0015	
07, 1500	20	98	72.5	0.0015	
08, 0800	20	98	81	0.0021	
08, 1000	20	98	83	0.0030	
08, 1200	20	98	83.5	0.0027	
08, 1600	20	98	85	0.013	
11, 0800	20	98	88.5	0.034	
11, 0900	20	98	89	0.033	
11, 0900	20	spray	87	0.066	RH and cell current changed immediately
11, 1200	20	∿100	91	0.081	
11, 1300	20	∿100	91.5	0.087	
11, 1300	20	spray	91.5	0.10	Cell current changed immediately
11, 1500	20	∿100	92.5	0.17	
11, 1500	20	spray	92.5	0.46	"
11, 1600	20	∿100	92.5	0.20	
11, 1800	20	∿100	92.5	0.25	
12, 0900	20	∿100	93	0.20	
12 1300	20	immersed	93	0.50	"
12, 1400	20	"	94	1.50	
12, 1500	20	"	95	1.30	
12, 1600	20	"	96	1.20	
780913	20	"	97	0.60	
14	20	"	98	0.30	
15	20	"	>98	0.20	
19	20	"	>98	0.11	
25	20	"	>98	0.08	
780926, 0800	+20	"	~100	0.08	
0900	+1	"	"100	0.02	
27, 0800	+1	"	"100	0.01	
0900	-10	"	"100	0.005	
780928, 0800	-10	"	"100	0.004	
1000	-20	"	"100	0.003	
1200	-20	"	"100	0.002	
780929, 0800	-25	"	"100	0.001	
1200	+3	"	"100	0.01	
1400	+3	"	"100	-0.003	
781001, 1000	+3	"	"100	0.005	
781002,	+10	"	"100	0.20	"
781003,	+10	"	"100	0.05	Unstable current
781005,	+22	"	"100	0.10	0.01-0.08

TABLE E. Measured cell current and relative humudity in series 4. /μA/cm^2/.

Time /days/	Cell number																REMARKS
	1		2		3		4		5		6		7		8		
	I	RH	I	RH	I	RH	I	RH	I	RH	I	RH	I	RH	I	RH	
0	-		+1.5		+0.02		0.225										Drying
1	-		+1.5		0		0.04		0		0		0		0		Out of test
2	-		+1.5		0.01		0.03		0		0		0		-0.003		
3	-		0.5														
4	-		2.5														
6	-		4.4		0.004		-0.001	100	+0.001		+0.001		0		-0.001		
7	-		max		0.004		+0.001		+0.001		0		-0.001		+0.001		
10	-		"		0.004		+0.008		0		0		0		+0.003		
13	-		2.0		0.004		+0.008		0		0		0		+0.003		Wetting in water
	-				+0.005		+0.12		0		0		0		-0.05		
16	-		+max		+0.005		+max		0		0		-0.001		-0.02		
17	-		"		+0.005		"		0		0		-0.001		-0.001		
20	-		"		+0.001		"		+0.001		+0.001		-0.001		+0.001		Wetting in 3%NaCl
22	-	76	"	85	+0.003		"		0	93	0	86	+0.001	98	+0.01	93	
27	-		"		+0.003	94	"	96	0	93	0	86	+0.001	99	+0.001	94	
34	-		max		0.08	94	max	96	0.001		0.001		0.001		0		
36	-		0.95		-		"		-		-		-		-		
42	-		max		0.01		"		0	90	0	84	0		0		
49	-		"		0.01	94	"	96	0	90	0	84	0	93	0	93	
45	-		1.1		0.01	94	"	96	0	92	0	83	0	88	0	84	
49	-	92	1.1	85	0.01		"		0.001	91	0.001	84	0.002	86	0.001	87	
55	-	86	1.3	91	0.01		"		0.001	92	0.001	86	0.003	86	-0.005	93	
67	-	87	1.1	93	0.05	93	"	97	0.001	93	0.001	86	0.003	86	+0.006	94	Drying
73	-		max		0.004		"		0.002		0.003		0.006		0.001		
75	-		0.88		0.004	91	4.2	91	0.002	90	0.003	84	0.003	81	0.001	91	
80	-	79	1.7	82	0.003	93	1.4	84	0.001	88	0.002	85	0.003	79	0.003	87	
87	-		1.9		0.003	92	1.3	82	0.001	88	0.002	84	0.003	77	0.003	86	
96	-		1.9		0.003		max		0.001		0.001		0.006		-0.001		Wetting in 3%NaCl

Table E, continued

Time /days/	Cell number															
	1		2		3		4		5		6		7		8	
	I	RH	I	RH	I	RH	I	RH	I	RH	I	RH	I	RH	I	RH
117	-				0.03		max		0.001		0.001		0.006		-0.001	
129	-		1.0		0.02		"		0.001		0.001		0.01		+0.01	
137	-	95	1.4	93	0.03	98	"	95	0.001	94	0.001	85	0.01	90	+0.01	95
138	-		1.4		0.02		"		0.001		0.001		0.01		-0.01	
146	-	96	1.2	93	0.02	97	"	95	0.001	95	0.001	85	0.01	91	-0.01	95
166	-		1.1		0.02	99	"	97	0.001	96	0.001	87	0.01	92	-0.01	96
180	-		1.1		0.002		"		0.001		0.001		0.01		0.005	
201	-		1.0		0.002		"		0.001		0.001		0.09		0.44	

TABLE A. Results, weight loss measurements, chapter 5.3.5. Steel not covered with mortar.

Sample number	w/c	Exp time days	RH %	Surface area cm^2	Corroded area %	Weight mg/cm^2	Mean corrosion µm/year		Remarks
							Total area	Corroded area	
83		475	60	35	75	1,8	1,8	2,4	
85		"	70	"	45	3,6	3,6	7,9	
87		"	80	"	95	3,9	3,8	4,1	
812		"	85	"	15	4,1	4,0	27	A small area corroded
813		"	90	"	50	2,1	2,1	4,1	
817		"	95	"	30	1,3	1,3	4,3	"
820		"	100	"	100	54,2	54	54	
821		"	100	"	100	56,2	55	55	
81		1003	60	35	30	1,7	0,5	1,7	
86		"	70	35	50	8,8	2,5	5,0	
89		"	80	35	100	4,5	1,3	1,3	
810		"	85	35	70	20,0	5,7	8,1	
815		"	90	35	40	53,0	15	38	

TABLE B. Results, weight loss measurements, chapter 5.3.5. Portland cement, CO_2 initiation.

Sample No	W/c	Exp time /days/	RH %	Surface area cm^2	Corr. area %	Weight loss mg/m^2	Mean corrosion µm/year		Remarks
							Total area	Corroded area	
068	0.70	59	60	51	2	0.0	-	-	
069	0.70	137	60	51	0	0.0	-	-	
0611	0.70	245	60	51	0	0.0	-	-	
0612	0.70	339	60	51	0	0.0	-	-	
077	0.70	59	70	51	5	0.0	-	-	
078	0.70	137	70	51	0	0.0	-	-	
0710	0.70	245	70	51	< 1	0.0	-	-	
0711	0.70	339	70	51	0	0.0	-	-	
0712	0.70	876	70	51	< 1	0.7	0.4	-	
087	0.70	59	80	51	2	0.0	-	-	
088	0.70	137	80	51	1	0.0	-	-	
0810	0.70	245	80	51	1	0.0	-	-	
0811	0.70	339	80	51	0	0.0	-	-	
0812	0.70	876	80	51	4	0.2	0.1	2.5	
0857	0.70	59	85	51	2	0.5	5.0	350	
0858	0.70	137	85	51	0	0.0	-	-	
08510	0.70	245	85	51	8	0.0	-	-	
08511	0.70	339	85	51	0	0.0	-	-	
08512	0.70	876	85	51	61	1.3	0.7	1.2	

Table B, continued

Sample No	W/c	Exp time /days/	RH %	Surface area cm^2	Corr. area %	Weight loss mg/m^2	Mean corrosion μm/year		Remarks
							Total area	Corroded area	
097	0.40	59	90	51	22	0.5	4.0	18	
0910	0.40	137	90	51	14	0.4	1.4	10	
098	0.40	245	90	51	57	0.7	1.3	2.4	
099	0.40	339	90	51	98	2.6	3.0	3.1	
0912	0.40	876	90	51	100	5.2	2.8	2.8	
0957	0.40	59	95	51	9	0.1	0.8	9.3	
0958	0.40	137	95	51	53	0.7	2.4	4.5	
09510	0.40	245	95	51	60	1.6	3.1	5.1	
09511	0.40	339	95	51	38	1.4	1.7	4.5	
09512	0.40	876	95	51	100	6.1	3.3	3.3	
017	0.40	59	100	51	5	0.2	1.2	23	
018	0.40	137	100	51	15	0.1	0.4	2.3	
0110	0.40	245	100	51	90	1.2	2.3	5.0	
0111	0.40	339	100	51	90	2.2	2.9	3.3	
0112	0.40	869	100	51	10	1.7	0.9	9.0-6.0	

Table B, continued

Sample No	W/c	Exp time /days/	RH %	Surface area cm^2	Corr. area %	Weight loss mg/m^2	Mean corrosion µm/year		Remarks
							Total area	Corroded area	
062	0.40	59	60	51	8	0.1	0.8	10.0	
063	0.40	137	60	51	100	0.4	1.4	1.4	
065	0.40	245	60	51	1	0.0	-	-	
066	0.40	339	60	51	0	0.0	-	-	
071	0.40	59	70	51	21	0.4	3.2	15.0	
072	0.40	137	70	51	4	0.0	-	-	
074	0.40	245	70	51	0	0.0	-	-	
075	0.40	339	70	51	100	0.2	0.2	0.2	
076	0.40	876	70	51	90	4.6	2.5	2.8	Sample in contact with salt sol.
081	0.40	59	80	51	6	0.5	4.0	66.0	
082	0.40	137	80	51	9	0.0	-	-	
084	0.40	245	80	51	0	0.0	-	-	
086	0.40	339	80	51	0	0.0	-	-	
085	0.40	876	80	51	10	0.8	0.4	4.0	
0851	0.40	59	85	51	2	0.4	3.2	210	
0852	0.40	137	85	51	1	0.0	-	-	
0854	0.40	245	85	51	~ 0	0.2	0.4	0.4	All surface uncoloured oxide
0855	0.40	339	85	51	0	0.0	-	-	
0856	0.40	876	85	51	~ 0	0.9	0.5	0.5	

Table B, continued

Sample No	W/c	Exp time /days/	RH %	Surface area cm^2	Corr. area %	Weight loss mg/m^2	Mean corrosion µm/year		Remarks
							Total area	Corroded area	
091	0.40	59	90	51	3	0.1	0.8	26.0	
093	0.40	137	90	51	1	0.0	-	-	
092	0.40	245	90	51	11	0.0	-	-	
095	0.40	339	90	51	100	1.4	1.8	1.8	
096	0.40	876	90	51	90	1.2	0.6	0.7	
0951	0.40	59	95	51	2	0.1	0.8	40.0	
0952	0.40	137	95	51	2	0.1	0.2	8.5	
0954	0.40	245	95	51	6	0.1	0.2	3.2	
0955	0.40	339	95	51	0	0.0	-	-	
0956	0.40	876	95	51	5	0.6	0.3	6.0	
012	0.40	59	100	51	4	0.1	1.6	10.0	
013	0.40	137	100	51	9	1.4	4.8	51.0	
011	0.40	245	100	51	4	0.9	1.7	43.0	
015	0.40	339	100	51	0	0.0	-	-	
016	0.40	876	100	51	2	0.5	0.3	15.0	

TABLE C. Results, weight loss measurements, chapter 5.3.5.
Slag cement (70% slag + 30% Slite Portland cement). CO_2-initiation.

Sample No	W/c	Exp time /days/	RH %	Surface area cm^2	Corr. area %	Weight loss mg/m^2	Mean corrosion µm/year		Remarks
							Total area	Corroded area	
162	0.40	59	60	46	22	1.4	11	50	
163	0.40	137	60	46	22	1.3	4.4	18	
165	0.40	245	60	46	10	0.4	0.8	7.6	
166	0.40	339	60	46	26	1.0	1.4	5.3	
171	0.40	59	70	46	22	0.8	6.4	29	
172	0.40	137	70	46	26	2.3	6.3	25	
174	0.40	245	70	46	48	0.8	1.5	3.2	
175	0.40	339	70	46	83	1.3	2.1	2.6	
176	0.40	876	70	46	100	35.9	19	19	Test solution
181	0.40	59	80	46	34	2.4	19	56	
182	0.40	137	80	46	30	2.6	8.0	26	
184	0.40	245	80	46	77	2.6	5.0	6.5	
185	0.40	339	80	46	100	3.2	4.4	4.4	
186	0.40	876	80	46	77	2.9	1.6	2.1	
1851	0.40	59	85	46	85	3.2	25	30	
1852	0.40	137	85	46	75	5.7	20	25	
1854	0.40	245	85	46	92	9.5	18	20	
1855	0.40	339	85	46	97	8.3	12	12	
1856	0.40	876	85	46	70	15.8	8.4	12	

Table C, continued

Sample No	W/c	Exp time /days/	RH %	Surface area cm^2	Corr. area %	Weight loss mg/m^2	Mean corrosion μm/year		Remarks
							Total area	Corroded area	
191	0.40	59	90	46	90	4.9	39	43	
196	0.40	137	90	46	100	3.9	13	13	
192	0.40	245	90	46	100	4.9	9.4	9.4	
193	0.40	339	90	46	90	7.3	10	11	
195	0.40	876	90	46	98	9.9	5.3	5.4	
1951	0.40	59	95	46	78	3.1	25	32	
1952	0.40	137	95	46	98	4.9	17	17	
1954	0.40	245	95	46	100	12.4	24	24	
1955	0.40	339	95	46	99	12.9	18	18	
1956	0.40	876	95	46	100	50.7	27	27	
111	0.40	59	100	46	98	1.8	13	13	
112	0.40	137	100	46	100	1.2	4.0	4.0	
114	0.40	245	100	46	100	2.1	4.0	4.0	
115	0.40	339	100	46	98	2.9	4.0	4.1	
116	0.40	876	100	46	100	2.7	1.4	1.4	

Table C, continued

Sample number	w/c	CO_2	5% $CaCl_2$	Cement type	Exp time days	RH %	Surf. area cm^2	Corr. area %	Weight mg/cm^2	Mean corrosion µm/year		Remarks
										Total area	Corroded area	
168	0,7	x		B	59	60	46	10	1,1	8,7	8,7	
169	"	x		B	137	"	"	100	0,5	1,7	1,7	
1611	"	x		B	245	"	"	58	0,9	1,7	3,0	
1612	"	x		B	339	"	"	19	0,8	1,1	5,7	
177	0,7	x		B	59	70	46	10	0,7	5,6	56	
178	"	x		B	137	"	"	15	0,0	-	-	
1710	"	x		B	245	"	"	20	0,5	1,0	4,8	
1711	"	x		B	339	"	"	21	0,7	1,0	4,5	
1712	"	x		B	876	"	"	100	45,3	24,	24	Sample in contact with test solution
187	0,7	x		B	59	80	46	50	1,8	15	29	
188	"	x		B	137	"	"	92	2,0	6,9	7,4	
1810	"	x		B	245	"	"	50	2,2	4,2	8,4	
1811	"	x		B	339	"	"	75	2,8	3,9	5,2	
1812	"	x		B	876	"	"	70	3,3	1,8	2,6	
1857	0,7	x		B	59	85	46	78	3,0	24	31	
1858	"	x		B	137	"	"	92	4,8	16	18	
18510	"	x		B	245	"	"	95	4,5	8,6	9,1	
18511	"	x		B	339	"	"	91	5,6	7,7	8,5	
18512	"	x		B	876	"	"	100	6,8	3,6	3,6	

Table C, continued

Sample No	W/c	CO_2	5%xp $CaCl_2$	Cement type	Exp. time days	RH %	Surf. area cm^2	Corr. area %	Weight loss mg/m^2	0-value	Mean corr. µm/year		REMARKS
											Total area	Corroded area	
197	0.70	x		B	59	90	46	95	3.6		29	30	
1912	0.70	x		B	137	90	46	100	5.8		20	20	
198	0.70	x		B	245	90	46	100	6.8		13	13	
199	0.70	x		B	339	90	46	100	6.6		9.1	9.1	
1910	0.70	x		B	876	90	46	100	8.6		4.6	8.6	
1957	0.70	x		B	59	95	46	100	3.5		28	28	
1958	0.70	x		B	137	95	46	100	4.9		17	17	
19510	0.70	x		B	245	95	46	99	7.8		15	15	
19511	0.70	x		B	339	95	46	100	10.5		15	15	
19512	0.70	x		B	876	95	46	100	24.3		13	13	
117	0.70	x		B	59	100	46	95	2.2		17	18	
118	0.70	x		B	137	100	46	100	2.5		8.5	8.5	
1111	0.70	x		B	245	100	46	55	3.2		6.1	11.1	
1112	0.70	x		B	339	100	46	100	3.6		5.0	5.0	

TABLE D. Results, weight loss measurements, chapter 5.3.5.
Slite Portland cement, initiation by 5% $CaCl_2$/cement.

Sample number	w/c	Exp time days	RH %	Surface area cm^2	Corroded area %	Weight mg/cm^2	Mean corrosion µm/year		Remarks
							Total area	Corroded area	
261	0,4	73	60	43	36	4,7	30	84	
262	"	153	"	"	91	7,1	22	24	
263	"	231	"	"	85	6,4	13	15	
264	"	339	"	"	58	6,8	9,4	16	
265	"	433	"	"	61	7,1	7,7	13	
266	"	970	"	"	100	14,9	7,2	7,2	
271	"	73	70	43	27	5,7	37	135	
272	"	153	"	"	44	10,8	33	75	
273	"	231	"	"	48	15,0	30	63	
274	"	339	"	"	22	13,6	19	85	
275	"	433	"	"	62	24,1	26	43	
276	"	970	"	"	51	21,8	11	22	
281	"	73	80	43	13	1,7	11	85	
282	"	153	"	"	25	7,9	24	97	
283	"	231	"	"	35	8,2	17	47	
284	"	339	"	"	53	18,0	25	47	
285	"	433	"	"	19	7,8	8,4	44	
286	"	970	"	"	59	22,9	11	19	
2851	"	73	85	43	27	5,3	34	130	
2852	"	147	"	"	28	8,6	27	98	
2853	"	231	"	"	35	11,4	23	66	
2854	"	339	"	"	60	23,6	33	54	
2855	"	433	"	"	40	15,0	16	41	
2856	"	970	"	"	57	37,3	18	32	

Table D, continued

Sample number	w/c	Exp time days	RH %	Surface area cm^2	Corroded area %	Weight mg/cm^2	Mean corrosion µm/year		Remarks
							Total area	Corroded area	
291	0,4	73	90	43	15	3,9	25	160	
292	"	153	"	"	15	9,6	29	200	
293	"	231	"	"	16	6,2	13	77	
294	"	339	"	"	9	12,2	17	190	
295	"	433	"	"	30	16,8	18	61	
296	"	970	"	"	40	26,6	13	33	
2951	0,4	73	95	43	11	3,6	23	210	
2952	"	153	"	"	15	9,6	29	200	
2953	"	231	"	"	6	3,6	7,3	115	
2954	"	339	"	"	3	2,0	2,7	97	
2955	"	433	"	"	35	29	31	88	
2956	"	970	"	"	16	24,7	12	75	
211	0,4	73	100	43	8	0,4	2,8	36	Incipient corrosion
212	"	153	"	"	7	1,4	4,3	61	
213	"	231	"	"	8	0,8	1,6	20	
214	"	339	"	"	7	2,7	3,7	53	
215	"	433	"	"	3	0,2	0,2	7,1	
216		970	"	"	-	0,0	-	-	

Table D, continued

Sample number	w/c	Exp time days	RH %	Surface area cm^2	Corroded area %	Weight mg/cm^2	Mean corrosion µm/year		Remarks
							Total area	Corroded area	
267	0,7	65	60	43	100	9,4	68	68	
268	"	111	"	"	100	11,3	48	48	
269	"	191	"	"	99	9,5	23	24	
2610	"	269	"	"	100	11,3	20	20	
2611	"	377	"	"	100	12,6	16	16	
277	0,7	65	70	43	95	11,3	81	85	
278	"	111	"	"	90	12,1	51	57	
279	"	191	"	"	90	12,6	31	34	
2710	"	269	"	"	99	16,7	29	29	
2711	"	377	"	"	93	21,8	27	29	
2712	"	471	"	"	94	23,5	23	25	
287	0,7	65	80	43	95	10,9	77	81	
288	"	111	"	"	82	13,7	58	70	
289	"	191	"	"	86	14,9	37	43	
2810	"	269	"	"	86	12,4	22	25	
2811	"	377	"	"	80	19,5	24	30	
2812	"	471			62	14,2	14	23	
2857	0,7	65	85	43	93	14,5	104	112	
2858	"	111	"	"	100	17,5	74	74	
2859	"	191	"	"	96	22,5	55	57	
28510	"	269	"	"	99	27,0	47	47	
28511	"	377	"	"	95	29,5	37	39	
28512	"	471	"	"	90	34,4	34	38	

Table D, continued

Sample number	w/c	Exp time days	RH %	Surface area cm^2	Corroded area %	Weight mg/cm^2	Mean corrosion µm/year		Remarks
							Total area	Corroded area	
297	0,7	65	90	43	16	8,7	63	390	
298	"	111	"	"	28	10,2	43	154	
299	"	191	"	"	31	7,7	19	61	
2910	"	269	"	"	35	10,1	18	50	
2911	"	377	"	"	44	17,0	21	48	
2912	"	471	"	"	42	19,2	18	43	
2957	0,7	65	95	43	28	9,2	66	240	
2958	"	111	"	"	28	8,9	38	140	
2959	"	191	"	"	36	11,2	27	77	
29510	"	269	"	"	41	14,8	26	62	
29511	"	377	"	"	45	13,5	17	37	
29512	"	471	"	"	62	34,4	34	55	
217	0,7	65	100	43	5	3,2	23	460	
218	"	91	"	"	8	1,6	6,7	81	
219	"	171	"	"	5	0,7	1,9	38	
2110	"	249	"	"	6	1,1	2,2	39	
2111	"	357	"	"	7	1,5	2,0	28	
2112	"	451	"	"	7	1,2	1,3	19	

Table D, continued

Sample number	w/c	Exp time days	RH %	Surface area cm^2	Corroded area %	Weight mg/cm^2	Mean corrosion µm/year		Remarks
							Total area	Corroded area	
461	0,40	140	60	42	49	4,0	13	27	
462	"	218	"	"	100	3,6	7,7	8	
471	0,40	140	70	42	21	9,0	30	140	
472	"	218	"	"	20	9,0	19	95	
481	0,40	140	80	42	23	7,2	24	100	
482	"	218	"	"	33	15,0	32	98	
4851	0,40	140	85	42	41	13,0	44	110	
4852	"	218	"	"	95	14,0	30	32	

Table D, continued

Sample number	w/c	Exp time days	RH %	Surface area cm^2	Corroded area %	Weight mg/cm^2	Mean corrsion µm/year		Remarks
							Total area	Corroded area	
491	0,40	140	90	42	14	10,0	33	230	
492	"	218	"	"	11	9,0	19	215	
4951	0,40	140	95	42	9	5,0	17	180	
4956	"	218	"	"	19	10,3	22	120	
411	0,40	140	100	42	4	0,9	3,0	75	
412	"	218	"	"	1	0,4	0,8	86	

Table D, continued

Sample number	w/c	Exp time days	RH %	Surface area cm^2	Corroded area %	Weight mg/cm^2	Mean corrosion µm/year		Remarks
							Total area	Corroded area	
467	0,70	140	60	42	96	11,1	37	39	
468	"	218	"	"	100	11,7	25	25	
477	0,70	140	70	42	82	12,3	41	50	
478	"	218	"	"	99	17,0	37	37	
487	0,70	140	80	42	69	16,7	56	81	
488	"	218	"	"	74	21,5	46	62	
4857	0,70	140	85	42	80	19,4	65	81	
4858	"	218	"	"	95	22,5	48	51	

Table D, continued

Sample number	w/c	Exp time days	RH %	Surface area cm^2	Corroded area %	Weight mg/cm^2	Mean corrsion µm/year		Remarks
							Total area	Corroded area	
497	0,70	140	90	42	42	17,1	57	140	
498	"	218	"	"	69	23,4	50	73	
4857	0,70	140	95	42	9	3,5	12	130	
4958	"	218	"	"	37	19,4	42	110	
417	0,70	140	100	42	4	0,8	2,6	68	Incipient corrosion
418	"	218	"	"	~0	-	-	-	

TABLE E. Results, weight loss measurements, chapter 5.3.5. Slag cement (70% slag + 30% Slite Portland cement) initiation by 5% $CaCl_2$/cement.

Sample number	w/c	Exp time days	RH %	Surface area cm^2	Corroded area %	Weight mg/cm^2	Mean corrosion µm/year		Remarks
							Total area	Corroded area	
361	0,40	67	60	43	53	10,5	73	140	
362	"	147	"	"	77	17,3	55	71	
363	"	225	"	"	51	17,0	35	70	
364	"	323	"	"	74	24,0	35	47	
365	"	417	"	"	83	24,2	27	32	
366	"	954	"	"	95	33,3	16	17	
371	0,40	67	70	43	28	14,0	98	350	
372	"	147	"	"	49	19,8	63	130	50% incipient corrosion
373	"	225	"	"	50	22,9	48	96	
374	"	323	"	"	30	21,0	30	100	
375	"	417	"	"	44	27,0	30	67	
376	"	954	"	"	50	39,0	19	38	
381	"	67	80	43	15	10,5	73	490	
382	"	147	"	"	33	15,7	50	150	Difficult to measure corroded area
383	"	225	"	"	86	30,5	63	74	
384	"	323	"	"	40	30,0	43	110	
385	"	417	"	"	45	33,0	36	81	
386	"	954	"	"	76	60,8	30	39	
3851	"	67	85	43	50	18,3	130	260	
3852	"	147	"	"	49	20,5	65	130	
3853	"	225	"	"	67	32,5	68	100	
3854	"	323	"	"	50	36,0	52	100	
3855	"	417	"	"	69	38,7	43	62	
3856	"	954	"	"	63	50,0	25	40	

Table E, continued

Sample number	w/c	Exp time days	RH %	Surface area cm^2	Corroded area %	Weight mg/cm^2	Mean corrosion µm/year: Total area	Mean corrosion µm/year: Corroded area	Remarks
391	0,40	67	90	43	30	13,2	92	310	
392	"	147	"	"	19	14,4	46	240	Incipient corrosion
393	"	225	"	"	24	12,3	26	110	in 100% corroded area
394	"	323	"	"	49	40,7	58	120	
395	"	417	"	"	43	35,0	38	95	
396	"	954	"	"	60	99,0	49	82	
3951	0,40	67	95	43	33	15,2	110	320	
3952	"	147	"	"	27	19,1	61	300	
3953	"	225	"	"	73	46,5	97	130	30% of surface area
3954	"	323	"	"	30	41,0	59	200	deep corrosion attack
3955	"	417	"	"	40	35,0	38	95	
3956	"	954	"	"	100	177,0	87	87	
311	0,40	67	100	43	30	1,4	9,7	32	
312	"	147	"	"	5	0,7	2,2	47	
313	"	225	"	"	15	3,5	7,3	56	Incipient corrosion
314	"	323	"	"	-	3,0	4,4	-	in 100% of surface
315	"	417	"	"	8	0,1	0,1	1,0	area
316	"	954	"	"	90	1,8	0,9	1,0	

Table E, continued

Sample number	w/c	Exp time days	RH %	Surface area cm^2	Corroded area %	Weight mg/cm^2	Mean corrosion µm/year		Remarks
							Total area	Corroded area	
367	0,70	67	60	43	100	11,1	78	78	
368	"	147	"	"	99	15,3	48	48	
369	"	225	"	"	100	16,2	34	34	
3610	"	325	"	"	95	19,5	28	30	
3611	"	417	"	"	70	19,8	22	31	
3612	"	954	"	"	99	20,7	10	10	
377	0,70	67	70	43	51	14,6	100	200	
378	"	147	"	"	87	23,0	73	84	
379	"	225	"	"	100	28,8	60	60	
3710	"	325	"	"	90	31,4	45	50	
3711	"	417	"	"	50	30,7	34	67	
3712	"	954	"	"	100	44,9	22	22	
387	0,70	67	80	43	50	17,1	120	240	
388	"	147	"	"	77	24,3	77	100	
389	"	225	"	"	100	31,5	66	66	
3810	"	325	"	"	90	40,6	59	65	
3811	"	417	"	"	79	39,6	43	55	
3812	"	954	"	"	80	59,4	29	36	
3857	"	67	85	43	88	10,3	72	82	
3858	"	147	"	"	96	17,0	54	56	
3859	"	225	"	"	100	15,8	33	33	
38510	"	323	"	"	96	18,6	27	28	
38511	"	417	"	"	92	19,0	21	23	
38512	"	954	"	"	98	25,2	12	12	

Table E, continued

Sample number	w/c	Exp time days	RH %	Surface area cm^2	Corroded area %	Weight mg/cm^2	Mean corrosion µm/year		Remarks
							Total area	Corroded area	
397	0,70	67	90	43	39	16,2	110	290	
398	"	147	"	"	48	22,8	73	150	
399	"	225	"	"	36	27,9	58	160	
3910	"	323	"	"	47	34,0	49	110	
3911	"	417	"	"	52	38,0	42	80	
3912	"	954	"	"	84	68,5	34	40	
3957	0,70	67	95	43	38	17,3	120	320	
3958	"	147	"	"	43	19,0	61	140	
3959	"	225	"	"	60	33,0	69	110	
39510	"	323	"	"	40	31,5	45	110	
39511	"	417	"	"	49	36,0	40	80	
39512	"	954	"	"	78	92,9	46	59	
317	0,70	67	100	43	10	1,5	11	110	
318	"	147	"	"	15	1,6	5,2	36	
319	"	225	"	"	5	1,2	2,6	52	
3110	"	323	"	"	-				Only not covered part corroded
3111	"	417	"	"	5	0,3	0,3	6,7	
3112	"	954	"	"	5	1,5	0,7	15	

TABLE F. Results, weight loss measurements, chapter 5.3.5. Varying relative humidity.

Sample No	W/c	CO_2	5%xp $CaCl_2$	Cement type	Exp. time days	RH %	Surf. area cm^2	Corr. area %	Weight loss mg/m^2	0-value	Mean corr. µm/year		REMARKS
											Total area	Corroded area	
073	0.40	x		P	30	50-100	51	45	0.1	0	2	4	Wetting once a week
0953	0.40	x		P	91	50-100	51	80	0.1	0.2	1	1	"
014	0.40	x		P	688	50-100	51	75	1	1	<1	1	"
079	0.70	x		P	30	50-100	51	80	0.5	0	8	10	"
0959	0.70	x		P	91	50-100	51	93	1.3	0.5	7	7	"
019	0.70	x		P	688	50-100	51	94	3	1	2	2	"
173	0.40	x		B	30	50-100	46	97	0.4	2	6	6	"
1953	0.40	x		B	91	50-100	46	100	0	6	-	-	"
113	0.40	x		B	688	50-100	46	100	2	1	1	1	"
179	0.70	x		B	30	50-100	46	100	62	0.5	31	31	"
1959	0.70	x		B	91	50-100	46	100	0.5	50	3	3	"
119	0.70	x		B	688	50-100	46	100	3	1	2	2	"
465	0.40		x	P	30	50-100	43	26	0.8	4	13	48	"
475	0.40		x	P	91	50-100	43	55	0	10	-	-	"
4855	0.40		x	P	688	50-100	43	100	7	10	5	5	"
495	0.40		x	P	688	50-100	43	90	10	10	7	8	"
4856	0.40		x	P	688	50-100	43	98	10	10	7	7	"
496	0.40		x	P	688	50-100	43	95	8	5	5	5	"

Table F, continued

Sample No	W/c	CO_2	5%xp $CaCl_2$	Cement type	Exp. time days	RH %	Surf. area cm^2	Corr. area %	Weight loss mg/m^2	0-value	Mean corr. µm/year		REMARKS
											Total area	Corroded area	
4611	0.70		x	P	30	50-100	43	100	0.1	11	2	2	Wetting once a week
4711	0.70		x	P	91	50-100	43	100	5	10	26	26	"
48511	0.70		x	P	688	50-100	43	95	17	10	12	12	"
4911	0.70		x	P	688	50-100	43	100	12	10	8	8	" *
48512	0.70		x	P	688	50-100	43	94	17	10	12	12	" *
4912	0.70		x	P	688	50-100	43	95	12	10	8	9	"
49511	0.70		x	P	688	50-100	43	99	9	10	6	6	"
49512	0.70		x	P	30	50-100	43	100	6	10	4	4	"
4111	0.70		x	P	91	50-100	43	98	7	1	5	5	"
4112	0.70		x	P	688	50-100	43	95	8	1	5	6	"
064	0.40	x		P	30	50-100	51	80	0.8	0	13.5	16	Wetting every day
0853	0.40	x		P	91	50-100	51	83	0.8	0	4	5	"
0610	0.70	x		P	30	50-100	51	100	0.7	0	11	11	"
0859	0.70	x		P	91	50-100	51	97	1.7	0	9	9	"
164	0.40	x		B	30	50-100	46	100	1.7	1	27	27	"
1853	0.40	x		B	91	50-100	46	100	0	6	-	-	"
1610	0.70	x		B		50-100	46	100	2.2	1	34	34	"
1859	0.70	x		B		50-100	46	100	2.4	1	12	12	"
464	0.40		x	P		50-100	43	42	0	4	-	-	"
474	0.40		x	P		50-100	43	71	9.7	10	50	70	"
4854	0.40		x	P		50-100	43	97	21	10	14	15	"
494	0.40		x	P		50-100	43	88	22	10	15	17	"
4954	0.40		x	P		50-100	43	90	10	10	7	8	"
414	0.40		x	P		50-100	43	60	8	1	5	9	"

*Insignificant 0-value.

Table F, continued

Sample No	W/c	CO_2	5%xp $CaCl_2$	Cement type	Exp. time days	RH %	Surf. area cm^2	Corr. area %	Weight loss mg/m^2	0-value	Mean corr. µm/year		REMARKS
											Total area	Corroded area	
4610	0.40		x	P		50-100	43	99	2	11	36	36	Wetting every day
4710	0.40		x	P		50-100	43	92	5	10	26	28	"
48510	0.40		x	P		50-100	43	95	33	10	22	24	"
4910	0.40		x	P		50-100	43	90	44	10	30	33	"
49510	0.40		x	P		50-100	43	70	34	10	23	33	"
4110	0.40		x	P		50-100	43	18	10	1	7	38	"
4853	0.40		x	P	688	40-60		95	13	10	9	9	
493	0.40		x	P	688	40-60		30	5	10	3	11	
4953	0.40		x	P	688	40-60		55	-	10	-	-	*
413	0.40		x	P	688	40-60		-	2	1	1	-	**
463	0.40		x	P	251	40-60	43	73	3	4	6	8	
473	0.40		x	P	251	40-60	43	60	19	10	35	59	
4858	0.70		x	P	688	40-60		10	17	10	12	120	
499	0.70		x	P	688	40-60		98	20	10	14	14	
4959	0.70		x	P	688	40-60		98	10	10	7	7	
419	0.70		x	P	688	40-60		90	2	1	1	1	
469	0.70		x	P	688	40-60		100	14	10	26	26	
479	0.70		x	P	688	40-60		100	15	10	28	28	

*Insignificant 0-value

** Metal covered with oxide layer.

TABLE G. Results, weight loss measurements, chapter 5.3.6.

Sample number	Reinforcement type	Cement type	w/c	Concrete cover /mm/	Crack width, mm		Moisture condition /RH%/	Exposure time /days/	Total steel area /cm^2/	Corr. area /cm^2)	Weight loss /mg/	Weight corr. area /mg/cm^2/	Depth of corrosion corroded area, /μm/
					designed	measured							
136	S10	Slite	0.70	15	0.10	0.10	100	82	~90	5.5	0	0	0
126	S10	Std	0.70	"	"	0.12	100	179	90	3.3	88	27	34
133	S10		0.70	"	"	0.10	100	722	90	2.3	18	7.8	10
142	S10		0.70	"	"	0.15	100	761	90	8.5	30	3.5	5
135	S10		0.70	30	0.10	0.10	100	82	90	2.2	0	0	0
125	S10		0.70	"	"	0.12	100	179	90	3.0	31	10	13
134	S10		0.70	"	"	0.10	100	722	90	2.8	8	2.9	4
141	S10		0.70	"	"	0.15	100	761	90	4.8	39	8.1	10
132	S10		0.70	15	0.30	0.30	100	82	90	6.8	0	0	0
138	S10		0.70	"	"	0.35	100	179	90	10.5	137	13	17
139	S10		0.70	"	"	0.35	100	722	90	5.0	12	2.4	3
127	S10		0.70	"	"	0.28	100	761	90	4.3	28	6.5	8
131	S10		0.70	30	0.30	0.30	100	82	90	6.8	0	0	0
137	S10		0.70	"	"	0.35	100	179	90	7.5	142	19	24
140	S10		0.70	"	"	0.35	100	722	90	3.3	23	7.0	9
128	S10		0.70	"	"	0.28	100	761	90	5.0	36	7.2	9
147	S10		0.70	15	0.10	0.08	80	82	90	2.5	0	0	0
151	S10		0.70	"	"	0.07	80	179	90	5.5	143	26	33
121	S10		0.70	"	"	0.18	80	722	90	5.8	15	2.6	3
143	S10		0.70	"	"	0.08	80	761	90	1.5	16	11	14

Table G, continued

Sample number	Reinforcement type	Cement type	w/c	Concrete cover /mm/	Crack width, mm		Moisture condition /RH%/	Exposure time /days/	Total steel area /cm^2/	Corr. area /cm^2)	Weight loss /mg/	Weight corr. area /mg/cm^2/	Depth of corrosion corroded area, /μm/
					designed	measured							
148	S10	Slite	0.70	30	0.10	0.08	80	82	~90	2.8	0	0	0
152	S10	Std	0.70	"	"	0.07	"	179	"	2.8	128	46	59
122	S10		0.70	"	"	0.18	"	722	"	5.0	14	2.8	4
144	S10		0.70	"	"	0.08	"	761	"	2.8	20	7.1	9
129	S10		0.70	15	0.30	0.30	"	82	"	4.0	0	0	0
150	S10		0.70	"	"	0.30	"	179	"	7.0	93	13	17
123	S10		0.70	"	"	0.32	"	722	"	11.0	26	2.4	3
145	S10		0.70	"	"	0.30	"	761	"	8.0	32	4.0	5
130	S10		0.70	30	0.30	0.30	"	82	"	5.0	0	0	0
149	S10		0.70	"	"	0.30	"	179	"	4.8	97	20	26
124	S10		0.70	"	"	0.32	"	722	"	9.0	21	2.3	3
146	S10		0.70	"	"	0.30	"	761	"	9.8	27	2.8	4
22	S10		0.50	15	0.10	0.15	100	82	"	3.5	0	0	0
32	S10		0.50	"	"	0.05	"	179	"	2.3	40	17	22
2	S10		0.50	"	"	0.10	"	722	"	3.8	18	4.7	6
29	S10		0.50	"	"	0.10	"	761	"	1.8	19	11	14
21	S10		0.50	30	"	0.15	"	82	"	2.8	0	0	0
31	S10		0.50	"	"	0.05	"	179	"	0.3	14	47	60
1	S10		0.50	"	"	0.10	"	722	"	2.3	7	3.0	4
30	S10		0.50	"	"	0.10	"	761	"	0.4	12	30	39
20	S10		0.50	15	0.30	0.30	"	82	"	2.5	0	0	0
38	S10		0.50	"	"	0.30	"	179	"	2.5	92	37	47
5	S10		0.50	"	"	0.32	"	722	"	2.0	12	6.0	8
36	S10		0.50	"	"	0.30	"	761	"	23.3	81	3.5	5

Table G, continued

Sample number	Reinforcement type	Cement type	w/c	Concrete cover /mm/	Crack width, mm		Moisture condition /RH%/	Exposure time /days/	Total steel area /cm^2/	Corr. area /cm^2)	Weight loss /mg/	Weight corr. area /mg/cm^2/	Depth of corrosion corroded area, /μm/
					designed	measured							
19	S10	Slite	0.50	30	0.30	0.30	100	82	~90	3.8	0	0	0
37	"	Std	"	"	"	0.25	"	179	"	2.5	52	21	27
6	"		"	"	"	0.25	"	722	"	3.8	8	2.1	3
35	"		"	"	"	0.30	"	761	"	8.8	24	2.7	4
23	"		"	15	0.10	0.10	80	82	"	1.7	0	0	0
13	"		"	"	"	0.10	"	179	"	4.0	58	15	19
7	"		"	"	"	0.10	"	722	"	19.8	48	2.4	3
12	"		"	"	"	0.10	"	761	"	3.8	11	2.9	4
24	"		"	30	"	0.10	"	82	"	0.4	0	0	0
14	"		"	"	"	0.10	"	179	"	3.5	79	23	29
8	"		"	"	"	0.10	"	722	"	9.0	19	2.1	3
11	"		"	"	"	0.10	"	761	"	2.7	16	5.9	8
3	"		"	15	0.30	0.30	"	82	"	4.0	0	0	0
17	"		"	"	"	0.30	"	179	"	5.0	26	5.2	7
34	"		"	"	"	0.20	"	722	"	1.8	14	7.8	10
27	"		"	"	"	0.25	"	761	"	4.0	14	3.5	5
4	"		"	30	"	0.30	"	82	"	4.3	0	0	0
18	"		"	"	"	0.30	"	179	"	4.0	22	5.5	7
33	"		"	"	"	0.20	"	722	"	1.8	15	8.3	11
28	"		"	"	"	0.25	"	761	"	1.3	16	12	16
62	"		0.35	15	0.10	0.10	100	82	"	3.8	0	0	0
54	"		"	"	"	0.10	"	179	"	6.0	24	4.0	5
40	"		"	"	"	0.10	"	722	"	1.3	7	5.4	7
55	"		"	"	"	0.10	"	761	"	6.8	14	2.1	2

Table G, continued

Sample number	Reinforcement type	Cement type	w/c	Concrete cover /mm/	Crack width, mm		Moisture condition /RH%/	Exposure time /days/	Total steel area /cm^2/	Corr. area /cm^2)	Weight loss /mg/	Weight corr. area /mg/cm^2/	Depth of corrosion corroded area, /μm/
					designed	measured							
61	S10	Slite	0.35	30	0.10	0.10	100	82	~ 90	1.5	0	0	0
53	"	Std	"	"	"	"	"	179	"	-	17	-	-
39	"		"	"	"	"	"	722	"	1.8	12	6.7	9
56	"		"	"	"	"	"	761	"	10.5	14	1.3	2
46	"	"	"	15	0.30	0.30	"	82	"	4.3	0	0	0
65	"		"	"	"	"	"	179	"	30.2	46	1.5	2
57	"		"	"	"	"	"	722	"	2.8	4	1.4	2
49	"		"	"	"	"	"	761	"	11.5	7	0.6	<1
45	"	"	"	30	0.30	"	"	82	"	2.0	0	0	0
66	"		"	"	"	"	"	179	"	2.5	26	10	13
58	"		"	"	"	"	"	722	"	1.3	3	2.3	3
50	"		"	"	"	"	"	761	"	12.8	11	0.9	1
52	"	"	"	15	0.10	0.10	80	82	"	2.3	0	0	0
43	"		"	"	"	0.10	"	179	"	4.0	45	11	14
67	"		"	"	"	0.08	"	722	"	2.8	7	2.5	3
48	"		"	"	"	0.14	"	761	"	14.3	30	2.1	3
51	"	"	"	30	"	0.10	"	82	"	1.5	0	0	0
44	"		"	"	"	0.10	"	179	"	2.3	45	20	25
68	"		"	"	"	0.08	"	722	"	2.3	3	1.3	2
47	"		"	"	"	0.14	"	761	"	6.8	14	2.1	3
64	"	"	"	15	0.30	0.30	"	82	"	11.8	0	0	0
42	"		"	"	"	0.30	"	179	"	9.3	56	6.0	7.7
60	"		"	"	"	0.28	"	722	"	19.5	36	1.9	2
69	"		"	"	"	0.33	"	761	"	4.3	12	2.8	4

Table G, continued

Sample number	Reinforcement type	Cement type	w/c	Concrete cover /mm/	Crack width, mm		Moisture condition /RH%/	Exposure time /days/	Total steel area /cm^2/	Corr. area /cm^2)	Weight loss /mg/	Weight corr. area /mg/cm^2/	Depth of corrosion corroded area, /µm/
					designed	measured							
63	S10	Slite	0.35	30	0.30	0.30	80	82	~ 90	7.0	0	0	0
41	"	Std	"	"	"	0.30	"	179	"	5.3	94	18	23
59	"		"	"	"	0.28	"	722	"	13.3	15	1.1	1
70	"		"	"	"	0.33	"	761	"	3.0	11	3.7	5
93	"	Slag*	0.50	15	0.10	0.10	100	82	"	6.8	57	8.4	11
95	"		"	"	"	"	"	179	"	6.3	57	9.1	12
87	"		"	"	"	"	"	722	"	6.5	52	8.0	10
97	"		"	"	"	0.05	"	761	"	6.0	66	11	4
94	"	"	"	30	0.10	0.10	"	82	"	3.0	10	3.3	4
96	"		"	"	"	"	"	179	"	3.8	42	11	14
88	"		"	"	"	"	"	722	"	5.3	38	7.2	9
98	"		"	"	"	0.05	"	761	"	5.0	42	8.4	11
90	"	"		15	0.30	0.30	"	82	"	10.3	4	0.4	<1
85	"		"	"	"	"	"	179	"	11.0	192	18	22
102	"		"	"	"	"	"	722	"	24.5	136	5.6	7
112	"		"	"	"	0.27	"	761	"	13.5	72	5.3	7
89	"	"	"	30	"	0.30	"	82	"	8.5	45	5.3	7
86	"		"	"	"	"	"	179	"	10.5	96	9.1	12
101	"		"	"	"	"	"	722	"	18.0	118	6.6	9
111	"		"	"	"	0.27	"	761	"	12.5	62	5.0	6
104	"	"	"	15	0.10	0.10	80	82	"	13.0	0	0	0
110	"		"	"	"	0.10	"	179	"	21.0	207	9.9	13
99	"		"	"	"	0.15	"	722	"	9.0	90	10	13
91	"		"	"	"	0.05	"	761	"	11.0	52	4.7	6

* (65% slag + 35% Slite Portland cement)

Table G, continued

Sample number	Reinforcement type	Cement type	w/c	Concrete cover /mm/	Crack width, mm		Moisture condition /RH%/	Exposure time /days/	Total steel area /cm^2/	Corr. area /cm^2)	Weight loss /mg/	Weight corr. area /mg/cm^2/	Depth of corrosion corroded area, /µm/
					designed	measured							
103	S10	Slag	0.50	30	0.10	0.10	80	82	~ 90	4.5	0	0	0
109	"		"	"	"	"	"	179	"	10.5	173	17	21
100	"		"	"	"	0.15	"	722	"	3.0	37	12	16
92	"		"	"	"	0.05	"	761	"	8.5	47	5.5	7
106	"	"	"	15	0.30	0.30	"	82	"	11.5	0	0	0
113	"		"	"	"	0.40	"	179	"	30.8	185	6.0	8
108	"		"	"	"	0.40	"	722	"	32.3	236	7.3	9
83	"		"	"	"	0.35	"	761	"	17.0	137	8.1	10
105	"	"	"	30	0.30	0.30	"	82	"	10.5	0	0	0
114	"		"	"	"	0.40	"	179	"	16.0	200	13	16
107	"		"	"	"	0.40	"	722	"	23.5	107	4.6	6
84	"		"	"	"	0.35	"	761	"	18.0	111	6.2	8
79	"	Slite Std	"	15	0.10	0.30	50 ⇄ 100	82	"	4.8	0	0	0
157	"		"	"	"	0.10	"	179	"	1.0	70	70	90
74	"		"	"	"	0.20	"	722	"	4.0	27	6.8	9
155	"		"	"	"	0.15	"	761	"	3.3	35	11	14
80	"	"	"	30	"	0.30	"	82	"	3.0	0	0	0
158	"		"	"	"	0.10	"	179	"	0	37	-	-
73	"		"	"	"	0.20	"	722	"	4.3	17	4.0	5
156	"		"	"	"	0.15	"	761	"	2.8	16	5.7	7
77	"	"	"	15	0.30	0.40	"	82	"	19.5	0	0	0
153	"		"	"	"	0.40	"	179	"	15.0	91	6.1	8
71	"		"	"	"	0.35	"	722	"	4.5	22	4.9	6
75	"		"	"	"	0.28	"	761	"	15.8	187	12	15

Table G, continued

Sample number	Reinforcement type	Cement type	w/c	Concrete cover /mm/	Crack width, mm		Moisture condition /RH%/	Exposure time /days/	Total steel area /cm^2/	Corr. area /cm^2)	Weight loss /mg/	Weight corr. area /mg/cm^2/	Depth of corrosion corroded area, /μm/
					designed	measured							
78	S10	Slite	0.50	30	0.30	0.40	50 → 100	82	~90	10.0	0	0	0
154	"	Std	"	"	"	0.40	"	179	"	9.3	84	9.0	12
72	"		"	"	"	0.35	"	722	"	3.8	27	7.1	9
76	"		"	"	"	0.28	"	761	"	8.0	70	8.8	11
15	"	"	"	15	0.10	0.05	3% NaCl	82	"	0	0	0	0
26	"		"	"	"	0.10-0.15	"	179	"	0	34	-	-
117	"		"	"	"	0.10	"	722	"	0.20	8	80	100
160	"		"	"	"	0.08	"	761	"	0	19	-	-
16	"	"	"	30	"	0.05	"	82	"	0	0	0	0
25	"		"	"	"	0.10-0.15	"	179	"	0	16	-	-
118	"		"	"	"	0.10	"	722	"	0.15	11	73	95
159	"		"	"	"	0.08	"	761	"	0	28	-	-
10	"	"	"	15	0.30	0.30	"	82	"	0	0	0	0
81	"		"	"	"	"	"	179	"	0	42	-	-
119	"		"	"	"	"	"	722	"	0	5	-	-
116	"		"	"	"	"	"	761	"	2.0	13	6.5	8
9	"	"	"	30	"	"	"	82	"	0	0	0	0
82	"		"	"	"	"	"	179	"	0	42	-	-
120	"		"	"	"	"	"	722	"	0	8	-	-
115	"		"	"	"	"	"	761	"	0.4	7	18	22

Table G, continued

Sample number	Reinforcement type	Cement type	w/c	Concrete cover /mm/	Crack width, mm		Moisture condition /RH%/	Exposure time /days/	Total steel area /cm^2/	Corr. area /cm^2)	Weight loss /mg/	Weight corr. area /mg/cm^2/	Depth of corrosion corroded area, /µm/
					designed	measured							
1	S 5	Slite	0.50	10	0.10	0.12	80	722	~130	0.4	7	18	23
15	"	Std	"	"	"	0.12	"	761	"	0.1	21	210	270
2	"		"	25	0.10	0.12	"	722	"	0.3	0	0	0
16	"		"	"	"	0.12	"	761	"	0.8	14	18	23
13	"		"	10	0.30	0.33	"	722	"	0.7	0	0	0
11	"		"	"	"	0.28	"	761	"	0.6	19	32	41
14	"		"	25	0.30	0.33	"	722	"	0.4	0	0	0
12	"		"	"	0.30	0.28	"	761	"	0.4	18	45	58
4	"		"	10	0.10	0.12	100	722	"	0.4	0	0	0
9	"		"	"	0.10	0.10	"	761	"	0.8	11	14	18
3	"		"	25	0.10	0.12	"	722	"	0	6	-	-
10	"		"	"	0.10	0.10	"	761	"	0.1	11	110	140
5	"		"	10	0.30	0.35	"	722	"	0.3	8	27	34
7	"		"	"	0.30	0.20	"	761	"	1.1	19	17	22
6	"		"	25	0.30	0.35	"	722	"	0.4	1	2.5	3
8	"		"	"	0.30	0.20	"	761	"	0.5	18	36	46
5	K 8		"	15	0.10	0.10	"	722	103	0.6	5	3	4
16	"		"	"	0.10	0.10	"	761	"	4.8	12	2.5	3

Table G, continued

Sample number	Reinforcement type	Cement type	w/c	Concrete cover /mm/	Crack width, mm		Moisture condition /RH%/	Exposure time /days/	Total steel area /cm^2/	Corr. area /cm^2)	Weight loss /mg/	Weight corr. area /mg/cm^2/	Depth of corrosion corroded area, /μm/
					designed	measured							
6	K 8	Slite	0.50	30	0.10	0.10	100	722	103	0.2	0	0	0
15	"	Std	"	"	0.10	0.10	"	761	"	0	6	-	-
9	"		"	15	0.30	0.30	"	722	"	1.5	11	7.3	9
2	"		"	"	0.30	0.28	"	761	"	2.3	10	4.4	6
10	"		"	30	0.30	0.30	"	722	"	0.8	17	21	27
1	"		"	"	0.30	0.28	"	761	"	0.8	0	-	-
13	"		"	15	0.10	0.12	80	722	"	0.4	6	15	19
3	"		"	"	0.10	0.08	"	761	"	9.0	0	-	-
14	"		"	30	0.10	0.12	"	722	"	0	9	-	-
4	"		"	"	0.10	0.08	"	761	"	3.3	0	-	-
7	"		"	15	0.30	0.28	"	722	"	2.3	19	8.3	11
11	"		"	"	0.30	0.30	"	761	"	3.3	0	-	-
8	"		"	30	0.30	0.28	"	722	"	1.5	10	6.7	9
12	"		"	"	0.30	0.30	"	761	"	6.5	0	-	-

Code: S10 = Smooth bar Ø 10 mm
K8 = Ribbed bar Ø 8 mm.

APPROXIMATION OF CORROSION RATE FROM BASIC DATA

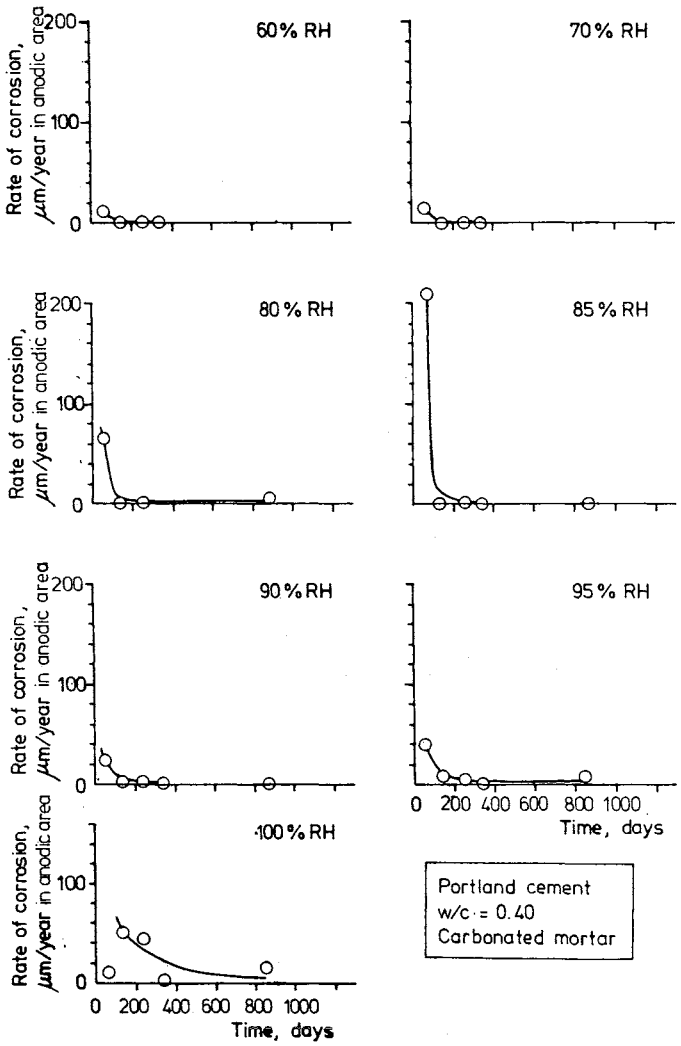

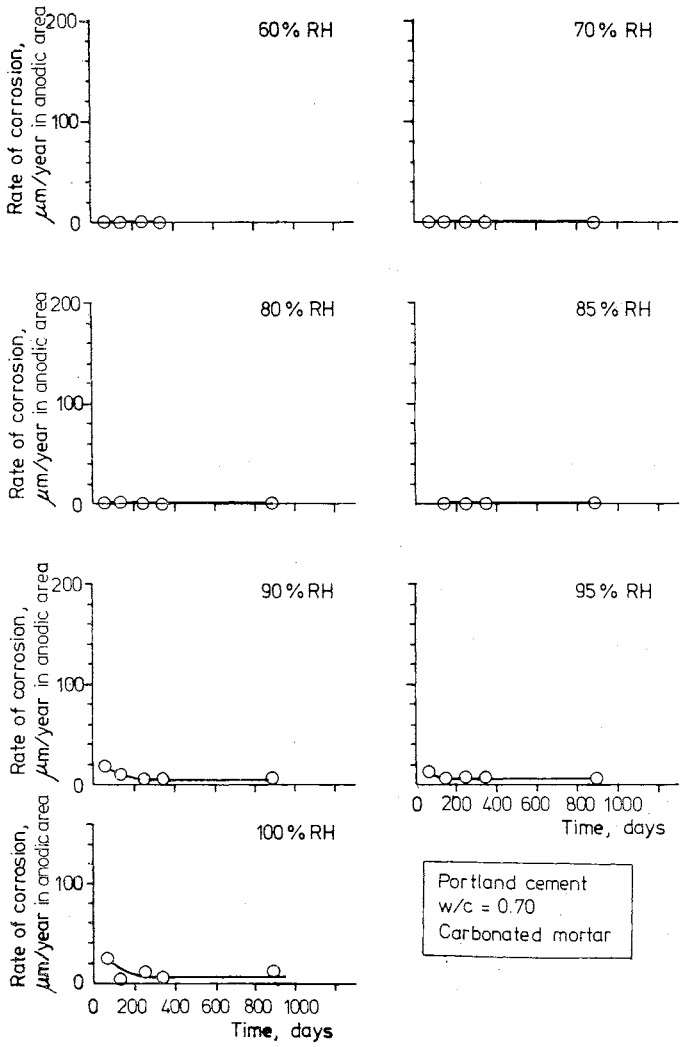
60% RH
70% RH
80% RH
85% RH
90% RH
95% RH
100% RH
Rate of corrosion, µm/year in anodic area
200
100
0
0 200 400 600 800 1000
Time, days
Portland cement
w/c = 0.70
Carbonated mortar

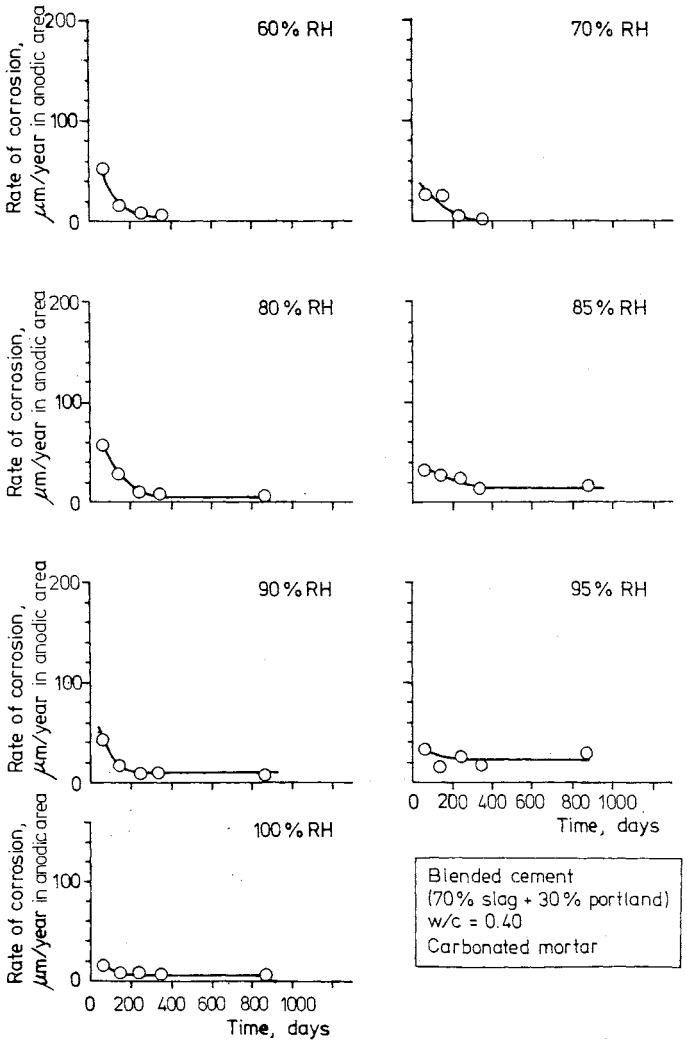
60% RH
70% RH
80% RH
85% RH
90% RH
95% RH
100% RH
Rate of corrosion, µm/year in anodic area
200
100
0
0 200 400 600 800 1000
Time, days
Blended cement
(70% slag + 30% portland)
w/c = 0.40
Carbonated mortar

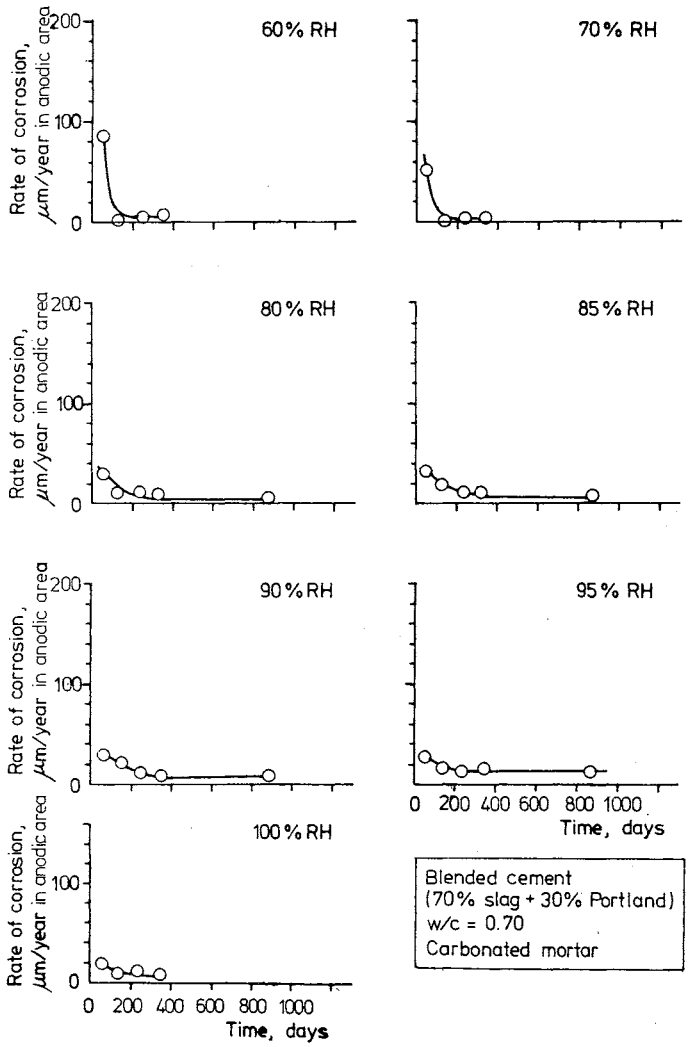
60% RH
70% RH
80% RH
85% RH
90% RH
95% RH
100% RH
Rate of corrosion, µm/year in anodic area
200
100
0
0 200 400 600 800 1000
Time, days
Blended cement
(70% slag + 30% Portland)
w/c = 0.70
Carbonated mortar

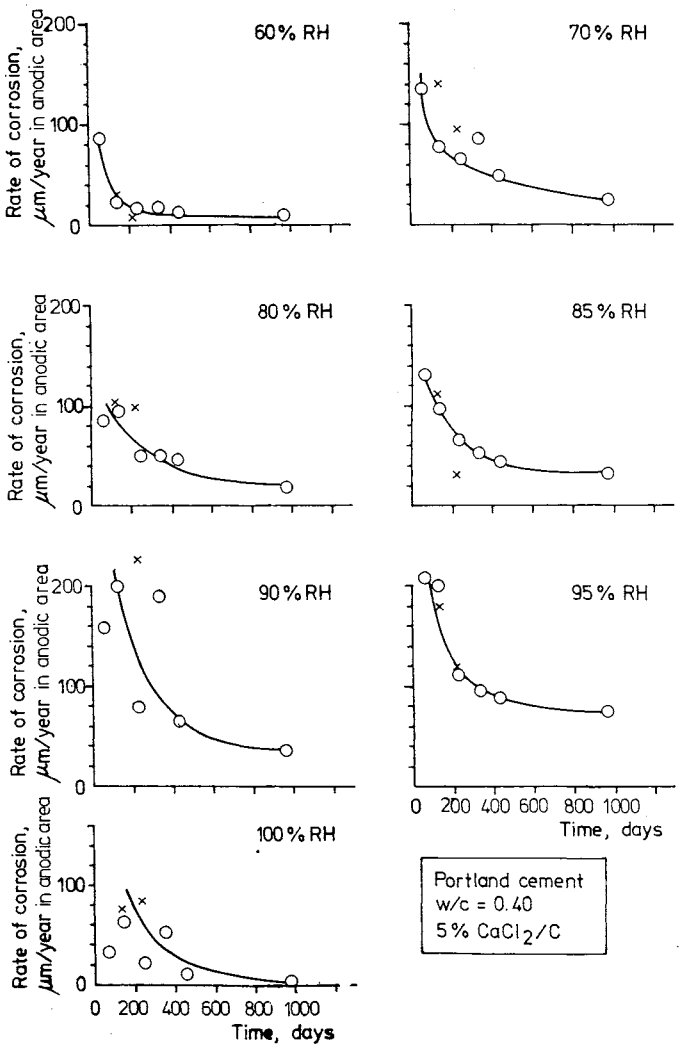
60% RH
70% RH
80% RH
85% RH
90% RH
95% RH
100% RH
Rate of corrosion, µm/year in anodic area
200
100
0
0 200 400 600 800 1000
Time, days
Portland cement
w/c = 0.40
5% CaCl2/C

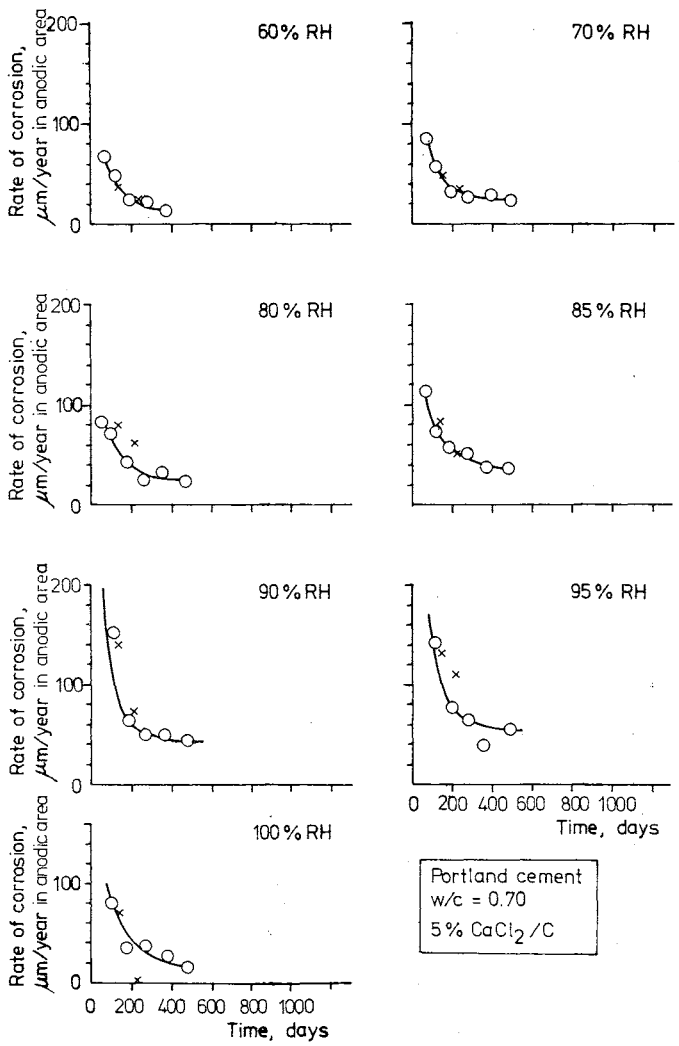
60% RH
70% RH
80% RH
85% RH
90% RH
95% RH
100% RH
Rate of corrosion, µm/year in anodic area
200
100
0
0 200 400 600 800 1000
Time, days
Portland cement
w/c = 0.70
5% CaCl2/C

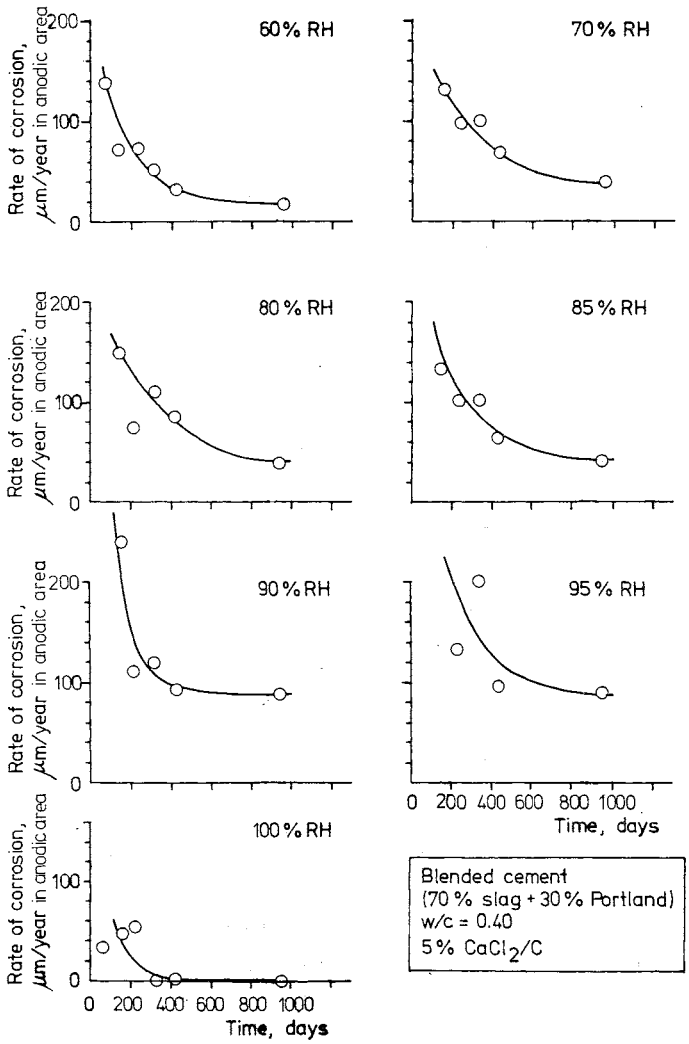
60% RH
70% RH
80% RH
85% RH
90% RH
95% RH
100% RH
Rate of corrosion, µm/year in anodic area
200
100
0
0 200 400 600 800 1000
Time, days
Blended cement
(70 % slag + 30 % Portland)
w/c = 0.40
5 % CaCl2/C

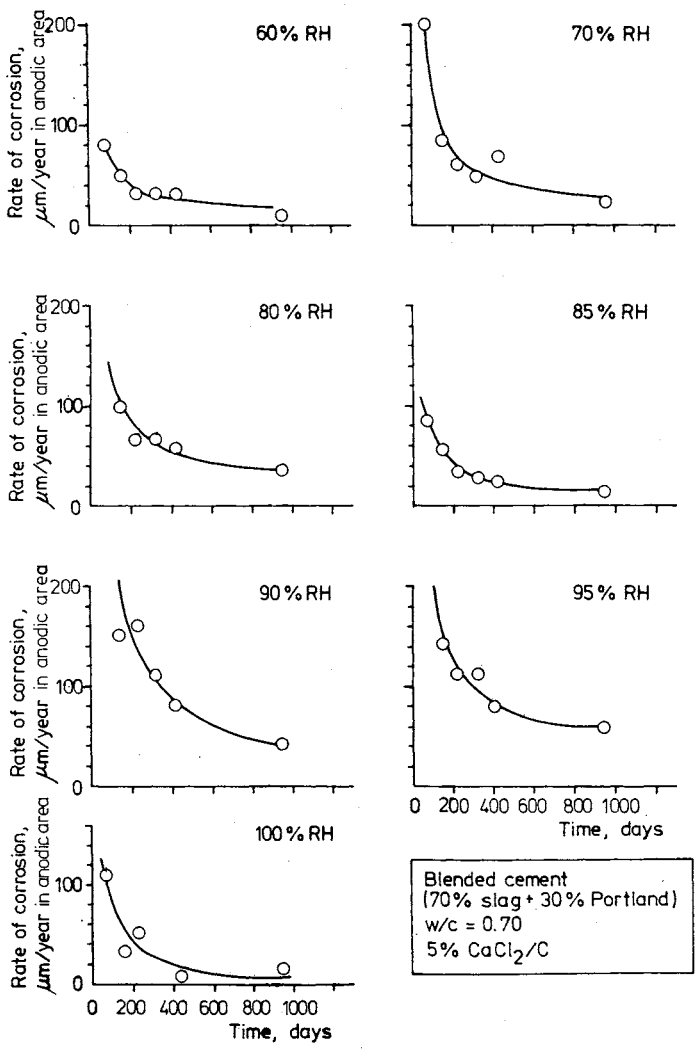
60% RH
70% RH
80% RH
85% RH
90% RH
95% RH
100% RH
Rate of corrosion, µm/year in anodic area
200
100
0
0 200 400 600 800 1000
Time, days
Blended cement
(70% slag + 30% Portland)
w/c = 0.70
5% CaCl2/C

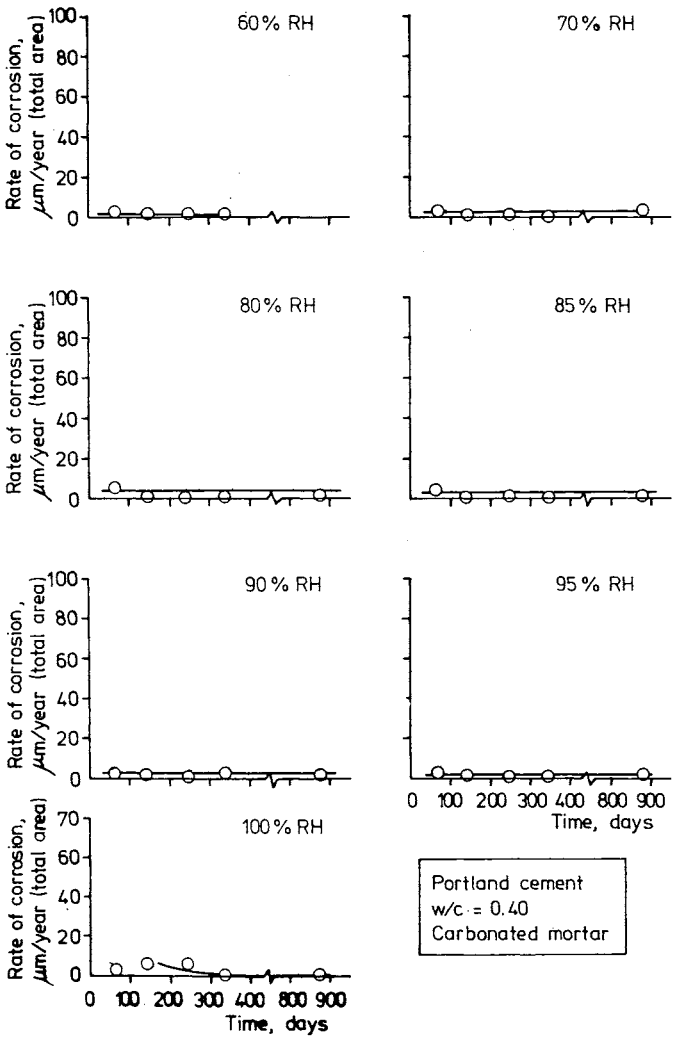
60 % RH
70 % RH
80 % RH
85 % RH
90 % RH
95 % RH
100 % RH
Rate of corrosion, µm/year (total area)
0 20 40 60 80 100
0 20 40 60 70
0 100 200 300 400 800 900
Time, days
Portland cement
w/c = 0.40
Carbonated mortar

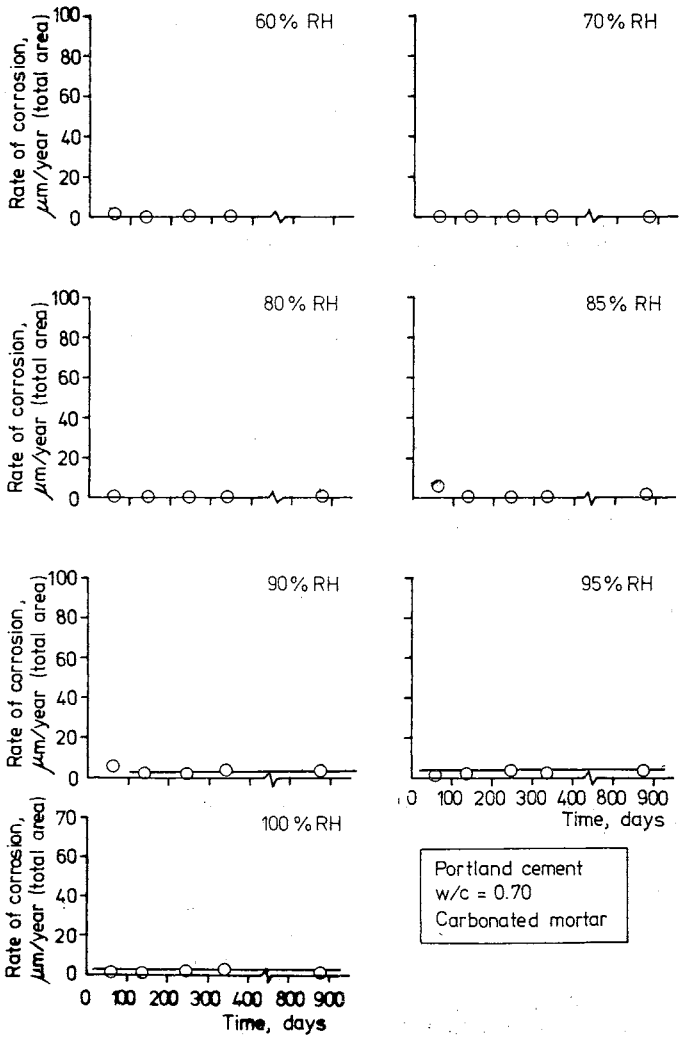
60% RH
70% RH
80% RH
85% RH
90% RH
95% RH
100% RH
Rate of corrosion, µm/year (total area)
0
20
40
60
80
100
0 100 200 300 400 800 900
Time, days
Portland cement
w/c = 0.70
Carbonated mortar

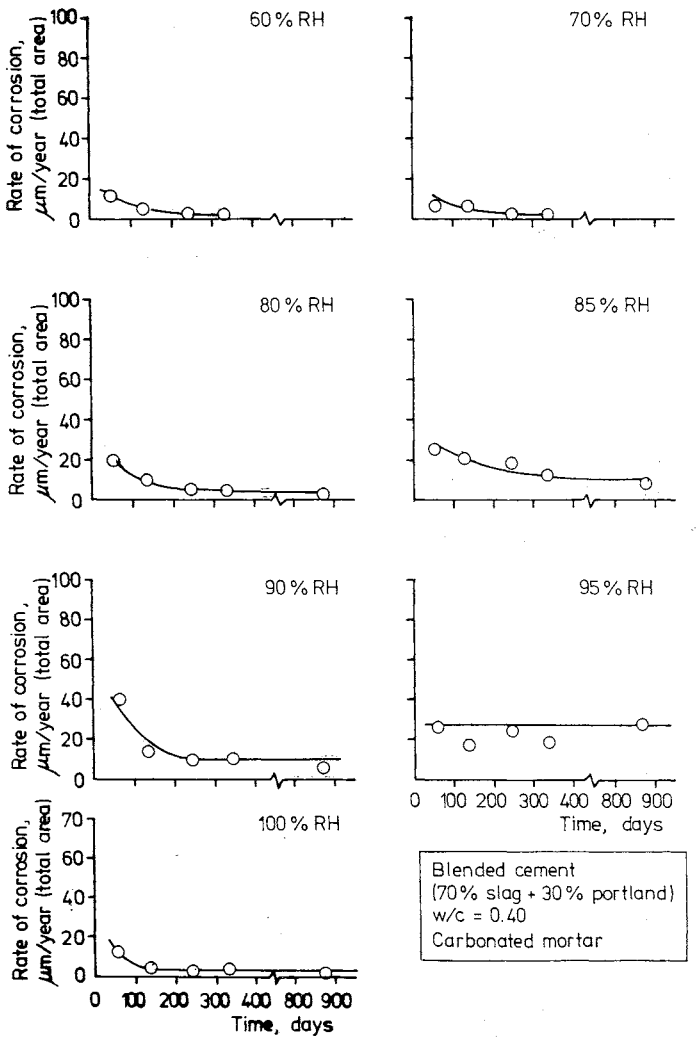
60 % RH
70 % RH
80 % RH
85 % RH
90 % RH
95 % RH
100 % RH
Rate of corrosion, µm/year (total area)
0
20
40
60
80
100
0 100 200 300 400 800 900
Time, days
Blended cement
(70 % slag + 30 % portland)
w/c = 0.40
Carbonated mortar

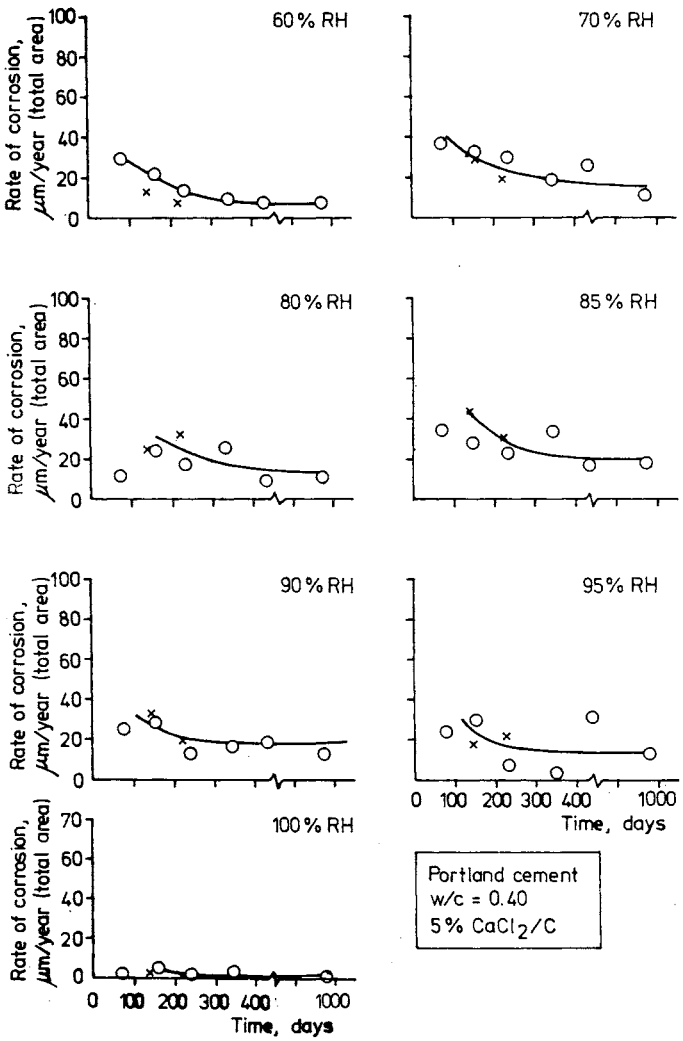
60 % RH
70 % RH
80 % RH
85 % RH
90 % RH
95 % RH
100 % RH
Rate of corrosion, µm/year (total area)
0
20
40
60
80
100
0 100 200 300 400 1000
Time, days
Portland cement
w/c = 0.40
5 % CaCl2/C

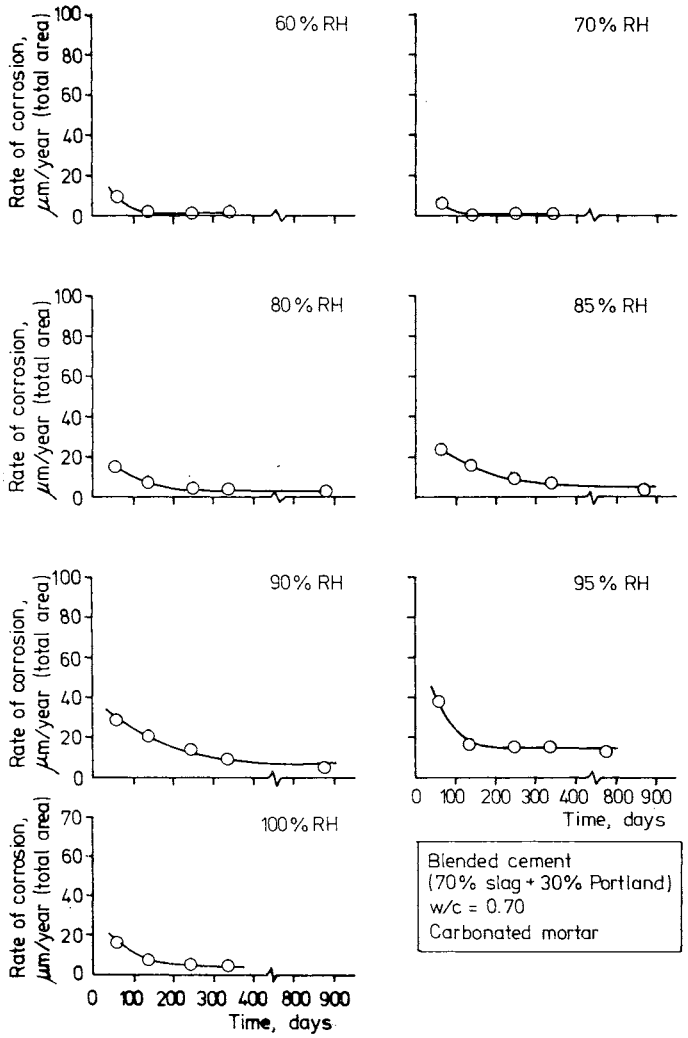
60 % RH
70 % RH
80 % RH
85 % RH
90 % RH
95 % RH
100 % RH
Rate of corrosion, µm/year (total area)
0
20
40
60
80
100
0 100 200 300 400 800 900
Time, days
Blended cement
(70% slag + 30% Portland)
w/c = 0.70
Carbonated mortar

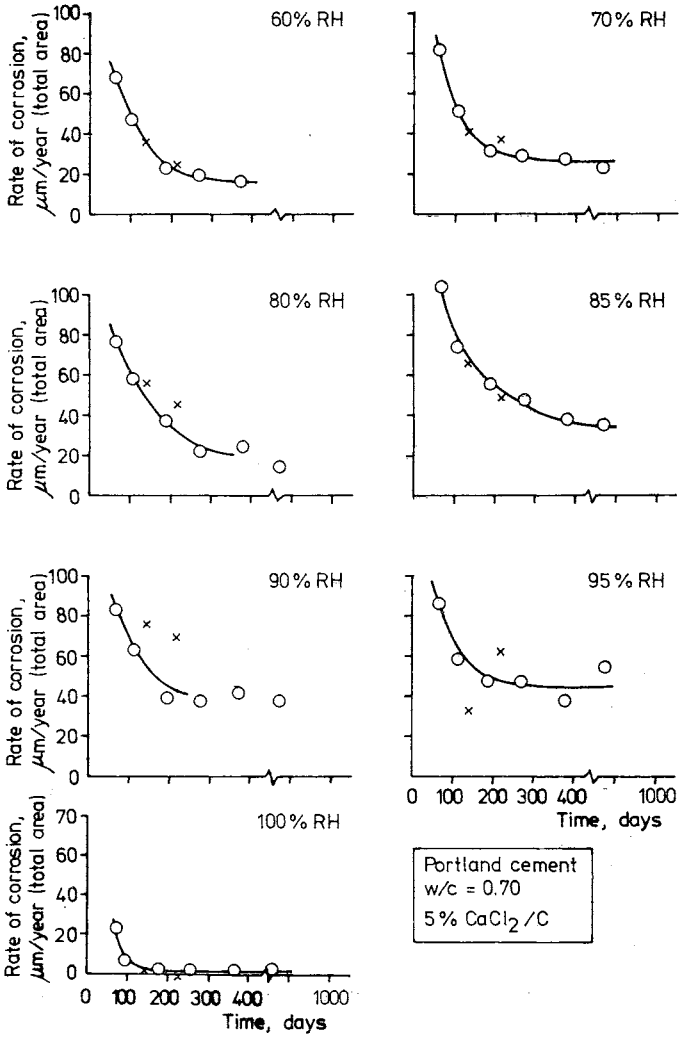
60% RH
70% RH
80% RH
85% RH
90% RH
95% RH
100% RH
Rate of corrosion, µm/year (total area)
0
20
40
60
80
100
0 100 200 300 400 1000
Time, days
Portland cement
w/c = 0.70
5% CaCl2 /C

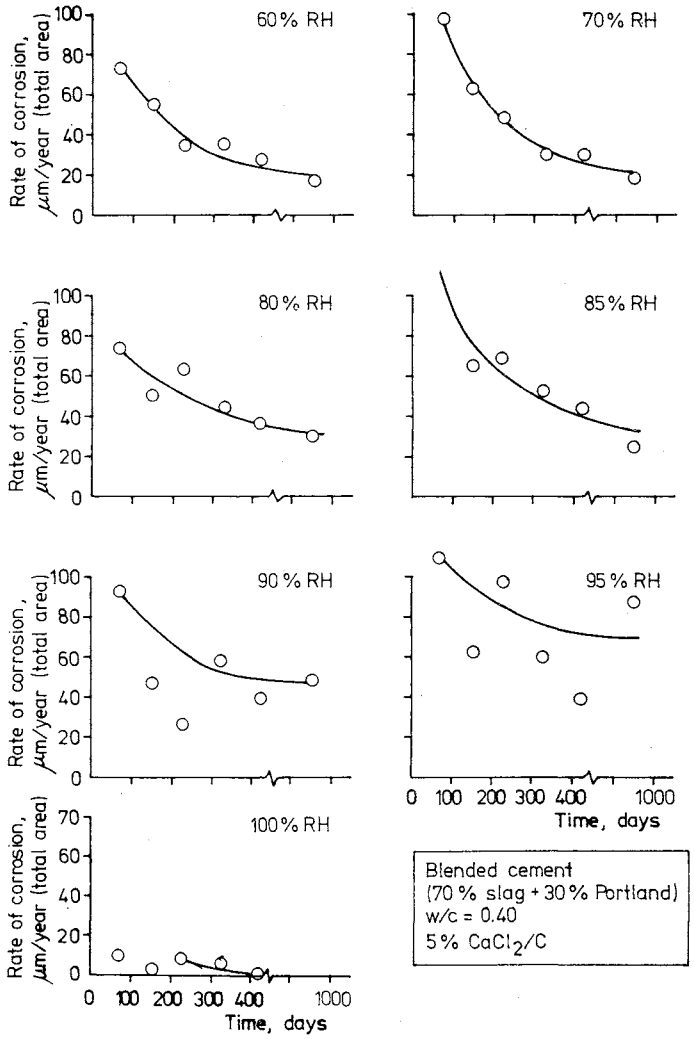
60 % RH
70 % RH
80 % RH
85 % RH
90 % RH
95 % RH
100 % RH
Rate of corrosion, µm/year (total area)
0
20
40
60
80
100
0 100 200 300 400 1000
Time, days
Blended cement
(70 % slag + 30 % Portland)
w/c = 0.40
5 % $CaCl_2$/C

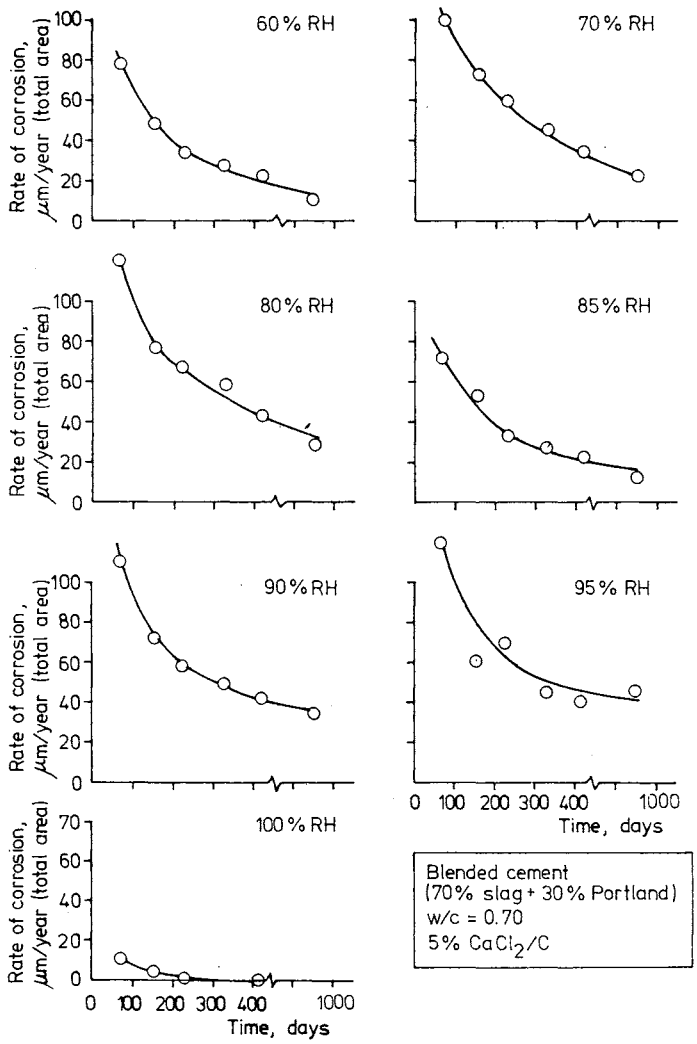
60 % RH
70 % RH
80 % RH
85 % RH
90 % RH
95 % RH
100 % RH
Rate of corrosion, µm/year (total area)
Time, days
0
20
40
60
80
100
200
300
400
1000
Blended cement
(70% slag + 30% Portland)
w/c = 0.70
5% $CaCl_2$/C

TABLE A. Results, diffusion tests, chapter 5.4.

Sample nr	Cement type	w/c	Dimension		Climate before test RH /%/	Weight in the drying period		Time /days	Position from inside /mm/	Measured concentration, chloride					D_{eff}
			ø /mm/	length /mm/		/gr/	/%/			Free /mg/l/	Total /mg/l/	Bound /mg/l/	Cl/C cem. /%/	OH, free /equiv/ l/	$/m^2/s$ $x10^{-12}$
1	P;P	0.4	19.5	30	100	-		66	0-5	10				1.2	
									5-8	10				0.87	
									8-11	20				-	
									11-14	40				-	
									14-19	800				1.1	
									19-21	8.000				-	
									21-24	15.000				0.11	5-70
									24-30	18.000				-	
2								543	0-8	4.400	14.000	9.000	0.39	1.4	
									5-13						
									12-15	5.600					
									13-19		24.000		0.65		
									17-23	8.400				0.99	1-5
									22-30	8.400	30.000	21.000	0.84		
3	P;P	0.4	19.5	50	100	-		447	0-8	20	1.000	1.000	0.03		
									5-10	20			-	0.82	
									10-14	-			-		
									14-19	600			-		
									19-23	2.600	12.000	9.000	0.34	-	
									23-28	5.000				0.71	
									28-33	8.000	20.000	12.000	0.55	0.35	
									33-36	12.000				0.34	
									36-40	-			-	-	
									40-45	-			-	-	
									46-50	12.000	29.000	17.000	0.79	0.10	3-10

CODE: P P = Slite Portland cement; paste
P M = " ; mortar
B P = Slag cement ; paste
B M = " ; mortar

Table A, continued

Sample nr	Cement type	w/c	Dimension		Climate before test RH /%/	Weight in the drying period		Time /days	Position from inside /mm/	Measured concentration, chloride					D_{eff}
			ϕ /mm/	length /mm/		/gr/	/%/			Free /mg/1/	Total /mg/1/	Bound /mg/1/	Cl/C cem. /%/	OH, free /equiv/ 1/	$/m^2/s$ $x10^{-12}$
1	P;P	0.4	19.5	30	100	-		66	0-5	10				1.2	
									5-8	10				0.87	
									8-11	20				-	
									11-14	40				-	
									14-19	800				1.1	
									19-21	8.000				-	
									21-24	15.000				0.11	5-70
									24-30	18.000				-	
2								543	0-8	4.400	14.000	9.000	0.39	1.4	
									5-13						
									12-15	5.600					
									13-19		24.000		0.65		
									17-23	8.400				0.99	1-5
									22-30	8.400	30.000	21.000	0.84		
3	P;P	0.4	19.5	50	100	-		447	0-8	20	1.000	1.000	0.03		
									5-10	20			-	0.82	
									10-14	-			-		
									14-19	600			-		
									19-23	2.600	12.000	9.000	0.34	-	
									23-28	5.000				0.71	
									28-33	8.000	20.000	12.000	0.55	0.35	
									33-36	12.000				0.34	
									36-40	-			-	-	
									40-45	-			-	-	
									46-50	12.000	29.000	17.000	0.79	0.10	3-10

Table A, continued

Sample nr	Cement type	w/c	Dimension		Climate before test RH /%/	Weight in the drying period		Time /days	Position from inside /mm/	Measured concentration, chloride					D_{eff}
			ϕ /mm/	length /mm/		/gr/	/%/			Free /mg/l/	Total /mg/l/	Bound /mg/l/	Cl/C cem. /%/	OH, free /equiv/ l/	/m^2/s x10^{-12}
1	P;P	0.60	19.5	30	100			71	0-5	800				0.27	
									5-9						
									9-12	2.700				0.20	
									12-17						
									17-21	10.000				0.11	
									21-26	15.000				0.11	
									26-30	17.000				0.08	12-14
2								439	0-7	6.400	33.000	27.000	1.53	0.16	
									7-11						
									11-14						
									14-19						
									19-24	7.000	34.000	27.000	1.58	0.14	
									24-30						6
									xx)	18.000				0.04	

xx) Test solution

Table A, continued

Sample nr	Cement type	w/c	Dimension		Climate before test RH /%/	Weight in the drying period		Time /days	Position from inside /mm/	Measured concentration, chloride					D_{eff}
			ϕ /mm/	length /mm/		/gr/	/%/			Free /mg/l/	Total /mg/l/	Bound /mg/l/	Cl/C cem. /%/	OH, free /equiv/ l/	$/m^2/s$ $x10^{-12}$
3	P;P	0.60	19.5	50	100			442	0-5	1.900	9.000	7.000	0.43	0.36	
									5-8						
									8-10	2.400	10.000	8.000	0.47		
									10-16						
									16-19	2.800				0.32	
									19-23		12.000		0.55		
									23-27	3.400	13.000	10.000	0.62		
									27-32						
									32-33						
									33-36	4.300				0.27	
									36-39						
									39-46		18.000		0.84		
									46-50	5.400	20.000	15.000	0.91	0.35	3-8

Table A, continued

Sample nr	Cement type	w/c	Dimension		Climate before test RH /%/	Weight in the drying period		Time /days	Position from inside /mm/	Measured concentration, chloride					D_{eff}
			ϕ /mm/	length /mm/		/gr/	/%/			Free /mg/l/	Total /mg/l/	Bound /mg/l/	Cl/C cem. /%/	OH, free /equiv/ l/	/m^2/s x10^{-12}
1	P;M	0.40	19.5	30	100			66	0-5						
									5-9						
									7-9	30					
									9-12	-					
									12-17	30				0.54	
									17-21	300				0.42	
									21-25	3.100				0.57	
									25-30	17.000					1-3
2								543	0-6	5.300	43.000	38.000	1.19		
									6-11						
									6-14						
									14-20	6.400	49.000	43.000	1.37	0.67	
									21-25	7.400					
									21-30	14.200	74.000	60.000	2.06	0.39	0.8-4
3	P;M	0.40	19.5	50	100			543	0-5	1.300	6.000	5.000	0.16		
									5-16						
									14-22	1.100	11.000	10.000	0.31		
									21-27						
									26-32	5.000				1.0	
									32-42						
									42-45	14.000				0.39	
									45-50	15.000	85.000	70.000	2.3		3-5

Table A, continued

Sample nr	Cement type	w/c	Dimension		Climate before test RH /%/	Weight in the drying period		Time /days	Position from inside /mm/	Measured concentration, chloride					D_{eff}
			ø /mm/	length /mm/		/gr/	/%/			Free /mg/l/	Total /mg/l/	Bound /mg/l/	Cl/C cem. /%/	OH, free /equiv/ l/	$/m^2/s$ $x10^{-12}$
1	P;M	0.60	19.5	30	100			71	0-6	60				0.32	
									6-10	660					
									10-13	1.800				0.18	
									13-18						
									18-22	7.000				0.18	
									22-26	14.000				0.09	
									26-30	18.000				0.08	7-10
2								539	0-8	7.700	40.000	32.000	1.86	0.54	
									8-10	8.400				0.24	
									8-16						
									16-23	10.000	47.000	37.000	2.18	0.23	
									23-28	10.000				0.19	4-6
3	P;M	0.60	19.5	30	100			428	0-5	11.000	37.000	26.000	1.73	0.55	
									5-11						
									11-16					0.49	
									16-19						
									19-24	11.000					
									24-26						
									27-30	12.000				0.12	5-11
4				50	100			428	0-7	2.600	13.000	10.000	0.61	0.17	
									7-11						
									11-16	4.000				0.19	
									16-24						
									24-30	7.500	29.000	21.000	1.36	0.30	
									30-34						
									34-40						
									40-44						
									44-47						
									47-50	12.000				0.15	7-12

Table A, continued

Sample nr	Cement type	w/c	Dimension		Climate before test RH /%/	Weight in the drying period		Time /days	Position from inside /mm/	Measured concentration, chloride					D_{eff}
			ø /mm/	length /mm/		/gr/	/%/			Free /mg/l/	Total /mg/l/	Bound /mg/l/	Cl/C cem. /%/	OH, free /equiv/ l/	$/m^2/s$ $x10^{-12}$
1	P;P	0.40	19.5	30	80	1.189	6.5	70	0-5	70				1.1	
									5-9	-				-	
									7-10	-				-	
									14-9	-				-	
									13-15	2.700				-	
									15-19	6.400				1.0	
									19-22						
									25-30	22.000				0.23	
2						1.202	6.6	510	0-3	-				-	
									3-6	6.200	21.000	15.000	0.59	0.47	
									6-9	4.300				-	
									9-13	7.000	24.000	17.000	0.65	-	
									13-15	8.000	27.000	17.000	0.74	-	
									15-19	-	27.000		0.74		
									19-21	13.200				-	
									21-23	-	34.000		0.94		
									23-25	14.800				0.34	
									25-30	-	41.000		1.12		

Table A, continued

Sample nr	Cement type	w/c	Dimension		Climate before test RH /%/	Weight in the drying period		Time /days	Position from inside /mm/	Measured concentration, chloride					D_{eff}
			ø /mm/	length /mm/		/gr/	/%/			Free /mg/l/	Total /mg/l/	Bound /mg/l/	Cl/C cem. /%/	OH, free /equiv/ l/	$/m^2/s$ $x10^{-12}$
1	P;P	0.60	19.5	30	80	2.265	14.4	63	0-7	3.200				0.24	
									7-11	4.200				0.29	
									11-15	5.600				0.30	
									15-21	6.800					
									21-25	15.000				0.11	
									25-30					0.20	
2						2.194	13.8	454	0-4	14.000	44.000	30.000	2.02	0.29	
									4-10						
									10-15						
									15-20						
									20-25						
									25-30	17.000	61.000	44.000	2.80	0.23	
									xx)	19.000					

xx) Test solution

Table A, continued

Sample nr	Cement type	w/c	Dimension		Climate before test RH /%/	Weight in the drying period		Time /days	Position from inside /mm/	Measured concentration, chloride					D_{eff}
			ϕ /mm/	length /mm/		/gr/	/%/			Free /mg/l/	Total /mg/l/	Bound /mg/l/	Cl/C cem. /%/	OH, free /equiv/ l/	/m^2/s x10^{-12}
1	P;M	0.40	19.5	30	80	0.474	2.2	510	0-9	6.200					
									6-12		46.000		1.29		
									10-13	8.000					
									13-19						
									19-24		92.000		2.57		
									24-30	17.000	110.000			0.25	
									27-30				3.16		
1	P;M	0.60	19.5	30	80	0.940	4.6	63	0-6	160					
									6-10	850				0.42	
									8-12	2.000				0.42	
									12-16	4.500				0.47	
									16-21	9.500				0.29	
									21-24	17.500				0.05	
									24-30	18.500				0.11	
2						0.994	4.9	510	0-6		53.000		2.48		
									5-12						
									12-14		63.000		2.93		
									14-18						
									18-22		76.000		3.56		
									22-26						
									26-30	18.500	74.000	55.000	3.46	0.41	

Table A, continued

Sample nr	Cement type	w/c	Dimension		Climate before test RH /%/	Weight in the drying period		Time /days	Position from inside /mm/	Measured concentration, chloride					D_{eff}
			ø /mm/	length /mm/		/gr/	/%/			Free /mg/l/	Total /mg/l/	Bound /mg/l/	Cl/C cem. /%/	OH, free /equiv/ l/	$/m^2/s$ $x10^{-12}$
1	P;P	0.40	19.5	30	50	1.939	10.7	69	0-6	1.200					
									8-11	6.500					
									11-16	12.000				0.51	
									16-20	14.000				0.36	
									20-24	18.500				0.26	
									24-26						
									26-30						
2						1.833	10.0	552	0-6	12.000	29.000	17.000	0.81	2.0	
									4-9						
									8-15	13.500					
									19-23						
									23-27	16.000	39.000	23.000	1.07	0.64	
									27-30						
3	P;P	0.40	19.5	50	50	3.074	10.3	552	0-4	2.200	10.000	8.000	0.27	1.7	
									4-11		11.000		0.29		
									8-16	5.500	15.000	9.000	0.41	1.8	
									16-19		17.000		0.47		
									18-23	8.400					
									22-28						
									28-31	11.000	24.000	13.000	0.67	1.2	
									32-43						
									41-47	18.000	32.000	14.000	0.89	0.85	
									47-50						

Table A, continued

Sample nr	Cement type	w/c	Dimension		Climate before test RH /%/	Weight in the drying period		Time /days	Position from inside /mm/	Measured concentration, chloride					D_{eff}
			ϕ /mm/	length /mm/		/gr/	/%/			Free /mg/l/	Total /mg/l/	Bound /mg/l/	Cl/C cem. /%/	OH, free /equiv/ l/	/m^2/s x10^{-12}
1	P;P	0.60	19.5	30	50	2.906	18.3	61	0-7	11.500				0.24	
									7-13	12.500				0.19	
									13-17	12.500				0.16	
									17-23	18.500				0.12	
									23-30						
2						2.978	19.1	453	0-4	13.000	37.000	24.000	1.70	0.19	
									4-8						
									8-13						
									13-18						
									18-28	15.000	50.000	35.000	2.31	0.12	
									23-30						
									xx)	18.000				0.05	
3	P;P	0.60	19.5	50	50	4.990	18.8	456	0-4	12.500	28.000	16.000	1.28	0.18	
									4-9		31.000		1.44	0.15	
									9-13						
									13-18						
									18-22						
									22-27						
									27-31						
									31-35						
									35-41						
									41-45		37.000		1.69		
									45-50	13.000	38.000	25.000	1.75	0.15	

xx) Test solution

Table A, continued

Sample nr	Cement type	w/c	Dimension		Climate before test RH /%/	Weight in the drying period		Time /days	Position from inside /mm/	Measured concentration, chloride					D_{eff}
			ϕ /mm/	length /mm/		/gr/	/%/			Free /mg/l/	Total /mg/l/	Bound /mg/l/	Cl/C cem. /%/	OH, free /equiv/ l/	$/m^2/s$ $x10^{-12}$
1	P;M	0.40	19.5	30	50	0.768	3.54	509	0-4	x)	26.000		0.72		
									4-7	"	39.000		1.09		
									11-13	"	41.000		1.14		
									20-30	"	57.000		1.59		
2	P;M	0.40	19.5	50	50	1.405	3.95	447	2-8	"	1.000		0.04		
									26-30	"	30.000		0.83		
									41-50	"	63.000		1.75		

x) Dry

Table A, continued

Sample nr	Cement type	w/c	Dimension		Climate before test RH /%/	Weight in the drying period		Time /days	Position from inside /mm/	Measured concentration, chloride					D_{eff}
			ϕ /mm/	length /mm/		/gr/	/%/			Free /mg/l/	Total /mg/l/	Bound /mg/l/	Cl/C cem. /%/	OH, free /equiv/ l/	$/m^2/s$ $x10^{-12}$
1	P, M	0.60	19.5	30	50	1.284	6.3	61	0-5	2.900				0.23	
									4-10	4.300				0.26	
									10-16	7.400				0.19	
									16-22						
									20-24	16.500				0.12	
									24-30	16.500				0.08	
2						1.309	6.4	552	0-4	14.000	51.000	37.000	2.37	0.85	
									4-8						
									8-12	14.000	51.000	37.000	2.37	0.58	
									11-19						
									19-21					0.54	
									23-30	15.000	93.000	78.000	4.37	0.30	
3	P, M	0.60	19.5	50	50	2.076	6.2	552	0-7	5.900	26.000	20.000	1.23	0.84	
									7-11	7.200				0.71	
									11-18						
									17-25						
									23-27	7.700	34.000	26.000	1.58	0.73	
									27-33						
									33-41	8.000				0.40	
									40-46	8.700	42.000	33.000	1.95	0.90	
									45-50	8.700				0.69	
									xx)	20.000					

xx) Test solution

Table A, continued

Sample nr	Cement type	w/c	Dimension		Climate before test RH /%/	Weight in the drying period		Time /days	Position from inside /mm/	Measured concentration, chloride					D_{eff}
			ϕ /mm/	length /mm/		/gr/	/%/			Free /mg/l/	Total /mg/l/	Bound /mg/l/	Cl/C cem. /%/	OH, free /equiv/ l/	/m^2/s x10^{-12}
1	B;M	0.40	19.5	30	100			455	0-5	x)	1.600		0.05		
									11-19	x)	2.800		0.09		
									25-29	x)	63.000		1.99		
2				50				455	0-4		1.000		0.03		
									4-7						
									7-11						
									11-15		1.000		0.03		
									16-22						
									23-32	250	2.000	2.000	0.06	0.16	
									32-39	2.400	4.000	2.000	0.12	0.14	
									37-45	4.800				0.13	
									45-50	20.000	53.000	33.000	1.67	0.13	0.6-1
1	B;P	0.40	19.5	30	100			455	0-6		600		0.02		
									6-9						
									9-17	200	900	700	0.03	0.27	
									17-24	1.400	2.400	1.000	0.08	0.25	
									24-30	8.000	15.000	7.000	0.48	0.14	0.3-0.7

x) Dry

Table A, continued

Sample nr	Cement type	w/c	Dimension		Climate before test RH /%/	Weight in the drying period		Time /days	Position from inside /mm/	Measured concentration, chloride					D_{eff}
			ϕ /mm/	length /mm/		/gr/	/%/			Free /mg/l/	Total /mg/l/	Bound /mg/l/	Cl/C cem. /%/	OH, free /equiv/ l/	$/m^2/s$ $x10^{-12}$
1	B;M	0.60	19.5	30	100			455	0-8		600		0.03		
									8-11						
									11-16						
									16-20	3.500				0.07	
									20-26	10.000	10.000	0	0.49	0.12	
									26-30	14.000	24.000	10.000	1.22	0.04	0.5-1
2				50				455	0-6	200	600	400	0.03	0.13	
									6-12						
									11-16	250				0.12	
									16-20						
									20-23	250				0.12	
									23-25		800		0.04		
									25-31	140				0.11	
									31-36	450				0.13	
									36-46	3.400					
									41-50	16.000	34.000	18.000	1.70	0.04	0.5-1

TABLE B. Results, evaporation tests, chapter 5.4.

Sample nr	Cement type	w/c	Dimension		Climate before test RH /%/	Weight in the drying period /gr/	Evaporation		Measured concentration					
			ϕ /mm/	length /mm/			Time /days/	Amount /gr/	Position from solution	Free /mg/l/	Total /mg/l/	Bound /mg/l/	Cl/C /%/	OH Free
20-1	PP	0.40	19.5	20	100	-	4	0.103	-	-	-	-	-	-
	PP	0.40	19.5	20	100	-	45	0.794	-	-	-	-	-	-
	PP	0.40	19.5	20	100	-	70	1.152	0-5	19.000				
									6-9	8.600				0.36
									9-14	6.800				
									14-17	50				
									17-20	*				
									xx)	19.000				0.17
20-2	PP	0.40	19.5	20	100	-	4	0.095	-	-	-	-	-	-
							45	0.676	-	-	-	-	-	-
							127	1.606	-	-	-	-	-	-
40-1	PP	0.40	19.5	40	100	-	4	0.117	-	-	-	-	-	-
							45	0.717	-	-	-	-	-	-
							127	1.558	-	-	-	-	-	-
40-2	PP	0.40	19.5	40	100	-	4	0.128	-	-	-	-	-	-
							45	0.738	-	-	-	-	-	-
							127	1.584	-	-	-	-	-	-
40-3							4	0.088	-	-	-	-	-	-
							45	0.639	-	-	-	-	-	-
							127	1.429	-	-	-	-	-	-
							535	5.128	-	-	-	-	-	-

*Dry
xx) Test solution
CODE: P P = Slite Portland cement; paste
P M = " ; mortar
B P = Slag cement ; paste
B M = " ; mortar
OH_{Free} = /equiv/ℓ/

Table B, continued

Sample nr	Cement type	w/c	Dimension		Climate before test RH /%/	Weight in the drying period /gr/	Evaporation		Measured concentration					
			ϕ /mm/	length /mm/			Time /days/	Amount /gr/	Position from solution	Free /mg/l/	Total /mg/l/	Bound /mg/l/	Cl/C /%/	OH Free
20-1	P M	0.40	19.5	20	100	-	4	0.161	-	-	-	-	-	-
							45	0.496	-	-	-	-	-	-
							72	0.670	0-5	15.000				0.07
									5-6	4.200				0.40
									6-11					
									11-13	1.360				
									13-17					
									17-20					
										18.000				0.07
20-2	P M	0.40	19.5	20	100	-	4	0.050	-	-	-	-	-	-
							45	0.367	-	-	-	-	-	-
							127	0.885	-	-	-	-	-	-
							4	0.101	-	-	-	-	-	-
							45	0.435	-	-	-	-	-	-
							127	0.986	-	-	-	-	-	-
							4	0.083	-	-	-	-	-	-
							45	0.805	-	-	-	-	-	-
							127	1.106	-	-	-	-	-	-

Table B, continued

Sample nr	Cement type	w/c	Dimension		Climate before test RH /%/	Weight in the drying period /gr/	Evaporation		Measured concentration					
			ϕ /mm/	length /mm/			Time /days/	Amount /gr/	Position from solution	Free /mg/l/	Total /mg/l/	Bound /mg/l/	Cl/C /%/	OH Free
40-1	P M	0.40	19.5	40	100	-	4	0.061	-	-	-	-	-	-
							45	0.372	-	-	-	-	-	-
							127	0.833	-	-	-	-	-	-
*40-2	P M	0.40	19.5	40	100	-	4	0.232		-	-	-	-	-
							45	0.600	-	-	-	-	-	-
							127	1.189	-	-	-	-	-	-
							535	3.738	-	-	-	-	-	-
40-3	P M	0.40	19.5	40	100	-	4	0.064	-	-	-	-	-	-
							45	0.420	-	-	-	-	-	-
							127	0.954	-	-	-	-	-	-
40-4	P M	0.40	19.5	40	100	-	4	0.066	-	-	-	-	-	-
							45	0.434	-	-	-	-	-	-
							127	0.994	-	-	-	-	-	-

*Salt deposit

Table B, continued

Sample nr	Cement type	w/c	Dimension		Climate before test RH /%/	Weight in the drying period /gr/	Evaporation		Measured concentration					
			ϕ /mm/	length /mm/			Time /days/	Amount /gr/	Position from solution	Free /mg/l/	Total /mg/l/	Bound /mg/l/	Cl/C /%/	OH Free
20-1	Pp	0.60	19.5	20	100	-	2	0.177	-	-	-	-	-	-
							44	5.889	-	-	-	-	-	-
							x) 69	6.588	0-4	18.000				0.20
									4-5	20.000				0.14
									5-9					
									9-12	33.000				0.26
									12-14					
									14-17	62.000				0.44
									17-20	92.000				1.96
									xx)	18.000				0.15
20-2	Pp	0.60	19.5	20	100	-	2	0.171	-	-	-	-	-	-
							44	4.149	-	-	-	-	-	-
							126	9.636	-	-	-	-	-	-
20-3							2	0.202	-	-	-	-	-	-
							44	4.904	-	-	-	-	-	-
							126	9.854	-	-	-	-	-	-
20-4							2	0.145	-	-	-	-	-	-
							44	3.989	-	-	-	-	-	-
							126	8.407	-	-	-	-	-	-

x) Crackled
xx) Salt solution

Table B, continued

Sample nr	Cement type	w/c	Dimension		Climate before test RH /%/	Weight in the drying period /gr/	Evaporation		Measured concentration					
			ϕ /mm/	length /mm/			Time /days/	Amount /gr/	Position from solution	Free /mg/l/	Total /mg/l/	Bound /mg/l/	Cl/C /%/	OH Free
40-1	Pp	0.60	19.5	40	100	-	2	0.137	-	-	-	-	-	-
							44	1.828	-	-	-	-	-	-
							126	4.578	-	-	-	-	-	-
40-2							2	0.161	-	-	-	-	-	-
							44	1.763	-	-	-	-	-	-
							126	4.304	-	-	-	-	-	-
							2	0.136	-	-	-	-	-	-
							44	1.642	-	-	-	-	-	-
							126	3.959	-	-	-	-	-	-
							534	14.088	0-11	-	-	-	-	-
									10-15					
									13-18					
									18-27					
									22-26	41.000	-	-	-	1.15
									27-37	58.000	-	-	-	1.63
									37-40	-	-	-	-	-
									xx)					0.20
40-4							2	0.215						
							44	2.171						
							126	5.534						

xx) Test solution

Table B, continued

Sample nr	Cement type	w/c	Dimension		Climate before test RH /%/	Weight in the drying period /gr/	Evaporation		Measured concentration					
			ϕ /mm/	length /mm/			Time /days/	Amount /gr/	Position from solution	Free /mg/l/	Total /mg/l/	Bound /mg/l/	Cl/C /%/	OH Free
20-1	PM	0.60	19.5	20	100	-	1	0.036	-	-	-	-	-	-
							43	1.187	-	-	-	-	-	-
							68	1.701	0-6	17.000				0.11
									6-9	18.000				0.26
									9-12	20.000				
									12-16	18.000				0.26
									16-18	26.000				0.39
									18-20	44.000				
									xx)	18.000				0.11
20-2							2	0.064	-	-	-	-	-	-
							44	1.183	-	-	-	-	-	-
							126	3.009	-	-	-	-	-	-
20-3							2	0.070	-	-	-	-	-	-
							44	1.289	-	-	-	-	-	-
							126	3.042	-	-	-	-	-	-
20-4							2	0.085	-	-	-	-	-	-
							44	1.233	-	-	-	-	-	-
							126	2.878	-	-	-	-	-	-

xx) Test solution

Table B, continued

Sample nr	Cement type	w/c	Dimension		Climate before test RH /%/	Weight in the drying period /gr/	Evaporation		Measured concentration					
			ø /mm/	length /mm/			Time /days/	Amount /gr/	Position from solution	Free /mg/l/	Total /mg/l/	Bound /mg/l/	Cl/C /%/	OH Free
40-1	P M	0.60	19.5	40	100	-	2	0.080	-	-	-	-	-	-
							44	0.971	-	-	-	-	-	-
							126	2.309	-	-	-	-	-	-
40-2							2	0.060	-	-	-	-	-	-
							44	0.978	-	-	-	-	-	-
							126	2.432	-	-	-	-	-	-
40-3							2	0.077	-	-	-	-	-	-
							44	1.129	-	-	-	-	-	-
							126	2.770	-	-	-	-	-	-
							534	9.288	-	-	-	-	-	-
									0-9	31.000				0.31
									3-7	31.000				0.30
									7-12	29.000				
									10-16	31.000				0.57
									15-23	33.000				0.58
									21-25	42.000				0.42
									25-32	58.000				
									30-34	100.000				
									34-40					
40-4							2	0.080						
							44	0.977						
							126	2.311						

Table B, continued

Sample nr	Cement type	w/c	Dimension		Climate before test RH /%/	Weight in the drying period		Evaporation		Measured concentration					
			ø /mm/	length /mm/		/gr/	/%/	Time /days/	Amount /gr/	Position from solution	Free /mg/l/	Total /mg/l/	Bound /mg/l/	Cl/C /%/	OH Free
21	P;P	0.40	19.5	20	80	0.785	6.6	4	0.055						
								48	0.971						
								129	2.509						
								139	2.663	0-2	20.000				
										2-6					
										6-10	16.000				
										10-13	13.000				
										13-17	10.800				
										17-20	6.000				
										xx)					0.10
22	P;P	0.40	19.5	20	80	0.814	6.8	4	0.096						
								48	1.153						
								129	2.782						
23	P;P	0.40	19.5	20	80	0.763	6.4	4	0.177						
								48	1.168						
								129	2.625						
41	P;P	0.40	19.5	40	80	1.539	6.3	4	0.017						
								48	0.576						
								129	1.912						

xx) Test solution

Table B, continued

Sample nr	Cement type	w/c	Dimension		Climate before test RH /%/	Weight in the drying period		Evaporation		Measured concentration					
			ϕ /mm/	length /mm/		/gr/	/%/	Time /days/	Amount /gr/	Position from solution	Free /mg/l/	Total /mg/l/	Bound /mg/l/	Cl/C /%/	OH Free
42	P P	0.40	19.5	40	80	1.577	6.5	4	0.014						
								48	0.525						
								129	1.891						
43						1.532	6.3	4	0.020						
								48	0.679						
								129	1.975						
21	P P	0.60	19.5	20	80	1.569	15.2	4	0.842						
								48	3.695						
								129	6.272						
								165	9.490	0-2	20.000				
										2-6					
										6-10	43.000				
										10-14					
										14-16	60.000				
										16-18	55.000				
										18-20					
										xx)					0.04
22	P P	0.60	19.5	20	80	1.545	14.9	4	0.823						
								48	4.066						
								129	6.330						

xx) Test solution

Table B, continued

Sample nr	Cement type	w/c	Dimension		Climate before test RH /%/	Weight in the drying period		Evaporation		Measured concentration					
			ø /mm/	length /mm/		/gr/	/%/	Time /days/	Amount /gr/	Position from solution	Free /mg/l/	Total /mg/l/	Bound /mg/l/	Cl/C /%/	OH Free
23	P P	0.60	19.5	20	80	1.285	11.8	4	0.563						
								48	2.805						
								129	6.177						
41	P;P	0.60	19.5	40	80	3.052	14.2	4	0.506						
								48	2.751						
								129	4.979						
42	P;P	0.60	19.5	40	80	2.932	13.6	4	0.426						
								48	2.728						
								129	4.497						
43	P;P	0.60	19.5	40	80	2.917	13.6	4	0.410						
								48	2.305						
								129	4.082						
21	P;M	0.40	19.5	20	80	0.297	2.1	4	0.019						
								48	0.288						
								129	0.952						
								139	1.015	0-6	18.500				
										6-13					
										13-16					
										16-20					
										xx)					0.04

xx) Test solution

Table B, continued

Sample nr	Cement type	w/c	Dimension		Climate before test	Weight in the drying period		Evaporation		Measured concentration					
			ϕ /mm/	length /mm/	RH /%/	/gr/	/%/	Time /days/	Amount /gr/	Position from solution	Free /mg/l/	Total /mg/l/	Bound /mg/l/	Cl/C /%/	OH Free
22	P;M	0.40	19.5	20	80	0.294	2.0	4	0.019						
								48	0.254						
								129	0.863						
23	P;M	0.40	19.5	20	80	0.312	2.2	4	0.018						
								48	0.250						
								129	0.858						
41	P;M	0.40	19.5	40	80	0.638	2.2	4	0.019						
								48	0.215						
								129	0.726						
42	P;M	0.40	19.5	40	80	0.587	2.0	4	0.018						
								48	0.217						
								129	0.741						
43	P;M	0.40	19.5	40	80	0.564	1.9	4	0.018						
								48	0.210						
								129	0.696						

Table B, continued

Sample nr	Cement type	w/c	Dimension		Climate before test RH /%/	Weight in the drying period		Evaporation		Measured concentration					
			ø /mm/	length /mm/		/gr/	/%/	Time /days/	Amount /gr/	Position from solution	Free /mg/l/	Total /mg/l/	Bound /mg/l/	Cl/C /%/	OH Free
21	P;M	0.60	19.5	20	80	0.608	4.5	4	0.316						
								48	1.770						
								129	3.349						
								165	3.895	0-4	27.000				
										4-9					
										7-12	33.000				
										12-14					
										14-17	45.000				
										17-20	50.000				
										xx)					0.05
22	P;M	0.60	19.5	20	80	0.633	4.6	4	0.342						
								48	1.850						
								129	3.522						
23	P;M	0.60	19.5	20	80	0.623	4.5	4	0.109						
								48	1.004						
								129	2.298						
41	P;M	0.60	19.5	40	80	1.369	5.0	4	0.162						
								48	1.136						
								129	2.422						

xx) Test solution

Table B, continued

Sample nr	Cement type	w/c	Dimension		Climate before test RH /%/	Weight in the drying period		Evaporation		Measured concentration					
			ϕ /mm/	length /mm/		/gr/	/%/	Time /days/	Amount /gr/	Position from solution	Free /mg/l/	Total /mg/l/	Bound /mg/l/	Cl/C /%/	OH Free
42	P;M	0.60	19.5	40	80	1.295	4.8	4 48 129	0.107 1.017 2.208						
43	P;M	0.60	19.5	40	80	1.281	4.7	4 48 129	0.036 1.285 2.637						

Table B, continued

Sample nr	Cement type	w/c	Dimension		Climate before test RH /%/	Weight in the drying period		Evaporation		Measured concentration					
			ϕ /mm/	length /mm/		/gr/	/%/	Time /days/	Amount /gr/	Position from solution	Free /mg/l/	Total /mg/l/	Bound /mg/l/	Cl/C /%/	OH Free
24	P;P	0.4	19.5	20	50	1.272	10.7	42	2.756						
								62	3.423						
								64	3.513	0-5	18.000	54.000	36.000	1.50	0.12
										5-8	22.000	52.000	30.000	1.44	0.12
										8-11	22.000	50.000	28.000	1.39	0.27
										11-13	29.000	49.000	20.000	1.35	0.37
										13-16	41.000	58.000	17.000	1.60	0.48
										16-20	52.000	68.000	16.000	1.88	1.06
										xx)	18.000				0.17
25						1.181	9.9	42	2.113						
								62	2.680						
26						1.259	10.6	42	2.215						
								62	2.810						
27						1.229	10.4	42	2.260						
								62	2.888						
28						1.239	10.4	42	2.192						
								62	2.805						
29						1.225	10.3	42	2.234						
								62	2.847						

xx) Test solution

Table B, continued

Sample nr	Cement type	w/c	Dimension		Climate before test RH /%/	Weight in the drying period		Evaporation		Measured concentration					
			ϕ /mm/	length /mm/		/gr/	/%/	Time /days/	Amount /gr/	Position from solution	Free /mg/l/	Total /mg/l/	Bound /mg/l/	Cl/C /%/	OH Free
44	P;P	0.40	19.5	40	50	2.459	10.0	42	2.058						
								62	2.696						
								124	4.227						
45						2.499	10.4	42	2.190						
								62	2.825						
								124	4.370						
46						2.471	10.3	42	2.091						
								62	2.730						
								124	4.260						
47						2.467	10.1	42	2.089						
								62	2.706						
								124	4.171						
48						2.541	10.5	42	2.224						
								62	2.882						
								124	4.447						
49						2.526	10.5	42	2.286						
								62	2.916						
								124	4.417						

Table B, continued

Sample nr	Cement type	w/c	Dimension		Climate before test RH /%/	Weight in the drying period		Evaporation		Measured concentration					
			ϕ /mm/	length /mm/		/gr/	/%/	Time /days/	Amount /gr/	Position from solution	Free /mg/l/	Total /mg/l/	Bound /mg/l/	Cl/C /%/	OH Free
24	P;P	0.60	19.5	20	50	2.017	19.3	42	4.078						
								62	6.129						
								64	6.305	0-4	21.000	44.000	23.000	2.02	0.13
										4-7	25.000	52.000	27.000	2.37	0.12
										7-9	27.000				0.13
										9-13	31.000	63.000	32.000	2.92	0.18
										13-15	44.000	58.000	14.000	2.66	0.27
										15-20	64.000	83.000	19.000	3.81	0.49
										xx)	20.000				0.14
25						1.955	18.6	42	3.889						
								62	5.989						
26						2.094	19.6	42	2.701						
								62	4.534						
27						2.009	19.3	42	3.780						
								62	5.815						
28						1.800	16.0	42	3.762						
								62	5.593						
29						2.004	20.0	42	4.544						
								62	6.910						

xx) Test solution

Table B, continued

Sample nr	Cement type	w/c	Dimension		Climate before test RH /%/	Weight in the drying period		Evaporation		Measured concentration					
			ϕ /mm/	length /mm/		/gr/	/%/	Time /days/	Amount /gr/	Position from solution	Free /mg/l/	Total /mg/l/	Bound /mg/l/	Cl/C /%/	OH Free
44	P;P	0.60	19.5	40	50	3.965	19.0	42	5.242						
								62	8.183						
								124	13.625						
45						3.896	18.6	42	4.137						
								62	6.458						
								124	11.180						
46						3.941	18.5	42	2.850						
								62	4.576						
								124	8.301						
48						3.870	18.0	42	4.325						
								62	6.533						
								124	10.998						
49						3.912	18.8	42	3.826						
								62	5.963						
								124	9.654						

Table B, continued

Sample nr	Cement type	w/c	Dimension		Climate before test RH /%/	Weight in the drying period		Evaporation		Measured concentration					
			ø /mm/	length /mm/		/gr/	/%/	Time /days/	Amount /gr/	Position from solution	Free /mg/l/	Total /mg/l/	Bound /mg/l/	Cl/C /%/	OH Free
24	P;M	0.4	19.5	20	50	0.490	3.4	41	0.819						
								60	1.056						
								63	1.091	0-5		53.000		1.48	
										5-8	18.000	43.000	25.000	1.19	0.10
										8-11					
										11-14					
										14-18	10.000	25.000	15.000	0.71	0.55
										18-20	12.000	23.000	11.000	0.63	
										xx)	18.000				0.07
25						0.541	3.8	41	0.841						
								60	1.090						
								122	1.814						
26						0.552	3.9	41	0.860						
								60	1.111						
								122	1.835						
27						0.507	3.5	41	0.726						
								60	0.956						
								122	1.626						
28						0.488	3.4	41	0.820						
								60	1.075						
								122	1.788						

xx) Test solution

Table B, continued

Sample nr	Cement type	w/c	Dimension		Climate before test RH /%/	Weight in the drying period		Evaporation		Measured concentration					
			ø /mm/	length /mm/		/gr/	/%/	Time /days/	Amount /gr/	Position from solution	Free /mg/l/	Total /mg/l/	Bound /mg/l/	Cl/C /%/	OH Free
44	P;M	0.40	19.5	40	50	1.015	3.5	41	0.475						
								60	0.686						
								122	1.281						
45						1.034	3.5	41	0.591						
								60	0.842						
								122	1.536						
46						1.018	3.6	41	0.532						
								60	0.785						
								122	1.479						
47						1.035	3.6	41	0.570						
								60	0.823						
								122	1.505						
48						1.032	3.6	41	0.437						
								60	0.653						
								122	1.252						
49						0.974	3.4	41	0.284						
								60	1.450						
								122	1.944						

Table B, continued

Sample nr	Cement type	w/c	Dimension		Climate before test RH /%/	Weight in the drying period		Evaporation		Measured concentration					
			ϕ /mm/	length /mm/		/gr/	/%/	Time /days/	Amount /gr/	Position from solution	Free /mg/l/	Total /mg/l/	Bound /mg/l/	Cl/C /%/	OH Free
24	P;M	0.60	19.5	20	50	0.828	6.0	41	1.335						
								60	2.020						
								62	2.111	0-4		39.000		1.85	
										0-7	18.000	42.000	24.000	1.95	0.08
										7-9		44.000		2.06	
										9-12	23.000				0.26
										12-14		46.000		2.14	
										14-17	33.000				0.71
										17-20	37.000	47.000	10.000	2.20	1.46
										xx)	18.000				0.11
25						0.858	6.4	41	2.035						
								60	2.896						
								122	5.006						
26						0.854	6.3	41	1.908						
								60	2.755						
								122	4.768						
27						0.877	6.5	41	1.652						
								60	2.442						
								122	4.381						
28						0.832	6.0	41	1.723						
								60	2.581						
								122	4.628						
29						0.874	6.4	41	1.798						
								60	2.625						
								122	4.553						

xx) Test solution

Table B, continued

Sample nr	Cement type	w/c	Dimension		Climate before test RH /%/	Weight in the drying period		Evaporation		Measured concentration					
			ϕ /mm/	length /mm/		/gr/	/%/	Time /days/	Amount /gr/	Position from solution	Free /mg/l/	Total /mg/l/	Bound /mg/l/	Cl/C /%/	OH Free
44	P;M	0.60	19.5	40	50	1.687	6.2	41	1.628						
								60	2.342						
								122	4.087						
45						1.710	6.3	41	1.547						
								60	2.333						
								122	4.231						
46						1.733	6.4	41	1.625						
								60	2.379						
								122	4.187						
47						1.750	6.5	41	1.867						
								60	2.752						
								122	4.806						
48						1.740	6.5	41	1.638						
								60	2.471						
								122	3.906						
49						1.689	6.2	41	1.687						
								60	2.506						
								122	4.408						

Table B, continued

Sample nr	Cement type	w/c	Dimension		Climate before test RH /%/	Weight in the drying period		Evaporation		Measured concentration					
			ϕ /mm/	length /mm/		/gr/	/%/	Time /days/	Amount /gr/	Position from solution	Free /mg/l/	Total /mg/l/	Bound /mg/l/	Cl/C /%/	OH Free
20-1	B;P	0.40	19.5	20	100	-		41	0.545						
								60	0.726						
								69	0.795	0-4	8.000				0.08
										4-6	460				0.37
										6-9	400				0.49
										9-11					
										11-13	600				0.58
										13-16					
										20-16					
										xx)	20.000				0.07
20-2								41	0.499						
								60	0.668						
								121	1.139						
20-3								41	0.517						
								60	0.694						
								121	1.196						
40-1	B;P	0.4	19.5	40	100			41	0.612						
								60	0.814						
								121	1.384						
40-2								41	0.594						
								60	0.796						
								121	1.359						
40-3								40	0.576						
								60	0.768						
								121	1.302						

xx) Test solution

Table B, continued

Sample nr	Cement type	w/c	Dimension		Climate before test RH /%/	Weight in the drying period		Evaporation		Measured concentration					
			ϕ /mm/	length /mm/		/gr/	/%/	Time /days/	Amount /gr/	Position from solution	Free /mg/l/	Total /mg/l/	Bound /mg/l/	Cl/C /%/	OH Free
20-1	B;M	0.40	19.5	20	100			41	0.423						
								60	0.568						
								73	0.652	0-5	10.200				0.10
										5-7	260				0.24
										7-10	470				0.22
										10-12	310				0.23
										12-16	310				
										16-20					
										xx)	20.000				0.05
20-2								41	0.353						
								60	0.491						
								121	0.899						
20-3								41	0.311						
								60	0.427						
								121	0.764						
40-1	B;M	0.40	19.5	40	100			41	0.379						
								60	0.521						
								121	0.942						
40-2								41	0.395						
								60	0.545						
								121	0.988						
40-3								40	0.377						
								60	0.516						
								121	0.920						

xx) Test solution

Table B, continued

Sample nr	Cement type	w/c	Dimension		Climate before test RH /%/	Weight in the drying period		Evaporation		Measured concentration					
			ø /mm/	length /mm/		/gr/	/%/	Time /days/	Amount /gr/	Position from solution	Free /mg/l/	Total /mg/l/	Bound /mg/l/	Cl/C /%/	OH Free
20-1	B;M	0.60	19.5	20	100			41	0.430						
								60	0.579						
								69	0.637	0-5	19.400				0.05
										7-5	940				0.13
										7-10					
										10-13	350				0.18
										13-16					
										16-20					
										xx)	19.000				0.05
20-2								41	0.460						
								60	0.619						
								121	1.069						
20-3								41	0.436						
								60	0.585						
								121	1.014						
40-1	B;M	0.60	19.5	40	100			41	0.456						
								60	0.616						
								121	1.076						
40-2								41	0.481						
								60	0.642						
								121	1.084						
40-3								41	0.464						
								60	0.623						
								121	1.079						

xx) Test solution

Table B, continued

Sample nr	Cement type	w/c	Dimension		Climate before test	Weight in the drying period		Evaporation		Measured concentration					
			ϕ /mm/	length /mm/	RH /%/	/gr/	/%/	Time /days/	Amount /gr/	Position from solution	Free /mg/l/	Total /mg/l/	Bound /mg/l/	Cl/C /%/	OH Free
21	B;P	0.40	19.5	20	50	1.368	11.5	38	1.199						
								57	1.428						
								121	2.004	0-4	11.600				
										4-7					
										7-8	8.000				
										8-12	7.200				
										12-14	5.500				
										14-16					
										16-18					
										18-20					
22								38	0.891						
								57	1.080						
								120	1.568						
23								38	0.769						
								57	0.976						
								120	1.514						
41	B;P	0.40	19.5	40	50	2.522	10.6	38	0.372						
								57	0.535						
								120	0.989						
42						2.750	11.8	38	0.357						
								57	0.517						
								120	0.975						
43						2.438	10.1	38	0.303						
								57	0.542						
								120	1.023						

Table B, continued

Sample nr	Cement type	w/c	Dimension		Climate before test	Weight in the drying period		Evaporation		Measured concentration					
			ϕ /mm/	length /mm/	RH /%/	/gr/	/%/	Time /days/	Amount /gr/	Position from solution	Free /mg/l/	Total /mg/l/	Bound /mg/l/	Cl/C /%/	OH Free
21	B;M	0.40	19.5	20	50	0.399	2.8	38	0.273						
								57	0.392						
								121	0.759	0-6	9.700				
										6-9					
										9-11					
										11-13					
										13-17					
										17-20					
22						0.451	3.2	38	0.279						
								57	0.397						
								120	0.751						
23						0.461	3.3	38	0.233						
								57	0.350						
								120	0.677						
41	B;M	0.40	19.5	40	50	0.777	2.7	38	0.286						
								57	0.413						
								120	0.783						
42						0.794	2.8	38	0.278						
								57	0.402						
								120	0.757						
43						0.791	2.8	38	0.281						
								57	0.408						
								120	0.779						

Table B, continued

Sample nr	Cement type	w/c	Dimension		Climate before test RH /%/	Weight in the drying period		Evaporation		Measured concentration					
			ø /mm/	length /mm/		/gr/	/%/	Time /days/	Amount /gr/	Position from solution	Free /mg/l/	Total /mg/l/	Bound /mg/l/	Cl/C /%/	OH Free
21	B;M	0.60	19.5	20	50	0.972	7.4	38	1.462						
								57	1.749						
								131	1.909	0-5	22.000				0.11
										5-7					
										7-9	24.000				0.09
										9-13	33.000				0.14
										13-16	41.000				0.14
										16-20					
										xx)	19.500				0.07
22						0.897	6.7	38	1.008						
								57	1.223						
								120	1.768						
23						0.963	7.2	38	1.195						
								57	1.435						
								120	2.027						
41	B;M	0.60	19.5	40	50	1.795	6.7	38	0.418						
								57	0.610						
								120	1.136						
42						1.877	7.0	38	0.424						
								57	0.626						
								120	1.183						
43						1.767	6.5	38	0.377						
								57	0.554						
								120	1.050						

xx) Test solution

TABLE C. Results, chlorides-admixtures used casting procedure, chapter 5.4.

Sample nr	Cement type	w/c	Dimension		Climate before test RH /%/	Weight in the drying period /gr/	Time /days	Position from inside /mm/	Measured concentration, chloride				
			ϕ /mm/	length /mm/					Free /mg/l/	Total /mg/l/	Bound /mg/l/	Cl/C cem. /%/	OH, free /equiv/ l/
0% Cl	P;P	0.50			100		400		600				xx)
0.50% Cl^-	P;P	0.50			100		400		7.500	14.000	7.000	0.50	0.10
0.25% Cl	P;P	0.50			100		400		5.000	7.000	2.000	0.25	
1.0% Cl	P;P	0.50			100		400		19.000	29.000	10.000	1.00	
1.25% Cl	P;P	0.50			100		400		20.000	36.000	16.000	1.25	0.13
1.50% Cl	P;P	0.50			100		400		20.000	43.000	23.000	1.50	0.25
2.00% Cl	P;P	0.50			100		400		36.000	58.000	32.000	2.00	
2.50% Cl	P;P	0.50			100		400		45.000	72.000	27.000	2.50	0.16

xx) Porosity = 45%
Cement content= 1290 kg/m^3

Table C, continued

Sample nr	Cement type	w/c	Dimension		Climate before test RH /%/	Weight in the drying period /gr/	Time /days	Position from inside /mm/	Measured concentration, chloride				
			ø /mm/	length /mm/					Free /mg/l/	Total /mg/l/	Bound /mg/l/	Cl/C cem. /%/	OH, free /equiv/ l/
0% Cl	P;P	0.50			100		400		350				xx)
							400		175				
							400		200				
							400		250				
							400		300				
0.25% Cl	P;P	0.50			100		400		875	7.000	6.000	0.25	
									1.050	7.000	6.000		
0.50% Cl	P;P	0.50			100		400		3.500	14.000	10.000	0.50	
									2.450	14.000	11.000		
									3.000	14.000	11.000		
0.75% Cl	P;P	0.50			100		400		10.000	22.000	12.000	0.75	
1% Cl^-	P;P	0.50			100		400		12.000	29.000	17.000	1.00	
1.5% Cl	P;P	0.50			100		400		17.500	43.000	25.000	1.50	
									14.000	43.000	29.000		
									15.000	43.000	28.000		

xx) Porosity = 45%
Cement content= 1290 kg/m^3

Photo 1.

Appearance of concrete surface before concrete cover was chipped off. Crack width approximately 2 mm.

Photo 2.

The same area as that shown in Photo 1 after the concrete cover had been chipped off. The stirrup is partly corroded all the way through. The rust thickness on the principal reinforcement amounts to about 1 mm. The concrete cover was about 15 mm. Little or no brown discolouration in the concrete around the steel.

Photo 3.

Older damage. In this case, ferric hydroxide has been liberated and has coloured the concrete surfaces brown. The corrosion thickness on the principal reinforcement is approximately 2 mm.

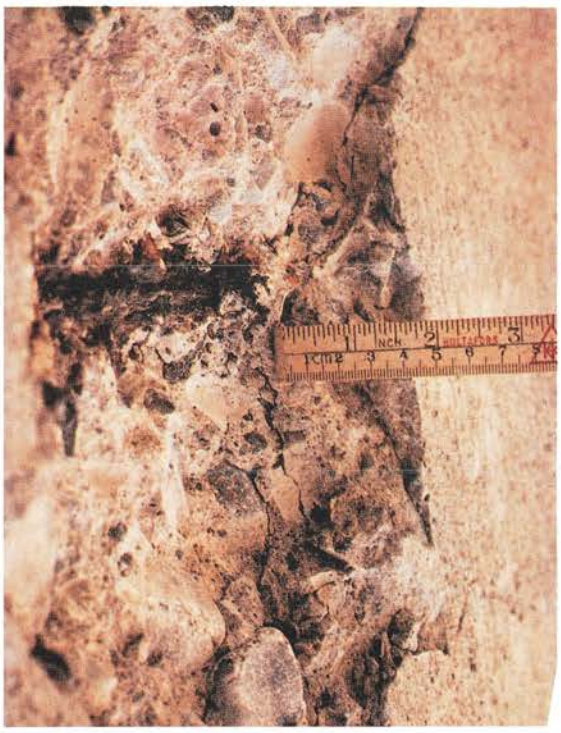

Photo 4.

Reinforcement severely attacked by corrosion, about 4 mm material loss. Concrete cover: approximately 30 mm. Concrete cracked in layers.

Photo 5. Photo of silo. Concrete chipped away to expose reinforcement in crack. Average centre-to-centre spacing 250 mm. Stipulated spacing 120 mm.

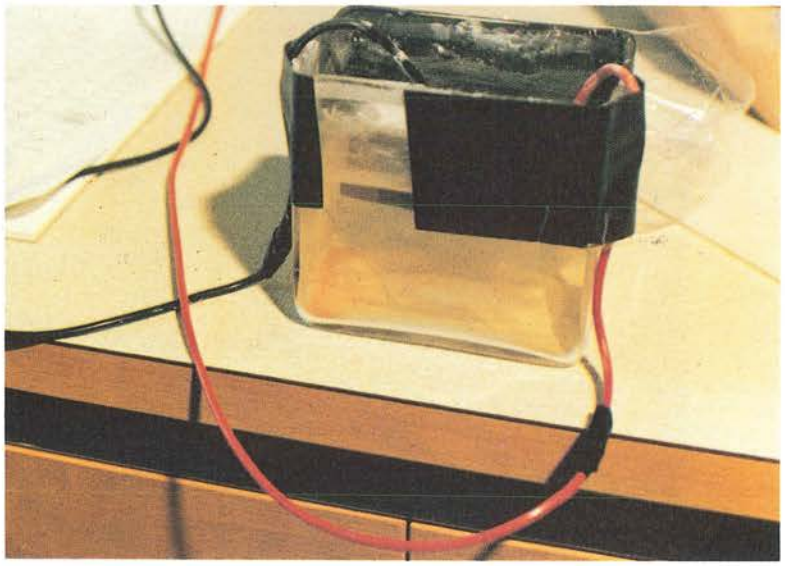

Photo 6. A corrosion cell which has been kept for 7 days in saturated $Ca(OH)_2$ solution without any visible attacks, and then placed in a saturated $Ca(OH)_2$ solution with 1% NaCl, showed corrosion attacks after 24 hours. A red sludge of ferric hydroxide can be seen in the bottom left hand part of the vessel.

Photo 7. Close-up of corrosion cell in preceding photo.

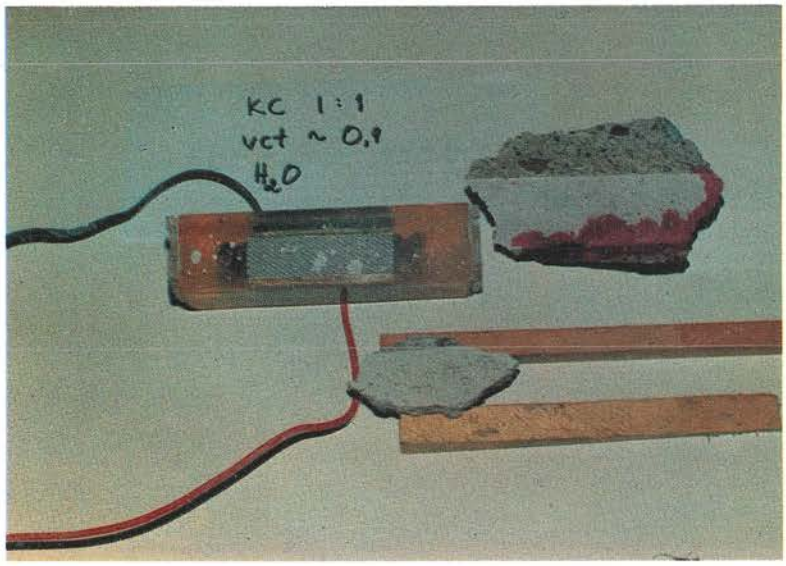

Photo 8. Corrosion cell after exposure to water for about 60 days. No changes in colour whatsoever as a result of corrosion can be seen. The phenolphthalein specimen is positive, in other words the specimen is not carbonated. Concrete quality: KC1-76, W/C approximately 0.8, concrete cover 7 mm.

Photo 9. Embedded corrosion cell after concrete had been chipped away.

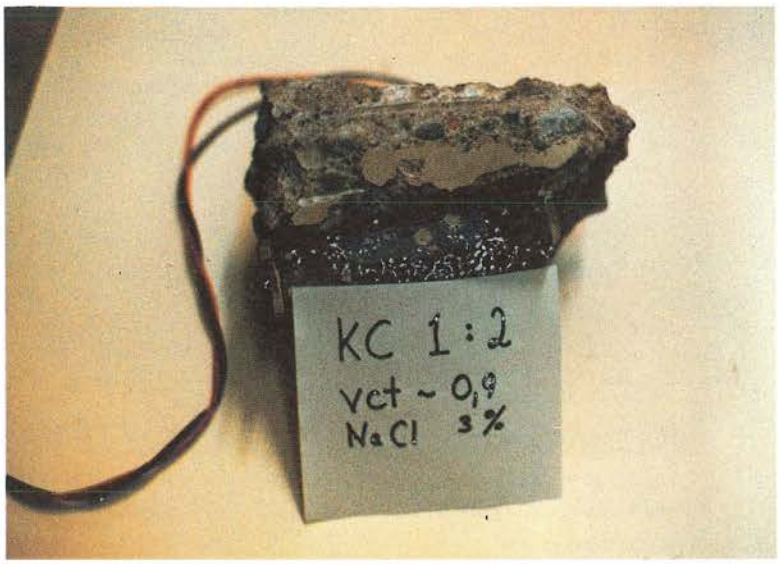

Photo 10. Corrosion cell after exposure to a 3% NaCl solution for about 60 days. A large quantity of corrosion products can be seen with the naked eye on the entire cell, particularly on the anodic areas. Concrete quality KC1-76, W/C approx. 0.8, concrete cover 7 mm.

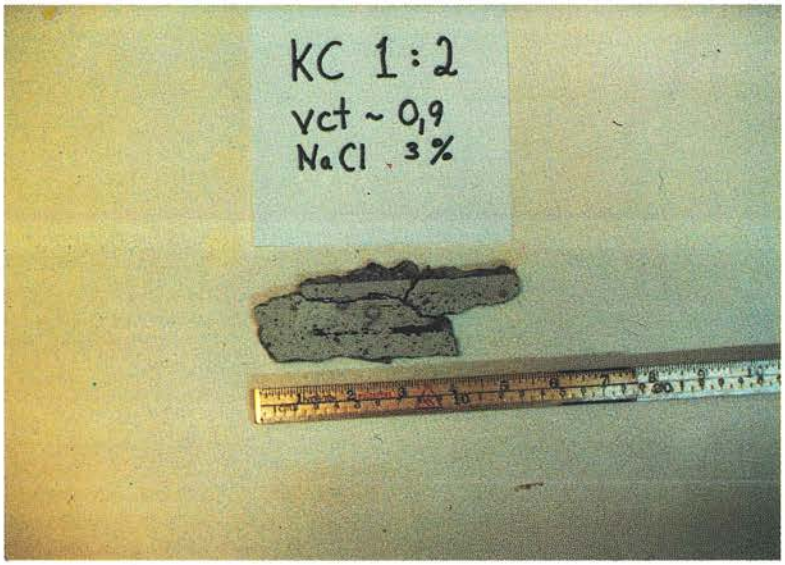

Photo 11. The concrete cover also showed clear marks of a corrosion attack.

Photo 12. The reinforcement bars (the reference bars) also showed signs of corrosion attacks where the corrosion cells had indicated this.

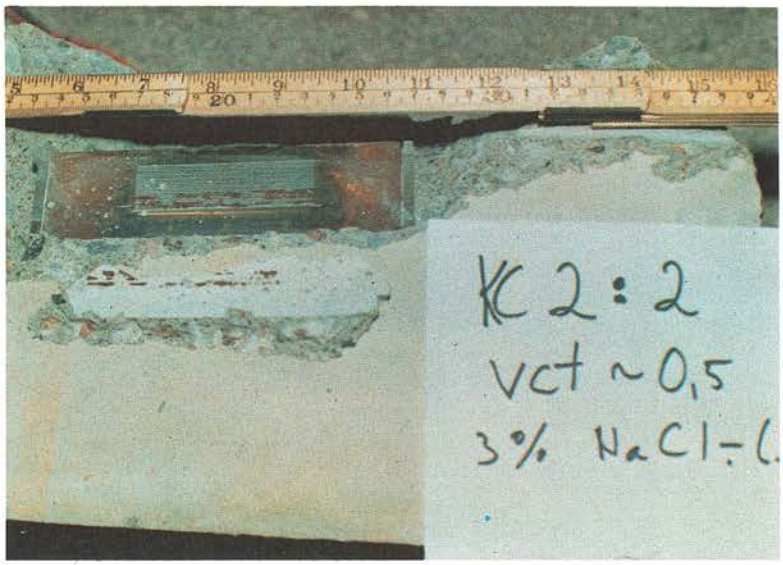

Photo 13. Corrosion attacks on corrosion cell stored in the concrete of higher quality. W/C approx. 0.5. The environment consisted of a 3% NaCl solution.

Photo 14. Corrosion cell in Series 1, cell No. 1 after conclusion of exposure.

Photo 15. Corrosion cell in Series 1, cell No. 2 after conclusion of exposure.

Photo 16. Corrosion cell in Series 1, cell No. 3 after conclusion of exposure.

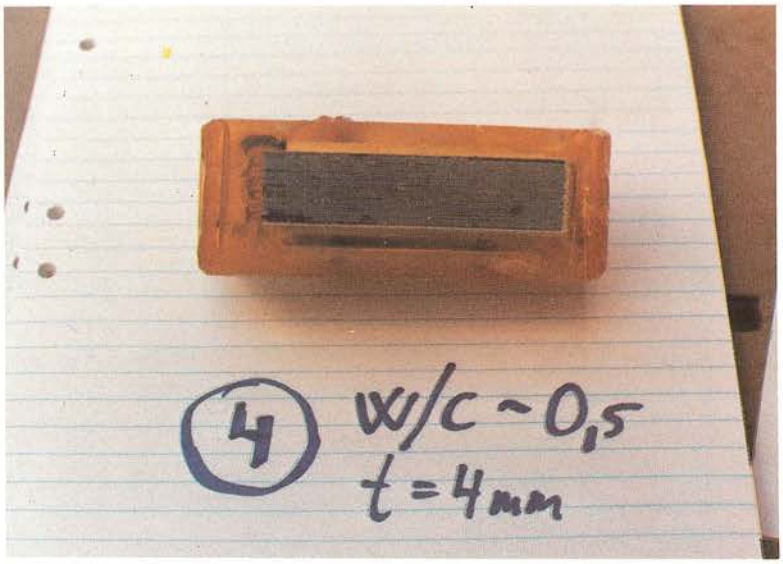

Photo 17. Corrosion cell in Series 1, cell No. 5 after conclusion of exposure.

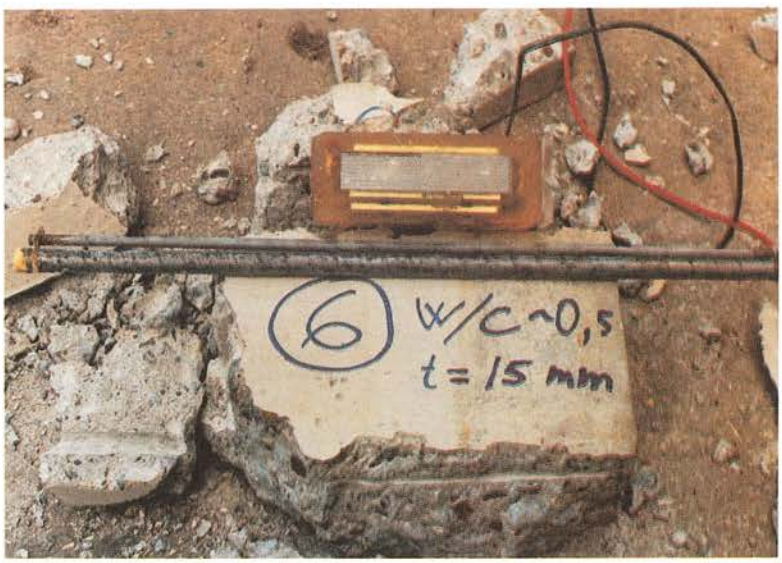

Photo 18. Corrosion cell in Series 1, cell No. 6 after conclusion of exposure.

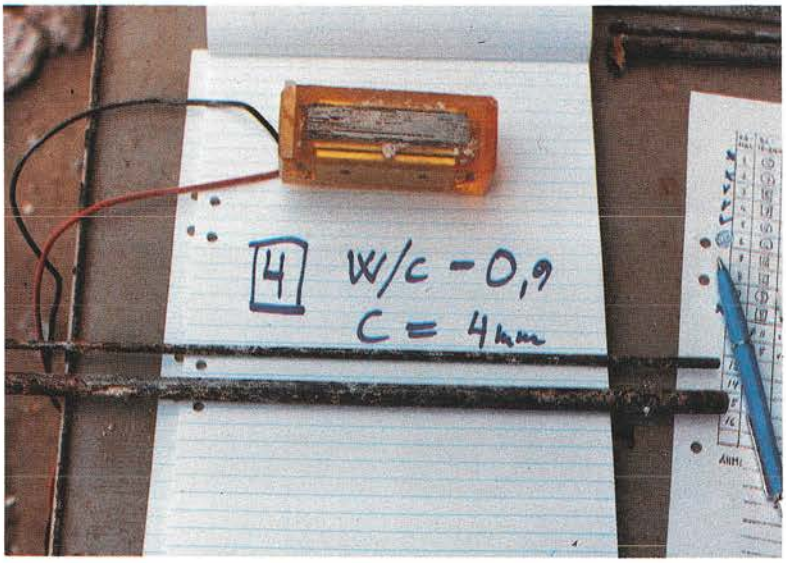

Photo 19. Corrosion cell in Series 1, cell No. 7 after conclusion of exposure.

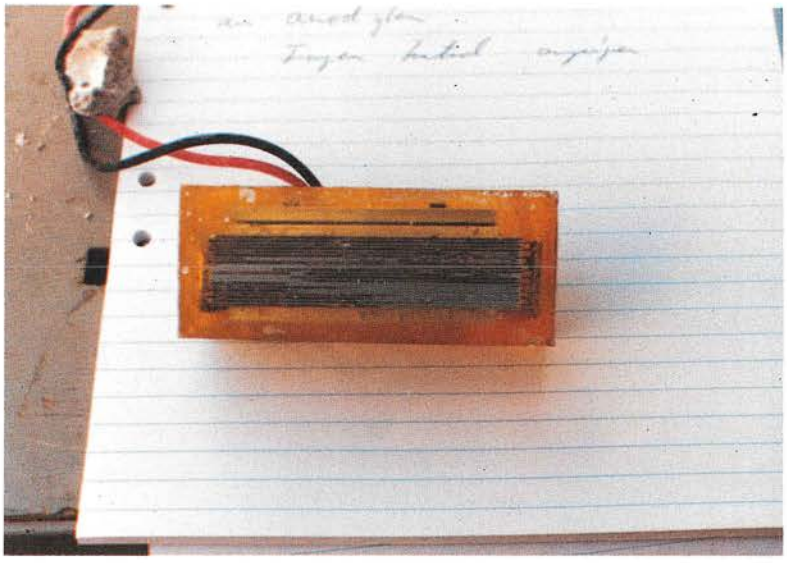

Photo 20. Corrosion cell in Series 1, cell No. 8 after conclusion of exposure.

Photo 21. Corrosion cell in Series 1, cell No. 9 after conclusion of exposure.

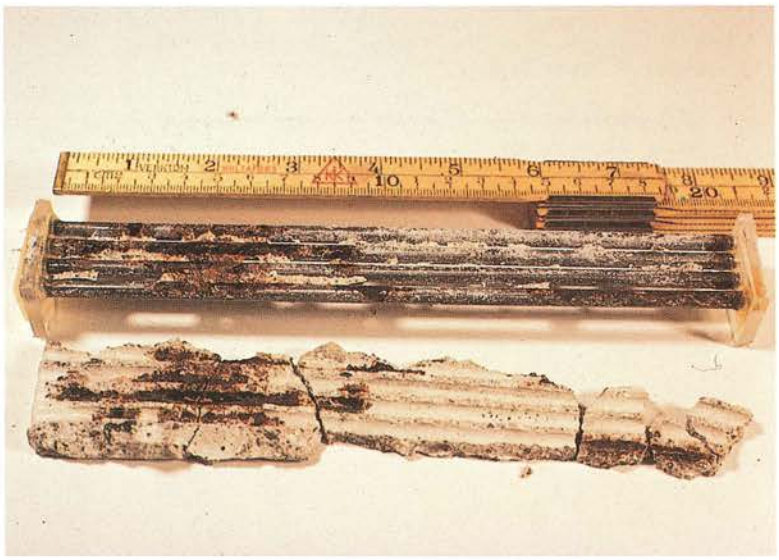

Photo 22. Corrosion cell in Series 1, cell No. 12 after conclusion of exposure.

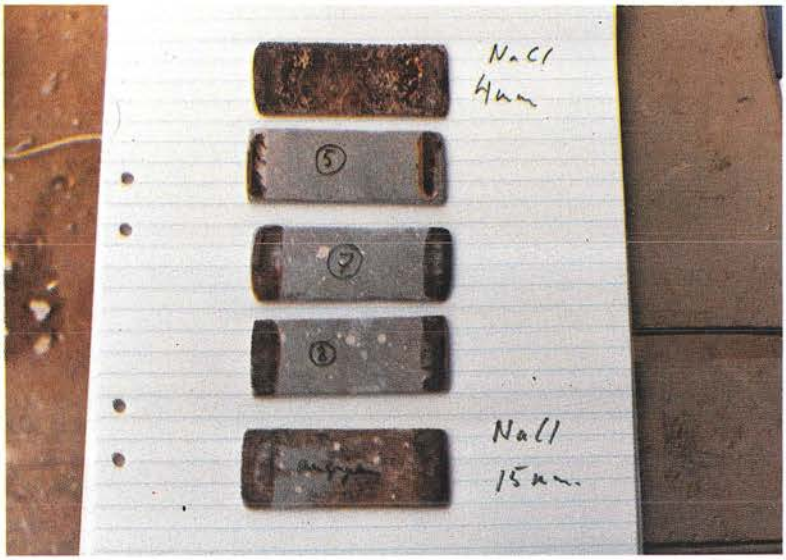

Photo 23. Steel plates contained in the same specimens as corrosion cells in Series 1. Counted from the top, the plates were contained in the following specimens:

W/C approx. 0.5, concrete cover 4 mm, 3% NaCl.	Corrosion cell 5
W/C approx. 0.5, concrete cover 4 mm, H_2O	Corrosion cell 1
W/C approx. 0.5, concrete cover 15 mm, H_2O	Corrosion cell 2
W/C approx. 0.5, concrete cover 15 mm, air	Corrosion cell 9
W/C approx. 0.5, concrete cover 15 mm, 3% NaCl	Corrosion cell 6

Photo 24. Anodic metal surfaces have received faint brown discolouring. Cell No. 1, in Series 2.

Photo 25. Unattacked corrosion cell. A varying oxide formation can, however, be seen along the cylindrical surfaces. When compared with the preceding photo, the differences are insignificant. Cell No. 4, in Series 2.

Photo 26. The entire corrosion cell has been attacked. Maximum pitting depth approximately 0.5 mm. Cell No. 10, in Series 2.

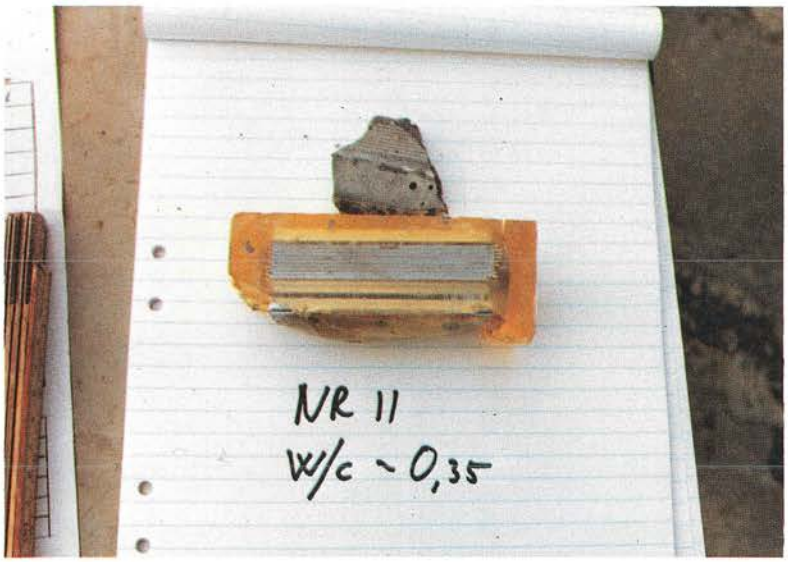

Photo 27. Corrosion cell where about 10% of the anodic area has begun to corrode. Cell No. 11, in Series 2.

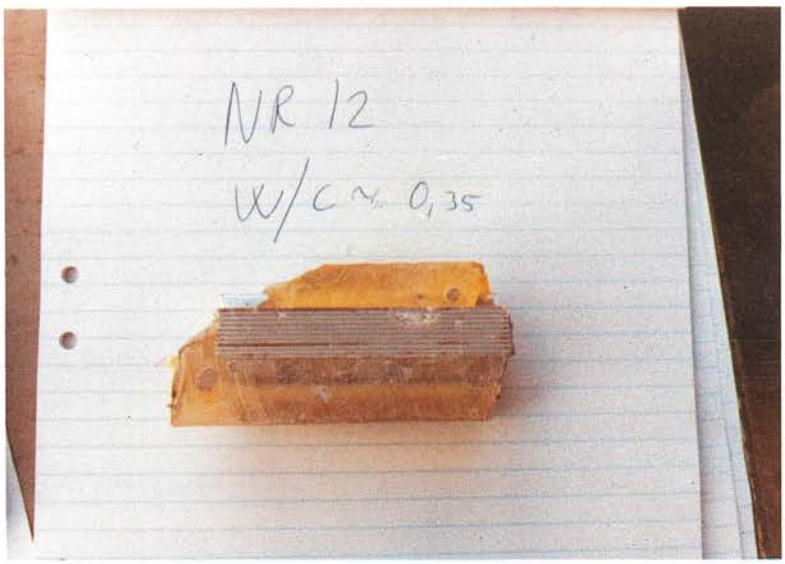

Photo 28. Corrosion cell where about 15% of the anodic area has begun to corrode. Cell No. 12, in Series 2.

Photo 29. Corrosion cell where about 20% of the anodic area has begun to corrode. Note that the three steel plates show no more than local corrosion. Cell No. 13, in Series 2.

Photo 30. State of reference bars after exposure in series in Series 2. A certain discolouration can be noted along the cylindrical surface of all bars and all bars show limited pitting for a maximum of 1% of the total area.

Photo 31. Corrosion cell of type C, in Series 3, KC6-78, after exposure. Note the marked corrosion in the centre which was connected as an anode during the measurements.

Photo 32. Corrosion cell in Series 3, KC6-78 which had been in carbonated concrete and then been subjected to wetting to study the cell current as a function of the relative humidity and temperature.

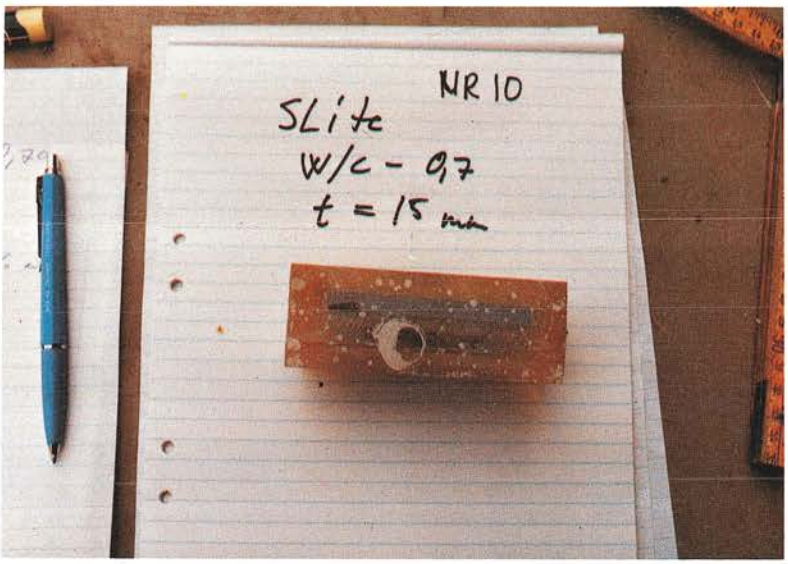

Photo 33. Cell No. 3 in Series 4 after exposure. Note the large void under the cell surface. Portland cement.

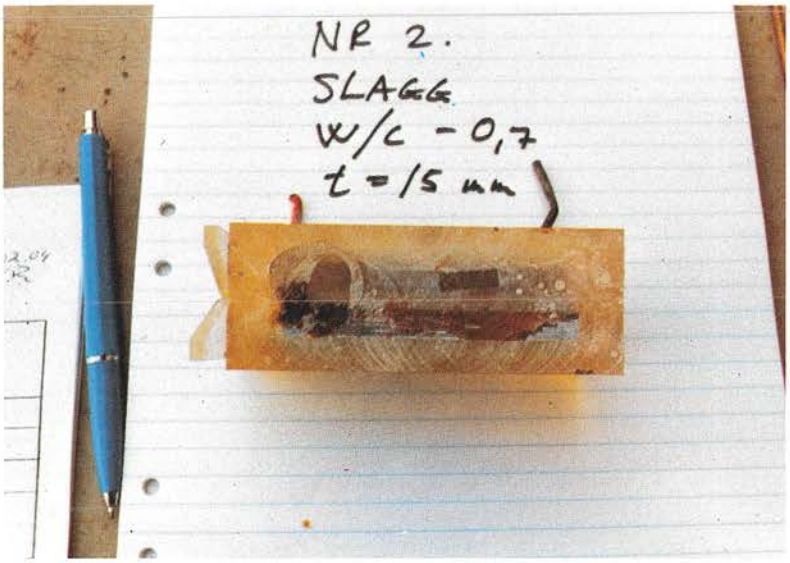

Photo 34. Cell No. 4 in Series 4. The attack started adjacent to a large void which was in contact with the exposure surface. Slag cement.

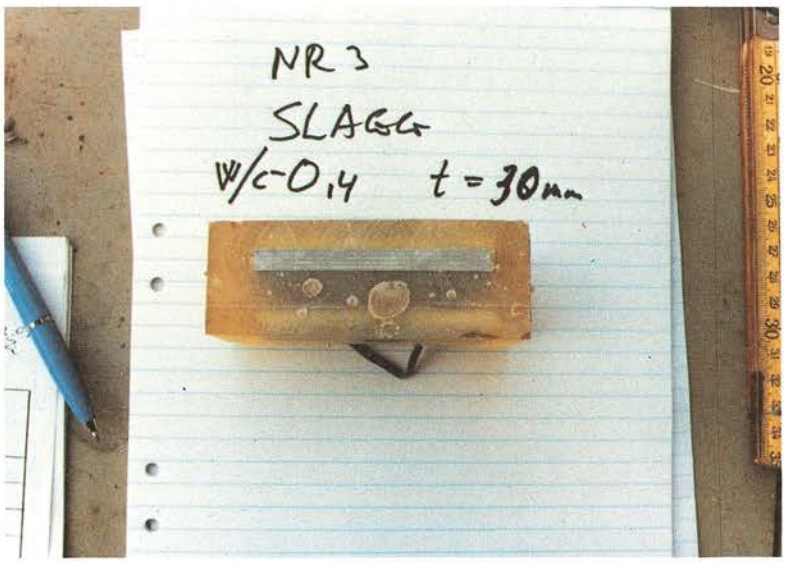

Photo 35. Cell No. 6 in Series 4. No visible corrosion attacks can be seen. Slag cement.

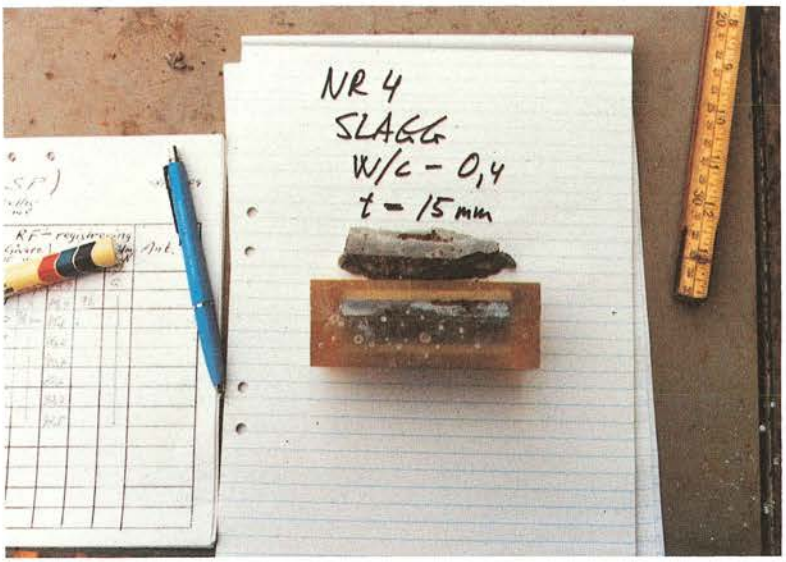

Photo 36. Cell No. 7 in Series 4. Slag cement.

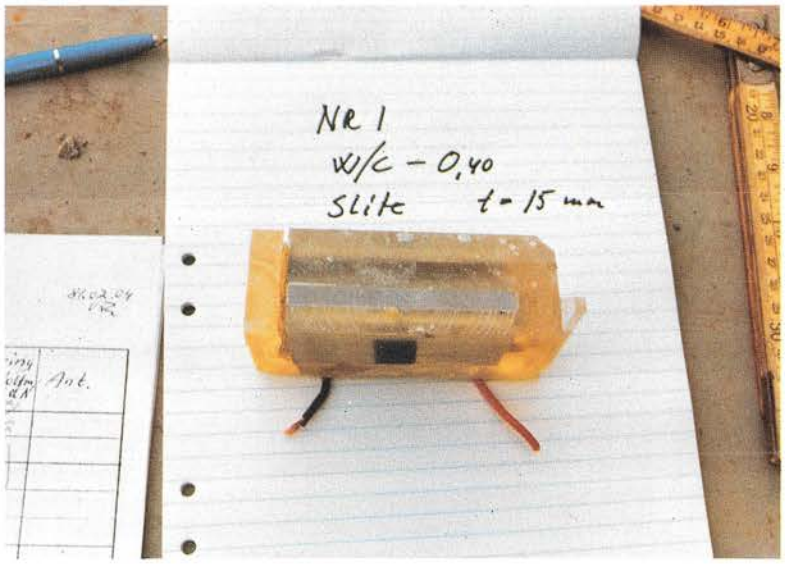

Photo 37. Cell No. 8 in Series 4. Slite Portland cement.

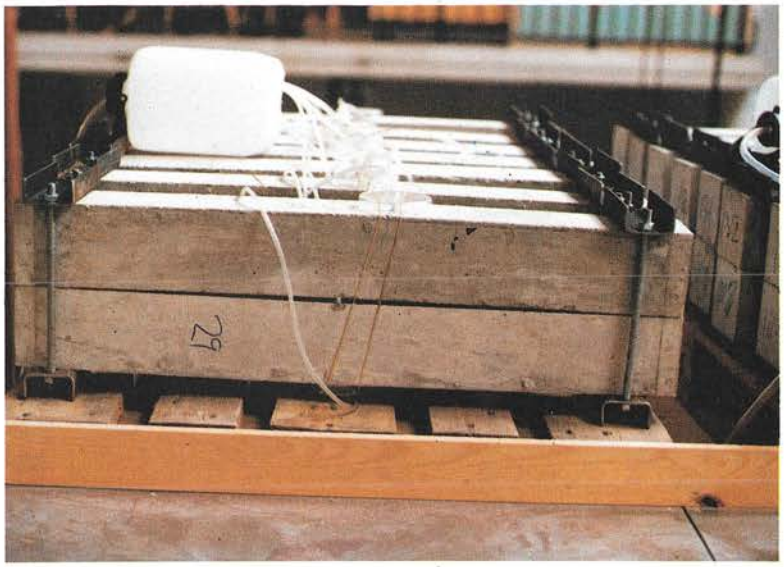

Photo 38. CO_2 initiation locally in crack by means of increased CO_2 content close to crack zone.

Photo 39. Corrosion of reinforcement in a traffic facility called Slussen in Stockholm where chlorides from road salt had initiated the corrosion process.

Photo 40. The process of corrosion stopped by repassivation or lack of O_2. Cathode cast into concrete, anode in waterfilled space. Exposure time 5 years.

Photo 41. Realkalization has occured in crack zones after increased relative humidity in the environment. Phenolphtalein test is positive.

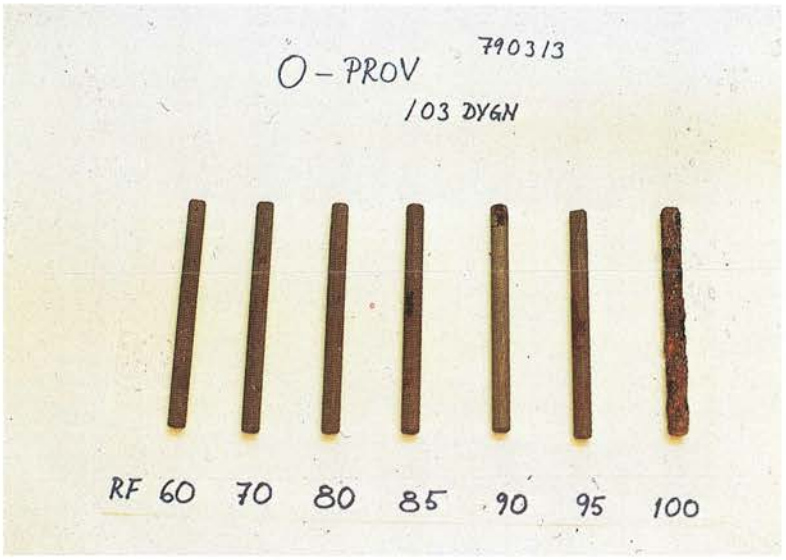

Photo 42. Bars after test exposed to different relative humidities. Exposure time 103 days.

Photo 43. Bars after test, cast into mortar with 5% $CaCl_2$ by weight of cement, exposed to different relative humidities. Exposure time 113 days, Slite Portland cement, W/C = 0.7.

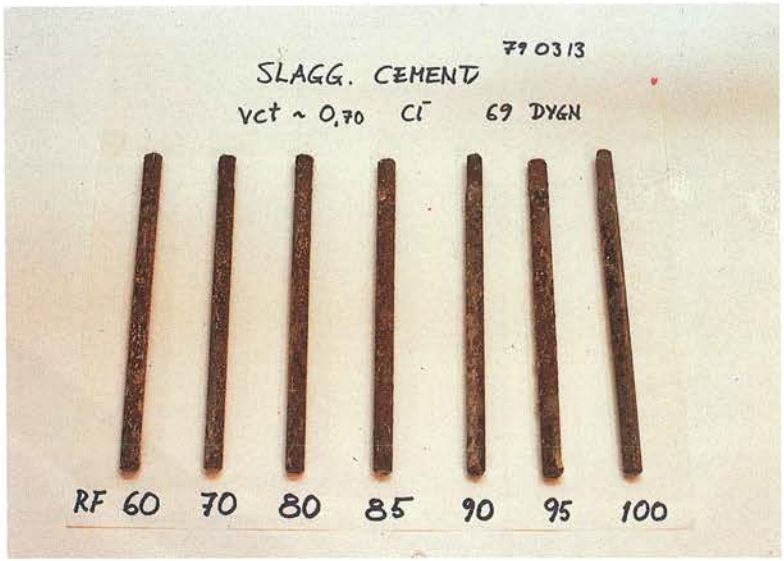

Photo 44. Bars after test, cast into mortar with 5% $CaCl_2$ by weight of cement, exposed to different relative humidities. Exposure time 69 days, slag cement, W/C = 0.7.

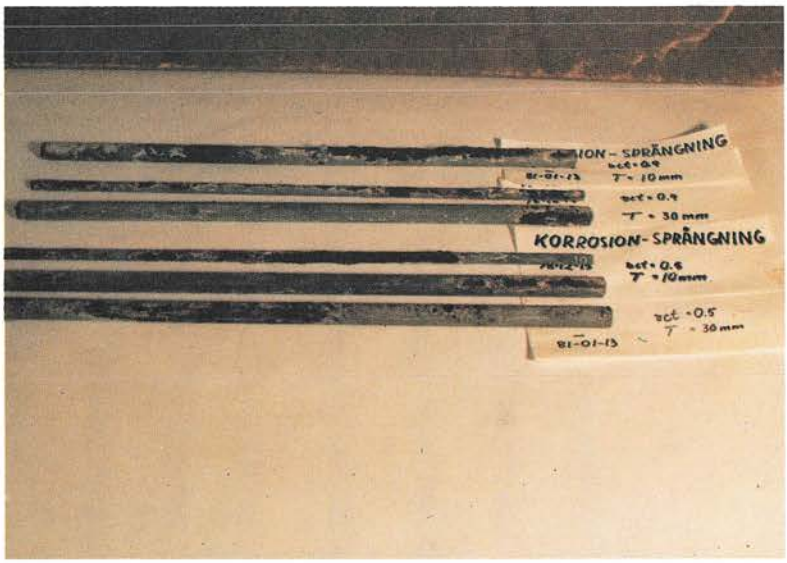

Photo 45. Cracked concrete cover as a result of reinforcement corrosion and bars after test according to chapter 5.3.7.

Notations in the photos:
vct = W/C
T = concrete cover